Corrosion of copper in antibacterial efficiency test

Jiaqi Luo

Corrosion of copper in antibacterial efficiency test

Dissertation

zur Erlangung des Grades

des Doktors der Ingenieurswissenschaften

der Naturwissenschaftlich-Technischen Fakultät

der Universität des Saarlandes

Von

Jiaqi LUO

Saarbrücken

2020

Tag des Kolloquiums:	10.12.2020
Dekan:	Prof. Dr. Jörn Walter
Berichterstatter:	Prof. Dr. Frank Mücklich
	Prof. Dr. Ralf Möller
	Prof. Dr. Jean-François Pierson
Vorsitz:	Prof. Dr. Christian Motz
Akad. Mitarbeiter:	Prof. Dr. Michel Vilasi
Mitglieder des	Dr. Régine Basséguy
Prüfungsausschusses:	Dr. Michael Stüber
	Dr. Tomáš Prošek

Thèse

Pour l'obtention du titre de :

DOCTEUR de L'UNIVERSITÉ DE LORRAINE

Spécialité : Sciences des Matériaux

présentée par :

Jiaqi LUO

Corrosion of copper in antibacterial efficiency test

Soutenue publiquement le 10.12.2020 à Sarrebruck devant le jury composé de :

Régine Basséguy	Directeur de Recherche, Laboratoire De Génie Chimique, University of Toulouse	Rapporteur
Michael Stüber	Senior Researcher, Institute of Applied Materials, Karlsruhe Institute of Technology	Rapporteur
Ralf Möller	Professor, Applied Science, Bonn-Rhein-Sieg University of Applied Sciences	Examinateur
Tomáš Prošek	Researcher, Technopark Kralupy, University of Chemistry and Technology Prague	Examinateur
Christian Motz	Professor, Experimental Methodology of Materials Science, Saarland University	Examinateur
Michel Vilasi	Professor, Institut Jean Lamour, University of Lorraine	Examinateur
Frank Mücklich	Professor, Functional Materials, Saarland University	Directeur de These
Jean-François Pierson	Professor, Institut Jean Lamour, University of Lorraine	Co-directeur de These

Institut Jean Lamour, UMR 7198, ARTEM – CS 50840-54011 Nancy Cedex

Université de Lorraine – Ecole doctorale Chimie – Mécanique – Matériaux – Physique (C2MP)

*To believe with **certainty**,*

*we must begin with **doubting**.*

Stanisław Leszczyński

Abstract, Zusammenfassung, Résumé

Metallic copper has been widely proved as a promising antibacterial surface. This work aims to investigate the copper corrosion phenomena mostly observed in a certain type of antibacterial efficiency test, the so-called droplet method. By performing various ex-situ metallurgical methods, chemical and morphological changes on copper surfaces were characterised, with which the copper ion content and antibacterial activity were correlated. All these findings not only help to understand the origin of the antibacterial copper ion release, but also shift the research focus back on the copper surface itself, suggesting how materials research can function in antibacterial surface design.

Metallisches Kupfer hat sich bereits mehrfach als eine vielversprechende antibakterielle Oberfläche erwiesen. Ziel dieser Arbeit ist es, die Kupferkorrosionsphänomene zu untersuchen, die am häufigsten bei einer bestimmten Art von antibakteriellen Wirksamkeitstests, der sogenannten Tröpfchenmethode, beobachtet werden. Durch die Durchführung verschiedener metallurgischer Ex-situ-Methoden wurden chemische und morphologische Veränderungen an Kupferoberflächen charakterisiert, mit denen der Kupferionengehalt und die antibakterielle Aktivität korreliert wurden. All diese Ergebnisse helfen nicht nur den Ursprung der antibakteriellen Kupferionenfreisetzung zu verstehen, sondern verlagern auch den Forschungsschwerpunkt zurück auf die Kupferoberfläche selbst, um zu zeigen, wie die Materialforschung für ein gezieltes Design antibakterieller Oberflächengestaltung funktionieren kann.

Le cuivre métallique a été largement prouvé comme une surface antibactérienne prometteuse. Ce travail vise à étudier les phénomènes de corrosion du cuivre principalement observés dans un certain type de test d'efficacité antibactérienne, appelé méthode des gouttelettes. En appliquant diverses méthodes métallurgiques ex-situ, des changements chimiques et morphologiques sur les surfaces de cuivre ont été caractérisés, avec lesquels la teneur en ions cuivre et l'activité antibactérienne ont été corrélées. Tous ces résultats permettent non seulement de comprendre l'origine de la libération d'ions cuivre antibactériens, mais aussi de recentrer la recherche sur la surface du cuivre elle-même, ce qui suggère comment la recherche sur les matériaux peut fonctionner dans la conception de surfaces antibactériennes.

Extended Summary

Pathogenic and antibiotic resistant bacteria are spreading across the world, concerning us all. They are too tiny to be easily noticed, therefore it is hard to tell if an object is contaminated or not. And most strikingly: they could survive on various types of surfaces for a long period. As a result, approaches such as cleaning and disinfection of frequently touched surfaces were developed, in order to restrain infections caused by bacteria. But meanwhile, another strategy is also receiving much attention: antibacterial surfaces.

Metallic copper has been widely proved as a promising antibacterial surface. This is mainly attributed to the release of copper ions, which could introduce damages in bacterial cells at multiple levels. To quantify the antibacterial efficiency of a certain surface, or to compare among several surfaces, antibacterial efficiency tests need to be performed. However, in these tests, the bacterial suspension is not only an object to be examined, but also an environmental factor introduced into such a corrosion system. Because it is exactly the corrosion reactions that release antibacterial copper ions, the interactions between copper surfaces and bacterial suspensions have significant impacts on antibacterial efficiency evaluation.

This work aims to investigate the copper corrosion phenomena mostly observed in a certain type of antibacterial efficiency test, the so-called droplet method. By performing various ex-situ metallurgical methods, chemical and morphological changes on copper surfaces were characterised, with which the copper ion content and antibacterial activity were correlated. Grazing incidence X-ray diffraction, Raman spectroscopy and scanning electron microscopy were applied for the former objective, while inductively coupled plasma mass spectrometry was employed for the latter one.

Some noteworthy features have been found, promoting the understanding of the roles of oxides, bacteria, and buffer solutions presenting in an antibacterial efficiency test. For example, diverse copper release kinetics have been recorded in different buffer solutions (phosphate-buffered saline, Na-4-(2-hydroxyethyl)-1-piperazineethanesulfonic acid, 0.9% saline); at the same time, the growth of Cu_2O could also be buffer-dependent. This oxide growth has been regarded as a barrier stopping copper surface from being directly corroded. This effect was further verified by introducing sputtered Cu_2O coating.

Next step was to investigate the effect of bacteria, as they are actually present in antibacterial efficiency test. In the case of bacterial suspension (*Escherichia coli* in phosphate-buffered saline), oxide growth could be sufficiently inhibited, which is linked to the copper accumulation effect by the bacteria. Meanwhile, localised corrosion phenomenon was revealed.

In addition, oxide growth and preferred corrosion sites have been further examined on electropolished copper coupons. Oxide growth can be described as a re-deposition process, and the

localised corrosion sites are microstructure dependent. It is thus found that the localised bacteria adhesion did not introduce extra corrosion attacks at that very spots, indicating the dominant role of buffer.

As a result, a further comparison was made between saline and pure water, where chloride demonstrated its significant factor in introducing localised corrosion. It accelerates copper ion release and enhances antibacterial efficiency. Features of atmospheric corrosion were obtained on saline pre-treated copper coupons.

All these findings not only help to understand the origin of the antibacterial copper ion release, but also shift the research focus back on the copper surface itself, suggesting how materials research can function in antibacterial surface design. On one hand, it is necessary to take the interaction between buffers and antibacterial surfaces into account, when interpretation of antibacterial efficiency is made. On the other hand, microstructural design could play a part in enhancing antibacterial efficiency, in which release of antibacterial substances is mainly fulfilled by corrosion.

Erweiterte Zusammenfassung

Pathogene und antibiotikaresistente Bakterien breiten sich weltweit aus, und betreffen uns alle. Sie sind zu winzig, um leicht gefunden zu werden, daher ist es schwer zu sagen, ob ein Objekt kontaminiert ist oder nicht. Am auffälligsten: Sie könnten auf verschiedenen Arten von Oberflächen lange Zeit überleben. Deshalb wurden Mittel wie die Reinigung und Desinfektion von häufig berührten Oberflächen entwickelt, um durch Bakterien verursachte Infektionen einzudämmen. Inzwischen wird aber auch einer anderen Strategie viel Aufmerksamkeit geschenkt: die antibakteriellen Oberflächen.

Metallisches Kupfer hat sich bereits mehrfach als eine vielversprechende antibakterielle Oberfläche erwiesen. Dies wird hauptsächlich auf die Freisetzung von Kupferionen zurückgeführt, die auf mehreren Ebenen zu Schäden in Bakterienzellen führen können. Um die antibakterielle Wirksamkeit einer bestimmten Oberfläche zu quantifizieren, oder zwischen mehreren Oberflächen zu vergleichen, müssen antibakterielle Wirksamkeitstests durchgeführt werden. Bei diesen Tests ist die Bakteriensuspension jedoch nicht nur ein zu untersuchender Gegenstand, sondern auch ein in ein solches Korrosionssystem eingebrachter Umweltfaktor. Da es genau die Korrosionsreaktionen sind, die antibakterielle Kupferionen freisetzen, haben die Wechselwirkungen zwischen Kupferoberflächen und Bakteriensuspensionen erhebliche Auswirkungen auf die Bewertung der antibakteriellen Wirksamkeit.

Ziel dieser Arbeit ist es, die Kupferkorrosionsphänomene zu untersuchen, die am häufigsten bei einer bestimmten Art von antibakteriellen Wirksamkeitstests, der sogenannten Tröpfchenmethode, beobachtet werden. Durch die Durchführung verschiedener metallurgischer Ex-situ-Methoden wurden chemische und morphologische Veränderungen an Kupferoberflächen charakterisiert, mit denen der Kupferionengehalt und die antibakterielle Aktivität korreliert wurden. Für das erstgenannte Ziel wurden Röntgenbeugung unter streifendem Einfall, Raman-Spektroskopie und Rasterelektronenmikroskopie eingesetzt, während für das letztgenannte Ziel die Massenspektrometrie mit induktiv gekoppeltem Plasma verwendet wurde.

Es wurden einige nennenswerte Merkmale gefunden, die das Verständnis der Rolle von Oxiden, Bakterien und Pufferlösungen bei einem antibakteriellen Wirksamkeitstest fördern. Beispielsweise wurden in verschiedenen Pufferlösungen unterschiedliche Kupferfreisetzungskinetiken aufgezeichnet (Phosphatgepufferte Salzlösung, Na-4-(2-Hydroxyethyl)-1-piperazinethansulfonsäure, Isotonische Kochsalzlösung 0.9%); gleichzeitig könnte die Entstehung von Cu_2O auch pufferabhängig sein. Dieses Oxidwachstum wurde als eine Barriere betrachtet, die die Kupferoberfläche vor direkter Korrosion schützt. Dieser Effekt wurde durch die Einführung einer gesputterten Cu_2O Beschichtung weiter verifiziert.

Der nächste Schritt war die Untersuchung der Wirkung von Bakterien, wie sie im antibakteriellen Wirksamkeitstest tatsächlich vorhanden sind. Im Falle einer Bakteriensuspension (*Escherichia coli* in Phosphatgepufferte Salzlösung) konnte das Oxidwachstum ausreichend gehemmt werden, was mit dem Kupferakkumulationseffekt durch die Bakterien zusammenhängt. Währenddessen wurde ein lokalisiertes Korrosionsphänomen aufgedeckt.

Darüber hinaus wurden das Oxidwachstum und bevorzugte Korrosionsstellen an elektropolierten Kupfercoupons eingehender untersucht. Oxidwachstum kann als ein Prozess der erneuten Ablagerung beschrieben werden, und die lokalisierten Korrosionsstellen sind mikrostrukturabhängig. Es wurde festgestellt, dass die Bakterienadhäsion selbst keine zusätzlichen lokalisierten Korrosionsangriffe einleitete, was auf die dominierende Rolle des Puffers hinweist.

In diesem Zuge wurde ein Vergleich des Korrosionseinflusses zwischen salzhaltigem und reinem Wasser gezogen, wo Chlorid seinen signifikanten Faktor bei der Ausbildung lokalisierter Korrosion zeigte. Es beschleunigt die Freisetzung von Kupferionen und verbessert die antibakterielle Wirksamkeit. Spezifische Merkmale der atmosphärischen Korrosion wurden an salzhaltig vorbehandelten Kupfercoupons untersucht.

All diese Ergebnisse helfen nicht nur den Ursprung der antibakteriellen Kupferionenfreisetzung zu verstehen, sondern verlagern auch den Forschungsschwerpunkt zurück auf die Kupferoberfläche selbst, um zu zeigen, wie die Materialforschung für ein gezieltes Design antibakterieller Oberflächengestaltung funktionieren kann. Einerseits ist es notwendig, bei der Interpretation der antibakteriellen Wirksamkeit die Wechselwirkung zwischen Puffern und antibakteriellen Oberflächen zu berücksichtigen. Zum anderen könnte die Gestaltung der Mikrostruktur eine Rolle bei der Erhöhung der antibakteriellen Wirksamkeit spielen, bei der die Freisetzung antibakterieller Substanzen hauptsächlich durch Korrosion erfolgt.

Résumé Détaillé

Les bactéries pathogènes et résistantes aux antibiotiques se répandent dans le monde entier et nous concernent tous. Elles sont trop petites pour être facilement remarquées, il est donc difficile de dire si un objet est contaminé, ou non. Et le plus frappant : elles peuvent survivre longtemps sur différents types de surfaces. C'est pourquoi des approches telles que le nettoyage et la désinfection des surfaces fréquemment touchées ont été développées, afin de limiter les infections causées par les bactéries. Mais en attendant, une autre stratégie fait l'objet d'une grande attention : les surfaces antibactériennes.

Le cuivre métallique a été largement prouvé comme une surface antibactérienne prometteuse. Cela est principalement attribué à la libération d'ions de cuivre, qui pourrait introduire des dommages dans les cellules bactériennes à plusieurs niveaux. Pour quantifier l'efficacité antibactérienne d'une certaine surface, ou pour comparer entre plusieurs surfaces, des tests d'efficacité antibactérienne doivent être effectués. Cependant, dans ces tests, la suspension bactérienne n'est pas seulement un objet à examiner, mais aussi un facteur environnemental introduit dans un tel système de corrosion. Comme ce sont précisément les réactions de corrosion qui libèrent des ions cuivre antibactériens, les interactions entre les surfaces de cuivre et les suspensions bactériennes ont des impacts significatifs sur l'évaluation de l'efficacité antibactérienne.

Ce travail vise à étudier les phénomènes de corrosion du cuivre principalement observés dans un certain type de test d'efficacité antibactérienne, appelé méthode des gouttelettes. En appliquant diverses méthodes métallurgiques ex-situ, des changements chimiques et morphologiques sur les surfaces de cuivre ont été caractérisés, avec lesquels la teneur en ions cuivre et l'activité antibactérienne ont été corrélées. La diffraction des rayons X en incidence rasante, la spectroscopie Raman et la microscopie électronique à balayage ont été appliquées pour le premier objectif, tandis que la spectrométrie de masse à plasma à couplage inductif a été utilisée pour le second.

Certaines caractéristiques remarquables ont été trouvées, favorisant la compréhension des rôles des oxydes, des bactéries et des solutions tampon se présentant dans un test d'efficacité antibactérienne. Par exemple, diverses cinétiques de libération du cuivre ont été enregistrées dans différentes solutions tampons (tampon phosphate salin, acide Na-4-(2-hydroxyéthyl)-1-pipérazine éthane sulfonique, Sérum physiologique 0.9%) ; en même temps, la croissance du Cu_2O pourrait également être dépendante de la solution tampon. Cette croissance d'oxyde a été considérée comme une barrière empêchant la corrosion directe de la surface du cuivre. Cet effet a encore été vérifié par l'introduction d'un revêtement de Cu_2O pulvérisé.

L'étape suivante consistait à étudier l'effet des bactéries, telles qu'elles sont réellement présentes dans le test d'efficacité antibactérienne. Dans le cas d'une suspension bactérienne (*Escherichia coli*

dans le tampon phosphate salin), la croissance de l'oxyde pourrait être suffisamment inhibée, ce qui est lié à l'effet d'accumulation du cuivre par les bactéries. Entre-temps, un phénomène de corrosion localisé a été révélé.

En outre, la croissance d'oxyde et les sites de corrosion préférés ont été examinés plus avant sur des coupons de cuivre électropoli. La croissance des oxydes peut être décrite comme un processus de redéposition, et les sites de corrosion localisés dépendent de la microstructure. On constate donc que l'adhésion localisée des bactéries n'a pas introduit d'attaques de corrosion supplémentaires, ce qui indique le rôle dominant du tampon.

En conséquence, une autre comparaison a été faite entre l'eau salée et l'eau pure, où le chlorure a démontré son facteur significatif dans l'introduction de la corrosion localisée. Il accélère la libération des ions cuivre et renforce l'efficacité antibactérienne. Les caractéristiques de la corrosion atmosphérique ont été obtenues sur des coupons en cuivre prétraités à la solution saline.

Tous ces résultats permettent non seulement de comprendre l'origine de la libération d'ions cuivre antibactériens, mais aussi de recentrer la recherche sur la surface du cuivre elle-même, ce qui suggère comment la recherche sur les matériaux peut fonctionner dans la conception de surfaces antibactériennes. D'une part, il est nécessaire de prendre en compte l'interaction entre les tampons et les surfaces antibactériennes, lors de l'interprétation de l'efficacité antibactérienne. D'autre part, la conception de la microstructure pourrait jouer un rôle dans l'amélioration de l'efficacité antibactérienne, dans laquelle la libération de substances antibactériennes est principalement assurée par la corrosion.

Contents

1. Background Information

This chapter covers three main domains related to the scope of this thesis. It starts with introduction of antibacterial surfaces: the reason why we need them, the circumstances where they can be applied, how they interact with bacteria, and how they are usually evaluated. After that, focus will be directed to copper materials, namely their specific antibacterial mechanisms and potential applications. In the third part, some concepts in corrosion science are presented, which are important for further analysis of the phenomena reported in the later chapters. In the end of this chapter, the way how this thesis is organised is also explained.

1.1. Antibacterial Surfaces

Exactly as it is written, "antibacterial" is a kind of effect that plays a significant part in fighting against bacteria. However, before going deep into it, some basic concepts of bacteria themselves would better to be mentioned. As Sun Tzu, a Chinese military strategist who wrote the book "The Art of War", has claimed 2500 years ago: if you know your enemy (as well as yourself), you will not be imperilled even in a hundred battles [1].

Bacteria are almost everywhere. However, most of them cannot be seen by the naked eye because of their micro-scale volume. They are thus regarded as microorganisms (or microbes). This tiny size can be attributed to their structures: they exist as single cells (unicellular organisms) and are classified as prokaryotes [2]. Nevertheless, even for such small beings, there is a great amount of variations in terms of their microscopic morphology, such as Cocci (spherical), Bacilli (rod-shaped), and Spirochetes (spiral or helical), etc.

Moreover, there are also different but delicate structures inside (cytoplasmic structures) or outside (*e.g.* cell wall, surface polymers, and flagella) the cell membrane, ensuring many important functions as well as metabolism for bacterial survival. These intracellular and extracellular structures are fitting the best targets for antibacterial strategies.

But why don't we like these tiny living things? Although not all bacterial species are always harmful to human beings, and sometimes we even need them, there are indeed pathogenic bacteria that do keep risking not just individuals but also the development of human civilisation. The Black Death, which resulted in estimated death from 75 to 200 million in Eurasia in only four years, was due to a bacterium called *Yersinia pestis* [3]. In the recent years, *Escherichia coli* known as *E. coli*, have led to foodborne outbreaks in every corner of the globe, hitting the headlines [4-6]. Even an inconspicuous skin wound on a child's leg could be the perfect place where next infection occurs,

eventually and unfortunately leads to an amputation, should proper medical treatment be missing. It is therefore important to find out substances that can influence bacteria, so that these types of scenarios could be prevented, or at least be better controlled.

For instance, there are substances that can completely kill bacteria, resulting in the actual cell death. These are classified as bactericidal agent. On the other hand, there are others that could only control the reproduction of bacteria, which are classified as bacteriostatic agent. Since both these effects inhibit the growth of bacteria, they are defined as antibacterial effects, and the corresponding substances are thus called antibiotic [7].

There has been almost 90 years since the first ever antibiotic Penicillin was discovered in the UK [8]. From then on, a range of antibiotics has been discovered, extracted, synthesised, and tested, one after another [9]. Many of them have become indispensable in clinical usage, saving millions of patients, again and again. Unfortunately, we are not the only one who are strengthening our "weapons", our "enemy" bacteria also have the same 90 years to develop themselves.

Many species/strains have developed the ability to resist one or even multiple types of antibiotics, challenging our limited methods in infection prevention and treatment. For example, multiple-resistant *Staphylococcus aureus* (MRSA) received the nickname as "superbug", as it is able to resist those common broad spectrum antibiotics such as methicillin and oxacillin, causing panic in public and concerns in hospital environmental sanitation [10]. Meanwhile, repeated and improper use of antibiotics increase their exposure to the environment, accelerating the rapid rise of antibiotic resistance [11]. Besides, other advanced treatments such as external fixation or implantation also place greater demands on the presence of antibacterial effect [12].

These are the reasons why the current antibacterial means are never enough, and new weapons are always highly demanded. Only together with multiple methods can we get the upper hand in the war against pathogenic bacteria.

1.1.1. Antibacterial Surfaces and Applied Fields

Among many newly developed methods, antibacterial surfaces are attracting widespread research interest [13]. This is because a surface could be a critical and multifunctional hub for the transmission of pathogens. Moreover, a contaminated surface not only serves as a reservoir for bacteria, but also as a hotbed, allowing them to grow and further defend themselves against antibiotics. For instance, some bacteria can form a "biofilm", a community of bacteria, after they stick to surface [14]. These biofilms are composed as well as surrounded by extracellular polymeric substances (EPS), forming networks that gather bacteria and distribute nutrients. Most importantly,

this kind of network acts as a “great wall” against the detrimental factors presented in the surrounding environment, making the traditional disinfection methods less effective.

These phenomena call for better understanding of the interactions between bacteria and surfaces. Advances in this aspect is beneficial for further exploring surfaces that could be unfavourable to the bacteria survival, namely the antibacterial surfaces. Nowadays, some circumstances have been identified to be in an urgent need of surface disinfection methods, where antibacterial surfaces could thus help meeting the demands.

1.1.1.1. Hospital Environment

As one could already imagine, hospitals are the places where numerous types of bacteria could be found, that are brought mostly but not only by patients. Meanwhile, patients themselves are also more vulnerable than others. Both these conditions give birth to a disastrous scenario: healthcare-associated infections (HAIs) [15]. Contaminated surfaces, unfortunately have been regarded playing a role in the transmission of the bacteria that are able to survive on top for a long period [16]. Well scheduled cleaning and disinfection procedures such as hydrogen peroxide vapour, ozone, and steam are currently necessary [17].

Other approaches are also assisting to reduce HAIs, one of which is to replace the frequent touched surfaces with antibacterial surfaces, which are also called “self-sanitising surfaces” in these scenarios. To verify the antibacterial effect of these surfaces, bacteria isolated from healthcare facilities or hospital environments were applied. Many copper surfaces have been demonstrated to be actively against *Acinetobacter baumannii* [18-20], *Klebsiella pneumonia* [19, 20], *E. coli* [19], *Pseudomonas aeruginosa* [19, 20], *Enterococcus faecalis* [21], *Enterococcus faecium* [21], MRSA [20], *Candida albicans* [20] , *Mycobacterium tuberculosis* [20], etc.

Furthermore, there are also a number of experiments being conducted in clinics or hospitals. In those actual environments, various touched objects such as handles [22], bed rails [23, 24], chairs [25], tables [24, 26], pens [27], push plates, and even toilet seats [28] were newly equipped with different types of copper surfaces. These experiments usually lasted for weeks or months and many positive results have been obtained.

To sum up, applying antibacterial surfaces are now universally accepted as an effective method to mitigate the bacterial burden in clinical environments. However, they are not designed to totally replace other existing disinfection methods. Applying multiple antibacterial approaches is still the key of battling against these severe bacteria induced scenarios. Indeed, the corresponding disinfection methods may need to be altered, so that the antibacterial effects obtained from these

advanced surfaces can be preserved and prolonged. In the case of copper surfaces, it has been preliminarily proven that they can be easily combined with the commercially available disinfectants [29].

1.1.1.2. In vivo Environment

Implant therapy is common in the present medical treatment. Many have been applied such as dental implants, orthopaedic implants, cochlear implants, and so on [30]. Principally, implants are designed to partially/fully fulfil the functions of missing parts of human bodies. Nevertheless, it is equally necessary to assure that the implants are accepted by the target tissues and promote their regeneration. Therefore it is crucial to effectively avoid infections around implants, namely implant-associated infections (IAIs) [31]. Especially for those non-degradable implants, infections could induce tissue damage or an implantation failure in a long term [32].

Bacterial adhesion and biofilm formation are often responsible for IAIs [33]. Consequently, the surface of implant has been developed to incorporate with antibacterial activity [34]. Different approaches have been tested depending on the specific *in vivo* environment where the implant is designed for [35]. For example, physical vapour deposition (PVD) could be applied to fabricate copper containing antibacterial coating on commercial titanium alloys [36], causing a biofilm inhibition without influencing the *in vitro* viability of normal human osteoblast. Besides, pin tract made of copper containing titanium bulk alloys has been analysed *in vivo*, where suppression of infection and outstanding osteoid-formation are simultaneously obtained [37]. On the other hand, for those where antibacterial substances are not included, micro-topography engineering which could be achieved by laser patterning, has also been demonstrated as an effective means to control bacterial adhesion as well as biofilm formation in an *in vivo* essay [38].

Although many ongoing studies are improving these strategies, other functions are gradually aimed to be incorporated. Such as low cytotoxicity, better biocompatibility [39] or disrupting different stages of the biofilm formation [40] are obtaining much attention.

1.1.1.3. Food Industries and Water Distribution Systems

Both of these aspects emphasise the present challenges of foodborne/waterborne bacteria. As processed foods have been provided increasingly in the market, food safety certainly attracts much attention from consumers. Although well-recognised protocols for producing and processing have been widely applied in food industry, they do not stop researchers from developing antibacterial

food contact surfaces.

On food contact surfaces where nutrients are provided, bacterial adhesion and reproduction could proceed even easier than other exposed surfaces [41]. Therefore, there is no doubt that endowing these surfaces with antibacterial activity will enable safer final products. Nevertheless, the uptake of the antibacterial substances by processed food also needs to be considered. Investigations are therefore in need not only to evaluate the antibacterial effects but also the acquisition of antibacterial substance by food. Copper is in a matter of fact an excellent candidate satisfying these two requirements. Research has shown its antibacterial effect against common foodborne bacteria such as *Salmonella enterica* and *Campylobacter jejuni*, while the amount of copper absorbed by chicken or pork remains low enough [42].

Situation becomes slightly divergent, when it comes to filters, pipes, and reservoirs in drinking water distribution systems and facilities, where the current threat mainly comes from biofilm [43]. Most notably, the existence of biofilm not just impairs the water quality, it could also result in localised corrosion, accounting for damage of drinking water pipe networks, and further affecting water quality with by-products of corrosion [44].

One general interest is related to the pipe materials, since they constitute the surfaces where bacteria could grow. For example, the copper-bearing stainless steel is a candidate for drinking water systems. It has been demonstrated to be helpful in killing planktonic bacteria and thereby inhibiting biofilm formation [45]. In addition, copper can also be installed as electrodes in the entry of pipe system, so that copper ions can be released (consumed) controllably under electric current and thus contribute to water disinfection [46].

1.1.1.4. Microbiologically Influenced Corrosion (MIC) in Shipping Industry

MIC is a type of corrosion which is introduced by microbes. Similar to the aforementioned situations in water distribution systems, attached bacteria firstly form biofilms. Instead of contaminating the aqueous surrounding, these biofilms could cause localised corrosion of the attached surface. In the case of shipping industry, it results in the reduction of structural lifetime. On the other hand, accumulation of bacteria could also evolve to biofouling to some extent, reducing the mobility of the vessel and increasing the energy consumption.

As a result, antibacterial or antifouling surface has been investigated to target these issues in such a specific environment. Take the copper-bearing stainless steel as an example for one more time, its antibacterial property has already be proven, by suppressing planktonic growth and biofilm caused by *Pseudomonas aeruginosa* in artificial seawater condition [47]. What's more, reduction

of the maximum MIC, pit depth, and the weight loss have been reported after copper was added [48], indicating its practical potentials in relevant applications.

1.1.2. Antibacterial Mechanisms

As described above, in each scenario, individual requirements need to be fulfilled. The good news is, different types of surface modification means have been consistently put forward and developed. Some methods that have been extensively investigated are briefly summarised below in two groups (**Figure 1.1**), depending on the window of opportunity. In other words, it is about which time phase these methods could take effect.

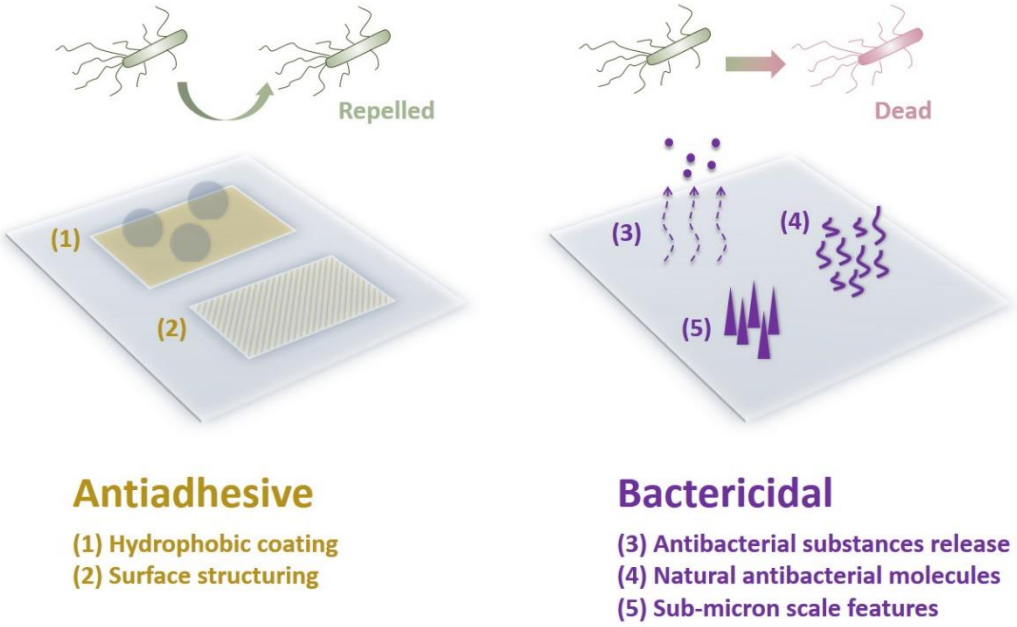

Figure 1.1 Schematic summary of antibacterial mechanisms covered in the main text.

1.1.2.1. Antiadhesive Surfaces

The first one is to prohibit bacterial adhesion in the first place. If it works, there will be no need for antibiotics substances in the following events. Especially for biofilm formation, prevention of bacterial adhesion is still the most effective strategy, since bacteria become much more resistant to environmental stress once biofilm is formed.

Some fundamental surface properties such as hydrophobicity could be applied to explore newly antiadhesive surfaces. Many studies have attempted to fabricate extraordinary hydrophobic surfaces

by coating techniques. For example, a Teflon-like film fabricated by plasma technique on micro/nano-textured PMMA was examined [49], showing low coverage of bacteria compared to control group. Besides, in spite of applying a totally different type of coating, modification of wettability could also be implemented simply by doping [50]. On the other hand, it has also been reported that the short-ranged hydrophobic interaction between surface and proteins on bacterial cell wall behave as the predominant force [51], concluding that higher force is needed to detach bacterial cells from hydrophobic surface. These studies seem to be contradictory, but this very complexity implies that it is worth considering every factor in each specific scenario: the way how tests are designed and performed, the interplay of bacteria, surface and the tested aqueous environment and so on.

Surface roughness or topography also plays an important part, as it affects how the cells could contact materials. It has been demonstrated that a stainless steel surface exhibiting a roughness in an appropriate range could reduce at least 10-fold of adhered bacteria [52]. This could be further related to the way how bacteria attach to relatively nano-scale rough surfaces: they were found to attach as individual single cell instead of a cluster. On the other hand, the size, type, and periodicity of nano-scale features on the surface also govern the bacterial adhesion [53], where the fundamental causes are still under discussion.

Another popular approach is based on functionalised molecules layers, owing the potential to repel bacteria. In one study, SiO_2 substrate was functionalised by immobilised polysaccharide molecules [54], in which an excellent repelling effect against *Staphylococcus aureus* (*S. aureus*) is shown. In another work, a grafted surface with long-chain zwitterionic poly(sulfobetaine methacrylate) has been proved to reduce bacterial accumulation both in short-term and long-term essays [55]. In general, it is their resistance to protein adsorption that eventually weakens the bacterial adhesion.

1.1.2.2. Bactericidal Surfaces

Once bacterial adhesion is unpreventable, another defence mechanism has to take over. These surfaces are called bactericidal surfaces, since they behave as an active antibiotic, inactivating further growth of attached bacteria or directly disrupting the bacterial cells. In the following sections of this thesis, the term “antibacterial” usually refers to “bactericidal” instead of “antiadhesive”.

To obtain antibacterial effect, one of the sufficient ways is to decorate the surfaces with well-known metallic antibacterial substances, such as silver and copper. These candidates are found to have strong antibacterial effect on a broad range of bacteria, mainly thanks to the toxicity presented

by their ionic form [56]. Certainly, these metals or their alloys can already be utilised as bulk materials [57]. Copper containing structural materials such as different types of copper-bearing stainless steel [47, 58, 59], are offering a promising solution. Furthermore, advanced coating techniques provide various possibilities to prepare antibacterial surfaces on the existing surfaces. Objects such as pure metals [60, 61], metal alloys [62, 63], composites [64, 65], oxides [36, 66], nano-structures [67, 68], doped layers [69, 70], etc. have been produced and tested to a great extent.

Antibacterial peptides [71] and chitosan [72] represent another group of effective antibacterial substances: natural molecules. Immobilisation of these molecules onto surfaces offer a practical way to lower the bacterial burden.

Recently, the micro-topography of surfaces is also demonstrated to have potential in interfering bacterial proliferation by physical damage/puncture. Black silicon and graphene-based materials are excellent examples in this sort. Black silicon refers to the silicon surface equipped with high aspect ratio sub-micron scale needles, which are usually modified by reactive-ion etching. It is inspired by a similar micro-topography that can be also found on dragonfly [73] or cicada [74]. During bacterial attachment or reproduction, bactericidal effect was therefore shown by the severe mechanical force induced by these sharp structures. Similarly, graphene sheet with blade-like edge can also cause pores at the bacterial cell wall and further damage [75].

However, a question should be asked when the primary layer of bacteria is disinfected, given that all these promising antibacterial strategies are based on direct contact with the corresponding surfaces. That is to say, how to maintain the potent antibacterial effect after the surface is fully covered with dead bacteria? This calls for a much complicated design of surface structure which could ensure a long-term antibacterial effect, through smartly releasing the attached bacteria [76].

1.1.3. Evaluations of Surface Antibacterial Effect

Antibacterial surfaces cannot be properly studied and compared, unless a certain method is selected and employed so as to evaluate the antibacterial effect. Thus, a number of antibacterial efficiency tests has been developed (**Figure 1.2**), revealing different aspects of different kinds of antibacterial surface depending upon the potential application conditions.

1.1.3.1. Droplet Method (Wet Plating Method)

This could be one of the most commonly used and reproducible evaluation methods [77-79]. In this method, it is also convenient to simulate different aqueous conditions (environmental factors). More

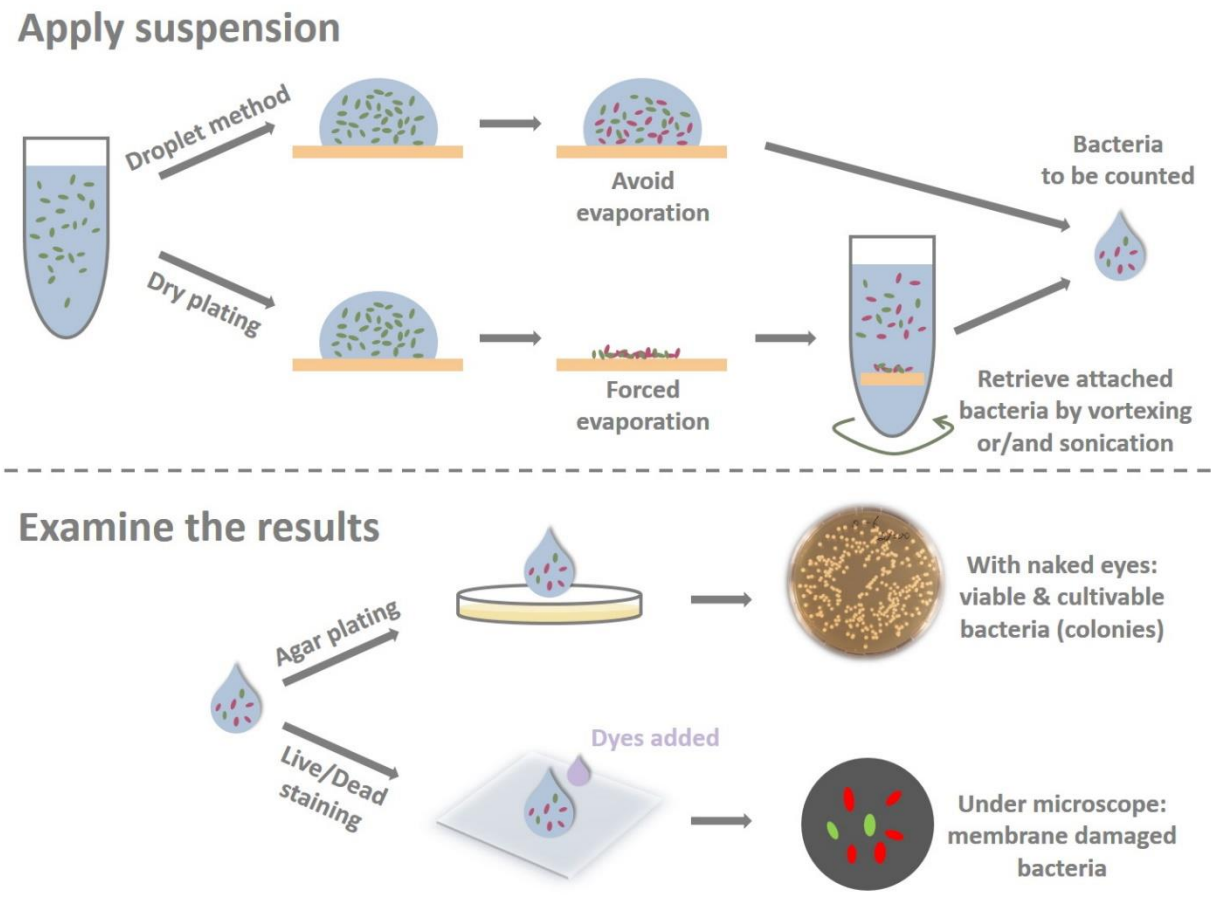

Figure 1.2 Schematic and simplified procedures of evaluation methods in laboratory for antibacterial surfaces.

precisely, it is also a method showing the number of cultivable bacteria after being inactivated by the surfaces investigated.

Briefly speaking, a certain strain of bacteria is selected and grown in nutrient broth, then harvested and suspended in buffer solution (hereinafter buffer). Afterwards, a certain amount of this suspension is applied as a droplet on the surface to be tested. Coupons are placed in a moist room where evaporation could be avoided to the most extent. After the set intervals are reached, the droplets will be repeatedly pipetted and partially withdrawn. With serial dilutions, bacterial concentration should be suitable (low enough) for plating on nutrient agar plates. Colonies will appear after proper incubation, representing the number/concentration of cultivable bacteria in the original droplet.

However, variations are sometimes introduced in the procedure. For example, the presence of carbon contamination could be simulated, simply by applying bacterial nutrient suspension [80, 81], instead of buffer suspension. Presented in another research, antibiotics were added into the buffer in order to test the joint antibacterial effect [82]. Other than keeping the inoculum as droplet,

approaches can be taken to force it to spread over the coupon (*e.g.* by covering a sterile plastic film [83]), so that the contact area is better controlled.

There are, nevertheless, two main issues need to be considered, since they tend to let this method count fewer actual survival. First, as mentioned previously, the final results could only reflect the quantity of bacteria that are cultivable. For those still viable but with supressed reproduction ability, they might not be able to grow as a colony and thus will not be counted [84]. Another issue is, the adhered bacteria could be missed. According to the time interval as well as the behaviours of bacteria, more and more bacterial cells could turn from planktonic mode to sessile mode. Repeated pipetting may not provide enough force to detach those bacteria. Alternatively, to achieve effective detachment of these sessile bacteria, ultrasonic bath and vortexing may be included if necessary [85].

1.1.3.2. Dry Plating Method

This is another popular method to simulate a frequent touched surface [21, 62, 80, 86]. “Dry” indicates that bacteria are not maintained in an aqueous condition during the inactivation period.

Similar to the droplet method, bacterial suspension is still required in the first place. Nevertheless, only a relatively small amount of droplet will be applied on the coupon. In the next step, this droplet could be dried naturally or manually by sterile air. As a consequence, only bacteria (and precipitates, if there is any) are left on the tested surface. Bacteria will be retrieved after a certain period of time, usually by sonication or vortexing in buffer. More effective approaches may be needed, since bacteria are forced to contact the surface in the first few minutes, which could result in a stronger adhesion compared to the droplet method. If the same agar plating evaluation (as described in the droplet method) is used, then only cultivable cells will be finally detected.

As mentioned above, this dry method could reflect the antibacterial efficacy for those touched surfaces, because in most of cases, these surfaces are equipped in daily atmospheric environment. Besides, this test could also be performed in a moist chamber where the humidity can be regulated on purpose [87]. This could be one of the advantages for researchers, as on some copper surfaces, it has been demonstrated that the relative humidity does influence the antibacterial activity [88]. Furthermore, it is universally observed that the bacterial killing rate obtained from this method is much higher than that from the droplet method [87, 89]. This suggests additional antibacterial mechanisms may take effect when bacteria come in close contact with the surfaces.

1.1.3.3. Live/Dead Staining

To overcome the drawback of the abovementioned methods regarding the unsatisfactory detection of viable but nonculturable bacteria, staining method is applied in some cases [90-92], supplementing the physiological state of the bacterial cells.

This method only focuses on the counting process: instead of diluting and plating the withdrawn bacteria suspension, fluorescent dyes are added to the withdrawn suspension. This stained bacterial suspension will be transferred to fluorescence microscopy and observed with appropriate filters.

One of the commercial pairs of dyes are SYTO9 and propidium iodide. Both of them are nucleic acid stains, nevertheless, have dissimilar penetrability through the cell membrane. SYTO9, which is a green-fluorescent stain, labels all live or dead bacteria. Propidium iodide, on the other hand, can only reach the nucleic acid inside bacteria only after the membrane is damaged. Afterwards, these bacteria will be stained fluorescent red. Therefore, if a bacterium simply turns nonculturable with intact membrane structure, it could still be correctly recognised as alive (green). Besides, as an improved method, it is also feasible to add staining suspension directly to the sample on the tested surface [92]. This approach includes detection of those adhered bacteria, without taking any efforts to detach them from the tested surfaces.

Another advantage of staining is that it could be easily combined with other approaches so as to extract more detailed information of the bacterial cell. For instance, the molecular cellular target sites of copper ions were once unclear. Well-designed mutagenicity assay and staining experiments together show that, increase of DNA breakage [89, 90] or mutation events [93] cannot be observed, unless the membrane damage occurred. Although these findings only reflect the specific type of bacterial strain, the method itself ensures the possibility of further exploring the copper attacking events.

On the other side, although such a method offers more actual and real-time information of the state of bacteria, the main challenge is still to quantitatively count and compare results obtained from different surfaces or conditions. For instance, a recent attempt has targeted to quantify the biomass represented by in-situ staining on antibacterial coating, where the trends were shown with a noticeable deviation [94]. Furthermore, if antibacterial substances target other parts of bacteria instead of cell membrane, staining method will not be able to identify actual cell death [92].

1.1.3.4. In vivo Tests

All those three methods aforementioned are *in vitro*, but lab environment can be extremely different

to the human body. To examine the actual antibacterial activity of implants, *in vivo* experiments seem to be indispensable in the final step of product development [35, 37, 40]. During *in vivo* tests, antibacterial effect of the prototype is supposed to be characterised by the final infection situations of the tissue, biofilm or bacterial adhesion located on the implants, and the release rate of antibacterial substances. Other possible negative aspects of the tested surface could also be studied, such as the potential weakening of cell adhesion and cytotoxicity.

1.1.3.5. Clinical Tests

So far, all the abovementioned *in vitro* methods are based on a certain simulated set-up. However, these set-ups may not reflect the actual environment. Therefore other methods are meant to be involved. Consider the applications aiming at the hospital environment as an example, clinical tests provide a direct way to check the effectiveness of antibacterial touched surfaces [27, 28, 95].

Although there is not yet a global standard how these tests should be performed, most of the current conducted tests were based on the following steps. Firstly, a certain number of wards or rooms should be selected for antibacterial surfaces installation. A similar and comparable of section in the same hospital should work as a control group. Secondly, detailed cleaning procedures as well as infection records of patients should be documented. Thirdly, a proper timetable is needed for collecting bacteria from the surfaces, in both tested and control groups. Fourthly, results will be compared considering the bacterial concentration collected as well as the type of bacteria isolated.

This kind of tests provide considerably sufficient and practical information of those to be used as potential touched surfaces. However, it takes an extremely long time and costs financial and human resources, making it impossible for every newly developed antibacterial surface. In the same manner, even some of the tested surfaces have shown positive results, the cost of applying into actual scenarios still needs to be considered [96].

1.1.3.6. Disk Diffusion Method

Also named as inhibition zone test, it is a quick but only qualitative measurement to compare across antibacterial substances based on their diffusion kinetics.

In short, nutrient agar plates are firstly spread with a number of bacteria on top. Before incubation, tested coupons (usually cut into same round shape) are separately placed upside down on the agar plates, so that the surfaces are in close contact with the bacteria. After incubation, for those coupons showing antibacterial effects, a circular zone without bacterial growth should appear

around the coupons. This zone is thus called inhibition zone. It is generally believed that the bigger the zone (diameter) is, the better antibacterial efficacy the tested surface has.

For those surfaces where release of antibacterial substances [97-99] is a key factor in suppressing bacterial growth, this disk diffusion method is rather practical and popular. The weakness of this method is also evident: as how it is called, the inhibition effect favours those antibacterial substances with higher diffusion efficiency. That is to say, it may hide the potential antibacterial effect of those surfaces where diffusible substances are not formed or direct contact is necessary [100].

1.2. Copper

Copper (Cu) with atomic number 29, which has been utilised in human civilisations for thousands of years, is still playing an indispensable role in modern industries [101]. For instance, owing to its high electrical conductivity as well as ductility, copper is always the best candidate for cables, connectors, and layers in electronic components. Furthermore, as an excellent thermal conductor, it is the most frequently used materials to fabricate heat sinks. The relatively great amount of known reserves around the world and its low price make these applications affordable.

In addition to serving as pure metal, copper alloys share some extensive applications in the modern world [102]. Bronze, a series of copper alloys mainly containing tin (Sn), has lower melting point for metallurgical processing, higher stiffness and corrosion resistance. Therefore it has been widely used in sculptures, bearings, and mechanical parts in ships. Brass, where zinc (Zn) is the main alloying element, has outstanding wear resistance and thus been applied in many parts in precise instruments. Alloying also helps to adjust the colour of the surfaces, adding its potential in decoration market.

On the other hand, copper and its alloys have become vastly popular in architectures, also thanks to its electrochemical stability: they do not easily react with water. However, oxidation could take place, covering copper surfaces with two possible native oxide layers: cuprous oxide (Cu_2O) and cupric oxide (CuO) [103]. These oxides usually turn the appearance of copper surface darker. Besides, together with oxygen (O_2), carbon dioxide (CO_2), and water (H_2O), intermediate products such as copper hydroxide ($Cu(OH)_2$) and copper carbonate hydroxide ($Cu_2(OH)_2CO_3$) could form, turning the surface into green colours.

For the biological process for both human and plants, copper is one of the essential elements [104]. On the other side, excess intake of copper could produce toxicity resulting in liver damage, but fortunately, total copper intake from daily food consumption is not supposed to easily exceed

the limit [105].

1.2.1. Copper as Antibacterial Candidate

For a long time, known for its purifying effect [106] just like silver, copper has been chosen for a food carriers and containers. It is the toxicity of copper towards cells that inspires exploration of its antibacterial effect. In the above sections, it can also be seen that similar concepts have been continuously developed into many examples to fight against bacteria in the modern society. Studies on copper-based materials can range from different forms of copper to divergent antibacterial mechanisms, which are briefly reviewed in the following sections, respectively.

1.2.1.1. Copper and Copper Alloys

Pure copper and its alloys are one of the most common forms to exploit the antibacterial effect of copper, which is in general achieved through two aspects:

Ionic copper. Copper has two ionic forms, cuprous ions (Cu^{+}) and cupric ions (Cu^{2+}). These two species can be obtained by corrosion of copper containing surfaces and thereby released into the environment. Bacteria, regardless of whether Gram-positive or Gram-negative, usually develop multiple ways reach copper homeostasis, such as enzymes that pump copper across the cytoplasmic membrane, or proteins that bind excess cytoplasmic copper [107].

That being said, by separately applying chelators of each type of ion, both species have been confirmed to be responsible for, to a certain degree, the antibacterial effect observed on copper surfaces [108]. On the other hand, another research that generated Cu^{+} by disproportionation and tested in a growth medium, recorded a stronger efficiency of Cu^{+}, while metallic copper did not even behave as an antibacterial candidate [109]. No matter how different these results are, it is still clear that discrepancy could be obtained in antibacterial tests from the same tested surface, should the applied medium contains substances that could bind any type of copper ions [80].

Several destructive effects introduced by copper ions have already been confirmed. Damage of bacterial cell membrane is one of those frequently observed [89, 90, 93]. As mentioned previously, this could be easily characterised by staining method, where bacteria with membrane disrupted will be stained because they become permeable to the specific dye. In addition, since the impaired cell integrity also results in leakage of intercellular contents, increase of these contents detected in buffer could be used as a proof, too.

Another route for copper ions to interfere bacterial cells is through genotoxic effect, namely

the damage of deoxyribonucleic acid (DNA). However, many studies have shown mutation and DNA damage are not observable when the leakage of membrane occurs, indicating that DNA might not the primary target [93, 110, 111]. But a study has indicated that in MRSA, DNA was degraded and bacteria were found inactivated even without membrane damage [92]. These facts together may suggest copper ions could be genotoxic, but it can only be observed when the membrane is not vulnerable.

The abovementioned phenomena are closely linked with the generation of reactive oxygen species (ROS) at the presence of copper ions [108]. Production of ROS such as hydroxyl radical (•OH) completed via the Fenton-like reaction intercellularly: hydrogen peroxide (H_2O_2) is catalised under Cu^+ (which consequently becomes Cu^{2+}). The unpaired electron of •OH has been proven to react with the unsaturated fatty acids on cell membrane, leading to its structural damage [90].

Similarly, interactions between copper ions and other substances in the environment are also found to be essential. For instance, presence of chloride ions (Cl^-) is believed to considerably accelerate the antibacterial process thanks to the generation and participation of reactive chlorine species (RCS), where Cu^+ again acts like catalyst [112].

Apart from the above multiple but indirect antibacterial effects via the formation of ROS, a direct toxicity is also being studied in the recent years: Cu^+ may damage enzymes by replacing iron in their iron-sulfur clusters [107]. This, together with the route of ROS formation, may provide hints in clarifying the difference in toxicity between Cu^+ and Cu^{2+}.

Metallic copper. Dry metallic copper surfaces are commonly seen in practical scenarios. Intriguingly, many studies have shown faster killing rates against bacteria in dry conditions, compared to the results obtained by droplet (wet/moist) methods [80, 87, 89, 113].

A major difference between these two methods is whether a close contact between bacteria and the tested surfaces is rapidly assured. In other words, for most of the bacteria presenting on dry surfaces, they could be influenced immediately after the experiment starts and do not have to wait for the copper ion diffusion (as in droplet methods). A longer actual/effective copper treated period is therefore achieved. Besides, the copper homeostasis is also considered less efficient on dry copper surfaces, owing to the lack of extracellular fluid [87].

Nevertheless, another viewpoint has been proposed based on the survival of bacteria that resistant to dry copper surface in moist (wet) testing [86]. Unexpectedly, the resistance developed to counter dry copper surface does not take any effects in the moist condition: these bacteria survived as poor as the negative control group (those without resistance to dry copper surface). That is to say, another individual antibacterial mechanism may exist on dry metallic coppers, which does not rely on the release of copper ions.

1.2.1.2. Copper Oxides

Copper oxides, without a doubt, share all the respects mentioned above in ionic copper, because of their relatively high solubility in aqueous conditions [114]. But comparison between metallic and oxides surfaces do not reach a globally accepted conclusion yet, with regard to their antibacterial efficiency [115, 116]. This could be ascribed to the fact that oxides have exclusive ways to enhance the antibacterial effect.

Photocatalytic effect. Consider CuO as an example, as a p-type semiconductor, electron excitation could occur under light irradiation. Electrons are thereby transferred from valence band to conduction band, leaving holes on the conduction band. These electrons could then combine with oxygen and form superoxide radicals ($O_2^{\bullet}$), while •OH can be produced from holes and water [117]. Both of them belong to ROS, as described above, contributing to the antibacterial efficiency [118].

Nano-scale effect. So far, decline in the antibacterial effects of copper or its oxides is not expected even though they are reaching nano-scale. On the contrary, their nano-particles could exhibit antibacterial effect not just by dissolution [119], but also by direct contact (and therefore can be influenced by aggregation) [120], likely resulting in non-oxidative stress [121].

1.2.2. Potential Applications

Based on these multifunctional antibacterial effects introduced by copper related substances, many attempts have been made to incorporate them into promising applications. Potential applications of antibacterial surfaces have been previously reviewed in detail, therefore focus will be shifted to the means of fabrication. Other research attentions are also briefly summarised.

1.2.2.1. Antibacterial Surfaces 1: Bulk Surfaces

Bulk surface applications usually require the whole workpiece to be made of the antibacterial copper or its commercial alloys. This kind of design fits those lightweight and frequently touched surface really well, no matter in the clinical environments, food industries, school, or public spaces [13]. Aside from applying copper (alloys), it is also practicable to obtain copper containing surfaces by doping, such as 1% copper doped titanium [37] and 3.9% copper doped stainless steel [122].

One of the advantages of the bulk surface attributes to its low requirement in wear resistance. Even the surface undergoes inevitable erosion, the freshly abraded and exposed surface with the

identical chemical composition still retain the same excellent antibacterial effect. On the other hand, this process helps to "release" the dead but adhered bacteria, avoiding full coverage of bacteria on the surface, which could be unfavourable for long-term antibacterial efficacy.

A number of research has been conducted directly on copper (alloys). In most of these cases, either droplet or dry evaluations were chosen. Regarding the tested strains, *S. aureus* and *E. coli* are a popular pair since they represent well-studied Gram-positive and Gram-negative bacteria, respectively. Besides, other common pathogenic bacteria or strains such as MRSA [92], *Enterococcus faecalis* [21], *E. coli* O157 [123], etc. have also been demonstrated to be vulnerable on copper surfaces such as C11000 (99.9% copper), C28000 (60% copper, 40% zinc), C51000 (95% copper, 5% Sn), etc. Nevertheless, a final wide-spectrum test should be done before serving these surfaces to the market.

However, compared to pure copper, it is common to find coupons made of copper alloys less effective [18, 19, 80]. This has been often linked with their lower copper contents, although the antibacterial efficiency or copper release level is not always proportional to the atomic/weight percentage of copper [124]. This phenomenon will be elaborated in the following corrosion section. Nevertheless, there are still hundreds of copper alloys that have been approved as antibacterial surfaces by Environmental Protection Agency (EPA) in the US, since they show a minimum 99.9% killing rate in 2 h against certain types of bacteria [125].

Owing to the fair stiffness and machinability of copper and some of its alloys, a few clinical tests have been already carried out. There are hospitals in the UK [28], Germany [95], South Africa [26], and the US [24], where copper surfaces have been installed in selected room and facilities. These studies have shown the considerable reduction of bacterial burden in the copper equipped environments: the number of microorganisms collected from the copper containing items was much lower; the rate of HAIs became significantly declined, and the like.

Nevertheless, some issues need to be discussed before fully applying copper surfaces, irrespective of where they are installed. As copper surfaces tend to be oxidised in atmosphere, a major concern is the compatibility of the existing cleaning method [95]. Even though copper oxides are demonstrated to be antibacterial, they are not necessarily desirable in these conditions. Therefore, a deeper knowledge is urgently needed in terms of copper surfaces aging, so that adequate innovation can be embedded in the present standard hygiene procedures.

1.2.2.2. Antibacterial Surfaces 2: Coatings & Thin Films

Advanced deposition techniques provide alternatives to obtain antibacterial copper surfaces,

without sacrificing other properties of the bulk materials/substrates, and potentially reducing the manufacturing cost. Moreover, deposition techniques can also be cooperated with substrates already with specific micro/nano-structures [126], strengthening the antibacterial effects.

For instance, relatively thick copper based coatings have been achieved by techniques such as laser cladding [78], electroplating [127], and spraying [128]. On one hand, not only the cost of the corresponding methods needs to be considered, but also whether the substrate is capable to withstand the coating process (*e.g.* high temperature or immersion in a certain solution). On the other hand, microstructure, micro-topography, and generation of side products (*e.g.* oxides) heavily depend on the coating approach and relevant parameters, which further determine the release of copper ions and thus the antibacterial efficacy. For example, electroplated copper owns smaller surface structures, which is considered to boost copper ion release; compared other spraying methods tested, cold spray introduces higher dislocation density and less oxidation, therefore shows a more outstanding antibacterial effect.

Thin films, particularly with nano-scale thickness, on the other hand, are more commonly to be prepared by PVD (such as thermo-ionic vacuum arc, sputtering, and so on.) [70, 129, 130] or chemical vapour deposition (CVD) [115, 131]. With these techniques, not only the precise compositions as alloys can be achieved [62, 132], but copper oxides [115, 130] or composites (*e.g.* Cu:C composite) [133] too. The antibacterial efficiency of thin films depends on similar properties as coating, which can be finely modified by the parameters of fabrication or post treatment.

To conclude, coatings or thin films are universal and economic ways to obtain antibacterial properties on targeted surfaces. However, their adhesion should be examined in the intended applied environment. So far, seldom research has attempted to evaluate from this respect.

In addition, there are also concerns regarding the durability of these surfaces, such as: how long will this layer deplete? Does it meet the designed lifetime? To examine its long-term performance, preliminary experiments have been designed to compare the antibacterial rate in some successive cycles [130, 131].

1.2.2.3. Micro/nano-scale and Embedding Materials

Especially for copper oxides, the antibacterial properties shown by their micro/nano-scale forms have been studied extensively, such as micro-particles [134], micro-crystals [135], nano-particles [120], nano-sheets [136], nano-wires [137], etc. Meanwhile, a huge range of chemical-based synthesis methods has been applied to produce copper containing micro/nano-scale materials, whereas green and eco-friendly synthesis methods have also been developed [138-140].

These micro/nano-scale copper containing materials are designed as candidates mainly for aqueous applications. Thus their antibacterial efficacy is frequently characterised by their minimum inhibitory concentration, rather than the aforementioned tests designed for antibacterial surfaces.

Likewise, antibacterial property of these micro/nano-scale materials are found to be closely associated with their sizes and morphologies. For instance, copper particles with smaller size reach a maximum antibacterial activity with a lower concentration, however, going through an evident decrease after 24 h [141]. The antibacterial efficacy of Cu_2O microcrystals were also found to be shape/morphology-dependent, attributing to the intrinsic antibacterial activity [142], or adsorption and desorption abilities towards bacteria [143] presented in different exposed crystal facets.

Another approach to apply these micro/nano-scale materials is to embed them into the existent surfaces, such as textiles and fabrics [144-146]. These loaded surfaces thereby obtain antibacterial property, which is accomplished by the release of the substances. In view of their flexibility, these surfaces have potential hygiene applications such as wound dressings and antibacterial food packaging [147]. Apart from being bonded to the flexible bulk substrates, these materials can also be immobilised on thin films [118, 148], further widening the antibacterial applications.

1.3. Corrosion

Metals in the nature are seldom found in a pure state. This is because pure element, in the majority of the cases, is not the most thermodynamically stable state. Most of them tend to react with the surrounding substances in atmosphere, waters, and soils. Compounds are consequently formed and remain in the natural environment. However, these compounds may not be the optimal forms to be directly employed in industries. Metallurgical operations have been thus developed, by which pure metals can be finally obtained [149]. But for the same reason, the state of these final products is not “final”. Depending on the storage/applied environments, they could again be driven to (partially) transform into compounds.

Corrosion is one of the significant routes realising this transformation. Corrosion describes a physicochemical process that happens on the surface with the environment [150]. On anodic sites, oxidation reaction transforms a metal (M) to its ionic form (M^{n+}, cations), which may also be further converted into metal hydrated ions, hydroxides, or oxides. Meanwhile, reduction reaction must accompany on the cathodic sites, consuming the electrons that leave the anodic sites. As it is shown, this process introduces variation in the oxidation state, therefore it is classified as an oxidation-reduction (redox) reaction. Since the change from pure element to its ionic/oxidised form usually causes mass loss of the original material, corrosion is generally regarded as a harmful process that

is meant to be prevented.

Just as widespread as bacteria, corrosion also happens everywhere. It has drawn much (or enough?) attention in a number of scenarios. For example, aqueous conditions in marine environment [151], drinking water distribution systems [152], oil and gas production industries [153], are all facing some serious corrosion problems. On the other side, studies in corrosion of historical artefacts in atmospheric conditions are also meaningful in protecting cultural heritage [154]. Furthermore, specific corrosion phenomena have also begun to be considered in other emerging areas, from automotive [155] and aerospace [156] industries to biomedical devices and biomaterials [157].

However, just like every coin has two sides, better comprehension of corrosion may also turn it into a highly practical tool. Taking materials science research as an example, etching has become one of the indispensable procedures in metallurgical research, aiming to selectively display grains and differentiate phases of the coupons investigated [158].

Back to the topic of this thesis, deterioration induced by corrosion serves positive functions too. After all, dissolution of the material from its original surface, in fact, provides an effective way for releasing substances from the surface. Especially on copper, it equally means the release of antibacterial copper ions. Hence the following sections will place emphasis on relevant aspects of copper corrosion.

1.3.1. Copper Aqueous Corrosion

Copper is one of the very few noble metals, having an excellent anti-corrosion tendency as silver and gold. For example, when one looks up in the reactivity series of metals, copper is regarded as one of the least reactive. This can be better understood from the aspect of electrochemistry/thermodynamic theory [159], as standard electrode potential (usually relative to the standard hydrogen electrode, SHE) aids to judge the direction of corresponding redox reaction. As the copper reduction reaction (Cu^{2+}/Cu) has a positive value (+ 0.342 V), it can thus be concluded that copper will not react with non-oxidising acid or generate hydrogen (by proton reduction or water reduction).

However, this is not the whole story of copper aqueous corrosion process, because the role of dissolved oxygen has not yet been considered. In oxygen free water, elaborate and long-term experiment has been designed so as to confirm corrosion only occurs to limited extent in accordance with the established thermodynamic data [160]. However, in near-neutral pH conditions where dissolved oxygen is not avoided, corrosion of copper can be induced as:

Reduction reaction (cathode):

$$O_2(g) + 2H_2O(l) + 4e^- \rightarrow 4OH^-(aq)$$

Oxidation reaction (anode):

$$Cu(s) \rightarrow Cu^{2+}(aq) + 2e^-$$

As can be seen, metallic copper is therefore transformed to its ionic form, representing the most important step for releasing copper ions from the metallic copper surface. Meanwhile, many other copper containing species may directly form, such as Cu_2O, CuO, $Cu(OH)_2$, and the like, consuming the copper ions presented in the aqueous environment.

1.3.2. Localised Corrosion

Electrochemistry tells how the corrosion reactions and phase transformations could happen, or even how to evaluate the corrosion rate, nevertheless, may have difficulties in describing the localised tendency at the micro/nano-scale [161]. Because most of the time, corrosion does not occur uniformly, even on a single-phase metallic surface. As the nature of electrochemical redox process, it is clear that some areas of the surface play the role of cathode. Insoluble reduction products could be found in these cathodic sites. Meanwhile, other parts of the surface serve as anodes. Anodes are the victim of corrosion, where dissolved metal ions are generated and released.

It is important to identify and further classify the corresponding localised corrosion phenomena. Since the more knowledge we have about various corrosion forms, the better the chance to realise antibacterial ion release. A few common localised corrosion behaviours closely related to this work (**Figure 1.3**) are addressed in brief as below.

1.3.2.1. Selective Corrosion

The term “selective corrosion” usually refers to the situation of some alloys, for the dissimilar corrosion resistance presented on one surface. According to the galvanic series, the element or phase that is less noble, acts as an anode and will be selectively corroded. For this reason, it is sometimes called as “de-alloying”.

Copper has been developed to a range of alloys sharing wide commercial interest. As most of the applied alloying elements are less noble compared to copper, it is not difficult to imagine the propensity of selective corrosion [162], not to mention the complex alloy phases that could formed. Among different kinds of copper alloys, brass is particularly vulnerable to this type of damage. A famous phenomenon is called dezincification, that is, zinc could be selectively removed, leaving

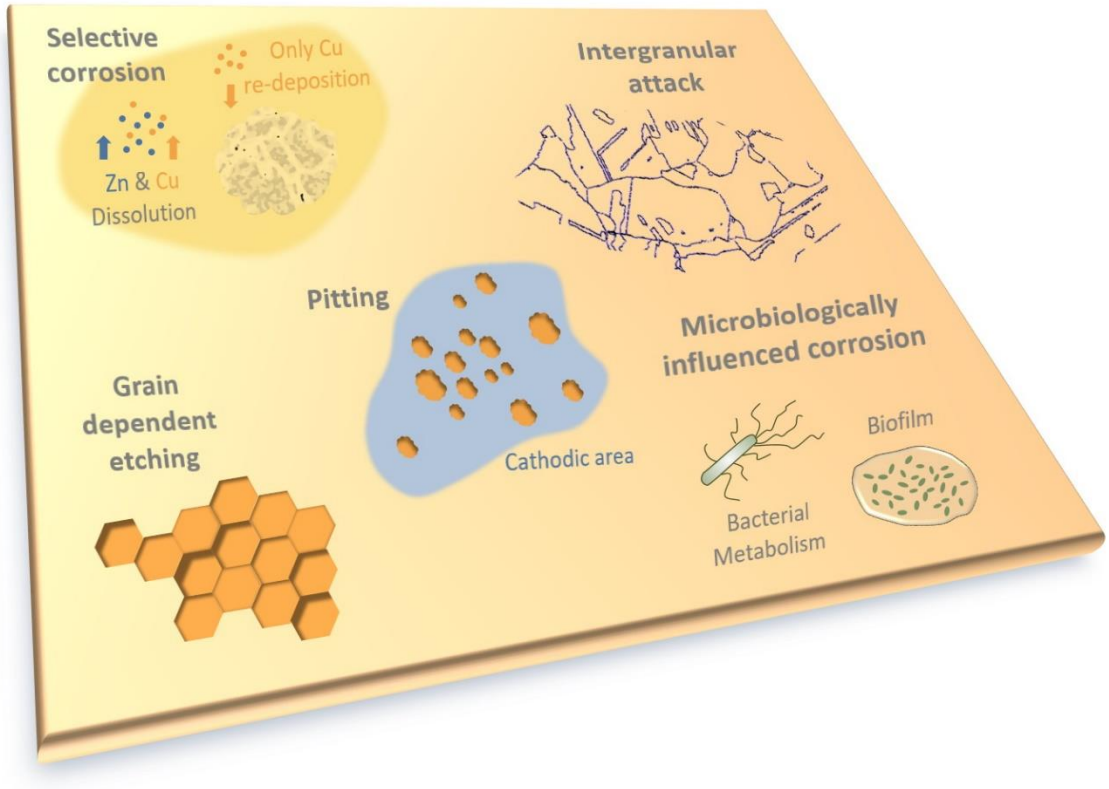

Figure 1.3 Schematic examples for localised corrosion.

copper in the matrix. Since copper alloys are also considered as candidates for antibacterial surfaces, this phenomenon has already been reported in artificial perspiration solution or bacteria contained environment [124, 163].

However, zinc (when it is less than 35 wt.%) does not exist as a secondary phase in brass. A solid solution should be found instead. Therefore, studies have suggested that this process is not simply governed by the selective dissolution [164], since both copper and zinc should have been removed from the crystal lattice at the same time. There should be a dissolution-precipitation (re-deposition) of copper that deviates the final composition from the original one, causing an "illusion" of selective dissolution. This has a meaningful implication in corrosion research: dissolution should not be easily considered as the end of the corrosion process, since the following reactions between aqueous species could continuously alter the corroded surface.

1.3.2.2. Intergranular Attack

This is not a typical type that can be observed on copper. Nevertheless, the significance of this type of corrosion lies in its relationship with material microstructure and its unique consequence: localised corrosion sites around grain boundaries.

One way to understand this phenomenon is to regard it as a similar type of selective corrosion. It is now the grain boundaries that are under severely attacked, acting as anode in the galvanic corrosion. The preferential dissolution of a grain boundary is usually attributed to its inhomogeneity, in respect to atomic defects and precipitated phases, which are likely brought by metallurgical process for bulk materials, or fabrication method/parameters for coating/thin films. However, existence of atomic defects is somehow inevitable, as they represent the nature of the locations where grains meet each other.

For the latter cause (precipitated phases), an appropriate heat treatment method would help, through their re-dissolution back into the matrix. Together with processing methods, the fractions of different types of grain boundary, which is defined by the misorientation between two neighbouring grains can be regulated. It has been demonstrated that these boundaries behave differently in terms of dissolution rate and corrosion tendency [165]. For example, coherent boundaries such as twin boundaries are usually regarded to have higher corrosion resistance [166, 167]. Furthermore, the shape of grain boundary (curved or relatively straight) is recently found closely relevant to the type of the corresponding boundary as well as its corrosion behaviour [168].

Another interesting scenario is how the predominant corrosion mechanism could shift after the initiation of intergranular attacks. That is to say, new situation could arise when the grain boundaries become geometrically lower, as a result of material loss. These uneven regions could have significant impacts on the mass transfer process, resulting in localised discrepancy in term of acidity, concentration of substances, and fluid flow rate compared to other intact near-surfaces. These will be further discussed in the following section related to pitting, as the scenarios share huge similarity.

In most of the cases, intergranular attacks are described to extend from the surface into the bulk materials crossing several grains. As a result, a cross section of the investigated surface would be the best approach to display the consequence [169]. However, in view of the relatively short corrosion periods covered by this thesis, only the initiation of intergranular attacks can be observed and considered. Therefore direct evaluation from top view has been selected.

1.3.2.3. Grain Dependent Etching

Contrary to the attacks occurring at grain boundaries, another type of corrosion targets the grains, which could also happen simultaneously alongside the intergranular attacks [165]. A variation of corrosion rate among different grains after polarisation is recently observed, by comparing the change in height using scanning tunnelling microscopy (STM) [170]. Interestingly, the reason behind does not solely come from the discrepancy in corrosion resistance of each single grain. It

also relates to the relatively potential difference among exposed grains nearby [171]. Therefore, any attempts to characterise the corrosion rate for a certain orientation would not succeed.

Moreover, it should be noted that it is in fact, not the bulk, but the exposed crystallographic facet of a certain grain that shows the electrochemical potential difference [172]. Therefore some facets act as anode and dissolve. However, since the exposed facets on an investigated polished surface usually lie on the orientation of their respective grains, this effect is still frequently considered to be grain dependent.

This kind of detailed information on grain scale, nevertheless, will not be collected or reflected in the macroscopic electrochemical measurement, where only the global response of the whole surface is recorded. Instead, technique like scanning electrochemical cell microscopy (SECCM) become promising in this circumstance [173], as electrolyte can be restricted by the tip and thus can be applied on just one grain. Influence from the neighbouring grains are likely to be isolated.

1.3.2.4. Pitting

This is another type of localised corrosion, which has been extensively observed on the grain surface. Compared to other localised corrosion phenomena, pitting usually evolves in a clear phase sequence that can be predicted [174, 175]. The first step is the “nucleation” of the pits, signified by the local breakdown of the existing oxide films. To exactly predict the initiation of pits is still difficult. Nevertheless, research has demonstrated that the nucleation sites could strongly favour the microstructural inhomogeneity sites, where dislocations [176] or climbs [177] are presented, but not necessarily following a one-to-one correspondence [178].

After a small pit appears, it is then the acidity and chemical concentration in such a micro-scale region that come to play. In the forthcoming pit growth phase, the inner parts of the pit act as anode, keep dissolving themselves and releasing metal ions. Meanwhile, the bare metal sites around the pit act as cathode, where reduction reactions occur simultaneously, increasing the pH. Around the pit, the dissolved metal ions may diffuse from the pit and form porous corrosion products (passive films) as a result of the local supersaturation. Formation of these products have two major effects. Firstly, they gradually close the pit, impeding the mass transfer between the pit and the outside environment; secondly, they could consume hydroxide (OH^-) and thereby lower the pH inside the pit, probably accelerating the pitting rate.

The final phase could be the seal of the pits. However, it does not necessarily signify the end of the pitting, while further corrosion could continue in the pits depending on each specific circumstance.

Another feature could be observed is called crystallographic etching. It leaves particular shapes of the pits or sub-microscopic steps on grains, which could even happen below the surface [179]. This can be explained partially based on the grain dependent etching that happens on the same grain [174, 175, 180]. That is to say, in a given circumstance, there are some atomic planes that dissolve faster than the others. In such a situation, the atomic planes that dissolved relatively slowly will disappear, and those most susceptible planes will gradually occupy the interior of pits.

External environmental variables usually have considerably strong influence on the formation of pits. In a number of instances, addition of chloride could form extra products such as copper chloride (CuCl) on copper surface, which might develop to pit sites if its transformation into Cu_2O is not sufficient [181]. However, Cu_2O membrane that separates the inner pitting region from the environment could in turn affect the pitting process [182].

Pitting rate is one of the important aspects in this phenomenon. Laser scanning microscopy (LSM) has been one of the powerful ex-situ tools to measure the depth of pits. However, only the early initiation of pits will be presented in this thesis, whose sizes are too small for the limited lateral resolution of LSM.

1.3.2.5. Microbiologically Influenced Corrosion (MIC)

This is also simply called microbial corrosion or bacterial corrosion, indicating the dominant role of microbes, mostly bacteria, in the aqueous corrosion process. Copper pipes in water distribution system is well known for universally risking this kind of corrosion since a long time [183, 184].

Once bacteria arrive on the surfaces or form biofilm, many local environmental components could be influenced. Enzymes and acidic metabolites (*e.g.* organic acids) could be aggressive, which will be continuously provided by the bacterial metabolism as long as they are viable. In the case of copper, not just the corroded substrate but also the passive layer can be influenced by these products, possibly affecting its protective capability [185]. For the same reason, concentration of other substances or dissolved gas species could be affected, altering the corrosion kinetics. For example, bacterial respiration is known for consuming oxygen in the aqueous environment [186]. Besides, coverage of bacteria compromises the fluid flow rate and mass transport, which could play a decisive factor on the corrosion process.

The type of corrosion also strongly depends on the special capability of the specific bacteria. Fox example, *Acidithiobacillus ferrooxidans* could oxidise Fe^{2+} to Fe^{3+} as a process of their metabolism, causing formation of $Fe(OH)_3$ precipitation, accelerating the anode dissolution kinetics [187]. On the other hand, iron-respiring bacteria can inversely reduce Fe^{3+} to Fe^{2+} by various

mechanisms [186]. In addition, sulphate-reducing bacteria (*e.g. Desulfovibrio desulfuricans*) could obtain energy from the environment by reducing sulfates (SO_4^{2-}) [187]. This causes hydrogen sulphide gas (H_2S) production and introduces severe corrosion on iron and steel. What's more, bacterial species may assist each other in biofilm, making the corrosion phenomena involved increasing complexity.

It has to be noted that, the micro-scale chemical or physical variations caused by bacteria or biofilm near the corroded surface could, however, decelerate the corrosion (*e.g.* by cutting down the oxygen content). That is to say, introducing bacteria or slight change of the environmental components could have multiple and complicated effects [188], which have to be characterised comprehensively in each specific case.

1.3.3. Other Issues of Copper Corrosion

As can be seen, the complexity of the corrosion environments presented later in this work will be rather complex. In order to focus more on the corrosion behaviours of copper, particularly a few independent issues still worth to be briefly mentioned.

1.3.3.1. Oxide Growth

Oxide growth is one of the most common and obvious chemical changes frequently observed on the corroded copper surfaces. Two thermodynamically stable oxides, namely Cu_2O and CuO can be individually identified depending on the corrosion conditions. Other corrosion products such as $Cu(OH)_2$ and $Cu_2(OH)_2CO_3$ are often found too. Whether ex-situ characterisation of the presence of these species is feasible also depends on their formation rates and scales. Especially when some have relatively high solubility in a specific condition [114], they directly dissolve and become non-detectable on the surface afterwards.

Traditionally, oxidation (particularly thermally) of metallic surfaces should be investigated with respect to diffusion of metallic atoms and oxygen, formation of the oxidised species, shift of the oxide front (interface between metal and oxide), and the like [189]. It is true that some general conclusions obtained from these perspectives are helpful in understanding the oxide formation on copper in aqueous conditions, however, may not describe all existing processes comprehensively.

For example, in the case of pitting corrosion, another special mode of oxide growth could be found assisted by the aqueous environment: re-deposition. As already described, the pit serves as an anode that dissolves copper ions into the solution. Meanwhile, oxide growth could be found on

the cathodic sites, namely the opening and the surrounding of the pit. Concentrations of the species as well as the electrons transferred through the metal (and grown oxide) could account for why this type of re-deposition reaction is restricted near the exposed surface, creating an "illusion" of direct oxidation of the metallic surface. Consequently, unlike in thermal oxidation process, diffusion of metallic/oxygen atoms at the oxide-metal interface becomes a minor concern. The oxide front should as well shift less obviously, as the metal on the interface does not go through an oxidation reaction.

Nevertheless, re-deposition could result in a layer composed of precipitates, or a solid-state grown film. Although in the latter case, there is no expected mass transfer between the layer and the original exposed metallic surface, this surface could still strongly influence how the re-deposited layer forms in the first beginning. For instance, studies have shown a similar copper oxide re-deposition process in solutions with copper containing substances [190], where some specific orientation relationships between copper grains and the newly deposited oxide layer were found. Carefully combing atomic force microscopy (AFM) [191] and STM [192, 193] with electrochemical polarisation, is was found that this lateral growth mechanism is simultaneously controlled by adsorption of oxygen species, surface reconstruction, and growth of stepped surface. These results therefore emphasise the assisting role of the substrate in the oxide nucleation phase.

There are many implications why oxide formation should be better considered in this thesis. First of all, having noticed the presence of oxides during antibacterial tests helps evaluate the actual antibacterial effect generated by metallic copper surface. Secondly, oxide growth consumes the existing antibacterial ionic copper in the aqueous environment, which is considered to be detrimental for antibacterial process and should be avoided. Moreover, more oxide coverage results in less metallic copper exposed to the environment, which could also impair the release of copper ions and better to be avoided [194].

1.3.3.2. Role of Chloride Ions

To simplify the discussion and to put forward the basic aspects of copper corrosion, thus far, only pure water has been taken into consideration in most of cases. Unfortunately, this simplified condition seldom reflects the actual environmental components. Especially in antibacterial efficiency test, buffers composed of different chemicals have to be applied, in order to ensure the survival of the bacteria. Among different compositions, sodium chloride (NaCl) is one of the common components, adjusting the osmotic pressure to a suitable level, or directly simulating the perspiration environment [124].

Cl^- are inevitably introduced into the aqueous environment. A recent study performing on copper-silver alloy surface has reported a better antibacterial property in the presence of Cl^- in buffers [195]. Attention should therefore be drawn to its possible reactions with copper surfaces or other substances in the solution. Studies [181, 196] have proposed how the presence of Cl^- interferes the corrosion process through the probable reactions listed below:

Reaction 1 (Adsorption of Cl^- and complex formation):

$$Cu(s) + 2Cl^-(aq) \rightarrow CuCl_2^-(aq) + e^-$$

Reaction 2 (Dissociation):

$$CuCl_2^-(aq) \rightarrow Cu^+(aq) + 2Cl^-$$

Depending on the concentration of the above substances, additional reactions can take place, which could inhibit further corrosion/dissolution of copper surface:

Reaction 3 (Deposition):

$$CuCl_2^-(aq) \rightarrow CuCl(s) \downarrow + Cl^-(aq)$$

Besides, Cu_2O could form in two ways based on the local pH conditions:

Reaction 4:

$$2CuCl(s) + H_2O(l) \rightarrow Cu_2O(s) + 2H^+(aq) + 2Cl^-(aq)$$

Reaction 5:

$$2CuCl(s) + 2OH^-(aq) \rightarrow Cu_2O(s) + H_2O(l) + 2Cl^-(aq)$$

Although Cl^- do not necessarily accelerate the corrosion process, it can be a causal factor of pitting corrosion in some cases [165, 181, 182]. As a result, chloride introduced by the buffers could add many complications in showing the antibacterial efficiency of copper surfaces, since it affects the release routes and rate of the antibacterial copper ions.

1.3.3.3. Aging of Surface

This section aims to cover the corrosion phenomena not anymore in aqueous condition, but simply in atmosphere. Concerning the lifespan of antibacterial metallic copper surfaces, it is important to realise how these surfaces could age in the specific conditions, and how these aging effects influence the antibacterial efficiency. Currently, as a cause of various types of structural failures and accidents, atmospheric corrosion on outdoor metallic surfaces such as bridges, mobiles, ships, and other architectures has been widely investigated. It provides a perfect introduction for aging analysis.

One major factor that needs to be constantly considered is the humidity. In relatively high humidity, salts deposited on a surface could go through a process called deliquescence [197]. This process allows the salts absorbing water from the atmosphere and thereby dissolving themselves on

the surface. A consequence of this process is to shift the near-surface environment to a quasi-aqueous condition, likely leading to many corrosion attacks.

However, even if the humidity is lower than the deliquescence point of a certain substance, it does not ensure that surface will be intact. Because water adsorption could still results in formation of monolayers of water on the surfaces [198], which may act similarly to bulk water. It is therefore possible for the salts to dissolve and its containing ions to further diffuse above the surface within this layer [199]. These dissolved ionic species and the monolayers of water together act as electrolyte. It thus again becomes a similar quasi-aqueous condition, which could be favourable for some corrosion reactions, aging not only the original salts deposited locations, but the surrounding areas too.

As mentioned in the previous section, NaCl is a common component for buffers applied in antibacterial tests, therefore it can be found on the tested surfaces even after the solution is withdrawn. NaCl is, unfortunately, one of the typical salts that has been confirmed to be active in both abovementioned effects [200]. However, having a deliquescence point around 75% relative humidity (RH), deliquescence transition in daily/lab environment might not be predominant, while diffusion of Cl^- within the adsorbed water monolayers could still age the copper surfaces.

1.4. Aims and Structure of this Thesis

To sum up, for copper and its relevant surfaces, it is corrosion that seems to determine the release of the antibacterial copper ions as well as the outcome of antibacterial efficiency test. This could further suggest that, in order to correctly interpret the results or trends obtained, one would better consider how the corrosion conditions and the corresponding consequences differ.

However, the evidence of such a correlation is still lacking. That is the reason why comprehensive characterisation of the corroded copper coupons in physiological environments is indispensable. For instance, investigation of micro-morphology or microstructure features provides information on the corrosion mechanisms that facilitate antibacterial copper ion release. Confirmation of corrosion products is, on the other hand, necessary for further analysis on the particular corrosion processes. In addition, evaluation of the aqueous environment itself reflects its potential impacts on corrosion as well. **Therefore multiple characterisation techniques were applied in this thesis, which will be introduced in detail in Chapter 2**.

Combining with these methods, this work targets the major issues as below:

- Will the corrosion behaviours of copper surface change when the aqueous condition is altered (*i.e.* in another buffer, or absence of microbes)?

- If yes, then how do these variations affect the release of copper ions as well as the antibacterial effects?
- Are there any dominant corrosion mechanisms can be observed during the antibacterial efficiency test?
- What kinds of corrosion products will form on the copper surface, and what are their impacts to the antibacterial process?

These questions will be partially and gradually answered as research developed in the following main chapters:

Chapter 3 initiated the attention of the how important a buffer could be in revealing antibacterial effect of metallic copper surface. Meanwhile, the roles of bacteria and Cu_2O formation are introduced and preliminary discussed. PBS and Na-HEPES were chosen, and the corrosion phenomena on copper as well as the antibacterial efficiency against *E. coli* were compared. Assisted by the results obtained from the well-defined sputtered Cu_2O coating coupon, three main features were observed:

- Corrosion behaviours shown on copper surface in two buffers have a huge impact on the antibacterial copper ion content and thus the antibacterial efficacy measured.
- Bacterial addition is an influential factor to the corrosion environment. It causes a discrepancy in copper ion release.
- Cu_2O formation may exist as a barrier layer hindering copper ion release, instead of promoting antibacterial effect.

To learn more from these observations, experiments were designed, and investigation was expanded in the following chapters.

Chapter 4 further characterised the corrosion phenomena introduced by PBS and discussed how they can be influenced by *E. coli* addition in the antibacterial efficiency test. It is found that when *E. coli* was added into PBS, formation of Cu_2O on copper surface was inhibited. These changes have been attributed to that fact that the bacteria cells passively accumulate copper ions by storing copper inside and promoting the formation of copper phosphate sub-micron particles outside. On the other hand, localised corrosion sites were revealed. Since it is at these sites where antibacterial copper ions are heavily released, the next chapter was designed to conduct comprehensive research on it.

Chapter 5 accomplished the investigation on electropolished copper coupon in PBS environment, offering details of how the corrosion attack and oxide growth occur. Distinct localised corrosion sites were identified along grain boundaries and on grains with specific orientations. Characterisation of oxide layer regarding its morphology and orientation, on the other

hand, depicts a re-deposition process. Interestingly, it is also worthwhile to mention that the addition of *E. coli* does not change the distribution of these preferential corroded sites. That is to say, the casual factor of such a localised corrosion phenomenon is still hiding in the buffer itself, which will be identified in the next chapter.

Chapter 6 narrows down the target to Cl^-. It introduces localised corrosion attacks on copper and assists atmospheric corrosion process. Copper ion release and antibacterial efficiency were compared between 0.9% saline and pure water. It is therefore clear that copper surface was corroded much severely in saline and thus killed *E. coli* faster. Furthermore, the residual NaCl deposits on copper surface introduced by saline showed a continuous aging effect in atmosphere, leading to formation of an additional Cu_2O layer and/or oxygen containing species.

2. Experimental Methods

2.1. Materials and Solutions Preparations

This section aims to cover the selection of materials and solutions applied in this work.

2.1.1. Bulk Materials

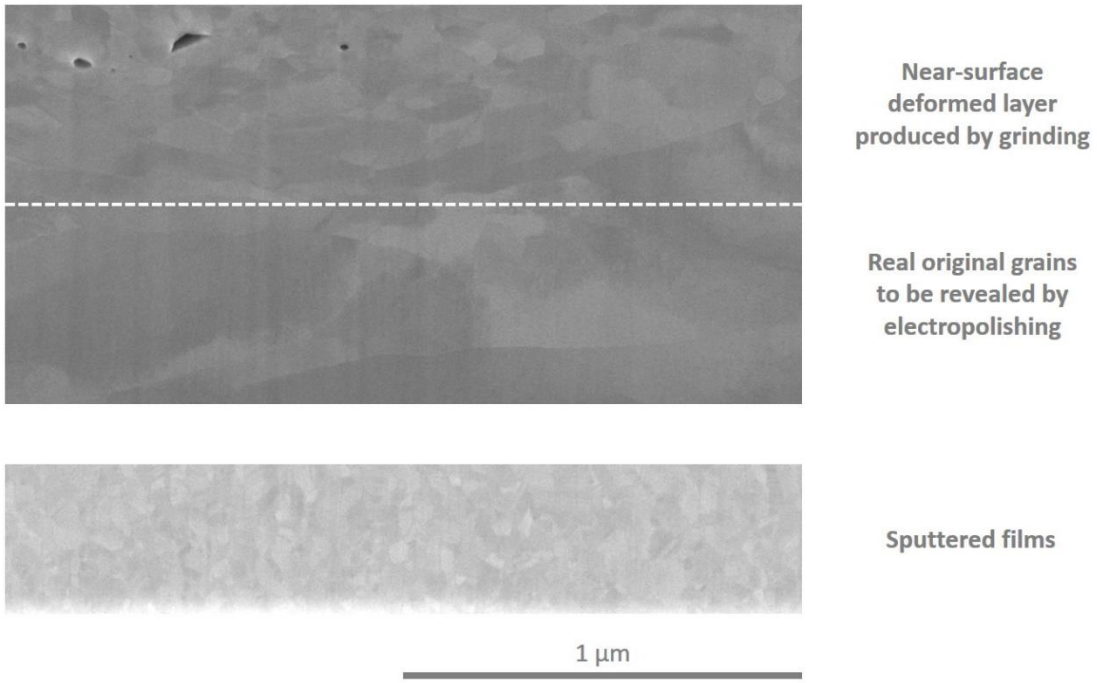

Figure 2.1 Comparison among exposed copper grains prepared by grinding, electropolishing, and sputtering, shown by their SEM cross-section images.

Pure copper (99.99%, K09, Wieland) was chosen for most of the experiments. There are mainly two types of surface finish that have been employed:

Ground copper coupons were mechanically ground with a silicon carbide sandpaper (stepped down to grit number P600), following a conventional metallurgical procedure. They were rinsed with water, cleaned with ethanol in an ultrasonic bath, and dried by air.

This type of surface was used in most of the experiments, for its simplicity and high reproducibility. It could represent the normal (which means not lab-level perfect) surfaces in daily lives.

Electropolished copper coupons were first mechanically ground and polished finishing with 1 µm diamond paste, and cleaned with soap. These coupons were electropolished in 85 wt%

orthophosphoric acid for 3 min at 2 V versus a copper slide. They were rinsed with water, cleaned with ethanol in an ultrasonic bath, and dried by air.

By electropolishing, not only has the copper surface become extremely smooth, but also have the original grains (with greater grain size) exposed, instead of the near-surface deform layer (**Figure 2.1**). These coupons helped to understand the correlation between microstructure and corrosion attacks.

2.1.2. Reactive Magnetron Sputtering

Apart from the copper coupons, a small portion of the experiments was performed on cuprous oxide (Cu_2O). These oxide surfaces were thin films fabricated by reactive magnetron sputtering technique (hereinafter sputtering).

Sputtering is a PVD method based on one (or many) source target(s) and a substrate. Both of them are placed in a vacuum chamber and connected with a specific power supply. Argon (Ar) usually serves as the sputtering gas, being ionised in the electric field between the target (cathode) and the substrate (anode). These ions will be further accelerated by the electric field and bombard at the target. This process generates sputtered ions/particles flying away from the target. Those reach the substrate could deposit and eventually form a layer on top. The term “magnetron” refers to the structure of cathode, where magnetic field is introduced in order to trap the electrons and thereby increase the ionisation efficiency. The term “reactive” indicates that reactive gas is introduced into the system along with Ar, so as to achieve a complex chemical composition of the deposited film.

To prepare Cu_2O films, microscope glass slide was chosen as the substrate. These substrates were cleaned by an ultrasonic bath with ethanol before being transferred into the sputtering chamber. Distance between substrates and Cu target (99.99%) was 50 mm. During the deposition, the sputtering pressure was maintained at 0.5 Pa, while Ar flow rate was 25 sccm and O_2 as 7 sccm. The sputtering power was provided with a constant current as 0.3 A (power around 150 W) by a pulsed-DC generator (Pinnacle, Advanced Energy). Frequency and off time were 50 kHz and 4μs, respectively. The total deposition time was 5 min.

The phase composition was examined by grazing incidence X-ray diffraction and Raman spectroscopy. Owing to such a totally different process compared to the conventional metallurgical fabrication, the crystallinity and microstructure of these thin films are supposed to exhibit a great distinction (**Figure 2.1**).

2.1.3. Solutions and Suspensions

These aqueous environments/conditions, in most of the cases, play the principle role in causing corrosion on the surfaces investigated. There are mainly two groups of solution that have been applied: one is the pure solutions, which is only composed of chemicals; another sort is bacterial suspension, that is to say, bacteria (live/dead) are added in these solutions.

Phosphate-buffered saline (PBS) was prepared with NaH_2PO_4. $1H_2O$ (Merck, Germany, final concentration 0.01 M), NaCl (VWR, Germany, final concentration 0.14 M) and pure water for analysis (Merck, Germany). Its pH value was adjusted by adding NaOH to 7.4, sterilised in an autoclave after preparation. Its buffer potential is provided by dihydrogen phosphate ($H_2PO_4^-$) and its conjugate base, namely hydrogen monohydrogen phosphate (HPO_4^{2-}).

Na-4-(2-hydroxyethyl)-1-piperazineethanesulfonic acid (Na-HEPES, final concentration 0.1 M) was prepared with HEPES FREE ACID (VWR, Germany) and pure water for analysis, and adjusted by NaOH in the same way as PBS, with a final pH of 7.0. Its buffer potential is provided by the protonation by the lone pair electrons on the amine and the deprotonation on the terminal hydroxy group.

Saline with various concentrations (default to be 0.9%) were prepared with NaCl (VWR, Germany), and pure water for analysis (Merck, Germany), sterilised in an autoclave after preparation.

Suspensions with bacteria. *E. coli* is well known as an ideal model organism for microbial study. *E. coli* K12 strain was grown aerobically overnight in Lysogeny Broth (LB) medium at 37 ºC in a water bath with a speed of 220 rpm. The stationary cells from culture were collected by centrifugation for 15 min at 5000×*g*, washed, and centrifuged three times with the corresponding buffer, and finally re-suspended in the same type of buffer. The initial average cell count in stationary phase was around 3×10^9 to 5×10^9 colony-forming unit (cfu)/ml.

Since *Staphylococcus cohnii* (*S. cohnii*) was observed with relatively lower mobility, it was therefore applied to examine the potential effects of fluid flow on corrosion. For the suspension with *S. cohnii*, except that the Tryptic Soy Broth (TSB) medium was applied for overnight culture, other parameters followed exactly the abovementioned protocol for *E. coli*.

Besides, the concentration of bacterial suspension can be easily adjusted during the re-suspension step. For example, a fivefold concentration *E. coli* saline suspension can be prepared by re-suspending in 0.2 mL of saline instead of the original amount 1 mL.

2.1.4. Corrosion Protocol

Corrosion test is an important part in this work, as most of the characterisations are done on those corroded coupons. The corrosion tests are designed as droplet exposure method (instead of immersion), in order to simulate almost the same procedures of antibacterial efficiency test to be mentioned in the following section. In brief, coupons of were placed in a water-saturated atmosphere at room temperature when droplets of 20 μL buffer or bacterial suspension (hereinafter sample) were applied on them with a pipette. After the set times, these samples were withdrawn. For coupons investigated in Chapter 3 and 4, they were dried in a ventilated room. Most of the coupons in Chapter 5 and 6 were then cleaned with ethanol in ultrasonic bath immediately after withdrawal.

In Chapter 5, to remove the corrosion products from the copper surface, coupons were immersed in 4 wt% hydrochloric acid (HCl) for 10 s, followed by water rinse and ethanol in ultrasonic bath. Extra and obvious attacks on copper surface after this acid treatment has not been observed.

In Chapter 6, in the test with various NaCl/bacterial concentrations, the treated surfaces were firstly wiped with detergent-dipped cotton pads in order to remove the adhered bacteria. As for the atmospheric aging experiments, the coupons remained unwashed. They were constantly kept in the lab atmosphere at room temperature, except for the time being characterised.

2.2. Characterisations Methods

In this section, brief overviews will be presented with respect to the characterisation approaches that have been utilised. It involves the purposes, general parameters, and notice for specific conditions if needed.

2.2.1. Grazing Incidence X-ray Diffraction

Phase analysis and confirmation are essential for corrosion investigation. Corrosion products and deposits can thus be identified, providing valuable information to further elucidate the corrosion process involved.

Grazing incidence X-ray diffractometer (GIXRD, Cu K_α with 1° grazing angle, PANalytical X'Pert PRO-MPD) is a helpful tool applied in the study. Similar to conventional X-ray

diffractometer, substances with different crystal structures can be indexed and distinguished, according to Bragg's law. By applying the incident X-ray beam with a grazing angle, the penetration depth of the beam is therefore limited. This becomes an advantage for sensitive surface analysis, since the core interest is the corrosion products attached on the coupon surface. In the majority of cases, they exist as a layer at nano-scale.

The spot of the X-ray beam (*i.e.* the lateral detection area) can be adjusted by inserting slit and mask with different sizes. Despite this, GIXRD is still a method that provides global information from the corroded surfaces.

Other than revealing the phase information from the corroded surfaces, GIXRD was also employed to confirm the preparation of sputtered thin films, or the precipitates deposited. However, since the detected diffraction planes are not always parallel to the coupon surface, information of preferential growth will be lost.

2.2.2. Raman Spectroscopy

To examine the corrosion products at a much smaller lateral scale, Raman spectroscopy (Raman, laser source with 532/633 nm, inVia, Renishaw) with a 50X optical microscope was applied.

Raman is designed based on the photon scattering effect of the specific bonds of a certain material. These scattering events generate a shift in energy of the photon, which is presented as the Raman shifts in the spectrum. Since the discrepancy and probability (*i.e.* intensity) of these shifts depend on the molecular vibrations of a substance, they provide fingerprint information for phase confirmation.

This is a method based on focused laser technique and therefore the information will be only collected from the area covered by the laser spot. With the applied configuration, the spot size is around two microns, therefore completely suitable for localised corrosion analysis.

2.2.3. Optical Microscopy

Optical microscope (OM, OLS4100, Olympus, 3D bright field mode) photos were captured so that the colour of the corrosion products covering the original coupon can be preserved. The colour recorded is the joint effect of the optical properties of the corrosion product and the substrate (**Figure 2.2**). Therefore it was applied to indicate the thickness difference of the same type of corrosion product, exclusively on the electropolished coupons after corrosion test.

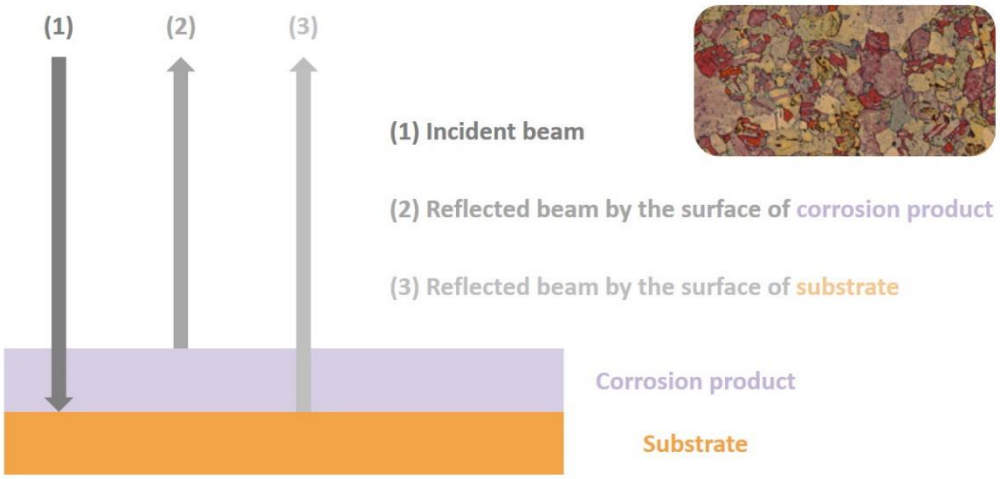

Figure 2.2 Schematic illustration of the application of OM in differentiating areas covered by oxides that are different in thickness.

2.2.4. Scanning Electron Microscopy

Scanning electron microscope (SEM, Helios NanoLab600, FEI) is a multi-functional system that was used to observe not only the corroded coupons but also the bacteria. In this section, only its image formation system is to be mentioned. The advantage of SEM in obtaining images of an object, is its lateral resolution. Compared to OM, SEM utilises electron beam instead of visible light for imaging, which has a much smaller wavelength (depending on its energy, *i.e.* acceleration voltage). Nano-scale spot can thus be obtained, making a similar fine resolution reachable.

However, in order to analyse images collected by SEM, it is also important to understand the electron beam-specimen interactions. The outcome of these interactions is further selectively collected by different type of detectors, forming images that reveal various properties of the coupons (**Figure 2.3**). In this work, two types of detector are mainly utilised, and for appropriate understanding of the results, some of their essential features are discussed below.

Secondary electron (SE) detector was applied to characterise the morphology of the top-surface as well as cross-section of the coupons. SE are defined as the electrons that ejected from the outer shell of a substance (under electron beam bombardment, in SEM). However, SE detector cannot differentiate the type/origin of the electrons. What it could do is to simply collect those electrons that have less kinetic energy, since that is one of the characteristics of SE. Because only those

generated by the near-surface materials can reach the surface and therefore be collected, SE images often reflect the near-surface condition and edge (topographic) effects.

On the other hand, backscatter electron (BSE) detector mostly aimed to explore the localised corrosion attacked sites already covered by corrosion products. Unlike secondary electrons, BSE are those originally from the incident electron beam, which are elastically scattered for several times, and finally escape the material surface. Since their trajectories could have reached much deeper and wider positions, they could help revealing the below-surface information but with poorer lateral resolution. BES images are also influenced by two additional effects, namely the compositional effect, and the electron channelling effect. The former one helps to preliminarily distinguish the density of an object according to the atomic number dependence. Grains with different orientation, on the other hand, could be distinguished by their crystallographic contrast thanks to the latter effect.

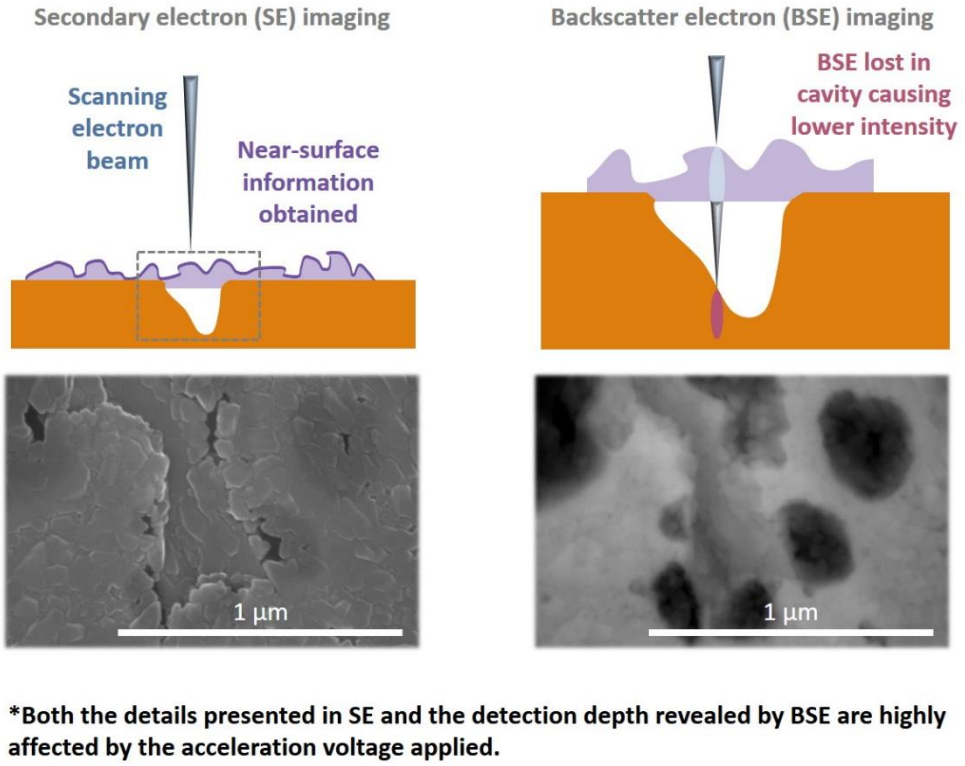

Figure 2.3 Illustration of origins of contrast collected by SE and BSE detector, respectively.

Nevertheless, one disadvantage of SEM is about its operating conditions, where vacuum environment is necessary. This suggested that only ex-situ characterisation can be made. Especially, owing to the complex structure and composition of bacteria, the observed morphology may not reflect the actual one before being transferred to the vacuum chamber.

Since different acceleration voltages have been chosen depending on the situations, they are further mentioned in the corresponding figure captions.

2.2.5. Electron Backscatter Diffraction Patterns

Electron backscatter diffraction (EBSD) patterns are generated by Bragg diffraction of the crystal planes. An EBSD pattern includes a certain amount of Kikuchi lines arranged in a certain way. These lines will be then indexed with the known/expected phases, from which the orientation of the corresponding crystal grain can be further derived.

However, a precise and correct indexing process assisted by software relies on an EBSD patterns with high quality. In other words, if part of the information is lost (*e.g.* incomplete pattern caused by the shadowing effect), it becomes necessary to apply manual indexing to extract the information aimed.

Results obtained from this method in Chapter 5 help to investigate the orientation relationship between the corrosion product and the substrate underneath. Data were collected with step sizes of 200 nm (for fine scan at local regions) or 1 μm (for fast scan at droplet edges) with an acceleration voltage of 20 kV in SEM.

2.2.6. Focused Ion Beam

Focused ion beam (FIB) is a useful tool integrated in SEM. Metallic ions (gallium, Ga, in this work) are emitted and accelerated by a strong electric field and focused on the coupon. This ion beam has two major functions: (1) to bombard, thus to destroy the coupon on purpose and (2) to assist deposition of addition material on the surface.

In this work, FIB has been applied, in most of the cases, to obtain cross-sectional views at the specific sites of the coupons, and to prepared lamella (a thin layer of material) for further analysis which will be addressed below. FIB assisted platinum (Pt) deposition of was also involved, so as to protect the near-surface from direct ion bombarding.

2.2.7. Scanning Transmission Electron Microscopy

Scanning transmission electron microscope (STEM, **Figure 2.4**) is one of the modes that can be applied in SEM. The object of this method is usually the lamella prepared by FIB. A lamella is a small portion of the investigated coupon. Polished by FIB with a final thickness less than 100 nm, then a portion of electron beam at 30 kV could therefore penetrate. Consequently, detectors are placed on the other side of the lamella (compared to the incident electron beam). The detector that

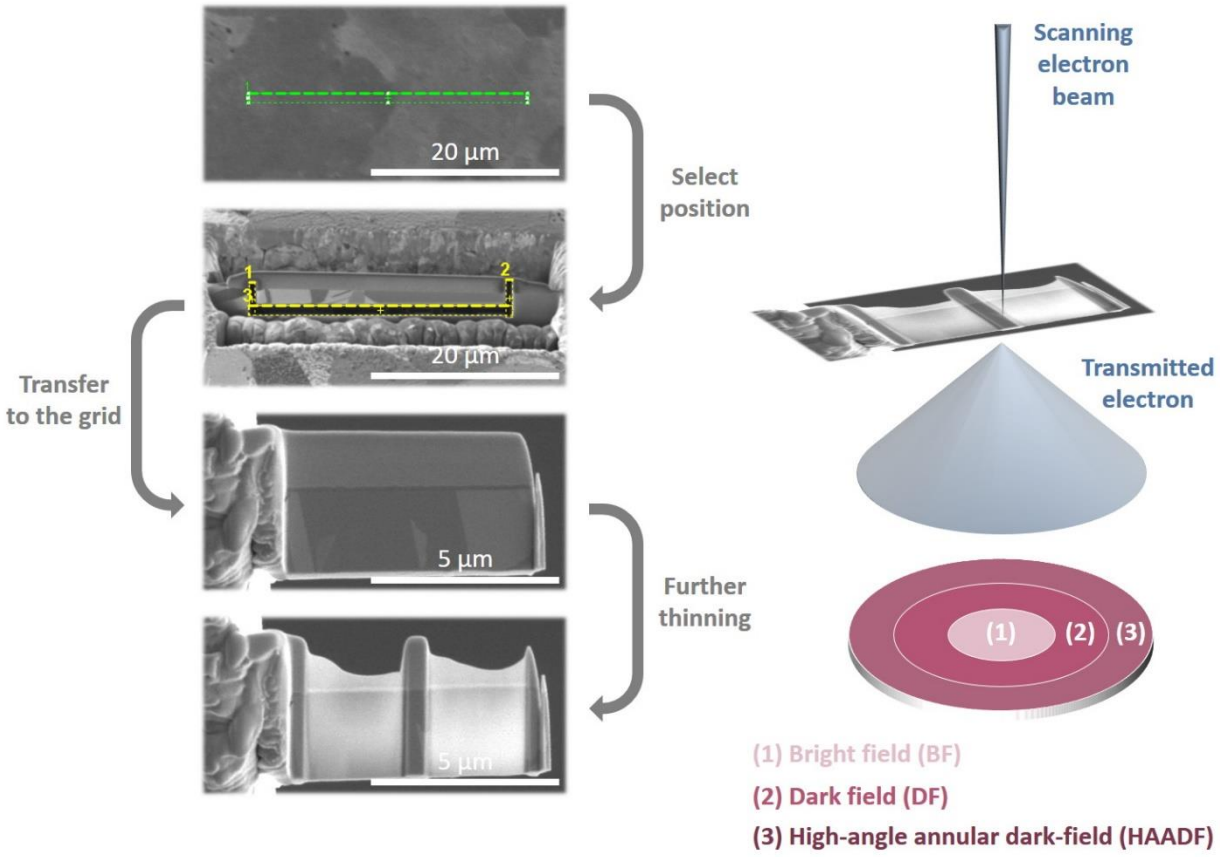

Figure 2.4 Illustration of lamella preparation by FIB as well as imaging principle of STEM.

placed near axis of electron beam is called bright field (BF), which aims to collect the transmitting electrons, preserving the microstructure information. From the axis outwards, there are dark field (DF) and high-angle annular dark-field (HAADF) detectors. Both are designed to detect those highly diffracted electrons, obtaining the compositional information.

Several characterisations have been carried out in Chapter 5 in order to closely survey the details of corrosion products and their relationship with the substrate.

Another example of STEM is in transmission electron microscope (TEM, JEM-ARM 200F, JEOL) in Chapter 4, applied with an accelerating voltage of 200 kV. Although it was operated in TEM, the electron beam was still focused as a spot. Tests were performed on the *E. coli* PBS suspension withdrawn from copper surface treatment after 3 h. Before having them transferred on a Ni grid for observation, they were diluted 1:10 with pure water for analysis.

2.2.8. Energy Dispersive X-ray Spectroscopy

Energy dispersive X-ray spectroscopy (EDS) is a function embedded in electron microscope system

so as to measure the X-ray distribution (intensity) as a function of its energy. Usually, for elemental composition analysis, it is the characteristic X-ray that produced by an inner shell electron ionisation process that needs to be further indexed and applied for comparison.

In this work, EDS in SEM is mainly applied to discover the chemical composition of bacteria (especially for copper), in spot mode with an acceleration voltage of 5 kV.

However, the lateral resolution of EDS is not simply determined by the spot size of the electron beam. For example, BSE inevitably generate X-ray from the atoms that stay far away from the original focus spot. Therefore, another EDS equipped along with TEM was also adopted in its STEM mode, with an acceleration voltage of 200 kV. Moreover, bacteria were transferred on a Ni grid (with thin carbon foil), unlike a bulk substrate in the SEM sample. This strongly reduces the unfavourable influence of BSE and allows precise elemental mapping.

2.2.9. pH Values Measurements

The pH values were obtained from pH-indicator strips (Merck, Germany), designed for a range from 6.5 to 10.0, with 5 gradations between 7.1 and 8.1, namely 7.1, 7.4, 7.7, 7.9, and 8.1. During the withdrawal process, 10 µL of various samples were applied on these strips.

2.2.10. Ion Release Measurement

The amount of copper ions that released from the coupon and presented in the samples was measured by inductively coupled plasma mass spectrometry (ICP-MS, 7500cx, Agilent). This technique involves two main parts, namely ICP and MS. ICP aims to transform the substances from particles to positive charged ions. Afterwards, these ions from the plasma will be transferred to MS, where ions can be separated according to their mass-to-charge ratio and individually measured.

For the samples to be directly measured, following almost every step of the corresponding corrosion protocol, only whenever the set time is reached, 10 µL samples were withdrawn by repetitive pipetting and diluted in 2.990 mL 1 wt% nitric acid (Merck, Germany).

For the measurement of supernatant in Chapter 4, every three 10 µL samples were transferred and mixed in SafeSeal 1.5 mL tubes. After being centrifuged for 5 min at 5 krpm, 10 µL of supernatant were collected and diluted in nitric acid as mentioned above.

For all samples, before being measured by ICP-MS, 3 µL of 10 mg/L scandium (Sc) and caesium (Cs) internal standard solutions were added to the samples. For calibration, standards with 0.1, 0.5, 2.5, 10, 50, 250, and 1000 µg/L of copper were used. After obtaining the results with a unit

of ppb, the final values with a unit of μM were calculated with the fold of dilutions and molar mass 63.55 g/mol for copper. The average values and standard deviation were obtained by three independent experiments.

2.2.11. Antibacterial Efficacy Test

In this work, droplet (wet-plating) method was chosen, whose pros and cons have been addressed in Chapter 1. Preparation of bacterial suspension has been presented as well. Take *E. coli* as an example, the test usually began by applying 20 μL of these re-suspended cells on the coupons in a water-saturated atmosphere at room temperature. After the set times, 10 μL samples were withdrawn by repetitive pipetting, serially diluted in PBS, and spread on LB agar plates (TSB agar plates for *S. cohnii*). Following incubation at 37 ºC for 24 h, the cfu on agar plates was counted and expressed in a way concerning both the fold of dilutions and relative to the original 20 μL samples. The average values and standard deviations were obtained by three independent experiments.

Results from the antibacterial efficiency tests are presented in two ways. In Chapter 3, they were drawn in a logarithmic scale, as a function of time. This facilitates the comparison of "log reduction" along the experimental time. While in Chapter 6, only the antibacterial efficiency in 1 h was investigated. Therefore "reduction rate" is also shown, which is calculated by dividing the number of deactivated bacteria (difference of cfu between the original values and the values obtained in 1 h) by the original number.

3. Buffer Comparison: PBS vs. Na-HEPES

In this chapter, the below peer-reviewed publication is going to be presented:

Early-stage corrosion, ion release, and the antibacterial effect of copper and cuprous oxide in physiological buffers: Phosphate-buffered saline vs Na-4-(2-hydroxyethyl)-1-piperazineethanesulfonic acid

Reproduced from Jiaqi Luo, Christina Hein, Jean-François Pierson, Frank Mücklich, *Biointerphases*, 2019, 14, (2021, 16 for Erratum) with the permission of AIP Publishing

DOI: 10.1063/1.5123039
DOI: 10.1116/6.0000835 (Erratum)

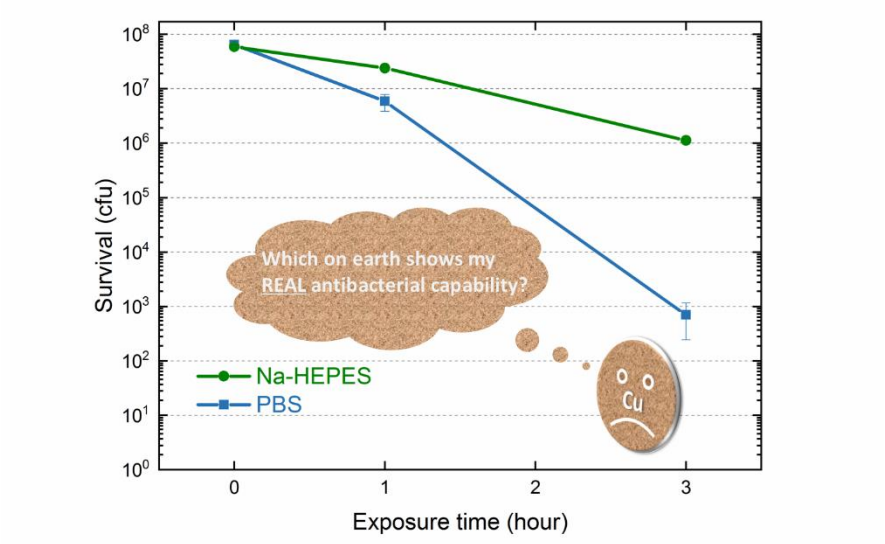

Contribution: Conceptualisation, Methodology, Validation (except from ICP-MS measurements and TEM observations), Investigation, Writing – Original Draft, Visualization, Project administration.

Early-stage corrosion, ion release, and the antibacterial effect of copper and cuprous oxide in physiological buffers: Phosphate-buffered saline vs Na-4-(2-hydroxyethyl)-1-piperazineethanesulfonic acid

Jiaqi Luo,[1,2,a)] Christina Hein,[3] Jean-François Pierson,[2] and Frank Mücklich[1]
[1]*Functional Materials, Saarland University, 66123 Saarbruecken, Germany*
[2]*Université de Lorraine, CNRS, IJL, F-54000 Nancy, France*
[3]*Inorganic Solid State Chemistry, Saarland University, 66123 Saarbruecken, Germany*

(Received 2 August 2019; accepted 21 November 2019; published 12 December 2019)

Copper surfaces are well known for their antibacterial effects due to the release of copper ions. This benefit has been shown in many antibacterial efficiency tests, however, without considering the corrosion behaviors of copper in the physiological solutions, which could play an indispensable role in ion release from the metallic surface. This study compared the ground copper surface and sputtered cuprous oxide (Cu_2O) coating in two common physiological buffers: phosphate-buffered saline (PBS) and Na-4-(2-hydroxyethyl)-1-piperazineethanesulfonic acid (Na-HEPES). The growth of the cuprous oxide (Cu_2O) layer was found on copper in pure PBS, inhibiting further copper ion release. In contrast, a continuous release of copper ions was recorded in Na-HEPES for 3 h, where no oxide formation was observed. The antibacterial efficiency of copper (against *E. coli*) was measured and discussed with the ion release kinetics in the presence of *E. coli*. Similar results were obtained from Cu_2O coating, ruling out its assisting role in showing the antibacterial property from copper surfaces, but they did indicate the importance of taking environmental parameters into consideration in interpreting the antibacterial efficiency of copper surfaces. *Published by the AVS.*
https://doi.org/10.1063/1.5123039

I. INTRODUCTION

Nowadays, there are many threatening situations caused by bacteria or other microbes. For example, we are not only facing the growth of Healthcare-Associated Infections,[1] but also the rapid rise of antibiotic resistance of microorganisms.[2] To confront them, a range of strategies have been developed. Particularly, antibacterial effects exhibited by various surfaces are attracting much attention. These surfaces could deactivate bacteria in different ways, including disturbing biofilm formation,[3] producing reactive oxygen species through photocatalytic reactions,[4] physically piercing cell wall,[5] releasing toxic ions,[6] etc. Copper,[7] copper alloys,[8] and copper incorporated materials[9] have been developed as popular antibacterial surfaces since copper ions are proven to cause damage on cell membranes, nucleic acids, and proteins.[10]

To obtain copper ions from the metallic copper surface, corrosion is a key step. It is no surprise that corrosion processes highly depend on the methods or conditions applied to measure the antibacterial efficiency. Because no matter in the film contact method[11] (where the bacterial suspension is spread on the coupon surface) or the wet-plating method[12] (where only a droplet of the suspension is placed), one factor can never be avoided: the physiological buffer. A buffer is applied in order to maintain a stable *p*H range and osmotic pressure for the survival of bacteria. Even in the so-called "dry" contact killing method,[13] bacteria still need to be prepared with the buffer, so as to be transferred onto the surfaces investigated. Buffers with complicated composition have also been applied, in order to simulate the organic contamination[14] or the synthetic perspiration environment,[15] which have practical meanings for everyday scenarios.

There are studies attempting to compare the antibacterial behavior of copper in different buffers,[12,16] where the relationship with the amount of copper ions was discussed. However, discussions were not extended to corrosion phenomena, namely, how copper ions were released. On the other hand, corrosion of copper never lacks research attention, unfortunately without correlating its antibacterial properties. For instance, regarding phosphate-buffered saline (PBS), a recent electrochemical analysis[17] confirms the corrosion species formed on the copper surface, showing the role of chloride ions in oxide formation. In another work,[18] corrosion resistance of copper was found to be grain-size dependent, which could be further applied in antibacterial surface design. It is also reported that other corrosion products such as $Cu_2Cl(OH)_3$ could form depending upon the composition of buffers and copper alloys themselves.[15]

Our research group also measured copper oxide formation during the antibacterial test,[16] although the emphasis was then shifted to the antibacterial effects of oxides themselves, on account of their promising antibacterial potentials.[19,20] As to our best knowledge, still very few studies have been performed to correlate corrosion and antibacterial effects. We now refocus on this issue. Our ongoing investigations have recently revealed the corrosion attacks on copper introduced by PBS (Ref. 21) and the additional influences induced by bacterial addition.[22]

[a)]**Electronic mail:** jiaqi.luo@uni-saarland.de

The purpose of this study is to better understand the relationship between corrosion and the antibacterial activity on copper surfaces. To better verify the relevant factors, cuprous oxide (Cu_2O) coating was also prepared by the sputtering method for comparison. Two buffers [PBS and Na-4-(2-hydroxyethyl)-1-piperazineethanesulfonic acid (Na-HEPES)] that introduced corrosion phenomena were characterized by *ex situ* metallographic means. Kinetics of copper ion release from two types of surfaces into two buffers are discussed, taking the role of bacteria into consideration, correlated with the antibacterial efficiency measured.

II. MATERIALS AND METHODS

A. Materials

Coupons of copper (99.99%, K09, Wieland) were first mechanically ground with a silicon carbide sandpaper (stepped down to grit number P600), then cleaned with ethanol in an ultrasonic bath, and finally dried by air. Cuprous oxide (Cu_2O) coating was fabricated on a microscope glass slide, by a reactive magnetron sputtering technique. Before being transferred into the sputtering chamber, the substrate was cleaned with ethanol in an ultrasonic bath. The distance between the substrate and the Cu target (99.99%) was 50 mm. During deposition, the sputtering pressure was maintained at 0.5 Pa, while the flow rate of argon and oxygen was 25 and 7 sccm, respectively. The sputtering process was performed with a constant current of 0.3 A (power around 150 W) by a pulsed-DC generator (Pinnacle, Advanced Energy). Frequency and off time were 50 kHz and 4 μs, respectively. The total deposition time was 5 min. Confirmation of its phase composition is shown in Fig. 1 in the supplementary material.[37]

B. Solutions

PBS was prepared with $NaH_2PO_4 \cdot 1H_2O$ (Merck, Germany, final concentration 0.01M), NaCl (VWR, Germany, final concentration 0.14M), and pure water for analysis (Merck, Germany), and its *p*H value was adjusted by adding NaOH to 7.4. Na-HEPES (final concentration 0.1M) was prepared with HEPES-free acid (VWR, Germany), pure water for analysis, and NaOH in the same way, with a final *p*H of 7.0. Both buffers were sterilized in an autoclave after preparation.

C. Corrosion protocol

To simulate the antibacterial efficiency test further described in Sec. II E, the droplet exposure method was applied to introduce corrosion. In brief, 20 μl of PBS or Na-HEPES was applied on coupons with a pipette. These coupons were placed in a water-saturated atmosphere at room temperature. After specific time intervals, these solutions were withdrawn with a pipette, and the coupons were simply dried in a ventilated room.

D. Surface characterization

The morphology of copper surfaces before and after the corrosion experiment was compared in a scanning electron microscope (SEM, Helios NanoLab600, FEI). Acceleration voltages will be further mentioned in the corresponding figure captions. For the phase confirmation of corrosion products forming on the surfaces, Raman spectroscopy (Raman, operating at 532 nm, inVia, Renishaw) was applied. Images and spectra were obtained within 24 h after corrosion treatment. Additionally, the phase composition of sputtered coating was examined by Raman and a grazing incidence x-ray diffractometer (Cu Kα with a 1° grazing angle, PANalytical X'Pert PRO MRD).

E. Antibacterial efficiency determination

The wet-plating test was used, whose details could also be referred to the previous publication.[12] In brief, the *Escherichia coli* (*E. coli*) K12 strain was grown aerobically overnight in a lysogeny broth (LB) medium at 37 °C in a water bath with a speed of 220 rpm. The stationary cells from 5 ml culture were collected by centrifugation for 15 min at 5000×*g*, washed and centrifuged three times with PBS or Na-HEPES accordingly, and finally resuspended in 5 ml of the same type of buffer. The test started by applying 20 μl of the bacterial suspension on the coupons that were placed in a water-saturated atmosphere at room temperature. When the set duration was reached, 10 μl samples were withdrawn by repetitive pipetting, serially diluted in PBS, and spread on LB agar plates. Following incubation at 37 °C for 24 h, the colony-forming unit (cfu) on agar plates was counted and expressed in a way concerning both the fold of dilutions and relative to the original 20 μl samples. The average values and standard deviations were obtained by three independent experiments.

F. Copper release determination

After the corresponding surface treatment (corrosion or the antibacterial efficiency test), 10 μl samples were withdrawn by repetitive pipetting and diluted in 2.990 ml 1 wt. % nitric acid (Merck, Germany). Before being measured by inductively coupled plasma mass spectrometry (ICP-MS, 7500cx, Agilent), 3 μl of 10 mg/l scandium and cesium internal standard solutions were added to the samples. For calibration, standards with 0.1, 0.5, 2.5, 10, 50, 250, and 1000 μg/l of copper were used. Original results with a unit of parts per billion were converted to the final results with a unit of μmol/l (μM), concerning both the fold of dilutions and molar mass 63.55 g/mol for copper. The average values and standard deviations were obtained by three independent experiments.

III. RESULTS AND DISCUSSION

A. Surface changes of copper in pure buffers

Among those studies focusing on the antibacterial property of copper, the status of the copper surface itself is rarely

examined. Therefore, in the current work, efforts were put into observing how the surface was transformed, first by high resolution SEM images shown in Fig. 1. As can be seen, the copper surface varied significantly when exposing to different buffers. In PBS, a considerable amount of small dispersed particles are found in 1 h. In a longer period, these corrosion products grew coarser and merged with each other, gradually covering a bigger portion of the original copper surface. On the other hand, in the case of Na-HEPES, the early-stage corrosion phenomena were less evident, since no corrosion product can be found even in 3 h. There are merely some submicrometer features with darker contrast and nanoscale topography differences [Fig. 2 in the supplementary material (Ref. 37)].

As the chemical composition of the corrosion products could be helpful, Raman was applied on the 3 h coupons. Their spectra are grouped with two colors in Fig. 2. Apart from the slight difference in the background intensity, other features are similar within each type of coupon. Three major Raman peaks (148, 219, and 637 cm^{-1}) found after PBS treatment are assigned to Cu_2O, confirmed by sputtered Cu_2O coating [Fig. 1 in the supplementary material (Ref. 37)] as well as results from the literature,[23] whereas no Raman peak was obtained from the Na-HEPES treated coupons, which is consistent with the findings of SEM.

The distinctions with regard to how copper surfaces evolved in two buffers are necessary in the following investigation. Because Cu_2O is the only corrosion product found in the case of PBS, the forthcoming experiment design is based on it. Therefore, it should be noted that this current result is unlike our early work[16] where an ellipsometer was applied and a layer of CuO was observed. Although ellipsometry is more sensitive to the ultrasurface properties and can be employed *in situ*, it is also a technique highly relying on a precise modeling process. For instance, the roughness can be a crucial factor in the model, but it is not easy to consider the sustained topographical change due to oxide growth. On the other hand, although the current results were obtained *ex situ*, the possible impacts have been excluded to a great extent by reducing the intervals between corrosion experiments and the SEM/Raman characterization. Hence, the exposure time can still be found as the most predominant factor. Furthermore, the Cu_2O growth in PBS has also been confirmed and characterized by versatile techniques in our recent studies,[21,22] where CuO has hardly been found.

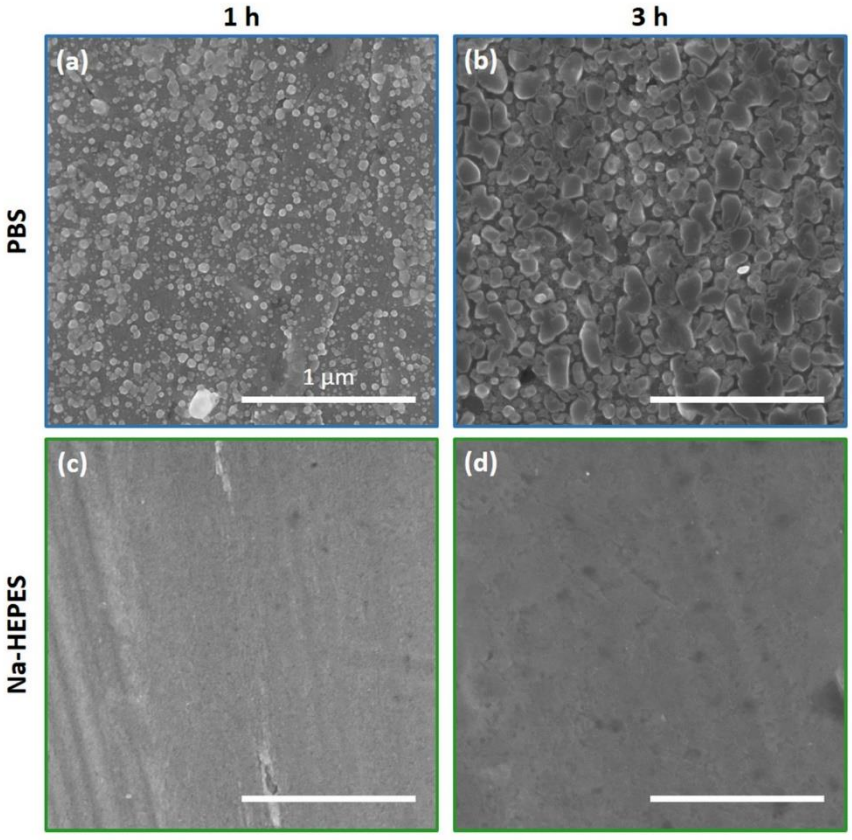

FIG. 1. Typical SEM images of the copper surface after 1 h [(a) and (c)] and 3 h [(b) and (d)] exposure to PBS [(a) and (b)] or Na-HEPES [(c) and (d)]. All images were obtained at 5 kV and share the same scale bars presented in (a).

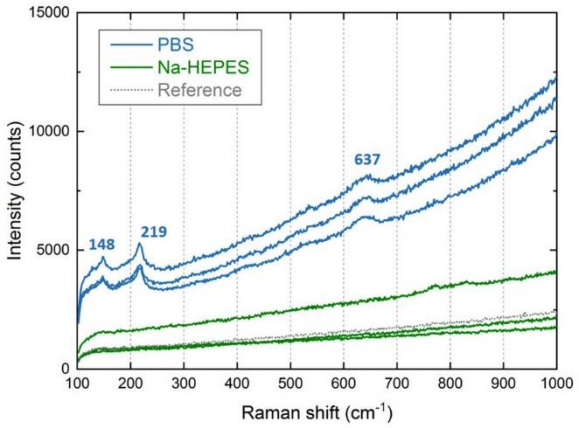

FIG. 2. Raman spectra obtained from the copper surface after 3 h exposure in two buffers. Three random locations were chosen from each sample represented by the same color. The reference spectrum was obtained from the copper surface without exposure to any solution.

B. Copper release and antibacterial efficiency

Apart from having the copper surface modified, corrosion also results in copper release into the applied droplets. The trends of copper content presented in the droplets along the time are plotted in Fig. 3 [values are listed in Table 1 in the supplementary material (Ref. 37)]. Two distinctive release patterns in these solutions are observed. At the start, copper release was rather rapid in PBS, but a plateau was already recorded after the first 30 min. More interestingly, a slight decline can be found from 1 h.

In contrast, a different path was recorded in Na-HEPES. In the first place, the average release rate was relatively low, with $1.87 \times 10^2\,\mu$M after 30 min, which was less than half of $3.41 \times 10^2\,\mu$M that was presented in PBS. However, the copper content kept rising in Na-HEPES, reaching almost a similar value as in PBS in 1 h. At the end of the test, this value ascended to more than one and a half times as in PBS, without any potential plateaus even until 9 h [Fig. 3 in the supplementary material (Ref. 37)].

Since the antibacterial activity is strongly correlated with copper content presented, the wet-plating test against *E. coli* was carried out and is displayed in Fig. 4. In PBS, the count of live bacteria reduced by already one log in 1 h and nearly five logs in 3 h. In comparison, the killing rate was considerably slow in Na-HEPES, which has a only two log deduction in 3 h. However, only a small section of these trends (before 1 h) could be positively associated with the above-mentioned copper release. The fact that the higher amount of copper released into Na-HEPES in the following hours did not as expected causes a corresponding increase in its killing rate.

One possibility why these two data sets fail to correlate with each other can be that the presence of *E. coli* has not been considered. A recent study[24] reported that the presence of bacteria in PBS significantly increased the copper content in the suspension. We, therefore, redesigned a similar experiment and verified this discrepancy and attributed it to the role of *E. coli*:[22] they accumulate copper, and thus, the formation of Cu_2O is inhibited. As the copper surface is not covered by Cu_2O, corrosion continues and consequently enhances copper content in the solution.

Therefore, the copper release in Na-HEPES was again measured, but with the presence of *E. coli*, as plotted in Fig. 5. The trend shown in pure Na-HEPES is similar to the one shown in Fig. 3, and only the absolute values are slightly different. This could be mainly ascribed to the fact that the state of the copper coupon where each droplet was deposited was not perfectly the same. However, adding *E. coli* into Na-HEPES did not change the trend dramatically, compared to the huge rise observed in the case of PBS.[22,24]

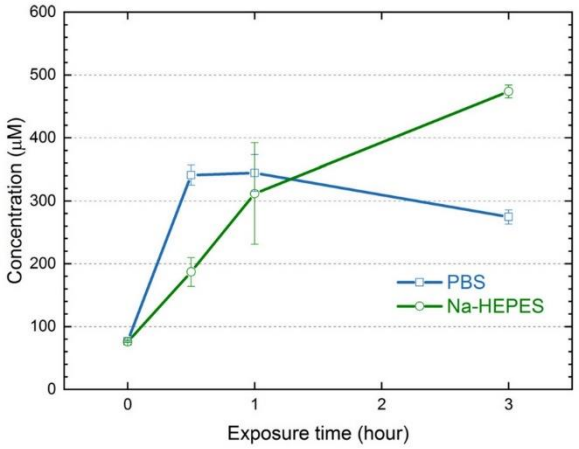

FIG. 3. Copper content released from the copper surface into PBS or Na-HEPES following various exposure periods. The error bars indicate the standard deviations calculated from three independent measurements.

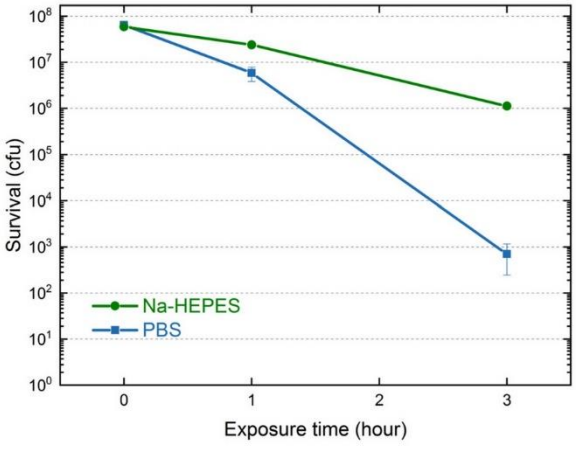

FIG. 4. Results of the antibacterial efficiency test against *E. coli* on copper in two buffers. The error bars indicate the standard deviations calculated from three independent measurements. The values at 0 h serve as controls, representing the cfu measured from both original suspensions when the 3 h samples were withdrawn.

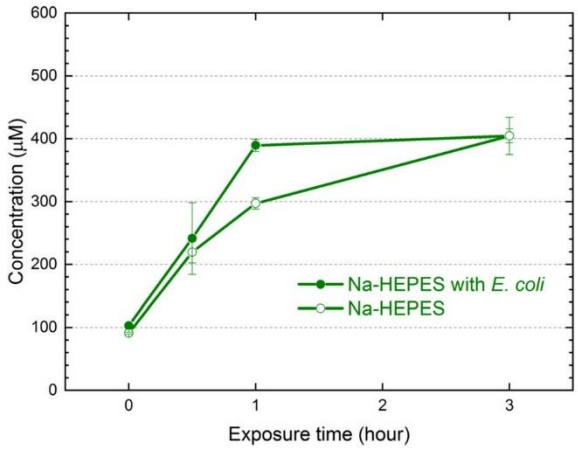

FIG. 5. Copper content released from the copper surface into the Na-HEPES and *E. coli* Na-HEPES suspension following various exposure periods. The error bars indicate the standard deviations calculated from three independent measurements.

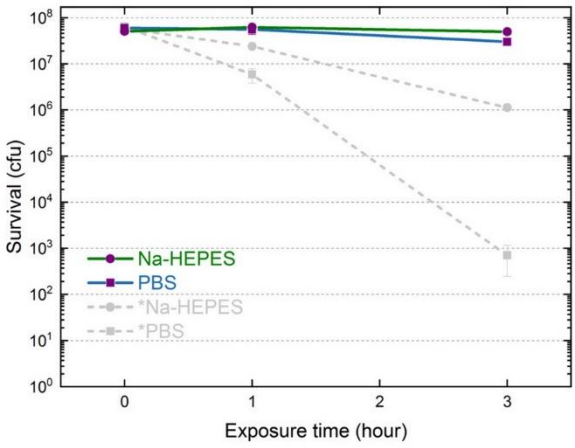

FIG. 6. Results of the antibacterial efficiency test against *E. coli* on Cu_2O coating in two buffers. The error bars indicate the standard deviations calculated from three independent measurements. The values at 0 h serve as controls, representing the cfu measured from both original suspensions when the 3 h samples were withdrawn. Trends shown with gray dashed lines represent the data already shown in Fig. 4 for comparison.

Only a higher value was recorded in 1 h (reason still unknown at the moment); nevertheless, the gap between two scenarios narrowed again in 3 h. In other words, copper release in pure Na-HEPES still approximately reflects a similar scenario with *E. coli* addition, but not in the case of PBS. Because of this, it is no surprise that *E. coli* were found being deactivated quicker in PBS.

Nowadays, in order to measure the release profile of the antibacterial substance, pure buffers rather than bacterial suspensions were widely used.[15,25,26] However, the current findings imply that the evaluation with pure buffers could have limits in representing the actual concentration of the antibacterial substance in the presence of bacteria. When this is the case (e.g., in PBS), bacterial suspensions should be applied. Besides, suspensions with dead bacteria can also be applied[22] so as to explore the impacts of bacteria in a more detailed way.

C. New insights provided by Cu_2O coating

Comparing these corrosion behaviors of copper in two buffers, it is not difficult to figure out that Cu_2O may play an indicative role. For example, since its formation in pure PBS could be considered as a barrier hindering direct ion release from the copper surface, bacteria that inhibit its formation thus allows continuous copper release.[22] On the contrary, since Cu_2O is not even detectable in pure Na-HEPES, bacterial addition does not cause further enhancement of copper release.

To better understand the role of this oxide, Cu_2O coupons were prepared by the sputtering method. Their phase information was confirmed and is given in Fig. 1 in the supplementary material,[37] although it has to be admitted that it is difficult to mimic the exact microstructure or surface roughness of copper coupons or the oxide formation. The antibacterial efficacy against *E. coli* measured in two buffers is shown in Fig. 6. In general, the Cu_2O surface was much less effective, compared to the copper surface. In 3 h, survival in PBS that is a bit less, however, is still higher than the 1 h value in Na-HEPES on copper. Similar Cu_2O coating produced by chemical vapor deposition also shows a weaker killing rate compared to copper coating.[20]

These observations, nevertheless, rule out the contributing role of Cu_2O in showing the antibacterial activity of the copper surface. That is to say, although to oxidize copper is a necessary step for releasing copper ions, Cu_2O itself does not necessarily exist as an essential direct/intermediate product. Simply supposing it does, then these Cu_2O coatings should have shown better (or at least equal) antibacterial efficiency compared to the copper surface because the route to release antibacterial copper ions should have been shortened.

It also needs to be noted that, unlike the antibacterial scenario introduced by copper oxide nanoparticles in the aqueous phase,[27] it was mainly the dissolution that transformed Cu_2O coating to copper ions so that the further bacterial membrane, nucleic acids, or protein could be mediated or undermined.[10] Therefore, to further explore how Cu_2O behaves in two buffers, copper release curves of the Cu_2O coating were also measured and are shown in Fig. 7. First of all, with the presence of *E. coli*, copper content kept increasing in both buffers but at a different rate. In 3 h, this value almost reached 400 μM in PBS, whereas less than 150 μM was recorded in Na-HEPES. This explains why on Cu_2O coating, *E. coli* in PBS were killed faster than those in Na-HEPES.

Besides, these release curves within each pure buffer show certain similarities with those obtained from the copper surface. Take PBS as an example, *E. coli* addition again promoted the copper release rate on the Cu_2O surface. This

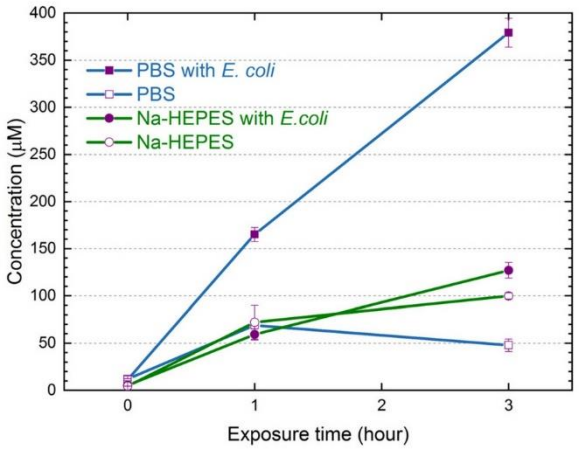

FIG. 7. Copper content released from Cu_2O coating into PBS, the *E. coli* PBS suspension, the Na-HEPES or *E. coli* Na-HEPES suspension following various exposure periods. The error bars indicate the standard deviations calculated from three independent measurements.

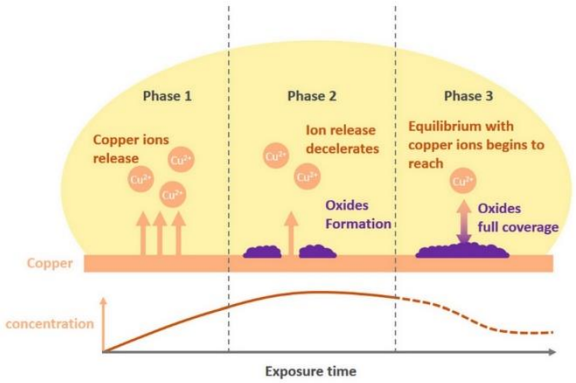

FIG. 8. Schematic model of corrosion phenomena on the copper surface in buffers. The time scale is only approximate. The section as a dotted line in concentration curves in Phase 3 signifies speculation from the current data.

effect was not dramatically influenced by the survival of bacteria, where more live bacteria were presented, compared to that on the copper surface. In addition, a slight decline is again observed in PBS after 1 h. On copper surface, this decline is considered as a result of oxide redeposition. However, this effect should be less predominant on originally oxide surface. It is, therefore, suggested that reactions between copper ions and other ingredients presented in PBS could happen, resulting in precipitation or redeposition of other species (e.g., copper phosphate[28]).

On the other hand, in Na-HEPES, bacterial addition did not markedly affect the release trend. Similar features are obtained on copper as well. This means that although the presence of *E. coli* and their additional copper accumulation effects could reduce the amount of copper ions, unlike in PBS, they are not governing the kinetics of corrosion of copper or dissolution of Cu_2O in Na-HEPES.

D. Copper transference in buffers

With the additional information of the Cu_2O surface, the transfer path of copper in these two buffers can be further summarized as shown in Fig. 8. In the beginning, corrosion happens when copper contacts the buffer droplet that contains a limited amount of copper ions. This process, which could be assisted by other species presented in the buffer (e.g., chloride ions), turns copper into its ionic form by corrosion, a key step transferring bulk copper into solution. In most of the cases, this leads to a rise of copper concentration in the buffer, hereafter named as "Phase 1."

The release rate varies from buffer to buffer due to their own corrosion properties. As the free copper content reaches a certain level, additional species could form in the solution, consuming copper content, marking the start of "Phase 2." In the case of PBS, oxide could redeposit on the copper surface[21] and gradually impede copper release (i.e., slowing down corrosion rate). Consequently, the concentration curve could be recorded as a slower rise.

As the oxide coverage is fulfilled, the condition for direct release of the copper surface may not exist anymore, which is classified as the outset of "Phase 3." Meanwhile, the remaining copper ions in the solution could keep forming oxides or other copper-contained species until each of their equilibrium is reached. Since these processes consume copper content and could lead to sedimentation, a reduction of copper concentration probably followed by another plateau is expected. A relatively complete path has been mapped in PBS presented in this study and the NaP_i buffer in another research.[12] The fact that they reached different plateau concentrations could be again associated with the properties of buffers, further resulting in the diversity of their corrosion rates, oxides/species formation rates, equilibrium conditions, etc.

Moreover, the timing of entering each phase can be changed with the presence of bacteria. On one hand, the existence of bacteria tends to postpone the formation of oxide, prolongs Phase 1, and thereby promotes copper release. On the other hand, since bacteria reduce the surrounding copper concentration, it could also promote ion release when the release kinetics is, to some extent, governed by it (e.g., the PBS-Cu_2O system). Since the copper surface in Na-HEPES is found staying in Phase 1 within the current experimental duration, adding bacteria does not alter its release curve, mainly because oxide formation has not even started. Future work is needed to track its release curve in much extended duration, if it is the aim to describe the whole corrosion process or equilibrium situation.

Nevertheless, one should notice that by ICP-MS measurement performed in this study, it was the total amount of copper present in the aqueous sample that has been measured, regardless of its existing form. Therefore, the amount of free copper ions may not be exactly reflected due to the possible formation of copper phosphate (in the case of PBS) or complex species (in the case of Na-HEPES). Furthermore, copper content that has been accumulated by the bacteria may return to the sample, adding complication to this scenario.

Both confirmation of the existing species and exact calculation should be helpful in depicting a more complete picture of the copper transfer path.

E. Practical hints for antibacterial surface research

For the antibacterial surfaces relying on a certain type of ion release such as copper and silver,[25] surface corrosion plays an essential role in the release process. To discuss corrosion phenomena, not only the surface (material) but also the applied solution/buffer (environment) should be taken into account because corrosion behaviors are likely to vary in different media.[29] It could affect the release kinetics of the antibacterial substance. The discrepancy of the antibacterial activity can thus be obtained from the same surface. In the current study, replacing PBS by Na-HEPES changed both the killing rate against *E. coli* shown by the copper coupon and Cu_2O coating. For the same reason, applying buffers with different *p*H values may already induce significant variation. It is, therefore, important to keep in mind that antibacterial efficiency shall be precisely addressed together with the characteristics of environment that are applied, rather than solely ascribed to the surface itself.

This perspective, however, adds difficulty and uncertainty in understanding or performing the antibacterial efficiency test. Take our former study[30] as an example, it reports the antibacterial effect of the cadmium surface, where silver as a widely known antimicrobial candidate was also included as a reference but has not shown an outstanding performance. This has been attributed to a low amount of silver ion release, as a result of insufficient corrosion. However, one cannot thereby claim that silver has a poor antibacterial activity, since this result could be simply caused by picking a "wrong" buffer, which could not efficiently corrode or interact with the silver surface.

Even a buffer could be "wrong" for some surfaces, in those widely used antibacterial efficiency tests [e.g., JIS Z 2801 (Ref. 31) and live/dead assays[32]], a certain buffer needs to be chosen and applied for all type surfaces. In other words, this fair protocol (every surface is treated with the same buffer) could be essentially unfair. One promising approach is to investigate the aimed medical environment before selecting the buffer and then select or design a buffer with specific composition, which could reflect the actual scenario to a great extent and thus the corresponding antibacterial efficiency. In this sense, studies that simulated the organic contamination[14] or synthetic perspiration[15] have set a meaningful and practical example.

From the perspective of materials research, there are many implications once the importance of corrosion is recognized. For instance, by modifying the corrosion tendency through alloying[33] or grain boundary engineering,[34] the corresponding antibacterial property could be better tailored. In the case of copper, we recently analyzed its localized corrosion sites in PBS, which could serve as a guideline in controlling the release of antibacterial copper ions.[21]

Moreover, characterizations of the formation of various corrosion products on antibacterial surfaces are recommended to be included. On one hand, identifying them helps revealing the possible modifications of the tested surface, especially during the killing process. On the other hand, since aging of the surface could influence bacterial behaviors (e.g., adhesion[35]), it becomes crucial to examine and recognize the actual surface status. Furthermore, the corrosion products themselves have potential to govern (or cease, in the case of Cu_2O) the ion release. That is to say, the release-time profile could be "programed," which could be beneficial for biocompatible medical applications.[36]

IV. SUMMARY AND CONCLUSIONS

In the first part of this work, we compared the corrosion phenomena on the copper surface caused by PBS and Na-HEPES. Pure PBS is favorable for the formation of Cu_2O acting as a barrier layer, whereas in Na-HEPES, no obvious oxide could be observed in 3 h; hence, copper concentration keeps rising in the whole experimental period. The difference in antibacterial efficiencies shown by the wet-plating test against *E. coli* has been better interpreted with the copper content measured with the presence of bacteria.

In the second part, sputtered Cu_2O coating was introduced to verify its role in corrosion of metallic copper and how the antibacterial activity is achieved/affected. Similar discrepancies in antibacterial effects and the ion release trend were obtained in two different buffers. These detailed results confirm its poorer antibacterial effect compared to metallic copper; on the other hand, they reveal a difference in corrosion kinetics in two buffers. All of these aspects strongly suggest the necessity of correlating antibacterial efficiency not only with the surfaces themselves but also with the specific environment applied.

ACKNOWLEDGMENTS

This study was supported by the Erasmus Mundus Joint European Doctoral Programme in Advanced Materials Science and Engineering (DocMASE, No. 512225-1-2010-1-DE-EMJD, European Commission) and the PhD-Track-Programme (No. PhD02-14, Franco-German University). The ICP-MS experiments were supported by Ralf Kautenburger from the chair of Inorganic Solid State Chemistry. The authors acknowledge Volker Presser and the Leibniz Institute for New Materials for the access of Raman spectrometer. J.L. thanks Marc Solioz at the University of Bern for critical reading and continuous support.

[1]H. T. Michels, C. W. Keevil, C. D. Salgado, and M. G. Schmidt, Health Environ. Res. Des. J. **9**, 64 (2015).
[2]T. Frieden, "Antibiotic resistance threats in the United States," U.S. Department of Health and Human Services, Centers for Disease Control and Prevention, 2013.
[3]K. Bazaka, M. V. Jacob, R. J. Crawford, and E. P. Ivanova, Appl. Microbiol. Biotechnol. **95**, 299 (2012).
[4]E. Unosson, M. Morgenstern, H. Engqvist, and K. Welch, J. Mater. Sci. Mater. Med. **27**, 1 (2016).
[5]E. P. Ivanova *et al.*, Small **8**, 2489 (2012).
[6]I. Ferreri, S. Calderon V, R. Escobar Galindo, C. Palacio, M. Henriques, A. P. Piedade, and S. Carvalho, Mater. Sci. Eng. C **55**, 547 (2015).

[7]J. O'Gorman and H. Humphreys, J. Hospital Infect. **81**, 217 (2012).
[8]H. Michels, S. Wilks, J. Noyce, and C. Keevil, "Copper alloys for human infectious disease control," https://eprints.soton.ac.uk/429845/.
[9]Y. Lou, L. Lin, D. Xu, S. Zhao, C. Yang, J. Liu, Y. Zhao, T. Gu, and K. Yang, Int. Biodeterior. Biodegrad. **110**, 199 (2016).
[10]G. Borkow and J. Gabbay, Curr. Med. Chem. **12**, 2163 (2005).
[11]M. Yasuyuki, K. Kunihiro, S. Kurissery, N. Kanavillil, Y. Sato, and Y. Kikuchi, Biofouling **26**, 851 (2010).
[12]C. Molteni, H. K. Abicht, and M. Solioz, Appl. Environ. Microbiol. **76**, 4099 (2010).
[13]C. E. Santo, N. Taudte, D. H. Nies, and G. Grass, Appl. Environ. Microbiol. **74**, 977 (2008).
[14]A. Różańska, A. Chmielarczyk, D. Romaniszyn, A. Sroka-Oleksiak, M. Bulanda, M. Walkowicz, P. Osuch, and T. Knych, Int. J. Environ. Res. Public Health **14**, 813 (2017).
[15]L. L. Foster, M. Hutchison, and J. R. Scully, Corrosion **72**, 1095 (2016).
[16]M. Hans, A. Erbe, S. Mathews, Y. Chen, M. Solioz, and F. Mücklich, Langmuir **29**, 16160 (2013).
[17]C. Toparli, S. W. Hieke, A. Altin, O. Kasian, C. Scheu, and A. Erbe, J. Electrochem. Soc. **164**, H734 (2017).
[18]O. Imantalab, A. Fattah-alhosseini, M. K. Keshavarz, and Y. Mazaheri, J. Mater. Eng. Perform. **25**, 697 (2016).
[19]M. Turalija, P. Merschak, B. Redl, U. Griesser, H. Duelli, and T. Bechtold, J. Mater. Chem. B **3**, 5886 (2015).
[20]I. A. Hassan, I. P. Parkin, S. P. Nair, and C. J. Carmalt, J. Mater. Chem B **2**, 2855 (2014).
[21]J. Luo, C. Hein, J.-F. Pierson, and F. Mücklich, Mater. Charact. **158**, 109985 (2019).
[22]J. Luo, C. Hein, J. Ghanbaja, J.-F. Pierson, and F. Mücklich, Micron **127**, 102759 (2019).
[23]L. Debbichi, M. C, Marco de Lucas, J. F. Pierson, and P. Krüger, J. Phys. Chem. C **116**, 10232 (2012).
[24]C. Hahn, M. Hans, C. Hein, R. L. Mancinelli, F. Mucklich, R. Wirth, P. Rettberg, C. E. Hellweg, and R. Moeller, Astrobiology **17**, 1183 (2017).
[25]E. Unosson, D. Rodriguez, K. Welch, and H. Engqvist, Acta Biomater. **11**, 503 (2015).
[26]S. Agnihotri, S. Mukherji, and S. Mukherji, Nanoscale **5**, 7328 (2013).
[27]S. Meghana, P. Kabra, S. Chakraborty, and N. Padmavathy, RSC Adv. **5**, 12293 (2015).
[28]G. He, W. Hu, and C. M. Li, Colloids Surf. B **135**, 613(2015).
[29]B. Millet, C. Fiaud, C. Hinnen, and E. M. M. Sutter, Corros. Sci. **37**, 1903 (1995).
[30]J. Luo, C. Hein, F. Mücklich, and M. Solioz, Biointerphases **12**, 020301 (2017).
[31]H. Kawakami, K. Yoshida, Y. Nishida, Y. Kikuchi, and Y. Sato, ISIJ Int. **48**, 1299 (2008).
[32]T. Diu, N. Faruqui, T. Sjöström, B. Lamarre, H. F. Jenkinson, B. Su, and M. G. Ryadnov, Sci. Rep. **4**, 7122 (2014).
[33]S. Sykes and J. W. Bond, J. Forensic Sci. **58**, 138 (2013).
[34]A. Vinogradov, T. Mimaki, S. Hashimoto, and R. Valiev, Scr. Mater. **41**, 319 (1999).
[35]M. B. Valcarce, J. P. Busalmen, and S. R. de Sánchez, Int. Biodeterior. Biodegrad. **50**, 61 (2002).
[36]G. A. Norambuena, R. Patel, M. Karau, C. C. Wyles, P. J. Jannetto, K. E. Bennet, A. D. Hanssen, and R. J. Sierra, Clin. Orthop. Relat. Res. **475**, 722 (2017).
[37]See supplementary material at https://doi.org/10.1063/1.5123039 for phase confirmation of Cu_2O coating, high resolution SEM images of Na-HEPES treated surface, and copper ion release in extended period.

Supplementary Information

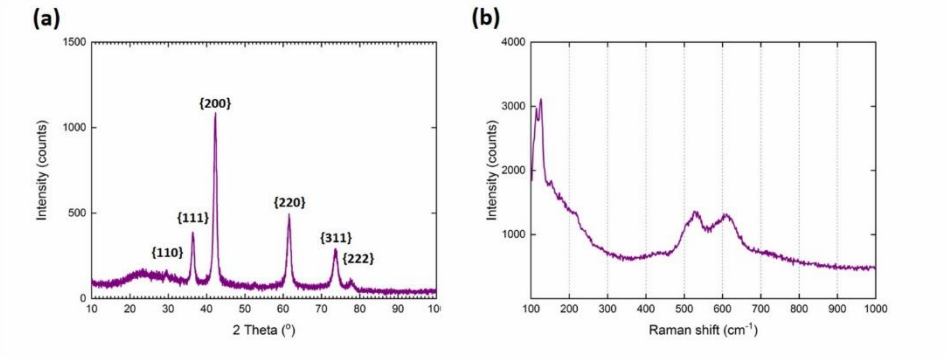

Supplementary Figure 1 | Grazing incidence X-ray diffractogram (indexed with JCPDS #75-1531) **(a)** and Raman spectrum **(b)** of sputtered coating on glass substrate, confirming Cu_2O as the predominant phase.

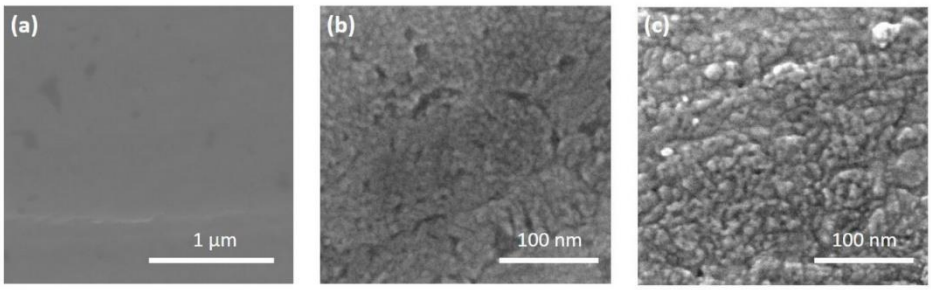

Supplementary Figure 2 | High resolution SEM images of copper surfaces before **(a & b)** and after **(c)** 3 h exposure to Na-HEPES (not from the same location). Images were obtained at 15 kV.

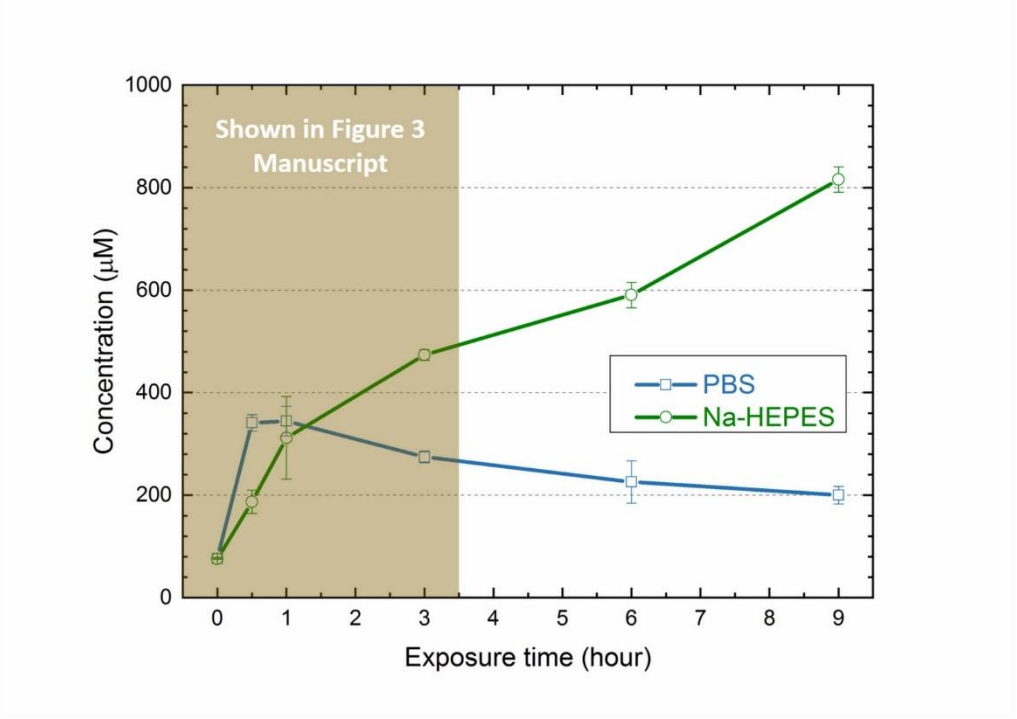

Buffer	Exposure time				
	30 min	1 h	3 h	6 h	9 h
PBS	341±15.9	345±29.0	275±11.3	226±41.5	200±17.2
Na-HEPES	187±23.0	312±80.6	474±10.3	591±24.7	816±81.5

Supplementary Figure 3 and Table 1 | The copper content (μM) released from copper surface into PBS or Na-HEPES as a function of exposure time. The error bars indicate the standard deviations calculated from three independent measurements, which are also shown in the table.

Biointerphases
A Journal of Biomaterials and Biological Interfaces
ERRATUM
avs.scitation.org/journal/bip

Erratum: "Early-stage corrosion, ion release, and the antibacterial effect of copper and cuprous oxide in physiological buffers: Phosphate-buffered saline vs Na-4-(2-hydroxyethyl)-1-piperazineethanesulfonic acid" [Biointerphases 14, 061004 (2019)]

Cite as: Biointerphases 16, 018601 (2021); doi: 10.1116/6.0000835
Submitted: 3 December 2020 · Accepted: 9 December 2020 ·
Published Online: 5 January 2021

Jiaqi Luo,[1,2,a] Christina Hein,[3] Jean-François Pierson,[2] and Frank Mücklich[1]

AFFILIATIONS

[1]Functional Materials, Saarland University, 66123 Saarbruecken, Germany
[2]Université de Lorraine, CNRS, IJL, F-54000 Nancy, France
[3]Inorganic Solid State Chemistry, Saarland University, 66123 Saarbruecken, Germany

[a]Author to whom correspondence should be addressed: jiaqi.luo@uni-saarland.de

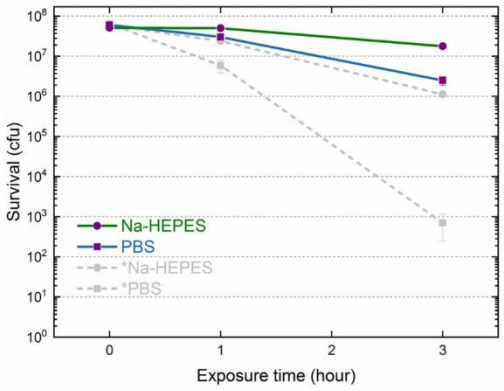

FIG. 6. Results of the antibacterial efficiency test against E. coli on Cu2O coating in two buffers. The error bars indicate the standard deviations calculated from three independent measurements. The values at 0 h serve as controls, representing the cfu measured from both original suspensions when the 3 h samples were withdrawn. Trends shown with gray dashed lines represent the data already shown in Fig. 4 for comparison.

In the original article,[1] Fig. 6 presents wrong survival (cfu) values of Cu_2O coating: Values at 1 h and 3 h were mistakenly plotted with those obtained at 30 min and 1 h, respectively. In the corrected figure, values at 1 h and 3 h are replaced accordingly. Values at 30 min (1 h in original version) are not plotted in order to keep the same format with Fig. 4 for better comparison.

This correction causes the following description in the second paragraph of Sec. III C to be invalid: "In 3 h, survival in PBS that is a bit less, *however, is still higher than the 1 h value in Na-HEPES on copper.*" Apart from this, other relevant discussion and conclusions are still intact.

The authors would like to apologize for any inconvenience caused.

REFERENCES

[1]J. Luo, C. Hein, J.-F. Pierson, and F. Mücklich, Biointerphases **14**, 061004 (2019).

4. Effects of Bacteria on Copper Surface in PBS

In this chapter, the below peer-reviewed publication is going to be presented:

Bacteria accumulate copper ions and inhibit oxide formation on copper surface during antibacterial efficiency test

Reproduced from Jiaqi Luo, Christina Hein, Jaafar Ghanbaja, Jean-François Pierson, Frank Mücklich, *Micron*, 2019, 127, with the permission of Elsevier

DOI: 10.1016/j.micron.2019.102759

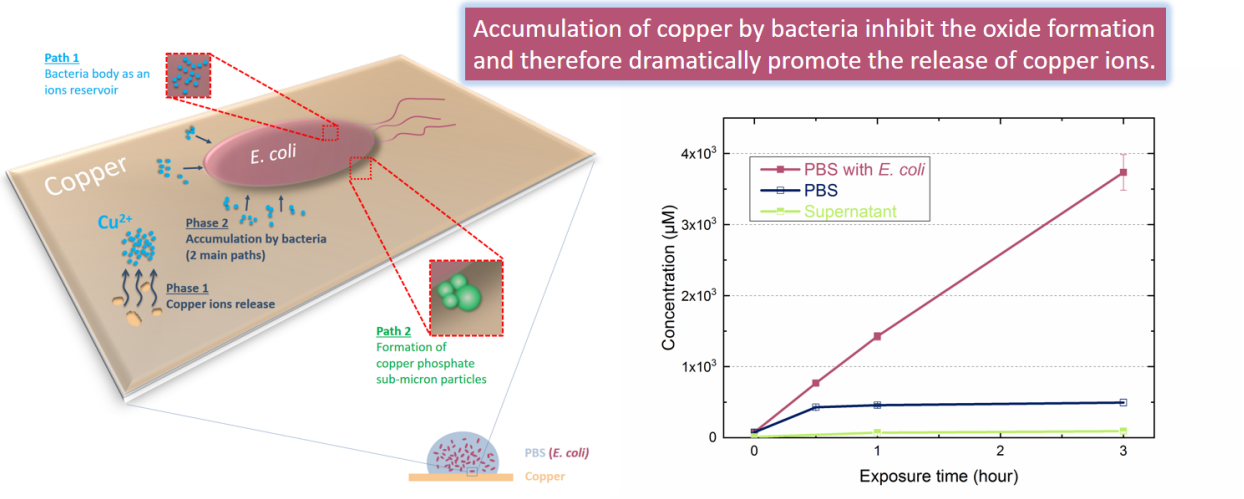

Contribution: Conceptualisation, Methodology, Validation (except from ICP-MS measurements and TEM observations), Investigation, Writing – Original Draft, Visualization, Project administration.

Micron 127 (2019) 102759

Contents lists available at ScienceDirect

Micron

journal homepage: www.elsevier.com/locate/micron

Bacteria accumulate copper ions and inhibit oxide formation on copper surface during antibacterial efficiency test

Jiaqi Luo[a,b,*], Christina Hein[c], Jaafar Ghanbaja[b], Jean-François Pierson[b], Frank Mücklich[a]

[a] Functional Materials, Saarland University, Germany
[b] Université de Lorraine, CNRS, IJL, F-54000, Nancy, France
[c] Inorganic Solid State Chemistry, Saarland University, Germany

ARTICLE INFO

Keywords:
Copper
Oxidation
Ions
ICP-MS
EDS
E. coli

ABSTRACT

Copper surface after antibacterial test against *E. coli* was examined in the aspect of corrosion. Results from scanning electron microscope (SEM), grazing incidence X-ray diffractometer (GIXRD) and Raman spectroscopy together confirmed less oxidation on copper surface with the presence of *E. coli*. The inhibition of the cuprous oxide (Cu_2O) layer instead ensured the continuous exposure of copper surface, letting localised corrosion attacks observable and causing a stronger release of copper ions. These phenomena are attributed to the fact that *E. coli* act as ions reservoirs since high amount of copper accumulation were found by energy dispersive X-ray spectroscopy (EDS).

1. Introduction

Copper has been drawing the attention of microbiologists in the recent years (Vincent et al., 2018; Turner, 2017; Rock et al., 2018; Muller et al., 2018). Copper and its ions, copper oxides as well as oxide nanoparticle, all of them have shown the toxicity against various bacteria or virus (Rosenberg et al., 2018; Rotini et al., 2017). This antimicrobial property brings copper into the hygiene market, and without a doubt, a great amount of studies have focused on this aspect. Copper or copper contained coatings (Wu et al., 2014; Souli et al., 2017), particles (Gilbertson et al., 2016; Ben-Sasson et al., 2016), fabrics (Dhineshbabu and Rajendran, 2016; Demir et al., 2015), textiles (Irene et al., 2016; Turalija et al., 2015), composites (Usman et al., 2016; Kara et al., 2016) are being fabricated and widely investigated, in terms of their antimicrobial efficiencies the relevant applications.

To determine the antimicrobial efficiency of a certain material, or more specifically of a surface, a certain method has to be applied. It allows us to measure the survival of microbe, to quantify the antibacterial efficacy, and in the end, to compare them. Most of these methods could be grouped into two main types that worth being briefly introduced. One is where no suspension with bacteria needs to be prepared, for instance, in the inhibition zone determination (Usman et al., 2016; Cano et al., 2018). The coupon to be tested will be placed on a nutrient agar plate already covered with bacteria. Since the antibacterial agents could release and further diffuse from the coupon, a gradient of antibacterial substance is supposed to form from the centre of the coupon outwards. After certain incubation periods, there should be a zone around the coupon where no obvious growth of colony is observed. The antibacterial efficiency can be thus compared by the size or radius of these zones. Moreover, this method may tell better the diffusion rate of the corresponding antibacterial substance on the agar plate. It is fairly popular in research especially in testing novel antibacterial composites or fabrics.

In another type of method, a drop of suspension composed of bacteria and buffer solution needs to be applied on the coupon. After several designed time points, part of the suspension is withdrawn. There are a number of approach to determine the bacterial survival in the suspension. One way to do this is by fluorescence microscopy (Wu et al., 2018; Ellinas et al., 2017), which is also often called Live/Dead staining test. In this test, a red-fluorescent indicator (often propidium iodide) is used to label the DNA after membrane damage happens, so as to distinguish whether bacteria are intact or not. Therefore the change of colour directly tells the killing effect of a substance. Another popular approach is to count the colony-forming unit (CFU) (Santo et al., 2011; Tripathy et al., 2017). The withdrawn suspension will be first properly diluted in series and then plated on an agar plate. The cultivable bacteria will grow as colonies that could be big enough to be identified and directly counted. This method not only produces highly statistical and reproducible results, but also allows to track the details of antibacterial efficiency as a function of time. This is why it has been chosen in most

* Corresponding author at: Functional Materials, Saarland University, Campus D3.3, 66123, Saarbruecken, Germany.
E-mail address: jiaqi.luo@uni-saarland.de (J. Luo).

https://doi.org/10.1016/j.micron.2019.102759
Received 14 August 2019; Received in revised form 23 September 2019; Accepted 23 September 2019
Available online 24 September 2019
0968-4328/

of our recent studies (Luo et al., 2017a; Hans et al., 2014, 2013), and again applied in this study.

Although all the methods listed above offer almost sufficient information of the survival of bacteria, nevertheless, there is a hidden respect not being considered: the coupons themselves. The bacteria are inactivated by the antibacterial agents, which are released from the specific surface in most of the cases. This indicates that the surface itself is also under a series of change along the time. In the case of copper, it is corrosion that should be further considered (Zhao et al., 2016; Liu et al., 2017). Furthermore, the corrosion phenomena occurring on the surface, in fact, also alter the surface itself during these antibacterial efficiency tests. In other words, these methods are not always charactering the initial surface, in contrary, a constantly changing surface. Take this into account have two main advantages: one is to know exactly the actual surface being characterised, the other one is to start exploring its potential aging effects when it comes to the daily life applications.

Oxidation is certainly drawing attention among the common corrosion phenomena. By mainly electrochemical means, copper oxides growth on copper or its alloys in buffer solution (Toparli et al., 2017) or synthetic perspiration (Foster et al., 2016) are recently reported. Different types of oxides (Cu_2O, CuO), hydroxide ($Cu(OH)_2$) or other corrosion products ($Cu_2Cl(OH)_3$) could be identified. Their thickness and in-depth distribution were correlated with different experimental conditions, such as the chemical composition of the original surface, the components of the applied solution and the contact period. However, there is a few research that has considered the aging of copper surface in a bacterial suspension, not to mention to probe the role of bacteria in this corrosion system. On the other hand, how bacteria interact with or influence by various kinds of metallic ions or particles have been extensively investigated, in terms of the transportation of ions and the accumulation in different organelles (Carter et al., 2014; Hohle et al., 2011). But again, bacterial influence on the surface through these effects are not the focus in these studies.

One recent research (Wakshlak et al., 2015) revealed the re-release of silver from the silver-killed bacteria back to the solution. It offers a hint about the interaction between ions enriched bacteria and their effect on the environment. Here in the current study, we extended the focus from the solution back to the initial ions releaser: the copper surface itself. The main question we aim to answer is: during the copper release process that kills bacteria, does the existence of these bacteria affect the corrosion process as well? Therefore we investigated the role of *E. coli* in copper surface chemical changes during the antibacterial efficiency test. Ex-situ approaches were performed to distinguish the changes in morphology and composition in the outermost copper surface. The inhibition effect of oxides was described and its possible causes were put forward, taking account of the role of bacteria on the amount of copper ion in suspension.

2. Materials and methods

2.1. Materials

Coupons of copper (99.99%, K09, Wieland) were first ground with a silicon carbide sandpaper (end with grit number as P600), then they were cleaned by an ultrasonic bath with ethanol and finally dried by air.

2.2. Solutions

Phosphate-buffered saline (PBS) was prepared with NaH_2PO_4. $1H_2O$ (Merck, Germany, final concentration 0.01 M), NaCl (VWR, Germany, final concentration 0.14 M) and pure water for analysis (Merck, Germany). Its pH value was adjusted by adding NaOH to 7.4, sterilised by an autoclave after preparation. The preparation of PBS with bacteria could also be referred to the antibacterial efficiency determination in previous publication (Molteni et al., 2010). In brief, the *E. coli* K12 strain was grown aerobically overnight in Lysogeny broth (LB) medium at 37 °C in a water bath with a speed of 220 rpm. The stationary cells from 5 mL culture were collected by centrifugation for 15 min at 5000 × *g*, washed and centrifuged three times with PBS, and finally resuspended in 5 mL of the same type of buffer solution. The initial average cell count was around 3×10^9–5×10^9 CFU/ml. For the suspension *S. cohnii*, the Tryptic soy broth (Fluka) medium was chosen.

2.3. Corrosion protocol

Coupons of copper were placed in a water-saturated atmosphere at room temperature when 20 µL of various solutions were applied on them with a pipette. After certain exposure time (30 min, 1 h, 3 h and 6 h), these solutions were withdrawn with a pipette and the coupons were dried in a ventilated room. These steps are chosen in order to keep it as similar as the antibacterial efficiency tests as described in our other research (Luo et al., 2017a; Hans et al., 2013).

2.4. Surface corrosion characterization

Scanning electron microscope (SEM, Helios NanoLab600, FEI) was used to compare the morphology of copper surfaces after various corrosion experiments. The chemical composition was obtained by Energy dispersive X-ray spectroscopy (EDS) with an acceleration voltage as 5 kV. For further confirmation of corrosion products covering the surfaces as well as the form of copper in bacteria, Raman spectroscopy (Raman, laser source with 633 nm, inVia, Renishaw) with a 50X optical microscopy (OM) and high resolution grazing incidence X-ray diffractometer (GIXRD, Cu Kα with 1 ° grazing angle, PANalytical X'Pert PRO-MPD) were applied. All these images and spectra were obtained within 24 h after corrosion treatment.

2.5. pH values measurements

The pH values were obtained from pH-indicator strips (Merck, Germany), designed for a range from 6.5 to 10.0, with 5 gradations between 7.1 and 8.1, namely 7.1, 7.4, 7.7, 7.9 and 8.1. During the withdrawal process described in Section 2.3, 10 µL of various solutions were separated and applied again on these strips.

2.6. Copper content determination

For the samples (PBS or PBS with *E. coli*) to be directly measured, following almost every step in the corrosion protocol, only whenever the exposure time is reached, 10 µL samples were withdrawn by repetitive pipetting and diluted in 2.990 mL 1 wt% nitric acid (Merck, Germany). For the measurement of supernatant, every three 10 µL samples were transferred and mixed in SafeSeal 1.5 mL tubes. After being centrifuged for 5 min at 5 krpm, 10 µL of supernatant were collected and diluted in nitric acid as mentioned above. For all samples, before measured by inductively coupled plasma mass spectrometry (ICP-MS, 7500cx, Agilent), 3 µl of 10 mg/l scandium and caesium internal standard solutions were added to the samples. For calibration, standards with 0.1, 0.5, 2.5, 10, 50, 250 and 1000 µg/L of copper were used. After obtaining the results with a unit of ppb, the final values with a unit of µM were calculated with the fold of dilutions and molar mass 63.55 g/mol for copper. The average values and standard deviation were obtained by three independent experiments.

2.7. Bacteria imaging and chemical mapping

Scanning transmission electron microscopy (STEM) mode of transmission electron microscopy (TEM, JEM-ARM 200 F, JEOL) was applied with a voltage of 200 kV. The bacteria were treated with copper surface for 3 h as described above. Before having them transferred on a Ni grid,

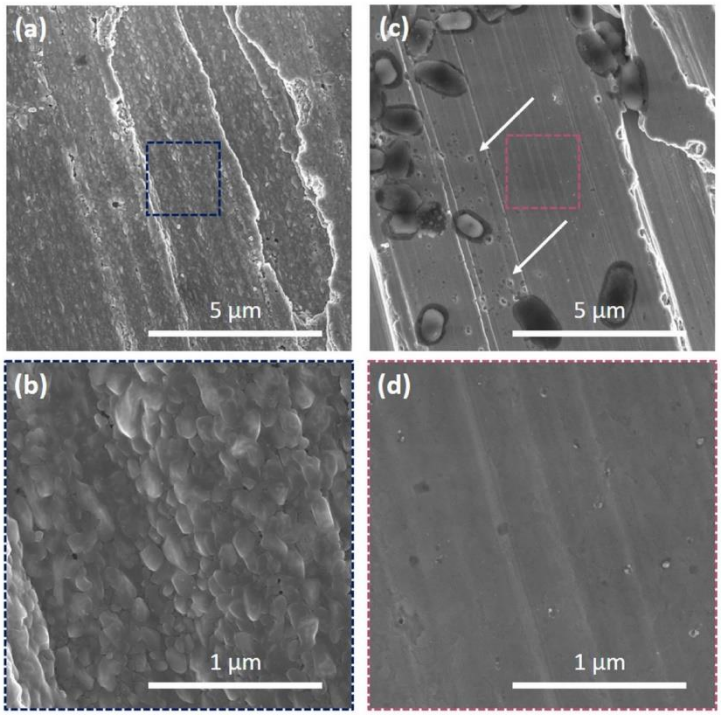

Fig. 1. Typical SEM images of copper surfaces after 3 h of exposure to PBS **(a–b)** and PBS with *E. coli* **(c–d)**. The dashed squares in **(a)** and **(c)** indicate the positions of the following higher magnification images **(b)** and **(d)**. The arrows indicate localised corrosion attacks.

they were diluted 1:10 with pure water for analysis.

3. Results and discussion

Evolution of surface morphology always reflects the corrosion behaviours. Therefore, to directly observe the corrosion phenomena on copper surface, high resolution SEM images were taken and shown in Fig. 1. After 3 h in pure PBS, granular sub-micron formation were found on the copper surface. Consequently, the as-ground morphology becomes less obvious. However, with the addition of *E. coli*, similar corrosion products can hardly be found. In addition to the remained bacteria, some area were suffering localised corrosion attacks, resulting in sub-micron scale pits. No other SEM observable features that can be identified on this bacterial treated surface. On the other side, it almost kept the original morphology of the untreated as-ground copper surface (SI, Fig. 1).

To further identify these corrosion products, GIXRD were applied to collect the near surface phase information presented in Fig. 2**(a)**. The range of diffraction peak of (111) planes of Cu_2O was chosen, since it is expected to be the strongest peak of the Cu_2O without any preferential orientation growth. A clear peak is recorded from the surface corroded by pure PBS, confirming the main corrosion products described above as crystallised Cu_2O. By contrast, the diffractogram from the coupon treated with *E. coli* suspension is rather flat.

Since no copper oxides related diffraction peaks could be assigned, Raman was applied owing to its higher sensitivity, where a slight oxidation is shown (Fig. 2**(b)**). Comparatively, these oxides signals are with lower background and less obvious oxides' peaks, especially around 149 cm^{-1} and 216 cm^{-1}. In addition, compared to the relatively large detection zone of GIXRD, Raman results could be correlated with more localised features. For example in Fig. 2**(c)**, some dark areas found in OM are confirmed by SEM as the positions where localised corrosion attacks occurred. In these positions, higher Raman signal of Cu_2O were recorded and shown in Fig. 2**(d)**. Although these localised corrosion sites are far smaller than the macroscopic pits that could be observed directly in OM, they do match the features described traditional pitting corrosion theories (Hoeppner, 1985). They describe the formation of corrosion products around the opening (cathode) of these cavities (anode). These product could gradually seal the pits, which has not yet been observed on our experiments though. Apart from small difference, all the above-mentioned findings confirm the considerable changes on copper surface after adding *E. coli* into PBS: the Cu_2O formation becomes less dominant and more non-uniform on copper surface.

Corrosion behaviour of a certain material is never an independent phenomenon: it is closely correlated to the surrounding environment which is applied, that is to say, the solutions (PBS or bacterial suspensions) on copper coupons. It is known from the Poubaix diagram of copper, that Cu_2O formation favours alkaline environment, while acidity increases, it dissolves and exists as cupric ions (Toparli et al., 2017). For this reason, although PBS is defined and prepared as a buffer solution, it would still be helpful to know whether the actual condition in these corrosion tests already exceeds the buffer capacity. Therefore, the pH values of the samples were checked and given in Table 1. For the original PBS, no matter with or without bacterial addition, their pH values were 7.4 as designed. However, in both cases, this value rose after corrosion tests, indicating an alkaline shift. Most importantly, when *E. coli* was added, the solution became even more alkaline, which theoretically should be more beneficial to the formation of Cu_2O. Therefore, there must be other reasons instead of the acidity that inhibit the oxide growth in bacterial condition.

To preliminarily verify if *E. coli* could interactive with Cu_2O actively, another case was designed to place *E. coli* PBS suspension on pure PBS treated copper surface (therefore with existing Cu_2O). Their GIXRD results (SI, Fig. 2) show that the previously formed Cu_2O layer does not change obviously after bacterial suspension treatment,

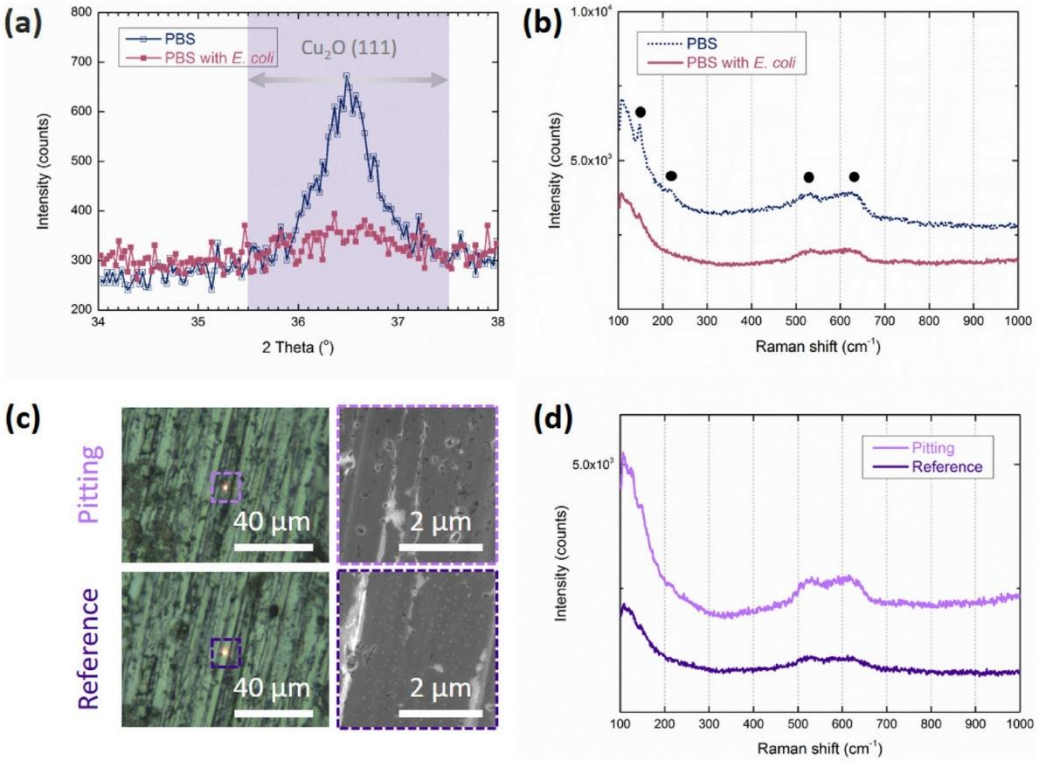

Fig. 2. (a) High resolution grazing incidence X-ray diffractograms in the range of (111) planes of Cu_2O (JCPDS#75-1531) and **(b)** typical Raman spectra obtained from copper surfaces after 3 h exposure to PBS and PBS with *E. coli*. **(c)** OM images and SEM images of two typical features obtained from the bacterial treated surface and **(d)** their Raman spectra from the same areas.

Table 1
The pH values of different solutions before and after 3 h corrosion tests on copper surface.

Solution	Before corrosion	After corrosion
PBS	7.4	7.7
PBS with *E. coli*	7.4	7.9
PBS with *S. cohnii*	7.4	7.9

suggesting that *E. coli* do not act as an active role in deteriorating Cu_2O layer.

After the examination of the corrosion products on these surfaces, we then shifted the interest to the solution, namely the withdrawn droplets. Copper content in pure PBS and *E. coli* PBS suspension were measured and plotted in Fig. 3. In pure PBS, the concentration of copper has quickly reached a plateau in 30 min, which at least lasted for 3 h. With *E. coli* addition, on the other hand, the curve evidently follows another trend: it significantly becomes higher in the whole period. The variety of these two patterns could be ascribed to the barrier effect of copper oxides coverage. As fewer oxides were found in the latter case, a bigger portion of bare copper was exposed to the solution, that is to say, can still be corroded by the solution. For this reason, release of copper ion can be thus less hindered and therefore copper content gradually increase could be observed. In addition, the shown copper content data can also be transferred into weight loss of the original surface if needed. Because for pure copper coupons, the amount of copper measured in solution should be equal to the weight loss. However, it should be noted that the contribution from the oxide growth will not be considered in this way as they are still attached to the original surface.

But why did the oxide growth rate slowdown so distinctly? Similar

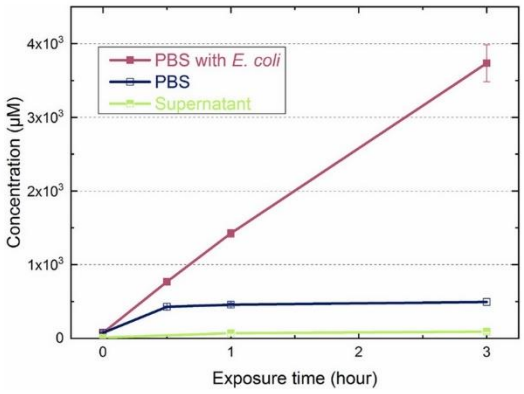

Fig. 3. Concentration of copper content in PBS, PBS with *E. coli* and its supernatant following various exposure periods. The error bars indicate the standard deviations calculated from three independent measurements.

trends of copper content were also reported with *S. cohnii* addition (Hahn et al., 2017). *S. cohnii* is a type of bacteria with less mobility, as shown in SI Fig. 3, its PBS suspension has rather similar corrosive influence on the copper surface: no obvious oxide layer could be found in 3 h. This helps us to exclude the potential effects induced by bacterial mobility that may change the local near-surface circumstance, such as substance concentration and fluid flow rate.

Now back to the rise of copper content, which was previously ascribed to the bonding effect of complexing agents (Hahn et al., 2017). Inspired by this aspect, another test was designed to detect the amount of copper in supernatant (green curve in Fig. 3). This result implies

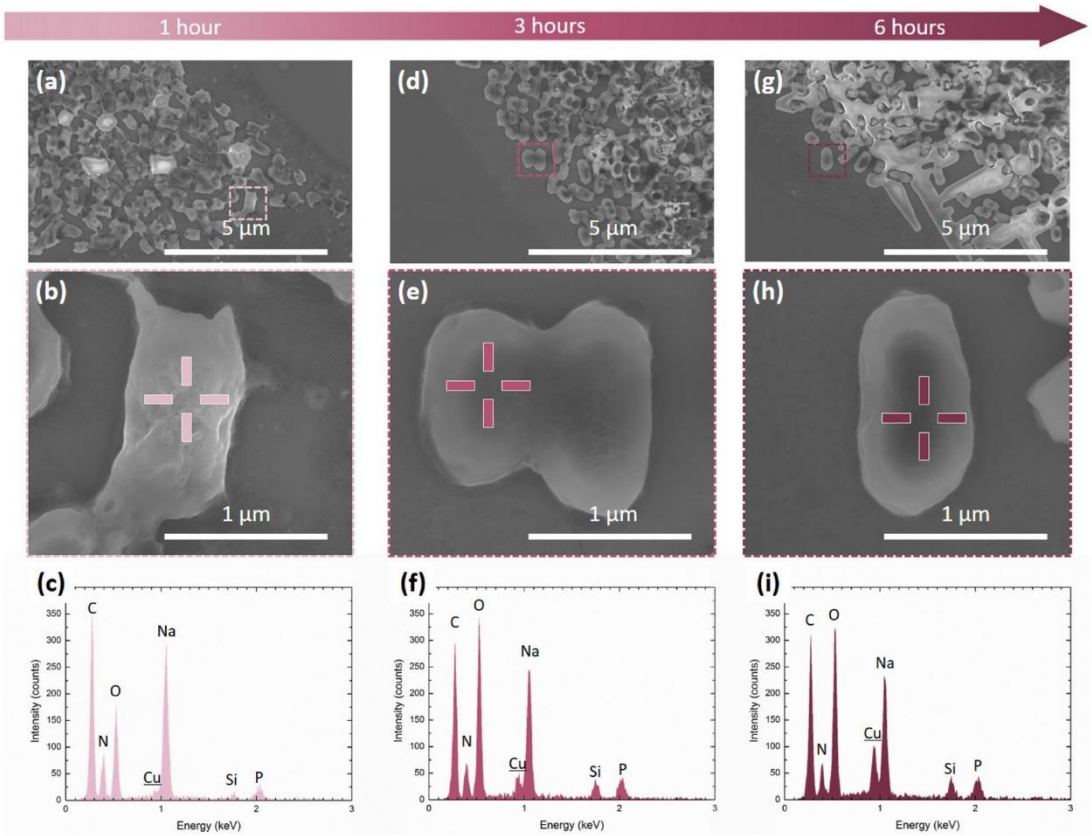

Fig. 4. Typical SEM images and EDS spectra from copper surface treated *E. coli* following various exposure periods, after being transferred to silicon wafer: **(a–c)** 1 h; **(d–f)** 3 h and **(g–i)** 6 h. The dashed squares indicates the position of the following higher magnification images. The cross shape indicators point out the positions where the corresponding spectra were collected.

another possibility. These values represent the amount of free copper ions in the suspension. They are relatively low, fewer than those in PBS by almost a factor around 5, in spite of the slight increase along the time. It could probably mean that the concentration of free copper ions are still far away from its equilibrium that leads to oxides formation.

Apparently, the following question needs to be answer could be: where are the rest of the huge amount of copper? Logically, if they are not in the supernatant, then they could only be with bacteria. Fig. 4 presents the copper treated *E. coli* observed by SEM. Prolonging the treatment time, in the first place, the shape of bacteria becomes more regular. However, since no fixation or drying steps were adopted in order to preserve the potential copper ion accumulation within bacteria, morphology of these bacteria might not be interpreted as their original state.

On the other hand, local elemental analysis done by EDS further provides more interesting information. First of all, the main elemental composition of *E. coli* itself is always considered as a combination of C, H, O and N (von Stockar and Liu, 1999). Other elements should be thus considered to have an environmental source. Therefore, the actual EDS on untreated *E. coli* (shown in SI Fig. 4) also revealed certain amounts of Na and P, which could come from the compositions of LB growth medium or PBS. Besides, signal of Si comes from the silicon substrate that is supporting the bacteria. The most significant finding belongs to those Cu peaks. Not only have their signal been successfully collected, their intensity also progressively increases proportional to treatment time. This trend indeed represents the copper amount accumulated by the bacteria, confirming both our results and the latest reported results obtained from ICP-MS measurements (Hahn et al., 2018).

As generally reported, 3 h is a period already assures at least 99.9% *E. coli* in PBS can be killed on copper surface due to the released copper ions (Hans et al., 2013). Interestingly, this accumulation process still continued after 3 h, as the intensity from Cu peak reached another higher value in 6 h. A similar test with sterile *E. coli* instead of viable *E. coli* was carried out, where bacteria were found with high copper content as well (shown in SI Fig. 5). This may indicate the observed accumulation process should not be considered as an active process fulfilled by the living bacteria or biofilm, but rather a passive process in this condition. Meanwhile, these results also suggest that the inhibition of oxides are not likely to be linked with the consequences of bacterial metabolism such as the consumption of oxygen.

Apart from this type of copper accumulation, the dissolved copper exists as another observable form. Fig. 5 reveals this on those bacteria after treated with copper surface for 3 h: there are some sub-micron particles with various sizes attaching on these bacteria. EDS spectra collected from these features tell more details from their composition. Position 1 represents the spectrum obtained from bacterium without particle coverage, acting as a contrast. The present elements resemble those discussed in the above section. The intensity of Cu is relatively higher, resulting from the fact that during this observation, these bacteria were still on copper surface, instead of having been transferred to silicon wafer in the previous case. Therefore this intensity also includes the characteristic X-ray excited from the copper surface under the bacterium due to its small size (more precisely, the thickness) of bacterium. On the other hand, the spectrum from position 2 centred on the sub-micron particle draws a different scene. The intensity of C, N and Na became less, based on the fact that the particle locates higher than

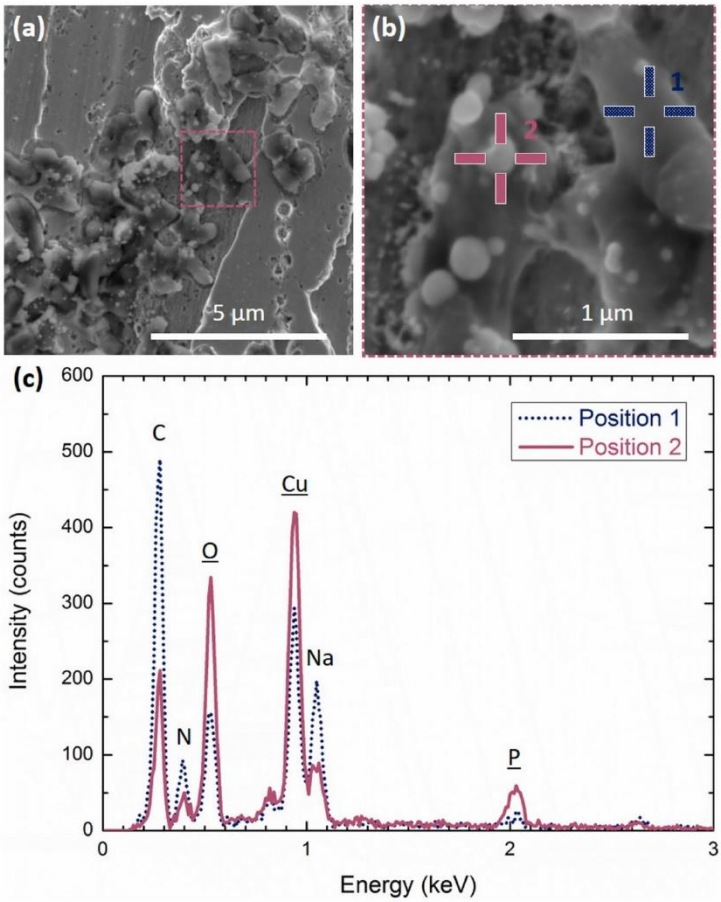

Fig. 5. Typical SEM images **(a–b)** and EDS spectra **(c)** from 3 h copper surface treated *E. coli*, on the original copper surface. The dashed squares indicates the position of the following higher magnification image. The cross shape indicators point out the positions where the corresponding spectra were collected.

the bacterium, and so there was less electrons reaching and exciting characteristic X-ray from the bacterium. Whereas the other three detected elements, namely O, Cu and P, were recorded with higher intensity. They should thus be considered as the main elemental composition of these particles.

Although no exact phase composition of these particles could be indexed from the current GIXRD results, studies (He et al., 2015; Luo et al., 2017b) did have shown that a popular approach to produce copper phosphate nano-particle is by appropriately mixing copper or its ions with phosphate solution. Unfortunately, we cannot directly conclude whether the bacteria promote the formation of the suspected copper phosphate particles (not the scope of our current study either). Nevertheless, we could still comment that they are more likely to grow on bacteria, and it does show us one of the forms how the copper content being stabilised in the solution instead of being free ions. Furthermore, since the above ICP-MS results only could show the sum of both accumulation of copper in bacteria and copper phosphate, it will be meaningful if future experiments are designed to show the proportion.

These sub-micron particles are easily found, mainly because their distribution on the surface of bacteria. However, for the dispersed copper that could only be detected by EDS, it is still yet to know whether they entered the bacteria or only attached with the outer membrane. STEM mode in TEM was therefore applied so as to collect the information of the elemental distribution, as shown in Fig. 6. BF image outlines the profile of bacteria better. While in the ADF image, it could already be observed that the sub-micron particles contain elements with higher atomic number, since higher intensity from these locations were recorded. This information is further confirmed by EDS mapping, where O, Cu and P were found highly concentrated in those regions. Another important fact could be extracted from the EDS mapping, is the distribution of copper in a bacterium. It is true that for a 2D top-view of a 3D object (the bacterium), it's hard to tell where the copper exactly are. However, one could still suppose that if the situation was that the copper only anchored on the outer membrane of a bacterium. In this case, the copper amount should be found a significant increase from the centre of the bacterium to its edge. This is because from a 2D top-view, the edge of a bacterium consists of overlap of the membrane in top-view that should have resulted in a higher copper content. But this has not been observed in the current result, suggesting that it is highly possible that those dispersed copper were located within the bacteria. To further investigate the more precise locations of copper, further work could be done by combing other more localised techniques such as NanoSIMS, with almost 100 nm lateral resolution (Kraft et al., 2006) combining with depth profiling. Another equally interesting information is about the state of these copper contents. Thus far have we applied GIXRD and Raman on the copper treated bacteria (shown in SI, Fig. 6), unfortunately no (or not enough) crystalline phase could be indexed.

With these observations, the role of bacteria in the antibacterial efficiency test (copper-PBS system) is summarised in Fig. 7. The first phase is the release of copper ions when the contact of suspension and

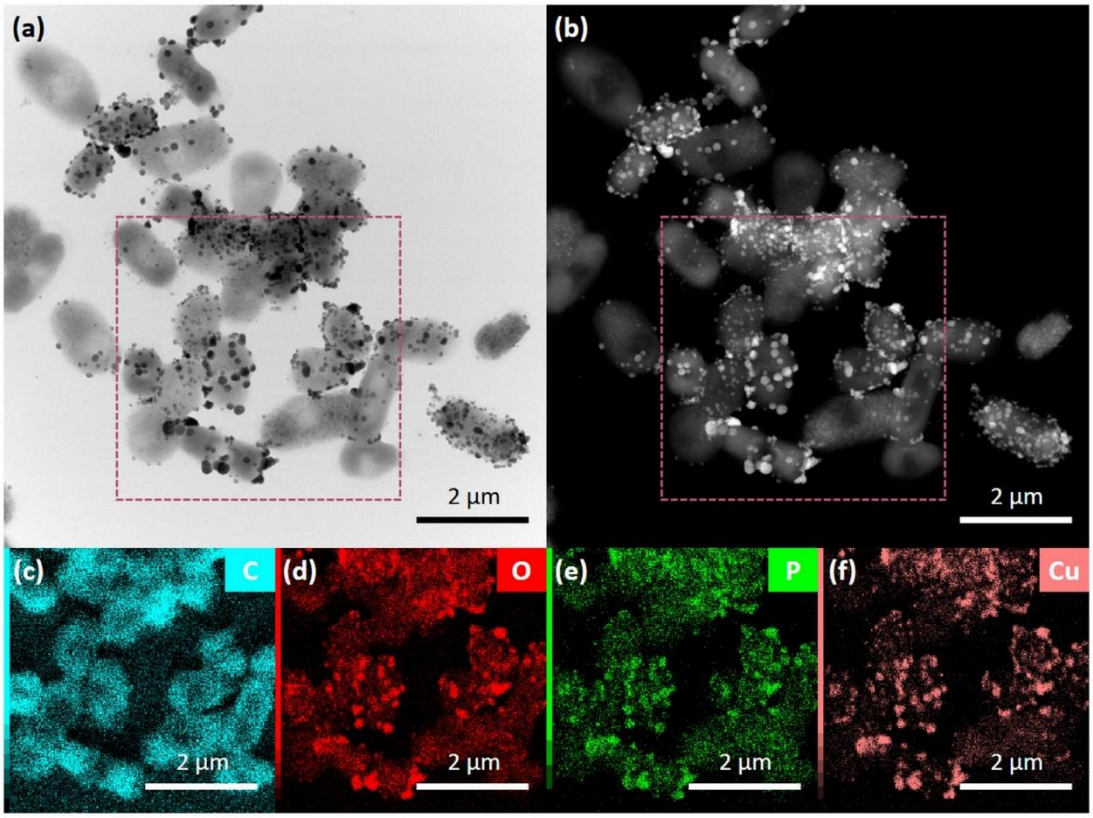

Fig. 6. Typical STEM observation from copper surface treated *E. coli* for 3 h: **(a)** BF image; **(b)** ADF image. The dashed squares indicate the position of the following chemical mapping: **(c)** carbon; **(d)** oxygen; **(e)** phosphorus and **(f)** copper.

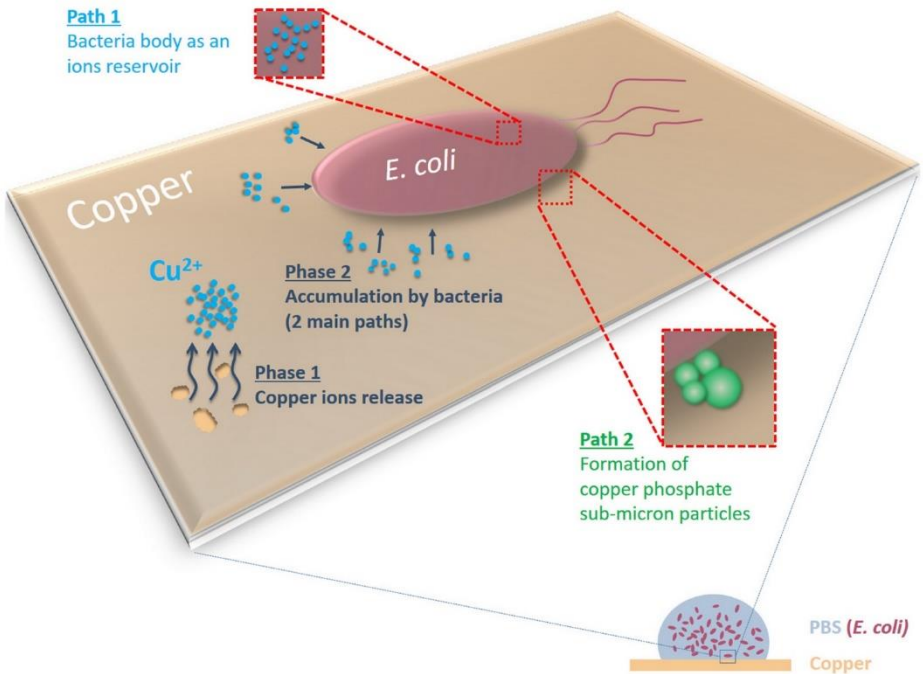

Fig. 7. Schematic description of the main paths of copper ions in PBS in the presence of *E. coli*.

copper surface begins, which leads to an increase of copper content in suspension. The existence of bacteria does not essentially alter this initial phase. However, when these ions "meet" the bacteria, they begin to be accumulated by the bacteria, with two main paths confirmed: one is through the absorption of the bacteria. It is not the first time to report that the microbe may act as a reservoir of metal ions (Veglio and Beolchini, 1997; Wang and Chen, 2009), but to link this behaviour not only to the surrounding solution environment but also another object (in this case: copper surface) sharing the same environment is still seldom considered. Another path is the formation of copper phosphate sub-micron particles. As the bacteria begin to collect free copper ions from the solution, the amount of the actual copper ions in the solution has been gradually consumed. This process keeps the amount of free copper ion low, favouring less the oxide formation. Exposure of copper surface without fully oxides coverage enables the continuous corrosion, explaining why the total amount of copper in the whole suspension is much higher.

At last, there are a few concerns that should be noticed basing on the current observations. For example, due to the additional effect introduced by bacteria, we should now realise the importance of interpreting the each corresponding scenario also with bacteria. In other words, although analysis of interaction between pure buffers and surface can help, but does not necessarily represent the actual situation (e.g. copper content level). On the other hand, the ion accumulation and its effects on corrosion process could be better validated, for instance, by well-defined experiments where copper content in the bacterial suspension can be precisely regulated. Moreover, further work should focus on the details of corrosion phenomenon on antibacterial copper as well as its consequences. Attempts to investigate how these changes could affect the antibacterial behaviour could also be meaningful.

4. Conclusions

This study focuses on copper surface evolution during the antibacterial efficiency test. The environmental components as well as the role of bacteria in buffer suspension were considered. Several concluding remarks are listed below:

- Copper surface oxidation in PBS is inhibited as the presence of *E. coli* in the suspension, confirmed by GIXRD and Raman. In contrast, without the Cu_2O coverage, localised corrosion attacks are much visible on the copper surface.
- Due to the absence of Cu_2O layer as an ion release barrier, the amount of copper ions released by the metallic surface strongly grows, where the plateau phase has not been reached in 3 h exposure.
- The released copper ions are found to be stored inside the bacteria and forming copper phosphate sub-micron particles outside the bacteria. These two main paths on one hand enhance the capacity of copper storage of the suspension, on the other hand, reduce the free copper ions in the suspension.
- This accumulation is considered as a passive process since viable bacteria is not the necessary condition.

Data availability

The data that support the findings of this study are available from the corresponding author on request.

Declaration of Competing Interest

None.

Acknowledgements

This study was supported by Erasmus Mundus Joint European Doctoral Programme in Advanced Materials Science and Engineering (DocMASE, 512225-1-2010-1-DE-EMJD, European Commision) and the PhD-Track-Programme (PhD02-14, Franco-German University). The ICP-MS experiments were supported by Dr. Ralf Kautenburger from the chair of Inorganic Solid State Chemistry. The authors acknowledge Prof. Volker Presser and Leibniz Institute for New Materials for the access of Raman spectrometer. Dr. Javad Najafi helped a lot to introduce the concept of bacterial mobility. Prof. Gert-Wieland Kohring and Dr. Fabio Pereira from Department of Microbiology in Saarland University offer valuable instruction in centrifugation procedure.

Appendix A. Supplementary data

Supplementary material related to this article can be found, in the online version, at doi:https://doi.org/10.1016/j.micron.2019.102759.

References

Ben-Sasson, M., Lu, X., Nejati, S., Jaramillo, H., Elimelech, M., 2016. In situ surface functionalization of reverse osmosis membranes with biocidal copper nanoparticles. Desalination 388, 1–8.
Cano, A.P., Gillado, A.V., Montecillo, A.D., Herrera, M.U., 2018. Copper sulfate-embedded and copper oxide-embedded filter paper and their antimicrobial properties. Mater. Chem. Phys. 207, 147–153.
Carter, K.P., Young, A.M., Palmer, A.E., 2014. Fluorescent sensors for measuring metal ions in living systems. Chem. Rev. 114, 4564–4601.
Demir, B., Cerkez, I., Worley, S.D., Broughton, R.M., Huang, T.-S., 2015. N-halamine-Modified antimicrobial polypropylene nonwoven fabrics for use against airborne Bacteria. ACS Appl. Mater. Interfaces 7, 1752–1757.
Dhineshbabu, N.R., Rajendran, V., 2016. Antibacterial activity of hybrid chitosan–cupric oxide nanoparticles on cotton fabric. Nanobiotechnology, IET 10, 13–19.
Ellinas, K., Kefallinou, D., Stamatakis, K., Gogolides, E., Tserepi, A., 2017. Is there a threshold in the antibacterial action of superhydrophobic surfaces? ACS Appl. Mater. Interfaces 9, 39781–39789.
Foster, L.L., Hutchison, M., Scully, J.R., 2016. Corrosion of Cu-5Zn-5Al-1Sn (89% Cu, 5% Zn, 5% Al, 1% Sn) compared to copper in synthetic perspiration during cyclic wetting and drying: the fate of copper. Corrosion 72, 1095–1106.
Gilbertson, L.M., Albalghiti, E.M., Fishman, Z.S., Perreault, F., Corredor, C., Posner, J.D., Elimelech, M., Pfefferle, L.D., Zimmerman, J.B., 2016. Shape-dependent surface reactivity and antimicrobial activity of nano-cupric oxide. Environ. Sci. Technol. 50, 3975–3984.
Hahn, C., Hans, M., Hein, C., Mancinelli, R.L., Mucklich, F., Wirth, R., Rettberg, P., Hellweg, C.E., Moeller, R., 2017. Pure and oxidized copper materials as potential antimicrobial surfaces for spaceflight activities. Astrobiology.
Hahn, C., Hans, M., Hein, C., Dennstedt, A., Mücklich, F., Rettberg, P., Hellweg, C.E., Leichert, L.I., Rensing, C., Moeller, R., 2018. Antimicrobial properties of ternary eutectic aluminum alloys. BioMetals.
Hans, M., Erbe, A., Mathews, S., Chen, Y., Solioz, M., Mücklich, F., 2013. Role of copper oxides in contact killing of bacteria. Langmuir 29, 16160–16166.
Hans, M., Támara, J.C., Mathews, S., Bax, B., Hegetschweiler, A., Kautenburger, R., Solioz, M., Mücklich, F., 2014. Laser cladding of stainless steel with a copper–silver alloy to generate surfaces of high antimicrobial activity. Appl. Surf. Sci. 320, 195–199.
He, G., Hu, W., Li, C.M., 2015. Spontaneous interfacial reaction between metallic copper and PBS to form cupric phosphate nanoflower and its enzyme hybrid with enhanced activity. Colloids Surf. B Biointerfaces 135, 613–618.
Hoeppner, D.W., 1985. Pitting corrosion: morphology and characterization. Framework. pp. 26.
Hohle, T.H., Franck, W.L., Stacey, G., O'Brian, M.R., 2011. Bacterial outer membrane channel for divalent metal ion acquisition. Proc. Natl. Acad. Sci. U. S. A. 108, 15390–15395.
Irene, G., Georgios, P., Ioannis, C., Anastasios, T., Diamantis, P., Marianthi, C., Philippe, W., Maria, S., 2016. Copper-coated textiles: armor against MDR nosocomial pathogens. Diagn. Microbiol. Infect. Dis. 85, 205–209.
Kara, S., Ureyen, M.E., Erdogan, U.H., 2016. Structural and antibacterial properties of PP/CuO composite filaments having different cross sectional shapes. Int. Polym. Process. 31, 398–409.
Kraft, M.L., Weber, P.K., Longo, M.L., Hutcheon, I.D., Boxer, S.G., 2006. Phase separation of lipid membranes analyzed with high-resolution secondary ion mass spectrometry. Science 313, 1948.
Liu, H., Xu, D., Yang, K., Liu, H., Cheng, Y.F., 2017. Corrosion of antibacterial Cu-bearing 316L stainless steels in the presence of sulfate reducing bacteria. Corros. Sci.
Luo, J., Hein, C., Mücklich, F., Solioz, M., 2017a. Killing of bacteria by copper, cadmium, and silver surfaces reveals relevant physicochemical parameters. Biointerphases 12, 020301.
Luo, Y.-K., Song, F., Wang, X.-L., Wang, Y.-Z., 2017b. Pure copper phosphate

nanostructures with controlled growth: a versatile support for enzyme immobilization. CrystEngComm 19, 2996–3002.
Molteni, C., Abicht, H.K., Solioz, M., 2010. Killing of Bacteria by copper surfaces involves dissolved copper. Appl. Environ. Microbiol. 76, 4099–4101.
Muller, M.P., MacDougall, C., Lim, M., Armstrong, I., Bialachowski, A., Callery, S., Ciccotelli, W., Cividino, M., Dennis, J., Hota, S., Garber, G., Johnstone, J., Katz, K., McGeer, A., Nankoosingh, V., Richard, C., Vearncombe, M., 2018. Antimicrobial surfaces to prevent healthcare-associated infections: a systematic review. J. Hosp. Infect. 92, 7–13.
Rock, C., Small, B.A., Thom, K.A., 2018. Innovative methods of hospital disinfection in prevention of healthcare-associated infections. Curr. Treat. Options Infect. Dis. 10, 65–77.
Rosenberg, M., Vija, H., Kahru, A., Keevil, C.W., Ivask, A., 2018. Rapid in situ assessment of Cu-ion mediated effects and antibacterial efficacy of copper surfaces. Sci. Rep. 8, 8172.
Rotini, A., Tornambè, A., Cossi, R., Iamunno, F., Benvenuto, G., Berducci, M.T., Maggi, C., Thaller, M.C., Cicero, A.M., Manfra, L., Migliore, L., 2017. Salinity-based toxicity of CuO nanoparticles, CuO-Bulk and Cu Ion to Vibrio anguillarum. Front. Microbiol. 8.
Santo, C.E., Lam, E.W., Elowsky, C.G., Quaranta, D., Domaille, D.W., Chang, C.J., Grass, G., 2011. Bacterial killing by dry metallic copper surfaces. Appl. Environ. Microbiol. 77, 794–802.
Souli, M., Antoniadou, A., Katsarolis, I., Mavrou, I., Paramythiotou, E., Papadomichelakis, E., Drogari-Apiranthitou, M., Panagea, T., Giamarellou, H., Petrikkos, G., Armaganidis, A., 2017. Reduction of environmental contamination with multidrug-resistant bacteria by copper-alloy coating of surfaces in a highly endemic setting. Infect. Control Hosp. Epidemiol. 38, 765–771.
Toparli, C., Hieke, S.W., Altin, A., Kasian, O., Scheu, C., Erbe, A., 2017. State of the surface of antibacterial copper in phosphate buffered saline. J. Electrochem. Soc. 164, H734–H742.
Tripathy, A., Sreedharan, S., Bhaskarla, C., Majumdar, S., Peneti, S.K., Nandi, D., Sen, P., 2017. Enhancing the bactericidal efficacy of nanostructured multifunctional surface using an ultrathin metal coating. Langmuir 33, 12569–12579.
Turalija, M., Merschak, P., Redl, B., Griesser, U., Duelli, H., Bechtold, T., 2015. Copper(i) oxide microparticles - synthesis and antimicrobial finishing of textiles. J. Mater. Chem. B 3, 5886–5892.
Turner, R.J., 2017. Metal-based antimicrobial strategies. Microb. Biotechnol. 10, 1062–1065.
Usman, A., Hussain, Z., Riaz, A., Khan, A.N., 2016. Enhanced mechanical, thermal and antimicrobial properties of poly(vinyl alcohol)/graphene oxide/starch/silver nanocomposites films. Carbohydr. Polym. 153, 592–599.
Veglio, F., Beolchini, F., 1997. Removal of metals by biosorption: a review. Hydrometallurgy 44, 301–316.
Vincent, M., Duval, R.E., Hartemann, P., Engels-Deutsch, M., 2018. Contact killing and antimicrobial properties of copper. J. Appl. Microbiol. 124, 1032–1046.
von Stockar, U., Liu, J.S., 1999. Does microbial life always feed on negative entropy? Thermodynamic analysis of microbial growth. Biochimica et Biophysica Acta (BBA) - Bioenergetics 1412, 191–211.
Wakshlak, R.B.-K., Pedahzur, R., Avnir, D., 2015. Antibacterial activity of silver-killed bacteria: the "zombies" effect. Sci. Rep. 5, 9555.
Wang, J., Chen, C., 2009. Biosorbents for heavy metals removal and their future. Biotechnol. Adv. 27, 195–226.
Wu, H., Zhang, X., Geng, Z., Yin, Y., Hang, R., Huang, X., Yao, X., Tang, B., 2014. Preparation, antibacterial effects and corrosion resistant of porous Cu–TiO2 coatings. Appl. Surf. Sci. 308, 43–49.
Wu, S., Altenried, S., Zogg, A., Zuber, F., Maniura-Weber, K., Ren, Q., 2018. Role of the surface nanoscale roughness of stainless steel on bacterial adhesion and microcolony formation. ACS Omega 3, 6456–6464.
Zhao, J., Xu, D., Shahzad, M.B., Kang, Q., Sun, Y., Sun, Z., Zhang, S., Ren, L., Yang, C., Yang, K., 2016. Effect of surface passivation on corrosion resistance and antibacterial properties of Cu-bearing 316L stainless steel. Appl. Surf. Sci. 386, 371–380.

Supplementary Information

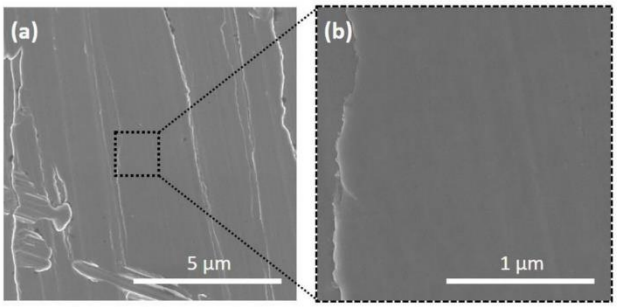

Supplementary Figure 1 | High resolution SEM images of as-ground copper surfaces. The dashed square in **(a)** indicates the position of the following higher magnification image **(b)**.

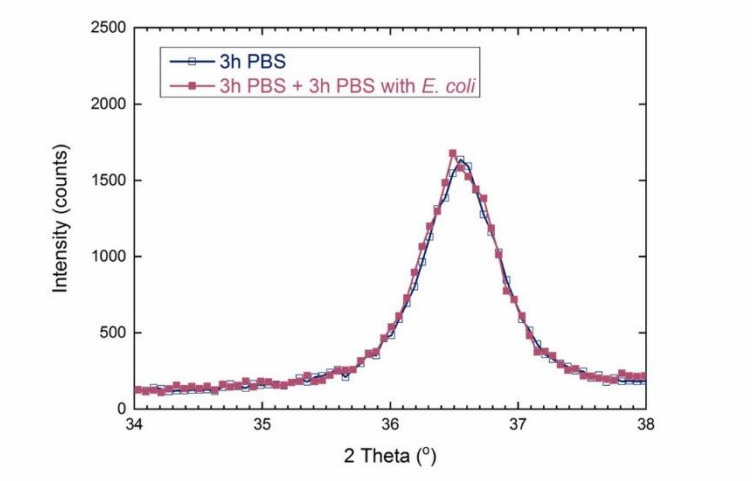

Supplementary Figure 2 | Grazing incidence X-ray diffractogram in the range of (111) planes of Cu_2O (#75-1531) of 3-hour PBS treated ground copper surface, and another 3-hour *E. coli* PBS suspension treated on the same surface.

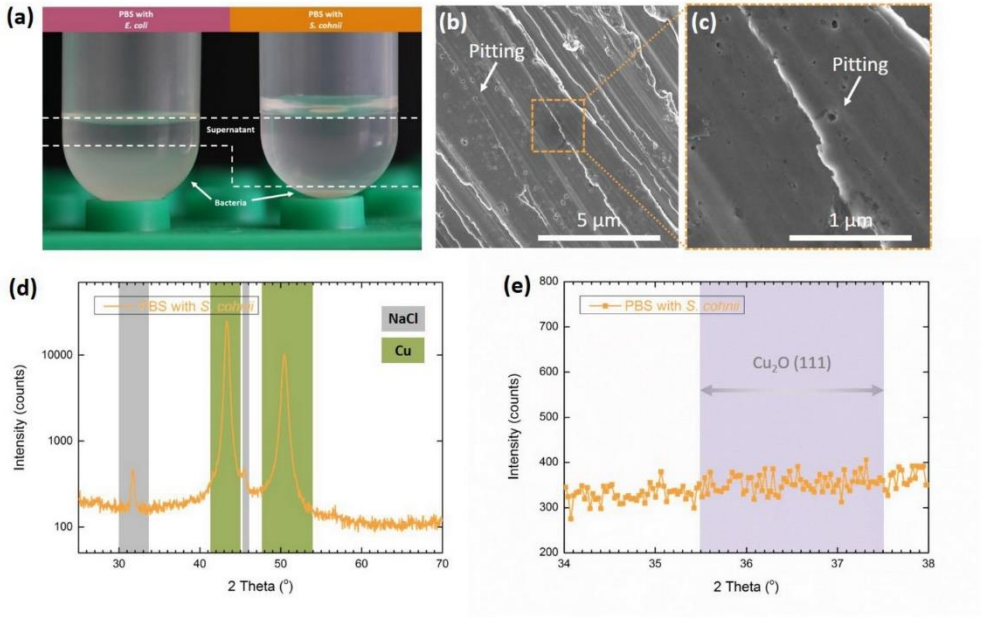

Supplementary Figure 3 | **(a)** Photo of PBS Suspension with *E. coli* or *S. cohnii* after one night standing, showing the less mobility of *S. cohnii* was observed. **(b-c)** Typical SEM images of copper surfaces after three hours of exposure to PBS with *S. cohnii*. Its grazing incidence X-ray diffractogram **(d)** and **(e)** a high resolution scan in the range of (111) planes of Cu_2O (#75-1531).

Experimental details: The growth of S. cohnii was with Tryptic soy broth (Fluka) medium, other parameters followed exactly the protocol for *E. coli* described in manuscript 2.2.

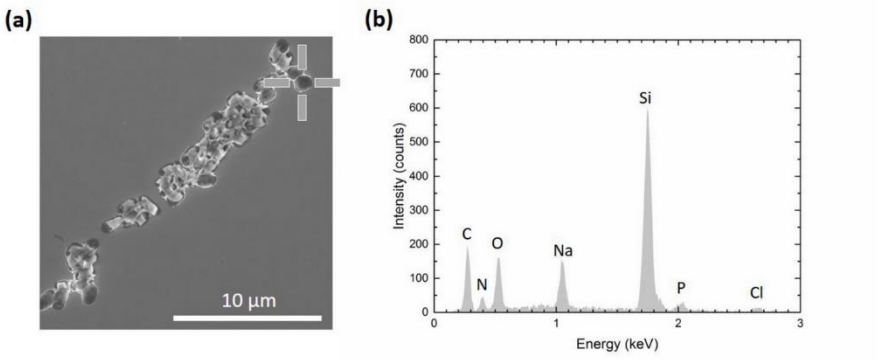

Supplementary Figure 4 | **(a)** Typical SEM imagesand **(b)** EDS spectrum from untreated *E. coli*. The cross shape indicator points out the position where the corresponding spectrum was collected.

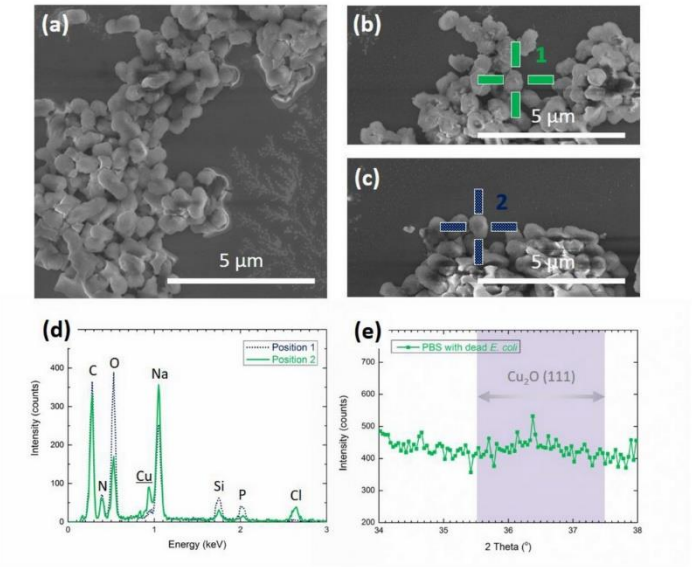

Supplementary Figure 5 | Typical SEM images of sterile *E. coli* on silicon wafer: **(a)** before and **(b-c)** after three hours of exposure to copper surface. The cross shape indicators point out the positions where **(d)** the corresponding EDS spectra were collected. Difference in copper content could be due to the fact that these bacteria only deposited on the surface randomly (but not through their own mobility). Those who deposited on a certain layers of bacteria were far away from the copper surface, having collected less copper. **(e)** High resolution grazing incidence X-ray diffractogram in the range of (111) planes of Cu_2O (#75-1531) of the copper after three hours of exposure to PBS with sterile *E. coli*.

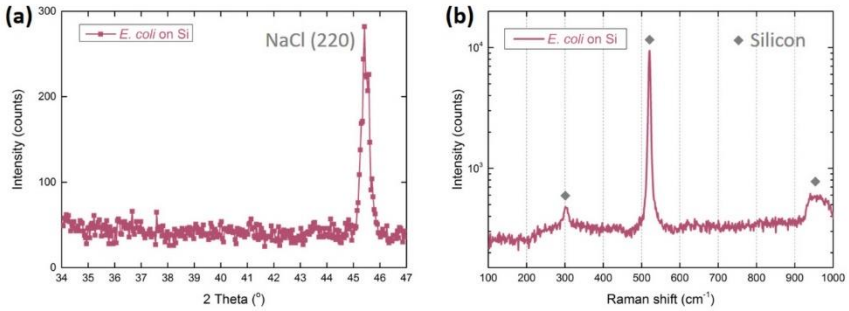

Supplementary Figure 6 | **(a)** High resolution grazing incidence X-ray diffractogram and **(b)** typical Raman spectrum, both obtained from silicon wafer with copper surface treated *E. coli* for 3 hours.

5. Corrosion Attacks and Oxide Growth on Copper Surface in PBS

In this chapter, the below peer-reviewed publication is going to be presented:

Localised corrosion attacks and oxide growth on copper in phosphate-buffered saline

Reproduced from Jiaqi Luo, Christina Hein, Jean-François Pierson, Frank Mücklich, *Material Characterization*, 2019, 185, with the permission of Elsevier

DOI: 10.1016/j.matchar.2019.109985

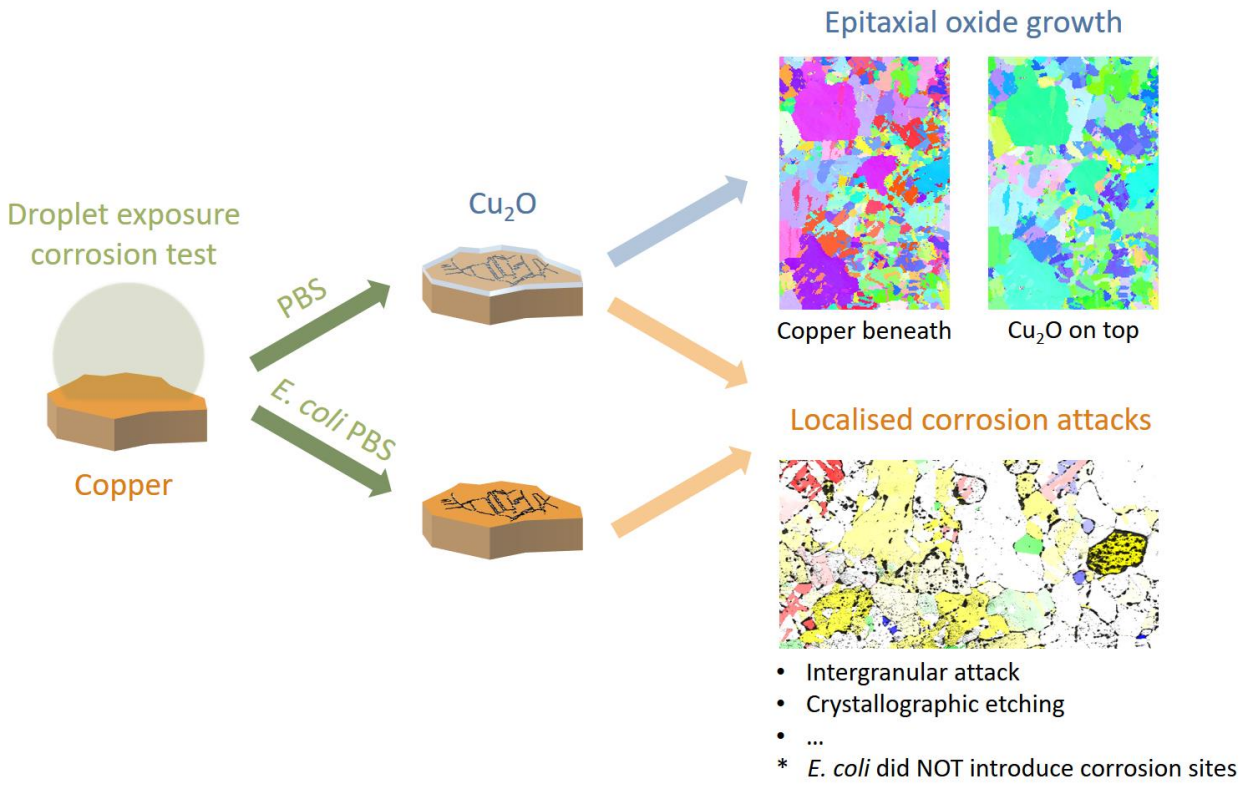

Contribution: Conceptualisation, Methodology, Validation (except from ICP-MS measurements), Investigation, Writing – Original Draft, Visualization, Project administration.

Materials Characterization 158 (2019) 109985

Contents lists available at ScienceDirect

Materials Characterization

journal homepage: www.elsevier.com/locate/matchar

Localised corrosion attacks and oxide growth on copper in phosphate-buffered saline

Jiaqi Luo[a,b,*], Christina Hein[c], Jean-François Pierson[b], Frank Mücklich[a]

[a] Functional Materials, Saarland University, 66123, Saarbruecken, Germany
[b] Université de Lorraine, CNRS, IJL, F-54000, Nancy, France
[c] Inorganic Solid State Chemistry, Saarland University, 66123, Saarbruecken, Germany

ARTICLE INFO

Keywords:
Copper
Cuprous oxide
PBS
Corrosion
Orientation
E. coli

ABSTRACT

Phosphate-buffered saline (PBS) is a buffer commonly used in antibacterial surface research. However, how copper surface varies in the buffer, in terms of corrosion attacks and oxide growth, is not yet fully recognised. In this study, PBS was applied as droplet on two types of copper surface: ground and electropolished. By scanning electron microscope (SEM), the similarities of their corrosion sites were compared, revealing the initiation of intergranular attack and orientation-dependent crystallographic etching. High resolution grazing incidence X-ray diffractometer (GIXRD), optical microscope (OM), Raman spectroscopy, and electron backscatter diffraction (EBSD) together provided detailed description of the epitaxial growth of cuprous oxide (Cu_2O) on electropolished copper. The amount of copper ions released from two types of surface were determined by inductively coupled plasma mass spectrometry (ICP-MS). By introducing *E. coli* into PBS, the inhibition of Cu_2O growth on electropolished coupon was observed. However, bacteria were found to hardly alter the corrosion mechanisms or the distribution of corrosion sites.

1. Introduction

Copper and its alloys have been regarded as important candidates in microbiology or hygiene market [1]. This should be credited to their capability to release copper ions, which have been proved to exhibit strong antimicrobial effect [2,3]. Therefore studies have been performed in order to understand phenomena such as cell damage and the mechanism of copper-DNA binding [4]. Tasks belong to materials researchers are, on the other hand, to figure out the approaches to incorporate copper into/onto different materials/surfaces [5–7], according to each of their application field [8–10]. Take the clinical environment as an example, touch surfaces made of coppers are promising in coping with not only those common germs such as *E. coli* or *S. aureus* [11–13], but also those deadly pathogenic strains/microbes such as *E. coli* O157 [14] and Norovirus [15].

Long-term efficacy is essential for daily touch surfaces. On one hand, bulk copper may be regarded as a self-healing antimicrobial touch surface. It is not difficult to imagine if the top layer of copper is destroyed, the newly-exposed surface, which is still copper, has the same antibacterial property as the original one. This ensures no substantial damage will be induced by daily touching, cleaning, or even scratching. However, oxidation of copper is not neglectable [16]. Its two regular oxides: cuprous oxide (Cu_2O) and cupric oxide (CuO) have also been revealed to have relatively weaker antimicrobial activity [17]. Therefore, some other ongoing studies also began to produce corresponding oxides on coppers [18], in order to better evaluate the changes in antibacterial performance as well as the role of oxides.

Another relevant concern is related to the methods applied to study surface antimicrobial efficacy. In these tests, microbes need to be transferred onto the coupons together with buffer solutions, in most of the cases, designed to cover the tested surfaces for the whole experimental periods [19]. The presence of these buffers could cause additional effects on the surface, which have been seldom addressed or considered in the existing research.

Phosphate-buffered saline (PBS) is one of the widely used physiological buffers in many microbiological and antibacterial studies [20–22]. In this buffer, disodium phosphate (Na_2HPO_4) or monosodium phosphate (NaH_2PO_4) helps to stabilise a pH of 7.4, when sodium chloride (NaCl) ensures a suitable osmotic pressure for microbes. However, these functions do not always secure a fair antimicrobial surface test. Two criteria should be further considered: first, does this buffer represent the specific environment (e.g. in everyday life) where the surface is applied? Second, does it play a neutral role, or will it instead bring additional effects into the tested system, altering the

* Corresponding author. Functional Materials, Saarland University, Campus D3.3, 66123, Saarbruecken, Germany.
E-mail address: jiaqi.luo@uni-saarland.de (J. Luo).

https://doi.org/10.1016/j.matchar.2019.109985
Received 6 August 2019; Received in revised form 26 October 2019; Accepted 26 October 2019
Available online 02 November 2019
1044-5803/

original surface status, and hence the antimicrobial performance?

To fulfil better the first criterion, artificial perspiration as an example, has been applied to simulate the scenario of daily touch surfaces in a few research [23,24]. However, the second criterion itself is somewhat contradictory, especially regarding copper surface. Continuous release of the antibacterial copper ions implies the original surface is undergoing chemical changes, which in many circumstances are, accomplished by corrosion attacks. Furthermore, these attacks generally do not just cause dissolution of the metallic surface, but also the formation of corrosion products, where growth of copper oxides become foreseeable.

Considering the corrosion attacks on copper, they have been abundantly investigated over the past decades. To analyse these attacks induced by PBS, certain known aspects are worth being briefly mentioned. First of all, it is the reactants that promote corrosion in the neutral condition as in PBS. Dissolution of copper is mainly promoted by dissolved oxygen instead of hydrogen ions [25]. However, PBS contains chloride ions (Cl^-), which is a reactive species especially promoting pitting corrosion [26]. Its existence also brings the possibility of more complex intermediate/final corrosion products such as copper chloride (CuCl) or dicopper chloride trihydroxide ($Cu_2(OH)_3Cl$) that could develop into different scenarios in pitting corrosion [27]. Pits themselves, have the bright side for microstructures studies, simply because defects such as dislocations are found to be the preferential pitting sites for most of the time [28]. For the same reason, localised corrosion attacks at grain boundaries and twin boundaries were also investigated [29], where high angle and incoherent grain boundaries are found to be corroded more easily. Meanwhile, grain orientation affects the corrosion resistance of the neighbouring boundaries [30,31]. Furthermore, under certain electrochemical conditions, etch pits occur on different grains are found to have crystallographic features, which can be highly related to the grain orientation [32].

Another aspect of the corrosion phenomena is the oxide growth. Analysis of this process enhances understanding of the (electro)chemical reactions involved. Usually, oxides are confirmed and further analysed by multiple phase analysis methods or electrochemical measurements [33]. However, the microscale details of the growth process itself seldom draw attention in the current existing research. To best our knowledge, there are only a few studies mentioning the epitaxial growth of Cu_2O on copper in aqueous environment [34], or deposition of epitaxial Cu_2O crystal in copper contained solution [35]. The focus of these investigations is the confirmation of orientation relationships that have also been previously reported in oxidation at elevated temperature [36,37], instead of the relevant corrosion processes.

Our recent study has reported the localised corrosion attacks that can be directly found on ground copper, since oxide growth is inhibited by the accumulation of copper in bacteria [38]. Therefore in the current study, more details from the corrosion aspect are revealed. In the first part of this work, we first revisited the corrosion sites on ground copper induced by PBS, but with another method, namely backscatter electron imaging. Afterward, the focus was diverted to both the localised corrosion attacks and oxide growth on electropolished copper. Additional ex-situ characterisations such as electron backscatter diffraction was conducted. Various results enable us to describe the detailed features of corrosion sites such as intergranular attack, crystallographic etching, and grains with certain preferential orientations. Moreover, the epitaxial growth of Cu_2O has also been recorded and analysed. Based on these results, the second part of the work applied *E. coli* PBS suspension for comparison, where the roles of bacteria on corrosion behaviours on copper were further discussed.

2. Materials and methods

2.1. Materials

Copper (99.99%, K09, Wieland) was chosen for both types of coupon: ground and electropolished. Ground coupons were mechanically ground with silicon carbide sandpaper (stepped down to grit number P600). Electropolished coupons were firstly mechanically ground and polished, finishing with 1 µm diamond paste, and cleaned with soap. Importantly, these coupons were electropolished in 85 wt% orthophosphoric acid (2 V, 3 min). After these grinding or polishing procedures, both types of coupon were rinsed with water, cleaned with ethanol in an ultrasonic bath, and dried by air.

2.2. Solutions

The preparation of PBS (0.01 M NaH_2PO_4. $1H_2O$, 0.14 M NaCl, pH about 7.4) and PBS with *E. coli* K12 can be referred to our recent publication [38]. For the bacterial suspension, the initial cell count was around 3×10^9–5×10^9 CFU/ml.

2.3. Corrosion protocol

To introduce corrosion on copper coupons, droplet exposure method (instead of immersion) was applied, in order to be kept as similar as the antibacterial efficiency tests performed in our other works [17,39]. In brief, 20 µL of PBS or *E. coli* PBS suspension was applied on coupons with a pipette. These coupons were placed in a water-saturated atmosphere at room temperature. After certain exposure time (1 h, 3 h, and 6 h), these solutions were withdrawn and the coupons were further cleaned with ethanol in an ultrasonic bath.

To remove the corrosion products from the coupon surface, acid etching was used. Coupons were immersed in 4 wt% hydrochloric acid (10 s), rinsed with water rinse, and cleaned with ethanol in an ultrasonic bath.

2.4. Surface characterization

Different functions of scanning electron microscope (SEM, Helios NanoLab600, FEI) were applied to observe copper surface after various corrosion experiments. Secondary electron detector (SE) was applied to describe the top-surface as well as cross-section of the coupons, while backscatter electron detector (BSE) depicted localised corrosion attacks exposed or covered by corrosion products. Acceleration voltages will be further mentioned in the corresponding figure captions. Transmission electron microscope lamella was prepared by focused ion beam (FIB) and finally attached on copper grid, so that scanning transmission electron microscopy mode (STEM) can be carried out at 30 kV, in order to survey the details of corrosion products. To investigate the orientation relationship between the corrosion products and the substrates underneath, electron backscatter diffraction patterns (EBSD) were collected at 20 kV, with step sizes of 200 nm (for fine scan at small regions) or 1 µm (for rapid scan at droplet edges). Optical microscope (OM, OLS4100, Olympus) photos were captured in 3D bright field mode to so that the colours induced by the corrosion products can be preserved. For further confirmation of these corrosion products covering the surfaces, Raman spectroscopy (Raman, operating at 633 nm, inVia, Renishaw) with a 50X OM and high resolution grazing incidence X-ray diffractometer (GIXRD, Cu Kα with 1° grazing angle, PANalytical X'Pert PRO-MPD) were applied. All these images and spectra were obtained within 24 h after the corresponding treatments.

2.5. Copper content determination

For the coupons to be measured, 10 µL samples were withdrawn by repetitive pipetting in the end of the corrosion protocol. To prepare the final samples for inductively coupled plasma mass spectrometry (ICP-MS, 7500cx, Agilent) measurement, they were first diluted in 2.990 mL 1 wt% nitric acid (Merck, Germany). Afterwards, 3 µl of 10 mg/l scandium and caesium internal standard solutions were added to the samples. For calibration, standards with 0.1, 0.5, 2.5, 10, 50, 250, and

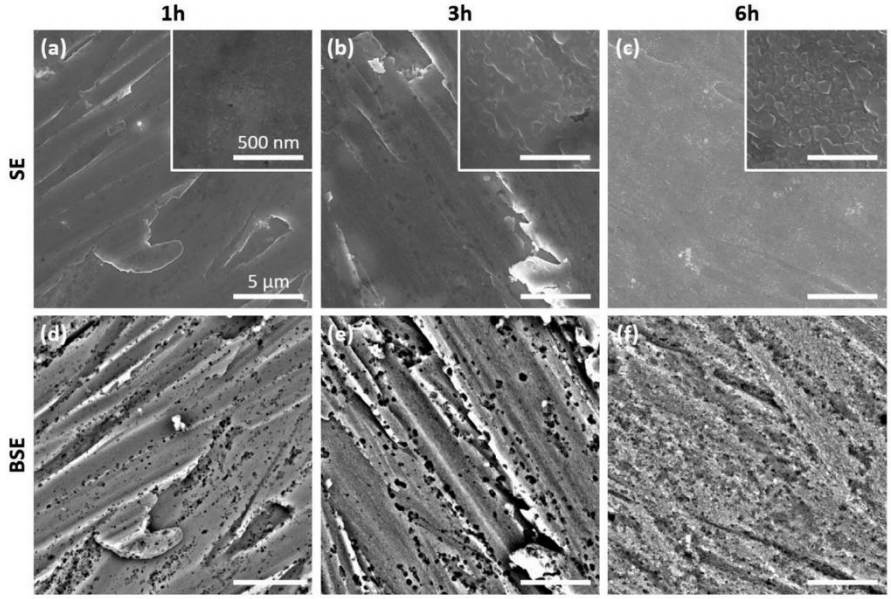

Fig. 1. Typical SEM images of ground copper surface after 1 h **(a & d)**, 3 h **(b & e)**, and 6 h **(c & f)** exposure to PBS. Same locations were imaged simultaneously with SE detector **(a–c)** and BSE detector **(d–f)** at 20 kV. All images share the same scale bars that presented in **(a)**.

1000 μg/L of copper were used. The original results with a unit of ppb were converted to the final values with μmol/L (μM), considering the fold of dilutions and molar mass 63.55 g/mol for copper. Results from ICP-MS represent the sum of every type of copper form presented in the samples. The average values and standard deviations were obtained by three independent experiments.

3. Results and discussion

3.1. From ground copper to electropolished copper: localised corrosion attacks, oxide growth, and copper release

Growth of Cu_2O on ground copper was observed in PBS, which has been preliminarily discussed in our previous study [38]. Here, special emphasis is placed on the copper substrate underneath. To obtain information not only from the upper oxide layer but also from the copper substrate covered, higher acceleration voltage (20 kV instead of 5 kV) was employed in SEM. From the SE images shown in Fig. 1(a–c), the growth of oxide over time is observed by the change of microscale topography. They are less evident as the scratches, since an electron beam with higher incident energy produces secondary electrons from a larger and deeper region of the sample, weakening the fine topographic contrast [40].

Nevertheless, dark dot-like zones became visible. They become much more obvious in the BSE images shown in Fig. 1(d–f). The size of these dots gradually increased as the corrosion prolonged from 1 h to 3 h. But when it extended to 6 h, they are hard to be located. Based on the origins of BSE contrast and the fact that no inclusion should be introduced during the corrosion process, it is thus suggested that each of these dark zone represents a cavity beneath the oxide coverage, as a result of localised corrosion attacks. Increase of these cavities in size implies that pitting continued. In the meantime it is the corrosion process that allowed the release of copper into solution. On the other hand, missing of these cavities in 6 h could be ascribed to a few causes. Firstly, it is clear that the oxide layer was getting thicker as a function of time, as a higher acceleration voltage is needed to detect the corrosion sites (SEM images in SI Fig. 1). Secondly, oxide could also grow inside these cavities, in another word, filling the cavities from inside (Raman spectra in SI Fig. 1).

Another important fact of these pits are their non-random distribution: along the scratches seems to be the favourable locations. Scratches that are introduced in grinding procedure do not simply represent height difference but also inhomogeneity of microstructure such as finer grain sizes and internal stress. Therefore this phenomenon is consistent with the previous study revealing pits distributed along dislocations [28]. That is to say, the state of copper surface has a huge influence on its corrosion behaviour, and in this case, the positions where pits initiate. As ground copper is always reported being covered by a deformed layer [41], it makes further analysis difficult if the aim is to comprehensively understand the correlation between the microstructure and the corrosion behaviours in PBS.

Therefore, electropolished copper were prepared, so that distinguishable grains could be revealed. Typical SE and BSE images of these coupons are displayed in Fig. 2. At the beginning of corrosion (1h), different “blocks” can be distinguished in the SE micrograph, indicating that grains were somehow corroded differently, leading to a topographic contrast. This contrast becomes ignorable as time goes by, since oxide layer began to form on all these grains covering those corrosion sites on grains. Results from BSE show a similar trend, but the origin of the contrast shown on 1 h coupon is different: it is mainly ascribed to the strong electron channelling effect of the copper grain orientation [40]. When it comes to the cavities (darker zones in BSE), their dimension kept increasing from 1 h to 6 h, symbolising continuous pit growth. Meanwhile, their locations were more regular: most of them are found lying along the copper grain boundaries, a sign of the initiation of intergranular attack.

Oxide layer on these electropolished coupons was growing thicker as well. To observe the pits underneath, low acceleration voltage is insufficient anymore for the long time corrosion coupons (SI Fig. 2). Besides, the oxide grown on these coupons has its own characteristic compared to that on ground copper. Typical cross-sectional SE images of these two coupons after 6 h corrosion are compared in Fig. 3 (a) and (b). Oxide layer on ground copper is relatively homogeneous in thickness, following the substrate topography. On electropolished copper, first of all, the aim of electropolishing protocol is confirmed, as a sharp edge with relatively low roughness copper surface is found. Secondly,

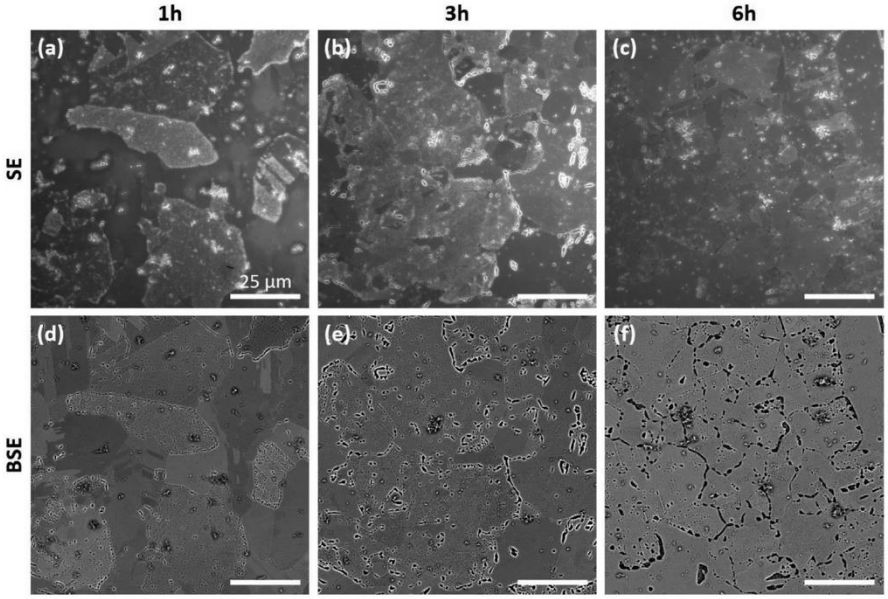

Fig. 2. Typical SEM images of electropolished copper surface after 1 h **(a & d)**, 3 h **(b & e)**, and 6 h **(c & f)** exposure to PBS. Same locations were imaged simultaneously with SE detector **(a–c)** and BSE detector **(d–f)** at 20 kV. All images share the same scale bars that presented in **(a)**.

the edge selected here as the copper-oxide interface is found still intact after corrosion. Furthermore, oxide grown on electropolished copper shows a particular phenomenon less visible on ground copper owing to the absence of near-surface deformed layer: the thickness of oxide seems to highly depend on the copper grain underneath.

Since FIB cross-sections are always too local and thus may lack of statistics, OM was applied to provide macroscopic details. The colour of these oxides in OM mainly depends on their thickness as a result of interference [42]. Therefore these OM photos (Fig. 3 (c–e)) suggest the localised similarity of the oxide thickness. Moreover, the intensity of oxide signal shown in GIXRD results could be regarded as a qualitative index of the oxide amount. In Fig. 3 (f) and (g), {111} diffraction peaks were compared since they are the most observable peaks for such a small amount of Cu_2O. It is evident that the sum of oxide grown on electropolished copper was fewer (also means slower in growth rate) than that on ground copper.

Corrosion not only introduces chemical changes on the surface, but also influences the environment, which is the solution in this case. For example, content of copper that released and entered the solution, is usually positively correlated with the antibacterial efficiency shown [17]. It could also tell the chemical interaction along the time. As shown in Fig. 4, the copper concentration in the droplet that contacted with electropolished coupons did not go through a decline phase as that with ground coupons. This phase could imply the occurrence of oxide coverage, which consumed copper ions by its formation, and at the same time, acted as a barrier stopping copper from direct release. However, owing to the exposure of distinct copper grains on electropolished coupon, oxide growth became more grain-dependent and therefore less homogeneous. One of the consequences is that it takes longer time for some certain grains to be fully covered by oxide. Therefore before this moment, copper ions are still allowed to be released directly. On the other hand, the ground copper released almost twice more copper ions in 1 h. This could mean that the electropolished copper actually has relatively higher corrosion resistance. It further implies that intergranular corrosion also dominates on ground coupons, since the existence of highly deformed layer is consisted of finer grains and thus owns a higher boundary density.

3.2. Re-deposition of oxide on copper grains

Since the oxide grown on electropolished copper has its distinct features, much attention is now drawn by it. For example, Fig. 5 presents some higher resolution micrographs of the oxide layer. Above all, boundaries exist among these oxides. Different parts of the oxide layer vary not only in contrast but also in sub-micron roughness/topography. If one looks carefully, it can be found that this slight difference is caused by the very fine facet-like features. These features are more distinguishable in those STEM images. The shapes of oxide on one grain are found to follow the same pattern. This pattern exists not just on the front side that was exposed directly by FIB (profiled red), it is also true for the other parts (profiled blue) that were covered by the Pt protection layer. And again, the copper grain shown here under the oxide seems to be still intact.

To better understand the microstructure of oxide grown on electropolished copper, EBSD was performed near the trace of droplets. Inverse pole figure (IPF) maps of coupons after 1 h and 6 h corrosion test are shown in Fig. 6 (a) and (c), respectively. It is clear that the edge of the droplet divides two regions that each has its own distinct orientation distribution. Although it has to be noted that, on the 1 h coupon, the orientation information on the droplet side may not simply represent the oxide layer. As shown in SI Fig. 3, the confidence index (CI) on the droplet side is much lower (and therefore darker). This CI indicator thus tells two facts: first, oxide layer grown in 1 h was still very thin, therefore EBSD detector also collected the Kikuchi patterns from the copper substrate below; second, similarity between the crystal structures of Cu_2O and copper leads to two similar sets of Kikuchi lines. The origins of these superposed diffractions are undistinguishable for the software. The CI values improve as the oxide grew thicker, implying that only Kikuchi lines from the upper part of the oxide layer was collected.

Back to the IPF maps, there is no doubt that sort of preferential oxide growth appeared, as the orientations presented by colours such as green, yellow, and blue become predominant on the droplet side. For the present, it seems more reasonable to call those oxides sharing a similar orientation as a “pseudo oxide grain”, since it is not easy to tell from definition whether they really belong to one grain (see SI Fig. 4).

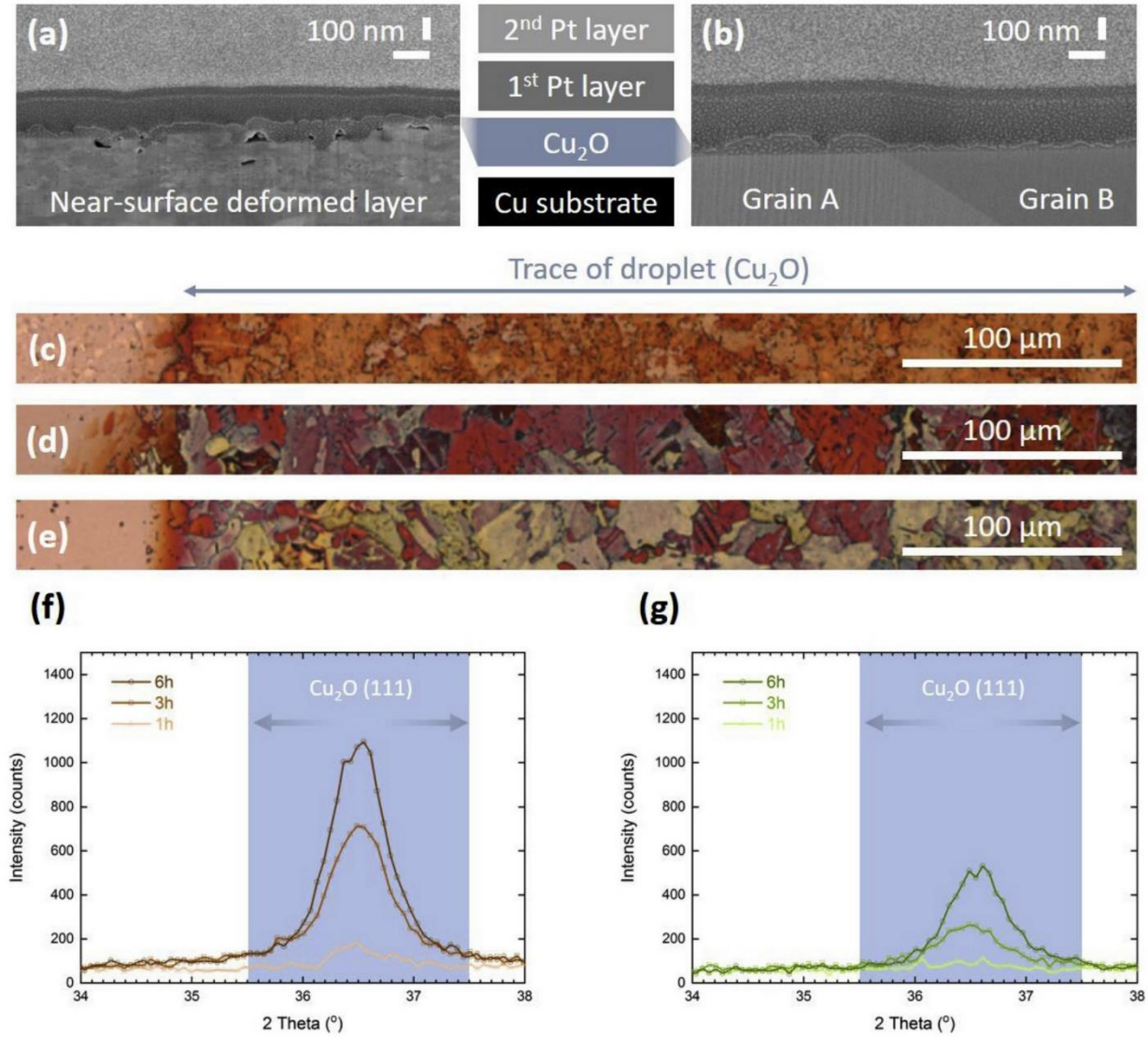

Fig. 3. Typical SEM cross-section SE images (5 kV) of ground copper **(a)** and electropolished copper **(b)** after 6 h exposure to PBS. Typical optical micrographs obtained from the edge of the droplet traces on electropolished copper surface after 1 h **(c)**, 3 h **(d)**, and 6 h **(e)** exposure to PBS. High resolution GIXRD results in the range of Cu_2O (111) planes (JCPDS#75–1531) obtained from ground copper surface **(f)** and electropolished copper surface **(g)** following various exposure periods in PBS.

Still, it is worth to mention that these pseudo oxide grains do not differ too much from the copper grains (outside the droplet) in size. This feature, together with the above STEM results, suggest certain crystallographic relationships may exist between the oxides and the copper substrate beneath.

To investigate this potential relationship, it is necessary to remove the oxide so as to obtain information from the copper grains underneath. This was accomplished by hydrochloric acid etching. EBSD of the same coupons at the same locations were obtained, whose IPF maps are shown in Fig. 6 (b) and (d). Comparing the regions outside the droplet with their un-etched state, only a small orientation drift is nevertheless inevitable because the extremely exact sample mounting is impossible. On the other hand, the former droplet sides share a similar orientation distribution as the outer regions, confirming that the acid etching is sufficient: the copper substrate was already exposed.

From a rough comparison amid Fig. 6, it is obvious that almost below every pseudo oxide grain there is a corresponding copper grain. To further investigate their orientation relationships, distribution of four certain crystal directions were chosen and re-drawn in Fig. 7, with certain degrees as tolerance. Their correspondences are considerably clear: the reason why “blue blocks” in IPF become dominant is that except from Cu_2O {111} preferential grown on Cu {111}, it is also common to find out Cu_2O {111} on Cu {001}. For the same reason, because of other two relationships, namely Cu_2O {101} // Cu {101} and Cu_2O {101} // Cu {113}, “green blocks” become popular too.

Similar orientation relationships have been reported when Cu_2O was found growing on copper single crystal in elevated temperature [36,37]. This is mainly attributed to the low misfit of copper atom positions in the interface between two phases. However, in those circumstances, growth of oxide depends on a series reactions such as capture of oxygen species, reconstruction of interface, further growth through diffusion of oxygen or oxygen vacancies, etc. [43] Also, there

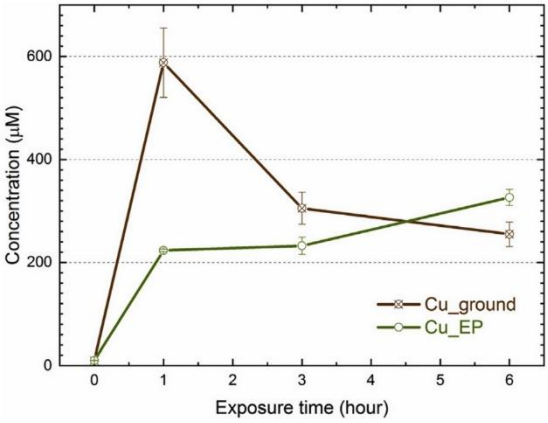

Fig. 4. Copper content in PBS following various exposure periods from ground copper surface (Cu_ground) and electropolished copper surface (Cu_EP). The error bars indicate the standard deviations calculated from three independent measurements.

are usually two consistently moving oxide fronts: the side exposed to the air and the oxide-metal interface, not just the former one shown in the current STEM results. In addition, this type of epitaxial growth was also found on copper single crystal when it was immersed in a copper contained solution where further considered as a deposition process [35].

These relevant examples are helpful in understanding the current study. The solution applied (PBS) for sure does not contain any copper species in the beginning, however, it becomes a copper contained solution once corrosion happens and copper ions are released. Afterwards, the process can be described similar to the epitaxial growth in thin films fabrication [44]. Firstly, copper oxide nucleation centres are formed. These nucleus are tiny, separate but sharing the same crystal orientation with that are also growing on the same copper grain. They keep growing as long as the copper ions in the solution are adequate, and finally merge with each other, becoming seemingly a pseudo grain. This type of growth is also statistically confirmed from the EBSD results. From this perspective, the reason why thickness of oxides differ from grains can also be explained: the growth rates are also orientation-dependent, i.e. grain-dependent. To sum up, the formation of Cu_2O on electropolished copper in PBS is a re-deposition process, assisted and accomplished by the copper ions presented in the solution, rather than a classical direct oxidation of the metallic surface in elevated temperature conditions.

3.3. Localised corrosion attacks on specific microstructures

Now that the oxide layer has been removed, an opportunity to check the corrosion sites on copper surface is provided. A localised EBSD scan was performed with a finer step size for the 6 h corrosion coupon and various forms of this scan are shown in Fig. 8. For example, image quality (IQ) map is an effective way to present the locations of pits or cavities, since these areas have less clear Kikuchi patterns, i.e. worse image quality. Combining carefully with the grain boundary map (possible obstacles see SI Fig. 5), it is clear that intergranular corrosion occurred at both twin boundaries and other grain boundaries. However, only small proportion of twin boundaries was found attacked, whereas other boundaries seem to be more susceptible to the corrosion attack. Former research has suggested that low angle grain boundaries and coherent/twin boundaries have higher corrosion resistance in Cl^- contained solution [29]. It is, nevertheless, fair to claim that only the latter preference is observed in this study, because the proportion of low

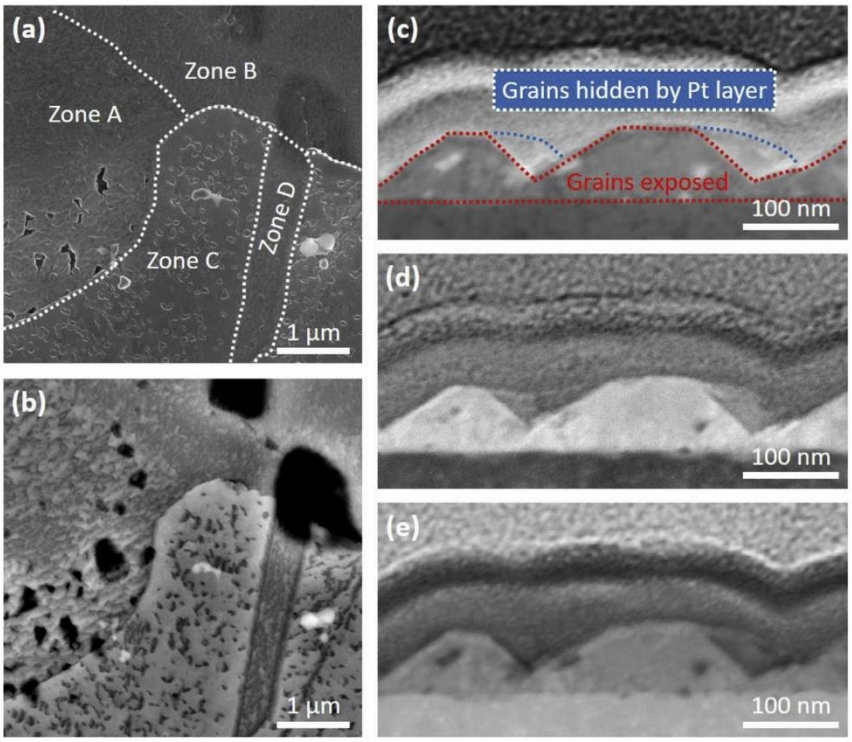

Fig. 5. High resolution SEM images of electropolished copper surface after 6 h exposure to PBS taken by SE detector **(a)** and BSE detector **(b)** at 5 kV. STEM cross-section images of the same coupon taken in: **(c)** bright field (BF), **(d)** dark field (DF), and **(e)** high angle annular dark field (HAADF).

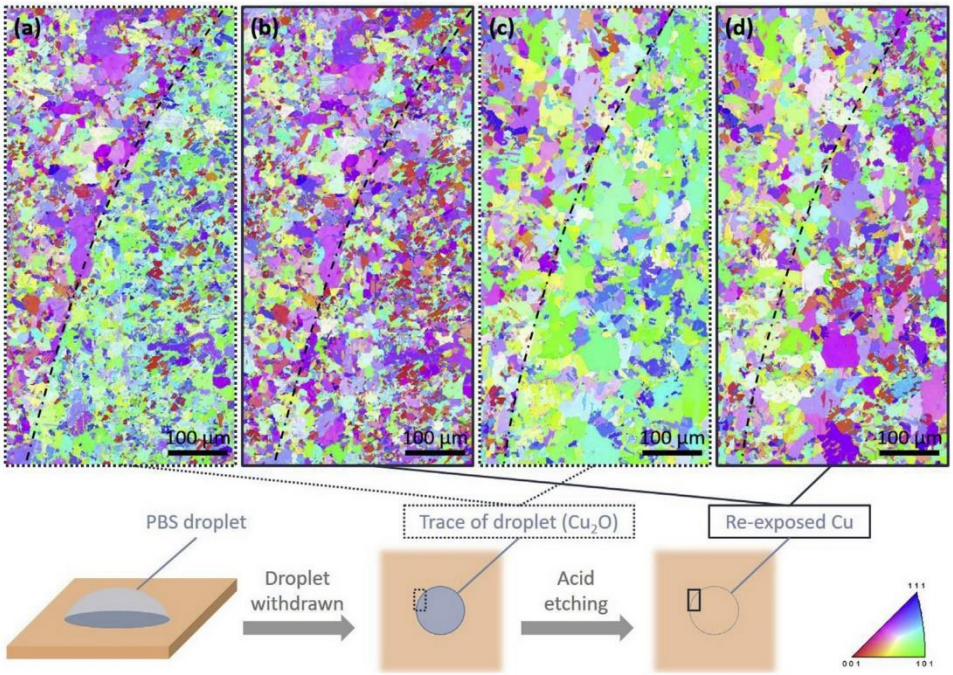

Fig. 6. EBSD results indexed and shown in the form of inverse pole figure (IPF) maps obtained from the edge of the droplet traces on electropolished copper surface after 1 h **(a–b)** and 6 h **(c–d)** exposure to PBS. The same areas were first sampled directly after exposure **(a & c)** and then after acid etching **(b & d)**. Long dash - dot lines indicate the edge of PBS droplets. A schematic description of the treatment process and the sampled location is shown below the maps. The legend is for the above IPF maps.

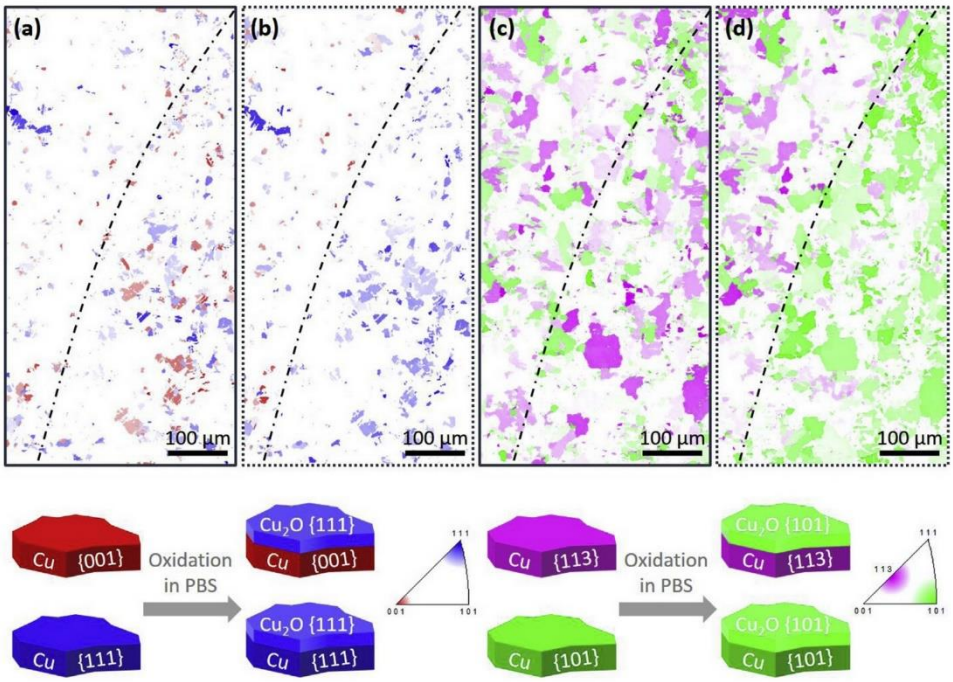

Fig. 7. Crystal direction (CD) maps extracted from the EBSD results obtained from the 6 h PBS treated electropolished copper surface after **(a & c)** and before **(b & d)** acid etching. The tolerance (maximum value) of misorientation angles of each CD are set as below: 10^0 for {001}; 15^0 for {111}; 12^0 for {113}; 15^0 for {101}.

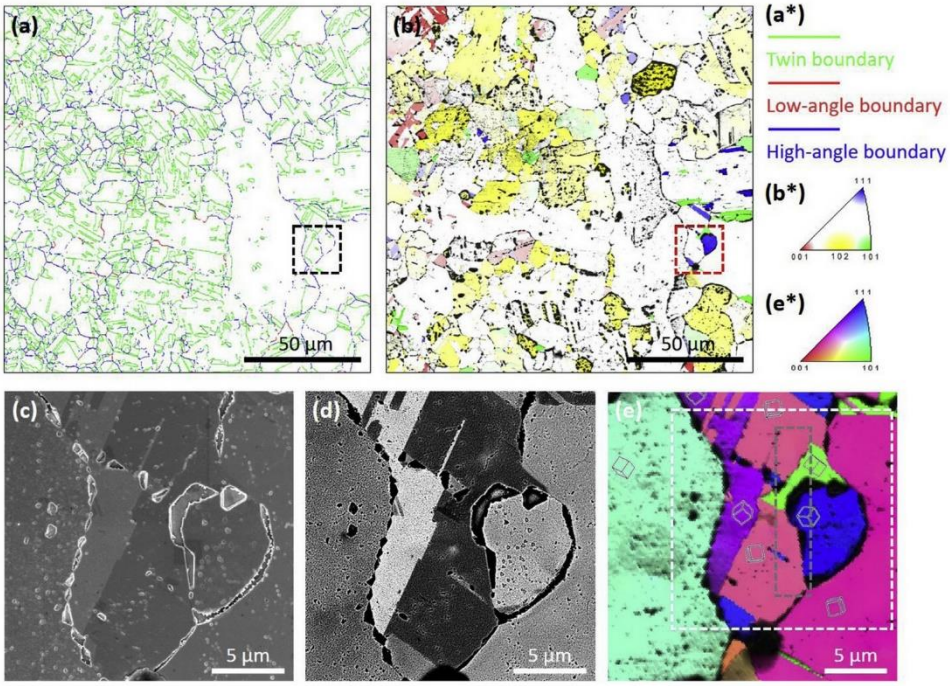

Fig. 8. Grain boundary networks **(a)** of electropolished copper surface after 6 h exposure to PBS and the following acid etching. Image quality (IQ) indicator and crystal direction (CD) map are combined in **(b)**, where threshold of IQ is set as 30% of the maximum measured value. High resolution SEM images of from the square region marked in **(a)** and **(b)** were taken by SE detector **(c)** and BSE detector **(d)** at 5 kV. EBSD result of the same region is shown within white dash squared in **(e)** as a combination of inverse pole figure (IPF) map and IQ map (threshold of 50%) with lattice indicators. The grey dash squared region is further presented in the following Fig. 9. Legend **(a*)** for **(a)** has defined Σ3 boundary as "twin boundary", grain boundary with misorientation from 5 to 15° as "low-angle boundary" and from 15 to 62.8° as "high-angle boundary". The legend **(b*)** which shows tolerance (maximum value) of misorientation angles in of each CD **(b)** are set as below: 10^0 for {001}; 10^0 for {101}; 10^0 for {111}; 13^0 for {102}. **(e*)** is the legend of **(e)**.

angle boundaries are relatively low and may not show the general trend even there is one.

Moreover, removal of oxide layer helps to find out the corrosion sites within grains. It happens to be less obvious on grains with regular Miller index planes ({001}, {101}, and {111}) parallel to the surface. On the contrary, for most of the grains suffering severe corrosion, they tend to share a closed crystal direction to {102}. However, it is also true that grain-dependent corrosion may not be simply related to the grains themselves: studies using in-situ scanning electrochemical microscopy (SECM) found out that the tip current measured on grains, which could symbolise the corrosion resistance, was also determined by the neighbour grains [30,31]. Scanning electrochemical cell microscopy (SECCM) can be a promising method for the future work, since the electrolyte can be restricted on a single grain [45], so that the likely influences from the neighbour grains should be isolated.

Specifically, high resolution SEM images (Fig. 8 (c–d)) provide details of the corrosion sites in terms of their shapes: SE images tell the bare facets exposed inside a cavity, while BSE images highlight the appearance of cavity itself. It is easily found that both these shapes follow certain patterns, reflecting the crystal direction of the grains they belong to (Fig. 8 (e)). This implies a result of crystallographic corrosion/etching, where the most dissolvable crystallographic planes were left and exposed [32,46]. Thus the shape of a cavity highly depends on the grain orientation. Identifying this mechanism helps to know better how preferential corrosion occurs as a quasi-two-step process. The first step is the initiation of the corrosion. Take grain boundaries as an example, they are generally believed to be less stable therefore favourable to corrosion. But once these unstable regions are corroded away, the rest are the relatively perfect grains on both sides of the original boundaries. However, corrosion does not necessarily stop, it could widen the cavity, not as a result of the unstable regions, but through crystallographic corrosion. Reactants (Cu^{2+} & Cl^-) and pH inside pits that are usually different from the bulk solution, should play an assistanting role in this step. Otherwise global nucleation of corrosion sites should have been observed, instead of the sustained developing of the existent attacked sites.

Since corrosion sites are always lower than the original surface, this means that these locations may not always be available for EBSD analysis. On one hand, due to the topographical shadow effect (i.e. projection effect), the corresponding relationship between the actual regions and patterns received may not match. On the other hand, the quality of Kikuchi patterns could worsen, therefore the orientation information of certain positions cannot be correctly identified by the software. Consequently, to compare and identify Kikuchi patterns manually could be a meaningful approach to extract those distorted information. Fig. 9 shows a region mainly composed by three identified grains and an intergranular attack site among them. Kikuchi patterns from these three grains are clear and distinguishable, providing eligible references for the following comparison. Kikuchi patterns from three positions inside the groove, nevertheless, are as expected with considerably worse contrast. Especially for position 2 and 3, a relatively large portion of EBSD camera did not receive any effective signal and thus looks completely dark. The reason is that those Kikuchi lines generated were blocked by the "cliff" of grain C. However, to carefully compare the recorded parts, one could still find out that all these three positions should be identical to each other. And most importantly, they can be classified as part of the pattern obtained from grain A. That is to say, although the so-called intergranular corrosion initiated in the grain boundary, the further expansion of the pit could be grain-preferential and therefore anisotropic, probably owing to the localised galvanic

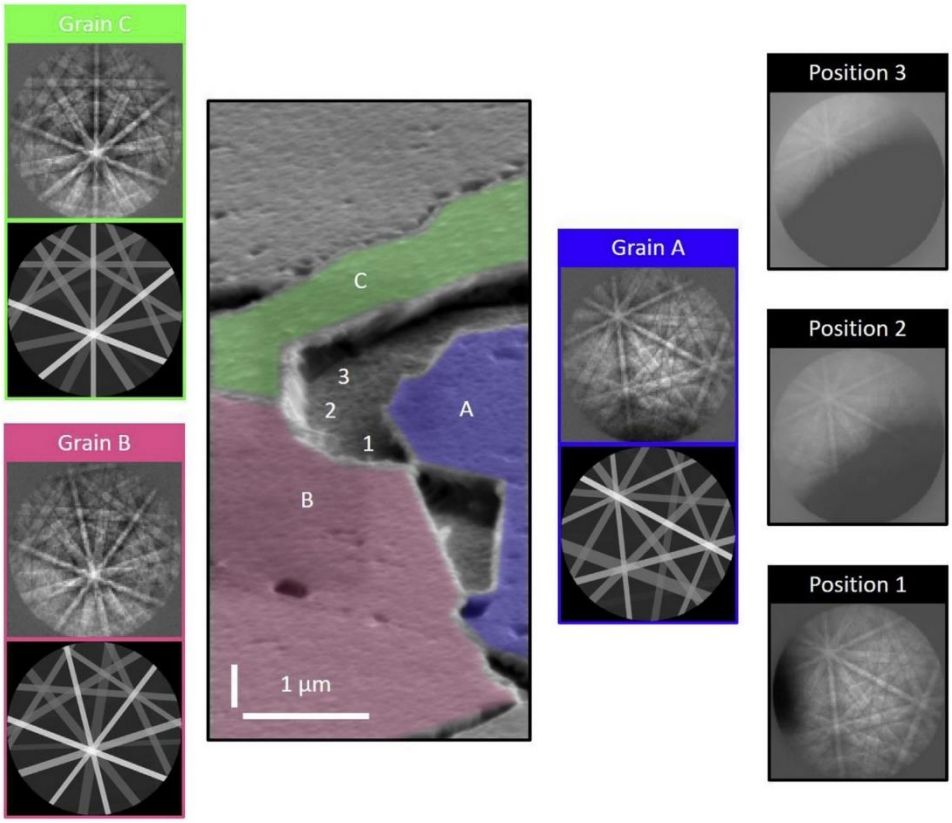

Fig. 9. SEM image (5 kV) of electropolished copper surface after 6 h exposure to PBS and the following acid etching, at a tilt angle of 70^0. Same region has been indicated in Fig. 8 (e). Actual or/and reconstructed Kikuchi patterns of the indicated grains (named by letters) or positions (named by numbers) are shown.

corrosion between two grains. In this case, the exposed surface is in fact part of grain A, suggesting that grain A was acting as anode for the whole corrosion period, suffering from most intense dissolution. Grain B and grain C, on the other hand, were cathodic sites and free from corrosion. These details are also the evidence of how neighbour grains could influence the tendency of intergranular attack.

3.4. Corrosion phenomena in E. coli PBS suspension

Thus far, we have obtained fundamental information from the copper-PBS system, which further fosters a better understanding in the corrosion phenomena if *E. coli* are presented. As shown in Fig. 10 (a), localised corrosion attacks are commonly found in this circumstance. These pits are following the similar distribution as those identified on PBS corroded coupon (originally shown in Fig. 1). On electropolished copper, Fig. 10 (b) and (c) also show similar corrosion sites as those introduced by pure PBS: some grains and some sections of grain boundaries were under severe attack. It should be noted that, these SEM observations were done without acid etching, since there were almost no GIXRD detectable oxide coverage formation (Fig. 10 (d)). This could be attributed to the roles played by bacteria, such as copper ion accumulation from the solution [38]. This argument is now further supported by the re-deposition mechanism of oxide growth described in previous section: copper ions are accumulated by the bacteria and therefore cannot be used to form oxide.

For the same reason, direct EBSD analysis of the corrosion sites becomes possible. Fig. 11 demonstrates very similar details of those preferential corroded sites in the presence of *E. coli*: grain boundaries and {102} direction grains are relatively vulnerable; marked intergranular attack and crystallographic etching are found as well. These similar features on electropolished coupons regardless of the presence of *E. coli* are together suggesting one fact: adding *E. coli* into PBS does not significantly change the major corrosion mechanisms on copper.

However, does this fact also mean that *E. coli* would not introduce new corrosion sites either? Observations shown in Fig. 12 can provide some hints. For example, except from the pits and the remained bacteria (owing to insufficient withdrawal), a huge amount of separate dark sites are found. They are different in size, but the largest ones are similar to the size of *E. coli* cell. After compared with the same feature under those bacteria remained, it is thus reasonable to deduct that these dark sites might represent the locations where the bacteria once were (i.e. before they were withdrawn). Their chemical information is unknown at the moment, as the BSE image already suggests its thinness, making in-situ EDS analysis impractical. However, it is much more noteworthy that the copper surface covered by these marks were not necessarily be corroded. The opposite is also true: the locations where pits appeared do not necessarily have these marks on/around them. This may verify the role of *E. coli* in the present corrosion experiment and thereby answer the abovementioned question: no new corrosion sites introduced exclusively by *E. coli* is found.

From another perspective, the existence of these dark marks convey a hidden message: *E. coli* tend to settle down and contact with the surface. It is no surprise that this happens to *E. coli* after they get killed because of the antibacterial nature of copper ions [39], and therefore lose their mobility. Although this type of contact does not show any influence in the corrosion attack on copper, it does reduce the area where copper is directly exposed to solution. Oxide re-deposition could

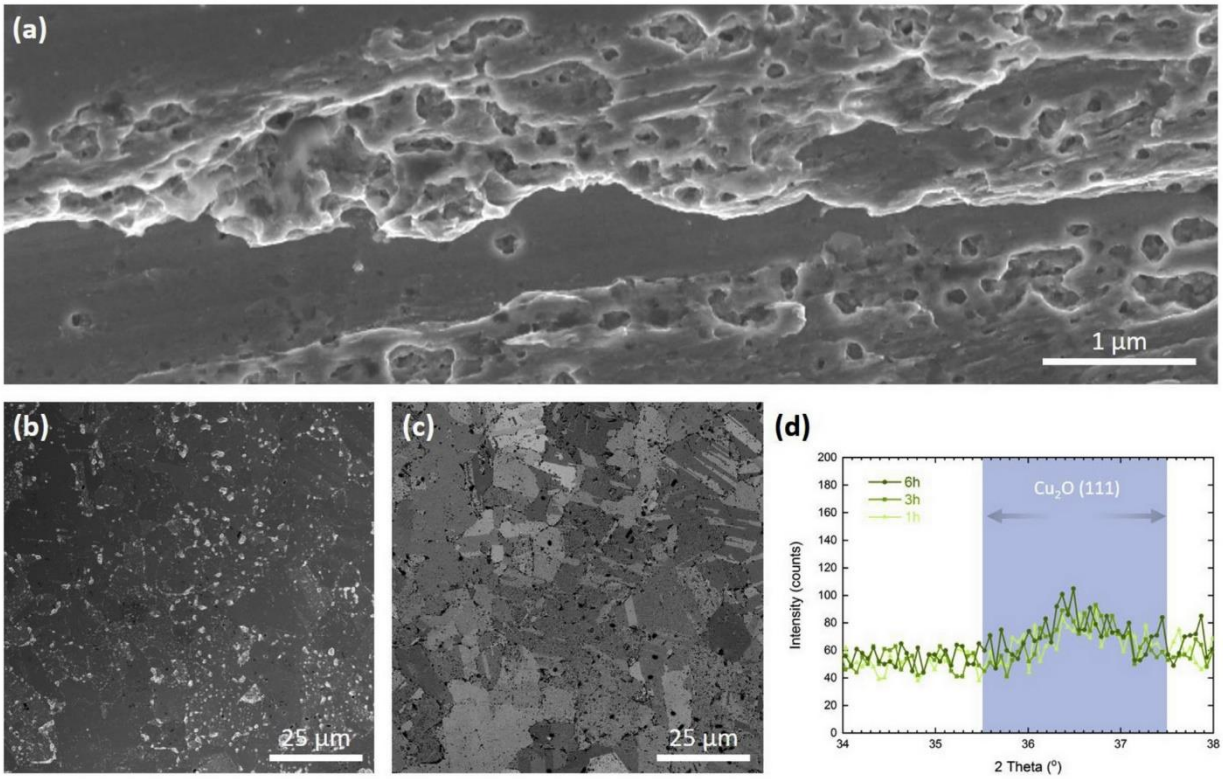

Fig. 10. Typical SEM image **(a)** of ground copper surface after 3 h of exposure to *E. coli* PBS suspension. SE image **(b)** and BSE image **(c)** were taken at the same region of an electropolished copper surface after 6 h exposure to *E. coli* PBS suspension. High resolution GIXRD result in the range of Cu_2O (111) planes (JCPDS#75–1531) obtained from electropolished copper surface **(d)** following various exposure periods in *E. coli* PBS suspension.

also be prevented in such a way.

Combined with other results discussed, a more comprehensive picture of antibacterial efficiency test is now shown, in terms of interplay between copper surface and bacteria in PBS environment, where corrosion should be considered as the key. On the other hand, efficient design of antibacterial surfaces could be expected based on the phenomena observed. For example, surface with finer grains contains longer grain boundary section should include more favourable corrosion sites to release antimicrobial copper ions. Preferred growth of copper thin films could also be applied to control exposed facet, resulting in a different corrosion resistance, which eventually leads to a controllable antibacterial activity. Furthermore, surfaces consisted of exposed crystallographic planes with lower oxide growth rate should benefit long-term application.

4. Conclusions

Chemical and morphological changes induced by PBS on copper surfaces were examined, which can be divided into two simultaneous process: localised corrosion attacks of copper surface and oxide growth on top. Some significant features and important implications found in these two processes are summarised below.

For localised corrosion attacks:

- Pitting sites were found along the scratches on ground copper. They grew in size from 1 h to 3 h, but become less distinguishable in 6 h.
- On electropolished copper, intergranular corrosion was the most predominant attack, where twin boundaries were less vulnerable. After an intergranular attack initiates on the grain boundaries, it can further develop in an extremely anisotropic way, probably due to localised galvanic corrosion between neighbouring grains.
- Copper grains have also shown different corrosion resistance. Those suffered much attack have orientations close to {102} planes parallel to the surface. The appearance of the corrosion sites indicates the occurrence of crystallographic etching.
- *E. coli* addition in PBS did not evidently change the characteristics of above-mentioned corrosion phenomena in 6 h experiment. No correlation has been found between the corrosion sites and the positions where bacteria locate.

For oxide growth:

- After same treatment durations, fewer amount of Cu_2O has grown on electropolished copper, which was less homogeneous than on ground copper. Distinction in the copper release trend could be one of the consequences.
- On electropolished copper, growth of Cu_2O can be regarded as an epitaxial re-deposition process, which leaded to a grain-dependent growth rate as well as a distinct difference in sub-micron surface morphology.
- Four major pairs of orientation relationships were found, namely Cu_2O {111} // Cu {001}, Cu_2O {111} // Cu {111}, Cu_2O {101} // Cu {101}, and Cu_2O {101} // Cu {113}, suggesting that it was the misfit of copper atom positions that mainly determine this re-deposition process.
- With addition of *E. coli* in PBS, oxide growth on electropolished copper was inhibited to a great extent.

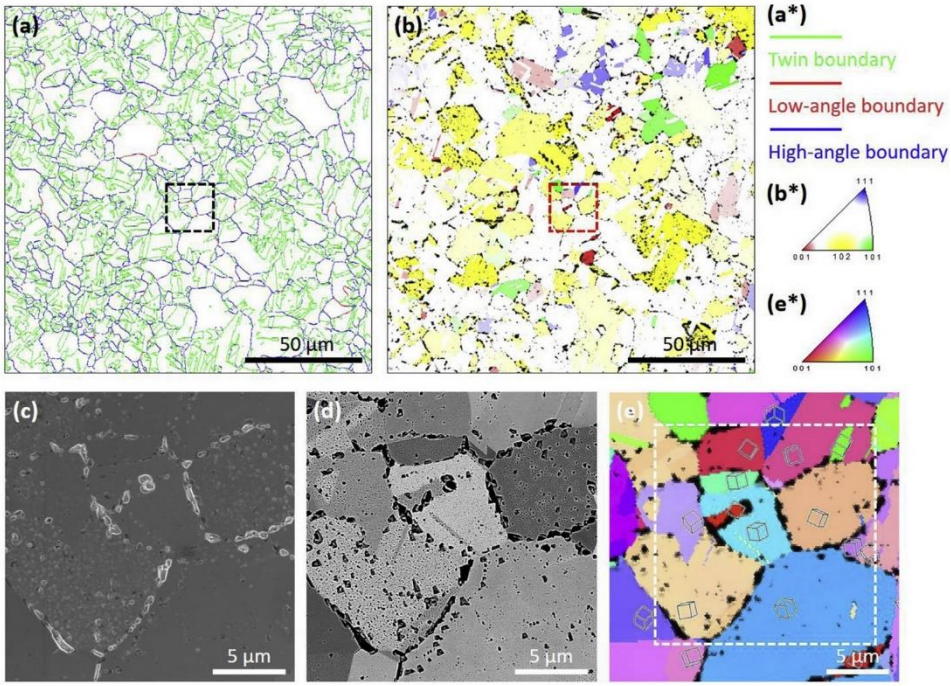

Fig. 11. Grain boundary networks **(a)** of electropolished copper surface after 6 h exposure to *E. coli* PBS suspension. Image quality (IQ) indicator and crystal direction (CD) map are combined in **(b)**, where threshold of IQ is set as 30% of the maximum measured value. High resolution SEM images of from the square region marked in **(a)** or **(b)** were taken by SE detector **(c)** and BSE detector **(d)** at 5 kV. EBSD result of the same region is shown within dash squared in **(e)** as a combination of inverse pole figure (IPF) map and IQ map (threshold of 50%) with lattice indicators. Legend **(a*)** for **(a)** has defined Σ3 boundary as "twin boundary", grain boundary with misorientation from 5 to 15° as "low-angle boundary" and from 15 to 62.8° as "high-angle boundary". The legend **(b*)** which shows tolerance (maximum value) of misorientation angles in of each CD **(b)** are set as below: 10^0 for {001}; 10^0 for {101}; 10^0 for {111}; 13^0 for {102}. **(e*)** is the legend of **(e)**.

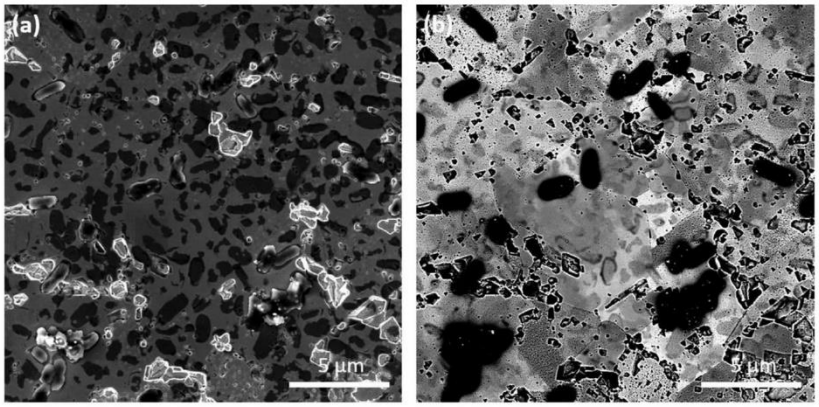

Fig. 12. SEM images of electropolished copper surface after 6 h exposure to *E. coli* PBS suspension were taken by SE detector **(a)** and BSE detector **(b)** at 5 kV.

Declaration of competing interest

The authors declare that they have no known competing financial interests or personal relationships that could have appeared to influence the work reported in this paper.

Acknowledgements

This study was supported by Erasmus Mundus Joint European Doctoral Programme in Advanced Materials Science and Engineering (DocMASE, 512225-1-2010-1-DE-EMJD, European Commission) and the PhD-Track-Programme (PhD02-14, Franco-German University). The ICP-MS experiments were supported by Dr. Ralf Kautenburger from the chair of Inorganic Solid State Chemistry. The authors acknowledge Prof. Volker Presser and Leibniz Institute for New Materials for the access of Raman spectrometer. We also thank Dr. Christoph Pauly for technical support and inspirational discussion in coupon preparation and characterisation. The kind suggestions received from the patient reviewer are instructive.

Appendix A. Supplementary data

Supplementary data to this article can be found online at https://doi.org/10.1016/j.matchar.2019.109985.

Data availability

The data that support the findings of this study are available from the corresponding author on request.

References

[1] M.P. Muller, C. MacDougall, M. Lim, I. Armstrong, A. Bialachowski, S. Callery, W. Ciccotelli, M. Cividino, J. Dennis, S. Hota, G. Garber, J. Johnstone, K. Katz, A. McGeer, V. Nankoosingh, C. Richard, M. Vearncombe, Antimicrobial surfaces to prevent healthcare-associated infections: a systematic review, J. Hosp. Infect. 92 (2018) 7–13.

[2] M. Vincent, R.E. Duval, P. Hartemann, M. Engels-Deutsch, Contact killing and antimicrobial properties of copper, J. Appl. Microbiol. 124 (2018) 1032–1046.

[3] R.J. Turner, Metal-based antimicrobial strategies, Microbial Biotechnology 10 (2017) 1062–1065.

[4] S.L. Warnes, S.M. Green, H.T. Michels, C.W. Keevil, Biocidal efficacy of copper alloys against pathogenic enterococci involves degradation of genomic and plasmid DNAs, Appl. Environ. Microbiol. 76 (2010) 5390–5401.

[5] R.K. Swarnkar, J.K. Pandey, K.K. Soumya, P. Dwivedi, S. Sundaram, S. Prasad, R. Gopal, Enhanced antibacterial activity of copper/copper oxide nanowires prepared by pulsed laser ablation in water medium, Appl. Phys. A 122 (2016) 1–7.

[6] S. Shinde, H. Dhaygude, D.-Y. Kim, G. Ghodake, P. Bhagwat, P. Dandge, V. Fulari, Improved synthesis of copper oxide nanosheets and its application in development of supercapacitor and antimicrobial agents, J. Ind. Eng. Chem. 36 (2016) 116–120.

[7] G. Sharmila, M. Thirumarimurugan, V.M. Sivakumar, Optical, catalytic and antibacterial properties of phytofabricated CuO nanoparticles using Tecoma castanifolia leaf extract, Optik - International Journal for Light and Electron Optics 127 (2016) 7822–7828.

[8] C. Hahn, M. Hans, C. Hein, A. Dennstedt, F. Mücklich, P. Rettberg, C.E. Hellweg, L.I. Leichert, C. Rensing, R. Moeller, Antimicrobial properties of ternary eutectic aluminum alloys, Biometals 31 (2018) 759–770.

[9] Y. Kang, J. Park, D.-W. Kim, H. Kim, Y.-C. Kang, Antibacterial and physicochemical properties of co-sputtered CuSn thin films, Surf. Interface Anal. 50 (2017) 138–145.

[10] A. Javid, M. Kumar, S. Yoon, J.H. Lee, J.G. Han, Size-controlled growth and antibacterial mechanism for Cu:C nanocomposite thin films, Phys. Chem. Chem. Phys. 19 (2017) 237–244.

[11] Y. Sun, V. Tran, D. Zhang, W.B. Wang, S. Yang, Technology and antimicrobial properties of Cu/TiB2 composite coating on 304 steel surface prepared by laser cladding, Mater. Sci. Forum 944 (2019) 473–479.

[12] V.M. Villapún, C.C. Lukose, M. Birkett, L.G. Dover, S. González, Tuning the antimicrobial behaviour of Cu85Zr15 thin films in “wet” and “dry” conditions through structural modifications, Surf. Coat. Technol. 350 (2018) 334–345.

[13] G.I. Nkou Bouala, A. Etiemble, C. Der Loughian, C. Langlois, J.F. Pierson, P. Steyer, Silver influence on the antibacterial activity of multi-functional Zr-Cu based thin film metallic glasses, Surf. Coat. Technol. 343 (2017) 108–114.

[14] S.L. Warnes, V. Caves, C.W. Keevil, Mechanism of copper surface toxicity in Escherichia coli O157:H7 and Salmonella involves immediate membrane depolarization followed by slower rate of DNA destruction which differs from that observed for Gram-positive bacteria, Environ. Microbiol. 14 (2012) 1730–1743.

[15] S.L. Warnes, C.W. Keevil, Inactivation of Norovirus on dry copper alloy surfaces, PLoS One 8 (2013) e75017.

[16] I. Platzman, R. Brener, H. Haick, R. Tannenbaum, Oxidation of polycrystalline copper thin films at ambient conditions, J. Phys. Chem. C 112 (2008) 1101–1108.

[17] M. Hans, A. Erbe, S. Mathews, Y. Chen, M. Solioz, F. Mücklich, Role of copper oxides in contact killing of bacteria, Langmuir 29 (2013) 16160–16166.

[18] M. Walkowicz, P. Osuch, B. Smyrak, T. Knych, E. Rudnik, Ł. Cieniek, A. Różańska, A. Chmielarczyk, D. Romaniszyn, M. Bulanda, Impact of oxidation of copper and its alloys in laboratory-simulated conditions on their antimicrobial efficiency, Corros. Sci. 140 (2018) 321–332.

[19] H. Kawakami, K. Yoshida, Y. Nishida, Y. Kikuchi, Y. Sato, Antibacterial properties of metallic elements for alloying evaluated with application of JIS Z 2801:2000, ISIJ Int. 48 (2008) 1299–1304.

[20] S. Wu, S. Altenried, A. Zogg, F. Zuber, K. Maniura-Weber, Q. Ren, Role of the surface nanoscale roughness of stainless steel on bacterial adhesion and microcolony formation, ACS Omega 3 (2018) 6456–6464.

[21] G. Wang, H. Feng, L. Hu, W. Jin, Q. Hao, A. Gao, X. Peng, W. Li, K.-Y. Wong, H. Wang, Z. Li, P.K. Chu, An antibacterial platform based on capacitive carbon-doped TiO2 nanotubes after direct or alternating current charging, Nat. Commun. 9 (2018) 2055.

[22] D. Wojcieszak, M. Mazur, D. Kaczmarek, P. Mazur, B. Szponar, J. Domaradzki, L. Kepinski, Influence of the surface properties on bactericidal and fungicidal activity of magnetron sputtered Ti–Ag and Nb–Ag thin films, Mater. Sci. Eng. C 62 (2016) 86–95.

[23] L.L. Foster, M. Hutchison, J.R. Scully, Corrosion of Cu-5Zn-5Al-1Sn (89% Cu, 5% Zn, 5% Al, 1% Sn) compared to copper in synthetic perspiration during cyclic wetting and drying: the fate of copper, Corrosion 72 (2016) 1095–1106.

[24] D.J. Horton, H. Ha, L.L. Foster, H.J. Bindig, J.R. Scully, Tarnishing and Cu ion release in selected copper-base alloys: implications towards antimicrobial functionality, Electrochim. Acta 169 (2015) 351–366.

[25] B. Beverskog, I. Puigdomenech, Revised pourbaix diagrams for copper at 25 to 300°C, J. Electrochem. Soc. 144 (1997) 3476–3483.

[26] S.M. Mayanna, T.H.V. Setty, Role of chloride ions in relation to copper corrosion and inhibition, Proc. Indian Acad. Sci. Sect. A 80 (1974) 184–193.

[27] A. El Warraky, H.A. El Shayeb, E.M. Sherif, Pitting corrosion of copper in chloride solutions, Anti-corrosion Methods & Mater. 51 (2004) 52–61.

[28] L.C. Lovell, J.H. Wernick, Dislocation etch pits and polygonization in high-purity copper, J. Appl. Phys. 30 (1959) 590–592.

[29] Y. Zhao, I.C. Cheng, M.E. Kassner, A.M. Hodge, The effect of nanotwins on the corrosion behavior of copper, Acta Mater. 67 (2014) 181–188.

[30] E. Martinez-Lombardia, V. Maurice, L. Lapeire, I. De Graeve, K. Verbeken, L. Kestens, P. Marcus, H. Terryn, In situ scanning tunneling microscopy study of grain-dependent corrosion on microcrystalline copper, J. Phys. Chem. C 118 (2014) 25421–25428.

[31] L. Lapeire, E. Martinez Lombardia, K. Verbeken, I. De Graeve, L.A.I. Kestens, H. Terryn, Effect of neighboring grains on the microscopic corrosion behavior of a grain in polycrystalline copper, Corros. Sci. 67 (2013) 179–183.

[32] D. Landolt, R.H. Muller, C.W. Tobias, Crystallographic factors in high-rate anodic dissolution of copper, J. Electrochem. Soc. 118 (1971) 36–40.

[33] C. Toparli, S.W. Hieke, A. Altin, O. Kasian, C. Scheu, A. Erbe, State of the surface of antibacterial copper in phosphate buffered saline, J. Electrochem. Soc. 164 (2017) H734–H742.

[34] J.P.G. Farr, A.J.S. McNeil, Epitaxy in the aqueous oxidation of (001) single crystal copper films, Surf. Technol. 8 (1979) 399–404.

[35] K.R. Lawless, G.T. Miller, Jnr, The epitaxial relationships of cuprous oxide formed on copper single crystals immersed in an aqueous solution of copper sulfate, Acta Crystallogr. 12 (1959) 594–600.

[36] T. Yamaguti, An investigation on oxidation of crystal surfaces with electron diffraction method, II. Copper single crystals, Proc. Physico-Mathematical Soc. Jpn. 3rd Series 20 (1938) 230–241.

[37] K.R. Lawless, A.T. Gwathmey, The structure of oxide films on different faces of a single crystal of copper, Acta Metall. 4 (1956) 153–163.

[38] J. Luo, C. Hein, J. Ghanbaja, J.-F. Pierson, F. Mücklich, Bacteria accumulate copper ions and inhibit oxide formation on copper surface during antibacterial efficiency test, Micron 127 (2019) 102759.

[39] J. Luo, C. Hein, F. Mücklich, M. Solioz, Killing of bacteria by copper, cadmium, and silver surfaces reveals relevant physicochemical parameters, Biointerphases 12 (2017) 020301.

[40] J.I. Goldstein, D.E. Newbury, J.R. Michael, N.W. Ritchie, J.H.J. Scott, D.C. Joy, Scanning Electron Microscopy and X-Ray Microanalysis, Springer, 2017.

[41] B.J. Cruickshank, A.A. Gewirth, R.M. Rynders, R.C. Alkire, In situ observations of shape evolution during copper dissolution using atomic force microscopy, J. Electrochem. Soc. 139 (1992) 2829–2832.

[42] D. Britz, A. Hegetschweiler, M. Roberts, uuml, F. cklich, Reproducible surface contrasting and orientation correlation of low-carbon steels by time-resolved beraha color etching, Mater. Perform. Charact. (2016) 5.

[43] K.R. Lawless, The oxidation of metals, Rep. Prog. Phys. 37 (1974) 231.

[44] Y. Wang, J. Ghanbaja, F. Soldera, P. Boulet, D. Horwat, F. Mücklich, J.F. Pierson, Controlling the preferred orientation in sputter-deposited Cu2O thin films: influence of the initial growth stage and homoepitaxial growth mechanism, Acta Mater. 76 (2014) 207–212.

[45] N. Ebejer, A.G. Güell, S.C.S. Lai, K. McKelvey, M.E. Snowden, P.R. Unwin, Scanning electrochemical cell microscopy: a versatile technique for nanoscale electrochemistry and functional imaging, Annu. Rev. Anal. Chem. 6 (2013) 329–351.

[46] J.H. Seo, J.-H. Ryu, D.N. Lee, formation of crystallographic etch pits during AC etching of aluminum, J. Electrochem. Soc. 150 (2003) B433–B438.

Supplementary Information

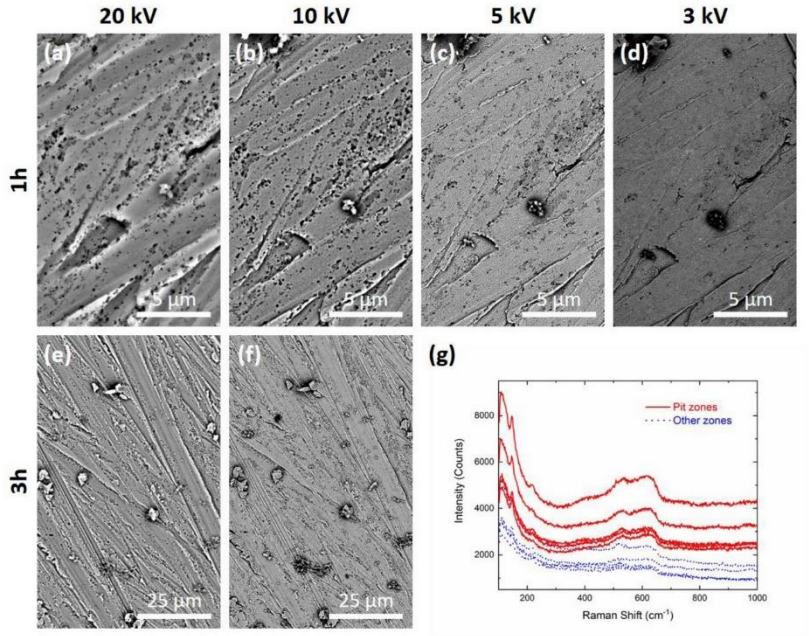

Supplementary Figure 1 | Typical SEM images of ground copper surface after 1 h **(a-d)** and 3 h **(e-f)** exposure to PBS imaged with BSE at different accelerating voltages (listed above each column). Raman spectra **(g)** of two types of locations obtained from the 3 h coupon are marked with different colours.

Brief interpretation: From the SEM images, the pits could still be distinguished at 5 kV for the 1 h corrosion coupon, while those on the 3 h coupon have already become much less observable even at 10 kV. These observations indicate the growth of oxide in thickness. The Raman results, on the other hand, show higher oxide signal from pits, suggesting the possibility of oxide growth inside the pits.

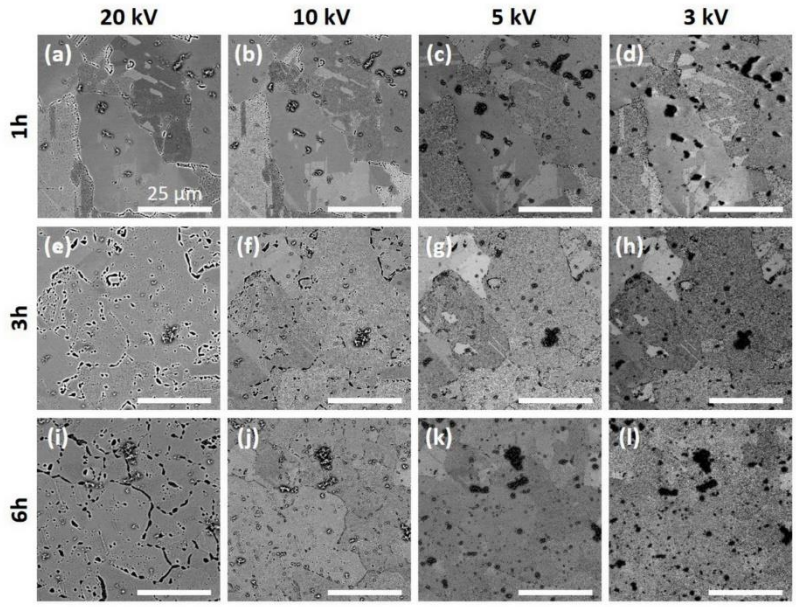

Supplementary Figure 2 | Typical SEM images of electropolished copper surface after 1 h **(a-d)**, 3 h **(e-h)** and 6 h **(i-l)** exposure to PBS imaged with BSE detector at different accelerating voltages (listed above each column).

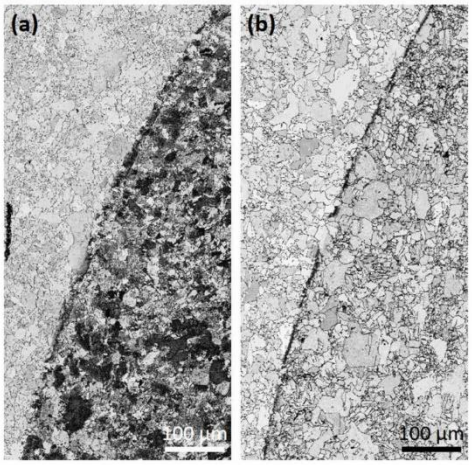

Supplementary Figure 3 | Confidence index (CI) indicator are extracted (threshold of 100%) from the EBSD results obtained from the edge of the droplets on electropolished copper surface after 1 h **(a)** and 6 h **(b)** exposure to PBS.

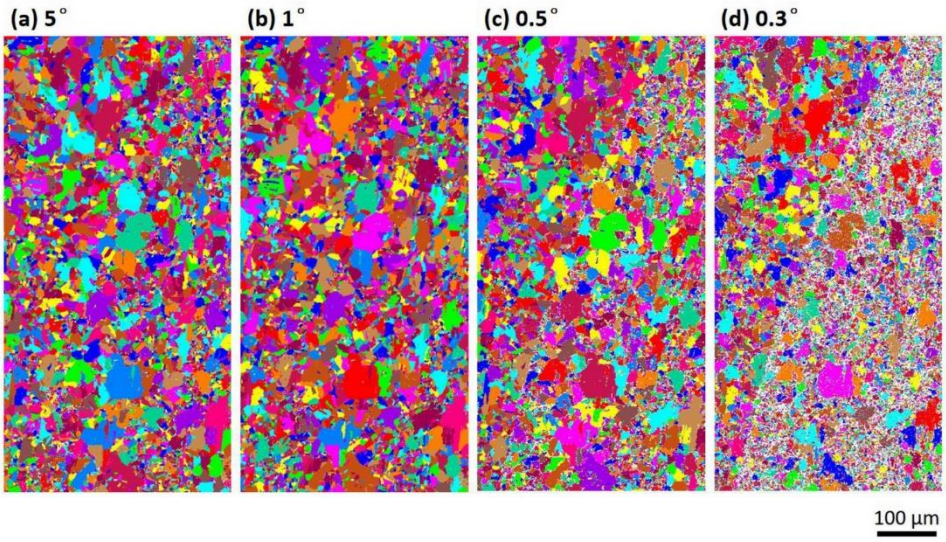

Supplementary Figure 4 | Unique grain colour maps extracted from the same region shown in Manuscript Figure 6 (c), defined with different misorientation angle criterion for grains.

Brief interpretation: It is clearly shown that as the maximum misorientation angle applied in grain definition decreases, changes on the droplet side is more obvious. This suggests the misorientation within pseudo oxide grains is relatively larger than that within copper grains.

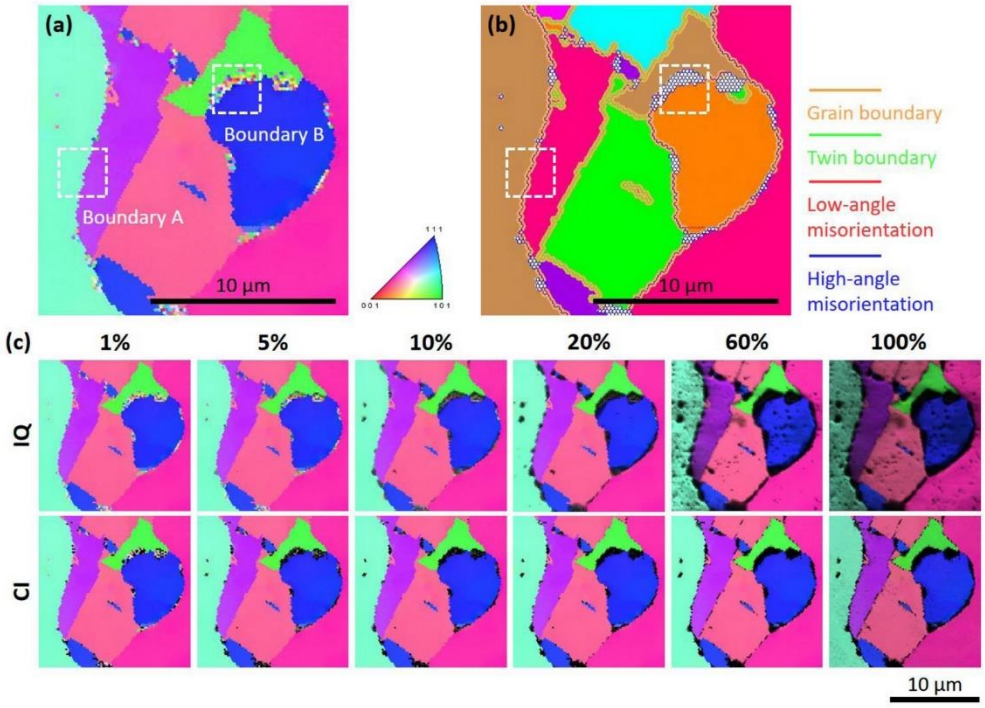

Supplementary Figure 5 | EBSD results extracted from the same region shown in Manuscript Figure 8 (e). There are **(a)** inverse pole figure (IPF) map, **(b)** unique grain colour map overlaid with boundaries map (grains have tolerance as 5 degree, Σ3 boundary has defined as "twin boundary", misorientation from 5 to 15 degrees as "low-angle misorientation" and from 15 to 62.8 degrees as "high-angle misorientation") and **(c)** a series of IPF maps that overlaid with image quality (IQ) or confidence indicator (CI) with different threshold values.

Brief interpretation: Intergranular corrosion may induce two typical types of boundaries indicated in squares "Boundary A" and "Boundary B". Type A represents the boundaries that have suffered from less deterioration, therefore the collected data points still have high values of IQ or CI, which allow their orientations to be correctly indexed. This allows the software further recognise these boundaries as grain boundaries. In this way, the misorientation values reflect the actual type of boundaries. However, for those locations endured severe corrosion (Type B), their data have extremely low CI (they already appear when the threshold is set as 5%). This could be attributed to low IQ resulted from the cavity. These data points cannot be grouped as one grain or classified into their original grains. Consequently, they form a number of data points with (usually high-angle) misorientation with each other, however, they would not be classified into grain boundaries by definition. In this case, the information of this type of original boundaries is lost.

6. Roles of NaCl in Aqueous Environment and Atmospheric Corrosion on Copper Surface

In this chapter, the below peer-reviewed publication is going to be presented:

Sodium chloride assists copper release, enhances antibacterial efficiency, and introduces atmospheric corrosion on copper surface

Reproduced from Jiaqi Luo, Christina Hein, Jean-François Pierson, Frank Mücklich, *Surfaces and Interfaces*, 2020, 20, with the permission of Elsevier

DOI: 10.1016/j.surfin.2020.100630

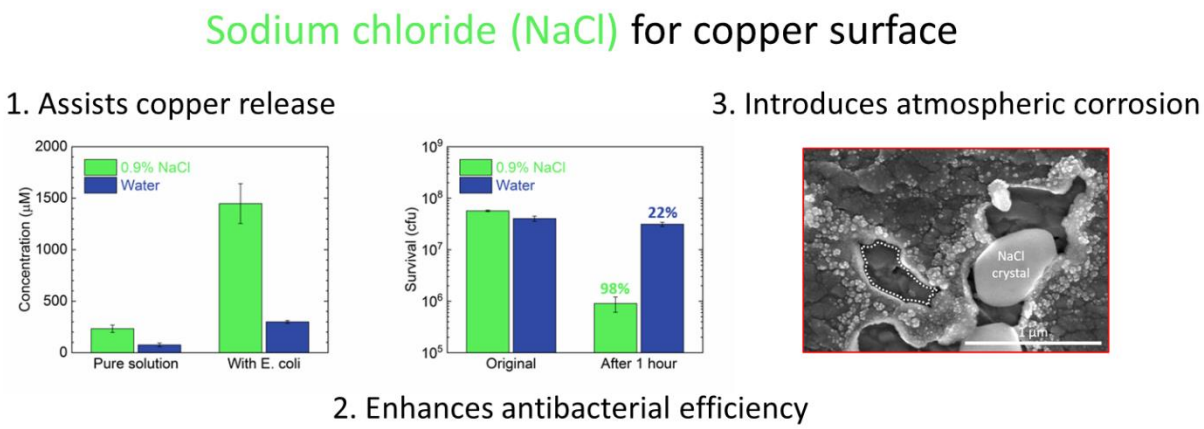

Contribution: Conceptualisation, Methodology, Validation (except from ICP-MS measurements), Investigation, Writing – Original Draft, Visualization, Project administration.

Surfaces and Interfaces 20 (2020) 100630

Contents lists available at ScienceDirect

Surfaces and Interfaces

journal homepage: www.elsevier.com/locate/surfin

Sodium chloride assists copper release, enhances antibacterial efficiency, and introduces atmospheric corrosion on copper surface

Jiaqi Luo[a,b,*], Christina Hein[c], Jean-François Pierson[b], Frank Mücklich[a]

[a] Functional Materials, Saarland University, 66123 Saarbruecken, Germany
[b] Université de Lorraine, CNRS, IJL, F-54000 Nancy, France
[c] Inorganic Solid State Chemistry, Saarland University, 66123 Saarbruecken, Germany

ARTICLE INFO

Keywords:
Copper
Cuprous oxide
Chloride
Corrosion
E. coli
Antibacterial surface

ABSTRACT

Sodium chloride (NaCl) is commonly found in physiological buffers. This study found out its additional but important role in antibacterial efficiency test by better corroding metallic copper surface. Combined with multiple characterisation methods including scanning electron microscopy, grazing incidence X-ray diffractometry, and inductively coupled plasma mass spectrometry, 0.9% saline was observed to cause localised corrosion attacks on copper surface, enhancing release of copper content. The 1 h killing rate against *Escherichia coli* was thus promoted from 22% (when re-suspended in pure water) to 98%. By a long-term observation (3-week), residual NaCl crystals on 0.9% saline treated copper surface were found partially disappeared in atmospheric environment, contributing to an additional Cu_2O layer forming above the treated surface. Besides, formation of oxygen-containing species was observed on fresh copper surface exposed by focused ion beam after saline treatment, suggesting a chloride-assisted atmospheric corrosion process.

1. Introduction

Antibacterial surfaces are drawing attentions in the recent years [1–3]. They can be applied as touched surfaces, having enormous potential demands in those heavily microbial burdened healthcare environments [4–6] as well as in our daily lives [7,8]. In order to verify and assess the antibacterial ability of newly fabricated surfaces, antibacterial efficiency tests were designed and carried out.

Nowadays, there are different types of evaluation methods such as dry plating [9], wet plating [10], agar disk diffusion [11], etc. Limited by the incubation of bacteria and transfer process of bacterial suspension, a certain medium must be introduced during these evaluations. This medium is usually called buffer, which provides a suitable aqueous environment for bacterial survival without further growth. Despite the wide selection of buffers, in most of the cases, two main requirements should be satisfied: (1) a manageable pH range and (2) a suitable osmotic pressure for the microbes. Take phosphate-buffer saline (PBS) as an example [12], it contains a pair of acid and its conjugate base so as to compensate the pH fluctuation around 7.4. For the second purpose, it is sodium chloride (NaCl) that plays the part.

As can be seen, the design of buffers mainly considers the needs of microbes. But when they are to be applied in antibacterial surface research, a question needs to be raised: should the potential interactions between buffers and surfaces also be considered? The answer may be "certainly". For example, copper-containing surfaces have been recently developed for antibacterial applications in various occasions [13–15]. Their antibacterial capability originates from the multifunctional antibacterial effects of copper ions [16]. To strongly interfere the survival of harmful microbes, copper ions should be efficiently released from the surfaces. As metallic surfaces, this release process is, most of the time, achieved by corrosion. The composition and the properties of buffer could become decisive, as they could facilitate or retard the corrosion process. Therefore, the solution and the copper surfaces together display how effective the antibacterial activity would be shown in antibacterial efficiency test.

Back to the example of PBS or other saline solutions, without a doubt, NaCl is expected to play an extremely important factor in revealing the antibacterial efficiency of copper surface. Electrochemical study has investigated the roles of chloride ions (Cl^-) in formation and transformation of corrosion product (CuCl, Cu_2O, $Cu(OH)_2$, etc.) [17], which could further affect the diffusion of copper ions [18]. In general, the presence of Cl^- also leads to a relatively corrosive environment for copper, depending on the concentration of Cl^- [19]. Meanwhile, it easily promotes pitting corrosion and further deterioration on the surface [20]. This could, on the contrary, contributes to the copper antibacterial efficiency. Because whenever the corrosion is enhanced, a

* Corresponding author at: Functional Materials, Saarland University, 66123 Saarbruecken, Germany.
E-mail address: jiaqi.luo@uni-saarland.de (J. Luo).

https://doi.org/10.1016/j.surfin.2020.100630
Received 2 July 2020; Received in revised form 23 July 2020; Accepted 5 August 2020
Available online 08 August 2020

faster dissolution process of the antibacterial substance (copper ions) is anticipated. For example, a latest study that evaluated antibacterial property of copper-silver surface has discovered the constructive effect of chloride addition in dissolving antibacterial copper ions [21]. Other experiments also suggest that Cu-Fenton chemistry, as one of the antibacterial mechanisms, could be accelerated by Cl^- [22], resulting in a better biofilm removal. On the whole, a different antibacterial efficiency is therefore highly expected in Cl^--containing environment.

Other than affecting the corrosion behaviour in media, it is noteworthy that NaCl deposits could induce atmospheric corrosion on dry surfaces. At high humidity levels, for instance, deliquescence of NaCl could happen, initiating micro-droplets formation on metallic surfaces and introducing further corrosion [23]. In lower humidity circumstances (below than 79% RH, deliquescence point of NaCl), where NaCl does not dissolve though, adsorption of water on the surface could form several layers that act as bulk water [24]. Diffusion of Cl^- could thus occur in this quasi-aqueous condition resulting in corrosion attack on copper [25]. Either way, tracking this atmospheric corrosion effect after antibacterial efficiency test may have significant implication for long-term product design [26].

Lately, we commenced focusing on buffers by comparing PBS and Na-4-(2-hydroxyethyl)-1-piperazineethanesulfonic acid (Na-HEPES) in terms of their impacts on evaluating the antibacterial performance of metallic copper and Cu_2O surface [27]. Corrosion behaviours introduced by PBS caught our attention, and therefore further experiments were designed to reveal the roles of bacteria [28] and to discuss the corrosion attacks and oxide growth [29]. Since PBS contains NaCl, this study narrows down to find out if NaCl plays an important factor as expected, in respect to corrosion. The primary objective is to explore how 0.9% saline affects the antibacterial efficiency test on metallic copper surface. Afterwards, the corrosion behaviours were compared among saline with different Cl^- or *Escherichia coli* (*E. coli*) concentrations. Finally, the following atmospheric aging effects resulting from the residual NaCl crystals on copper surface were also characterised.

2. Materials and methods

2.1. Materials

Copper (99.99%, K09, Wieland) coupons were ground with a silicon carbide sandpaper (stepped down to grit number P600), then cleaned with ethanol in an ultrasonic bath, finally dried by air.

2.2. Solutions

Saline with various final concentrations (0.45%, 0.9%, and 1.8%) was prepared with NaCl (VWR, Germany) and pure water for analysis (Merck, Germany). PBS was prepared with NaH_2PO_4. $1H_2O$ (Merck, Germany, final concentration 0.01 M), NaCl (VWR, Germany, final concentration 0.14 M) and pure water for analysis, and its pH value was adjusted by adding NaOH to 7.4. These buffers were sterilised in an autoclave after preparation.

The preparation of bacterial suspension will be described in Section 2.6. Besides, a fivefold concentration *E. coli* NaCl suspension was simply prepared by re-suspending bacteria in 0.2 mL of saline instead of its original volume 1 mL. A tenth fold diluted *E. coli* NaCl suspension was prepared in the similar manner (*i.e.* by re-suspending bacteria in 10 mL saline).

2.3. Corrosion protocol

Droplet of 20 μL pure solution or *E. coli* suspension was applied on ground copper surfaces with a pipette. These copper coupons were placed in a water-saturated atmosphere at room temperature for 3 h. Solutions or suspensions were then withdrawn with a pipette. These steps are chosen to simulate the antibacterial efficiency test further described in Section 2.6.

If not specified, the coupons were then cleaned with ethanol in an ultrasonic bath immediately after withdrawal of droplet. However, for the tests with various NaCl or bacterial concentrations (Section 3.4), the treated surfaces were firstly wiped with detergent-dipped cotton pads in order to remove the adhered bacteria. On the other hand, for some tests designed for atmospheric aging experiments (Section 3.5), the coupons remained unwashed. They were constantly kept in the lab atmosphere at room temperature, except for the time being characterised.

2.4. Surface characterization

Different functions of scanning electron microscope (SEM, Helios NanoLab600, FEI) were employed to observe copper surfaces after various corrosion experiments. Secondary electron detector (SE) was applied to examine the top-surface as well as cross-section of the coupons. Meanwhile, with backscatter electron detector (BSE), localised corrosion attacks covered by corrosion products were explored. Acceleration voltages will be further mentioned in the corresponding figure captions. The chemical composition of bacteria was obtained by energy dispersive X-ray spectroscopy (EDS) at 5 kV. Optical microscope (OM, OLS4100, Olympus) photos were captured in 3D bright field mode. For further confirmation of the corrosion products covering the surfaces, high resolution grazing incidence X-ray diffractometer (GIXRD, Cu K_α with 1° grazing angle, PANalytical X'Pert PRO-MPD) was applied. In the atmospheric aging experiments, focused ion beam (FIB) was applied to fabricate fresh cross-section of the copper coupon after corrosion treatment, using gallium ions with an accelerating voltage of 30 kV. Images and spectra were obtained within 24 h after the corresponding corrosion treatments, except from the atmospheric aging experiments.

2.5. Copper content determination

After corresponding surface treatment, 10 μL samples were withdrawn by repetitive pipetting and diluted in 2.990 mL 1 wt% nitric acid (Merck, Germany). Before being measured by inductively coupled plasma mass spectrometry (ICP-MS, 7500cx, Agilent), 3 μL of 10 mg/L scandium and caesium internal standard solutions were added to the samples. For calibration, standards with 0.1, 0.5, 2.5, 10, 50, 250, and 1000 μg/L of copper were used. Original results with a unit of ppb were converted to the final values with μmol/L (μM), concerning both the fold of dilutions and molar mass 63.55 g/mol for copper. The average values and standard deviations were obtained by three independent experiments.

2.6. Antibacterial efficiency determination

Wet-plating test was used, whose details can be referred to a previous publication [10]. In brief, the *E. coli* K12 strain was grown aerobically overnight in Lysogeny broth (LB) medium at 37 °C in a water bath with a speed of 220 rpm. The stationary cells from 1 mL culture were collected by centrifugation for 15 min at 5000 × *g*, washed and centrifuged three times with the corresponding solutions, and finally re-suspended in 1 mL of the same type of solution. The test commenced by applying 20 μL of these re-suspended bacteria on the coupons, which were placed in a water-saturated atmosphere at room temperature. After 1 h, 10 μL samples were withdrawn by repetitive pipetting, serially diluted in PBS and spread on LB agar plates. Following incubation at 37 °C for 24 h, the colony-forming unit (cfu) on agar plates was counted and expressed in a way concerning both the fold of dilutions and relative to the original 20 μL samples. The average values and standard deviations were obtained by three independent experiments.

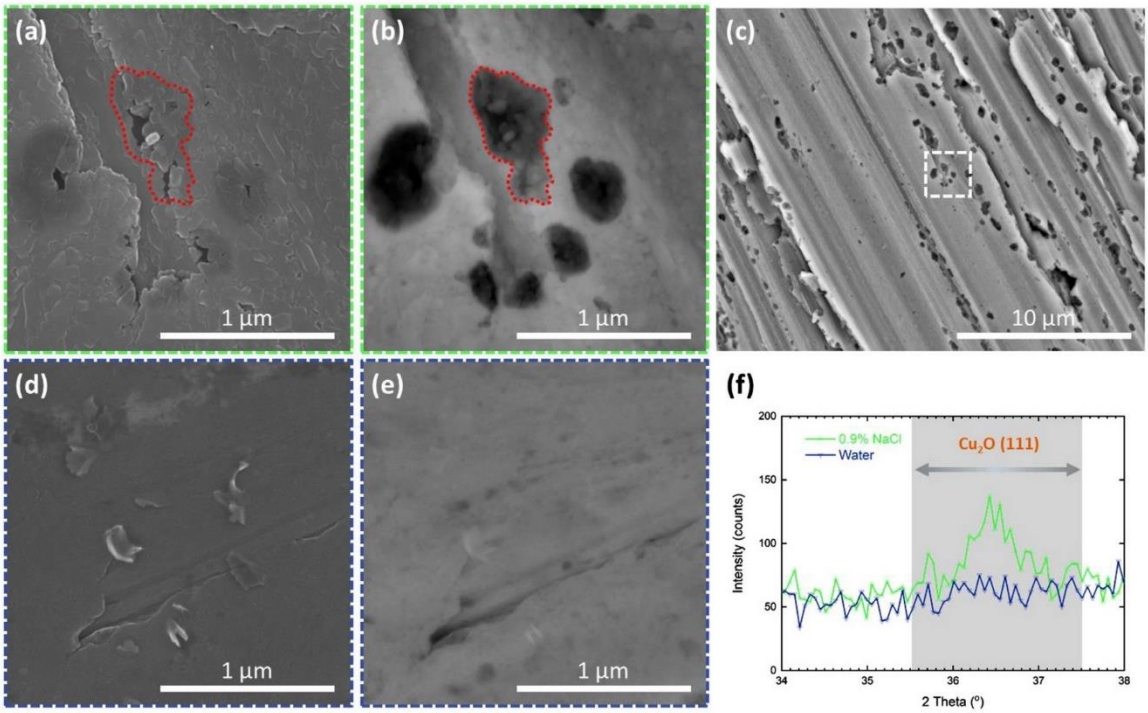

Fig. 1. Typical SEM images of ground copper surfaces after 3 h exposure to 0.9% NaCl **(a-c)** or pure water **(d, e)**. Images were obtained by SE detector **(a, d)** and BSE detector **(b, c, e)** at 20 kV. The dotted lines in **(a, b)** surround a typical localised corrosion zone. Images **(a, b)** correspond to the square dash marked region in **(c)**. High resolution GIXRD results **(f)** in the range of (111) planes of Cu_2O (JCPDS#75-1531) obtained from these surfaces.

3. Results and discussion

3.1. Corrosion of copper surface in 0.9% NaCl and pure water

Before analysis of the actual antibacterial efficiency test, this study first focuses on the corrosive effects introduced by 0.9% NaCl (this concentration is hereafter simply referred to as "saline") without bacteria. For instance, Fig. 1 (a-c) shows the morphological change and formation of corrosion product on the copper surface after 3 h exposure to this environment. Uniformly distributed sub-micron corrosion products are evident in SE image. Meanwhile, at some locations, much lower intensity was recorded in BSE (therefore darker), indicating missing of material underneath the corrosion product. These cavities signify where localised deterioration took place. Variation of microstructure definitely has impacts on the initiation of these localised attacks [30]. The distribution of these attacks can be mostly referred to a recent study [29], where how electropolished copper surface corroded by PBS droplet was investigated in detail.

Coupon exposed to pure water for the same duration is shown for comparison purposes in Fig. 1 (d and e). Fewer features can be summarised: no obvious additional product coverage nor localised corrosion sites. Therefore, it can be preliminarily concluded that, adding NaCl into pure water significantly varies the environmental corrosivity towards copper.

The corrosion product formed on copper was further examined by high resolution GIXRD shown in Fig. 1 (f). Crystalline Cu_2O has been identified as the major product after saline treatment, but not in pure water. Similar observation was obtained from potentiostatic polarisation [20], highlighting the formation of intermediate product CuCl, followed by the formation of Cu_2O and initiation of pits in a temporal sequence. However, CuCl is not identified in the current study. Meanwhile, the cavities were found being gradually covered by Cu_2O films, instead of destroying the films. Therefore, dissolution-precipitation or re-deposition mechanism [27] seems to be more appropriate in explaining the oxide growth: the exceeding copper ions gather near the copper surface and form oxide.

3.2. Corrosion of copper surface in bacterial suspensions

By adding *E. coli* (hereafter referred to as "bacteria"), solution becomes suspension, some corrosion behaviours on copper surface thus alter accordingly, as can be found in Fig. 2. In saline, localised corrosion attack is still predominant, which can be easily recognised from the BSE images. SE image usually shows more morphological details, but the above-mentioned (Section 3.1) sub-micron corrosion product Cu_2O forming in pure solution can hardly be seen. The missing diffraction peak of Cu_2O (111) in GIXRD also matches this observation. Highly similar phenomena were recently reported in the case of PBS [28], which could help interpret the current scenario: it is attributed to the bacterial accumulation effects of copper ions. Copper concentration near surface is thus reduced and oxide growth is inhibited.

Without oxide coverage, a considerable amount of cavities, as a result of localised corrosion attacks, become visible even in SE mode. Those invisible ones, on the other hand, may imply another mechanism of pit initiation: a Cu_2O membrane could be found, separating the inner pitting region from the aqueous environment and promoting further pitting corrosion under the uppermost copper surface [31]. Similar sites have also been observed in the intermetallic particles induced crystallographic pitting grown beneath the surface [32], suggesting galvanic couple could be considered in the current scenario.

In the case of pure water, its bacterial suspension has not introduced distinct morphological or chemical changes on copper surface. These contrasts suggest the important roles of *E. coli*: although its presence inhibits the formation of Cu_2O, it does not affect the major corrosion attacks (especially in saline) or cause additional corrosion effect (especially in pure water). In other words, it is still the properties of

J. Luo, et al. Surfaces and Interfaces 20 (2020) 100630

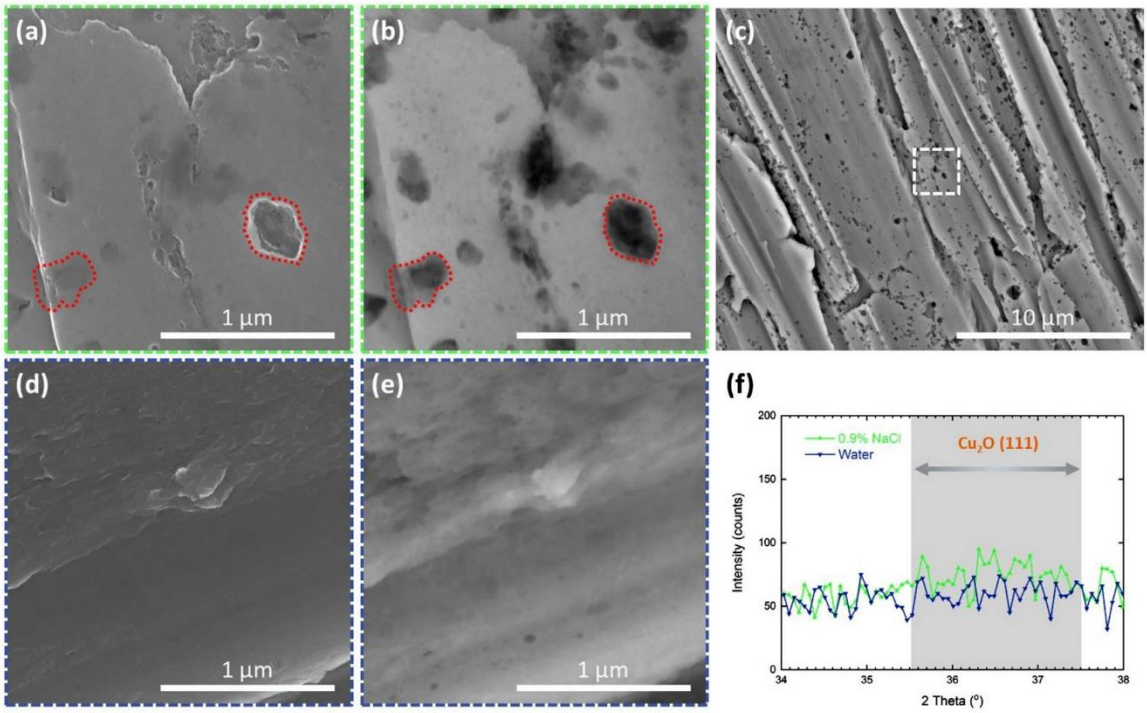

Fig. 2. Typical SEM images of ground copper surfaces after 3 h exposure to *E. coli* 0.9% NaCl suspension **(a-c)** or *E. coli* pure water suspension **(d, e)**. Images were obtained by SE detector **(a, d)** and BSE detector **(b, c, e)** at 20 kV. The dotted lines in **(a, b)** indicate two types of localised corrosion site. Images **(a, b)** correspond to the square dash marked region in **(c)**. High resolution GIXRD results **(f)** in the range of (111) planes of Cu_2O (JCPDS#75-1531) obtained from these surfaces.

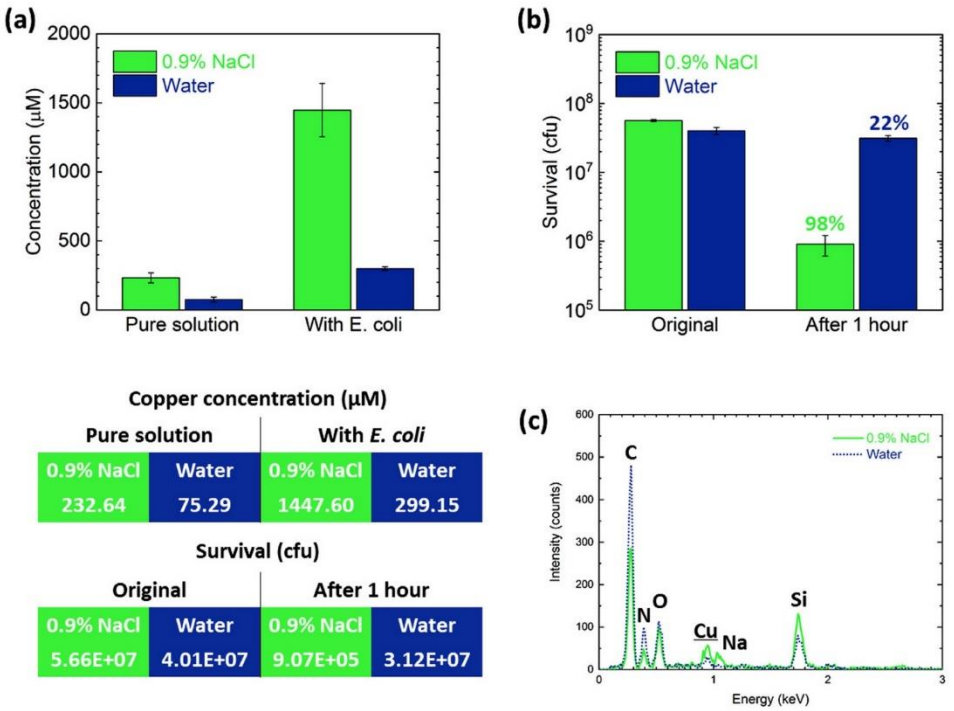

Copper concentration (μM)

Pure solution		With *E. coli*	
0.9% NaCl	Water	0.9% NaCl	Water
232.64	75.29	1447.60	299.15

Survival (cfu)

Original		After 1 hour	
0.9% NaCl	Water	0.9% NaCl	Water
5.66E+07	4.01E+07	9.07E+05	3.12E+07

Fig. 3. Copper content **(a)** in 0.9% NaCl or pure water, with or without *E. coli* after 3 h exposed to ground copper surfaces. Antibacterial efficiency of ground copper surfaces **(b)** against *E. coli* in two different suspensions in 1 h. The error bars indicate the standard deviations calculated from three independent measurements. Percentages in **(b)** above the bars represent the killing rate in 1 h (compared to the "Original" data). Average values from **(a)** and **(b)** are listed in the tables. Typical EDS results **(c)** collected from the bacterium (*E. coli*) transferred onto silicon wafer after being treated with copper surface in two suspension for 3 h.

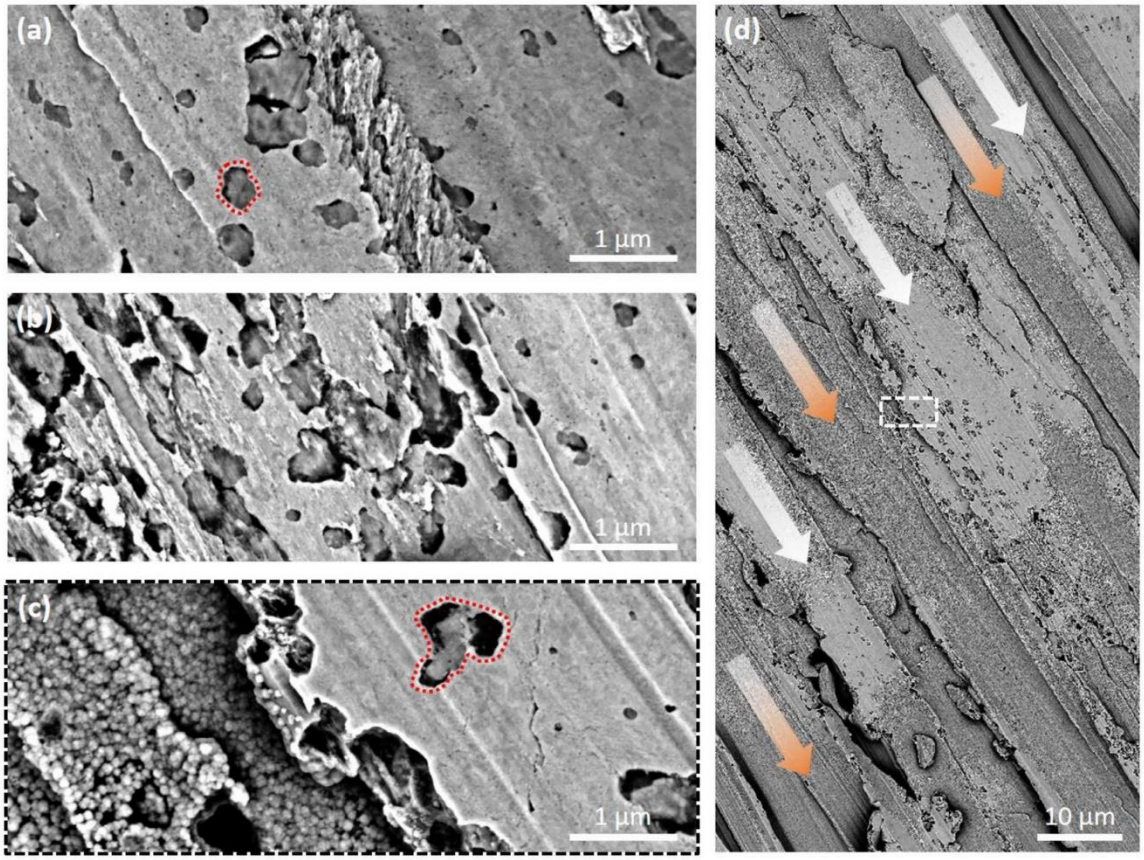

Fig. 4. Typical SEM images (BSE, 5 kV) of ground copper surfaces after 3 h exposure to *E. coli* suspension with different NaCl concentration: **(a)** 0.45%; **(b)** 0.9%; **(c)** 1.8%. The dotted lines in **(a, c)** indicate typical localised corrosion cavities. Image **(c)** corresponds to the square dash marked region in **(d)**. The orange arrows in **(d)** indicate regions with oxide growth, while the white arrows for those without.

solution that determine the corrosion process.

From the microbiological perspective, addition of bacteria introduces not only bacteria themselves, but also their metabolism as well as the products of it. Bacterial respiration, for example, is one of the universal processes frequently discussed, as it could help reducing oxygen content in the aqueous environment [33]. Meanwhile, dissolved oxygen happens to play an indispensable factor in the corrosion of metallic copper in aqueous [34] or Cl^--containing environment [35]. However, in the following sections, this aspect will be further ruled out from the present conditions.

3.3. Copper release and antibacterial efficiency

In the above sections, the corrosion behaviours of copper surface were revealed, in terms of how it varies after being exposed to different solutions or suspensions. But apart from this, it is also meaningful to investigate the effects of corrosion on the contacting droplet itself. For instance, the rise of copper content measured by ICP-MS shown in Fig. 3 (a) offers valuable information. First of all, it is evident that the copper content measured from the bacterial suspension is higher than its corresponding pure solution. This can be again correlated with the role of bacterial addition summarised above: since bacteria decrease the amount of free copper ions in solutions, it favours a continuous release kinetics. This particularly affects the situation in saline, as it suppresses the formation of Cu_2O, which could have formed as a barrier layer reducing the metal/solution interface [27] as well as retarding ion diffusion [18].

Another marked discrepancy is found between saline and pure water: the amounts of copper presented in saline are, in both cases, evidently higher than that in pure water. This trend matches the SEM observation: copper surface always suffers from more detectable localised corrosion attacks in saline. This is likely attributed to Cl^-, which has been regarded as an accelerator of corrosion on metallic surfaces most of the time [36]. With respect to copper, there was also study conducted on the relationship between Cl^- concentration and corrosion rate [19]. It shows that the Cl^- attachment allows complex formation and thereby promotes a faster ion release.

Additionally, it is still worth noting that neglectable variations of surface topography does not necessarily represent similar copper release level. In the case of pure water, although SEM results do not indicate significant difference, its bacterial suspension does enhance copper release by about three times, from 75.29 μM to 299.15 μM (data listed in the table in Fig. 3). This suggests that it is the uniform corrosion that dominates the copper release in pure water, instead of localised corrosion.

Copper content presented in suspension is also positively related to the surface antibacterial efficiency, as presented in Fig. 3 (b). Bacteria in both suspensions were grown from the same broths and thence share similar original concentration. Merely in 1 h, their survival already parted ways: around 98% were killed in the saline suspension, while only 22% was recorded in pure water. Not surprisingly, these numbers match the difference of copper content evaluated in ICP-MS discussed

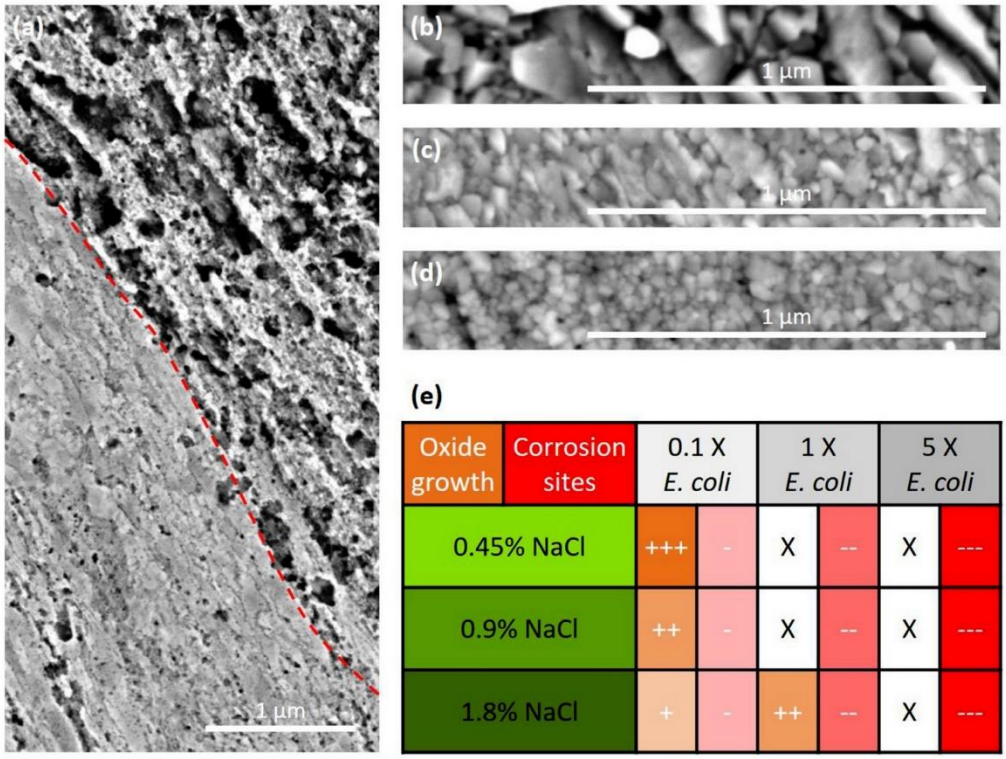

(e)

Oxide growth	Corrosion sites	0.1 X *E. coli*		1 X *E. coli*		5 X *E. coli*	
0.45% NaCl		+++	-	X	--	X	---
0.9% NaCl		++	-	X	--	X	---
1.8% NaCl		+	-	++	--	X	---

Fig. 5. Typical SEM images (BSE, 5 kV) of ground copper surfaces after 3 h exposure to **(a)** fivefold *E. coli* 1.8% NaCl suspension; **(b)** tenth fold diluted *E. coli* 0.45% NaCl suspension; **(c)** tenth fold diluted *E. coli* 0.9% NaCl suspension; **(d)** tenth fold diluted *E. coli* 1.8% NaCl suspension. Dash line in **(a)** separates the severe corrosion zone from the almost intact zone. Table **(e)** summarises the characteristics of oxide growth and corrosion sites in different conditions: more "+" represents bigger particle size; more "-" represents smaller localised corrosion sites; "X" represents situations where particle coverage was rarely observed.

above and that accumulated in the bacterium compared in Fig. 3 (c): Stronger Cu L_α radiation at 0.930 keV was recorded from the bacteria killed in saline.

These comparisons demonstrate how corrosion behaviour and antibacterial efficiency are correlated: even though same type of microbe was tested on same type of metallic copper surface, the composition of the solution can dictate the release of antibacterial substance and thus result in a different antibacterial efficiency. Saline, a relatively corrosive solution, causes a higher amount of copper release (at least within a certain period), raising the copper concentration and enabling a faster killing rate against *E. coli*. A recent study [21] conducted by another research group also found out a similar role of Cl^- in enabling sufficient corrosion on not only copper and but also copper-silver alloy to deactivate *S. aureus*.

Two additional remarks may help further interpreting the antibacterial efficiency results. Since the killing rate follows the same trend of the increasing copper content, it cannot be estimated in the current experiment, how much of the antibacterial efficiency was assisted by the Cl^- accelerated Cu-Fenton reaction [22] or other combined effects [37]. On the other hand, one may notice that pure water is not a buffer, but a low osmolarity environment in the strict sense. Hypoosmotic shock does not necessarily lead to cell death [38], but even if it does, the contribution of copper in reaching a 22% killing rate should be considered even lower.

3.4. Effects of NaCl concentration and E. coli concentration on copper

Since the effects of NaCl and *E. coli* in this corrosion system have been preliminarily identified, additional experiments were designed to explore these effects. Fig. 4 (a-c) compare the effects of NaCl concentration on the corrosion behaviours of copper surface. For all these selected concentrations, copper was subjected to a similar type of localised corrosion attacks. As the NaCl concentration increases, the expansion of cavities is observed, identified by imaging contrast in BSE. Besides, contrast can also be found even within a single cavity. This implies that the localised attack inside the cavity is not uniform. On the other hand, oxide growth is ignorable in both 0.45% and 0.9% suspensions. But when it added up to 1.8%, huge areas covered by submicron oxides are found. Meantime another striking feature is also observed regarding the distribution of oxide on copper surface: they only grew on specific locations.

According to the re-deposition mechanism discussed (at the end of Section 3.1), oxide growth usually corresponds to excessive copper ions. Therefore, the emergence of oxide could be attributed to a faster corrosion kinetics in a high Cl^- concentration scenario, where the amount of copper ions exceeds the accumulation capacity of *E. coli*. However, as the bacteria presenting in the droplet are supposed to be well-mixed, their copper accumulation effect should be distributed evenly on the surface. That is to say, the localised copper ion concentration is expected similar across the whole near surface. Therefore, other than copper concentration, there must be another factor governing the preferential locations of oxide growth.

As it can be seen in Fig. 4 (d), oxide coverage seems to follow the grinding marks. It strongly suggests its correlation with the state of the original copper surface (*e.g.* microstructural or morphological difference introduced by the grinding procedure). In other words, variation of the state of the surface might dominate the distribution of cathodic sites, where oxide growth prevails. To design similar experiments on electropolished copper surface may help, as it did reveal the crystallographic dependency of copper corrosion in PBS [29].

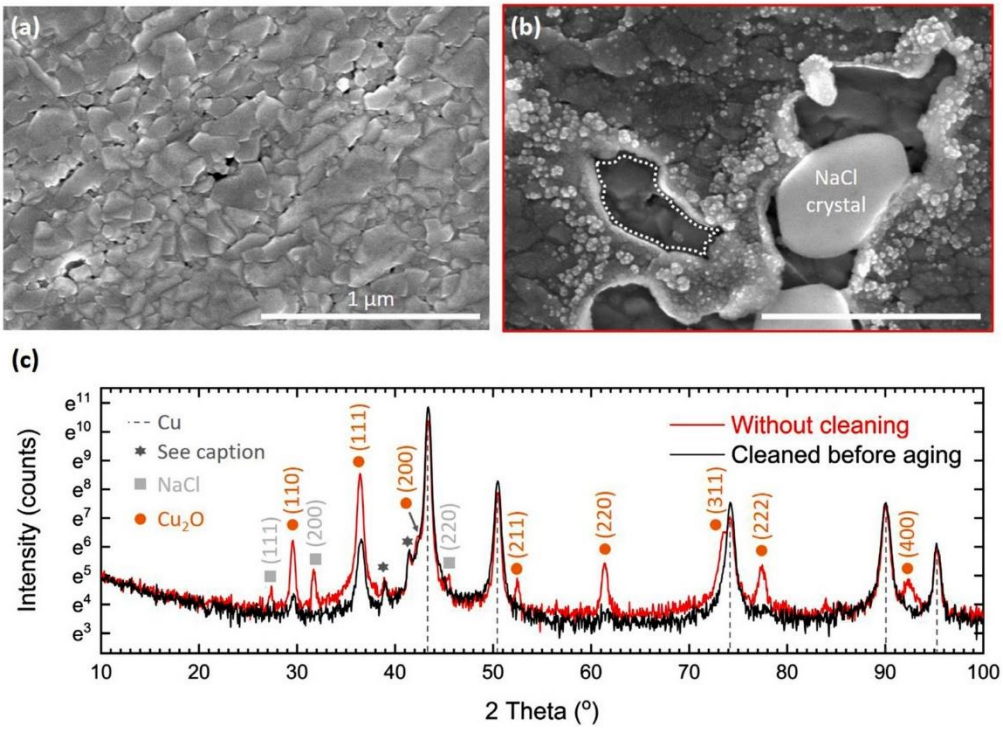

Fig. 6. Typical SEM images (SE, 5 kV) of ground copper surfaces 3 weeks after 3 h exposure to 0.9% NaCl solution. Coupon shown in **(a)** has been ultrasonic cleaned by ethanol immediately after the 3 h corrosion experiment, while **(b)** was kept without further cleaning. Both images share the same scale bars that presented in **(a)**. The dotted region in **(b)** indicates the missing of NaCl crystal as well as the exposed original oxidised copper surface. High resolution GIXRD results **(c)** obtained from these surfaces 12 weeks after the original treatment. Cu (JCPDS#04-0836), NaCl (JCPDS#05-0628), and Cu_2O (JCPDS#75-1531) were applied to index the patterns. The diffraction peaks marked with hexagonal star (★) represent diffraction of Cu (111) planes under Cu-K_β and W-$L_{\alpha 1}$.

To verify the role of ion accumulation effect introduced by *E. coli*, another corrosion test was conducted with 1.8% NaCl, whereas fivefold *E. coli* was re-suspended. After the same duration, oxide coverage can hardly be seen on copper surface, as shown in Fig. 5 (a). Surge of the amount of bacteria boosts both the capacity and efficiency of the ion accumulation, compensating the increase of copper release in high Cl^- concentration. Besides, higher bacterial concentration did not affect the selective distribution of localised corrosion sites, indicating that the corrosion mechanism stays the same. However, the size of cavities did shrink, and they are easy to be found connected altogether. Meanwhile, even on the locations that are free from severe localised corrosion, slight degradation can be observed, as the grinding marks can hardly be found. It is unclear at the current stage, but these phenomena could be related to but not limited to the variation of local chemical concentration (Cl^- or chemicals produced by bacterial metabolism), local fluid flow rate (induced by the mobility of bacteria), etc.

On the other hand, with lower bacterial concentration (tenth fold diluted), oxide coverage can always be found in whole series of NaCl concentration (Fig. 5 (b-d)). Oxide particles with bigger size are noticed in lower NaCl concentration. That is, NaCl concentration has an impact on the nucleation density of oxide. The trend of how NaCl and bacterial concentration influence oxide growth and corrosion attacks are qualitatively summarised in Fig. 5 (e).

3.5. Atmospheric corrosion caused by residual NaCl crystals

So far, the impacts of NaCl on copper surface have only been discussed during corrosion test or antibacterial efficiency test. However, even though the saline will be withdrawn afterwards, some NaCl residues could stay on the copper surface. These NaCl crystals are found to continue playing a decisive part in the copper aging process.

Fig. 6 compares the copper surfaces observed 3 weeks after having been exposed to saline. Coupon shown in Fig. 6 (a) has been cleaned immediately after the saline was withdrawn in the end of the corrosion test, therefore no NaCl crystal was remained. In this case, the oxide coverage is found unchanged in 3 weeks. However, coupon that has not been cleaned properly experienced significant changes, as shown in Fig. 6 (b). Firstly, a secondary layer with a slightly different roughness formed on the previous Cu_2O coverage. Moreover, the reason why some uncovered previous Cu_2O can be located, is likely related to the NaCl crystals (with brighter colour in SE mode) lying aside: it is assumed that these uncovered zones were also originally covered by the NaCl crystals. Nevertheless, these crystals gradually disappeared during the 3-week atmospheric aging.

From GIXRD results, two facts have been clearly shown. First, NaCl residues were efficiently cleaned by the current protocol, as much weak diffraction signals are found on the cleaned coupon. Second, more Cu_2O diffraction peaks with higher intensity appeared from the coupon without cleaning, confirming the newly grown secondary layer is mainly composed of Cu_2O as well.

Intriguingly, this kind of aging effect does not occur only on the directly treated copper surface. As shown in Fig. 7, a hole on the copper coupon was fabricated by FIB, immediately after the corrosion test without applying cleaning protocol. This exposes some “fresh” areas beneath the original surface. “Fresh” is here defined as having not directly “met” the saline, since they were still inside the bulk copper during the corrosion test. OM image taken straightway after FIB operation (*i.e.* Day 0) recorded some bright zones, not just in the hole, but also around it, as a result of Ga ion beam bombardment. The areas inside the hole that are darker were due to rougher topography,

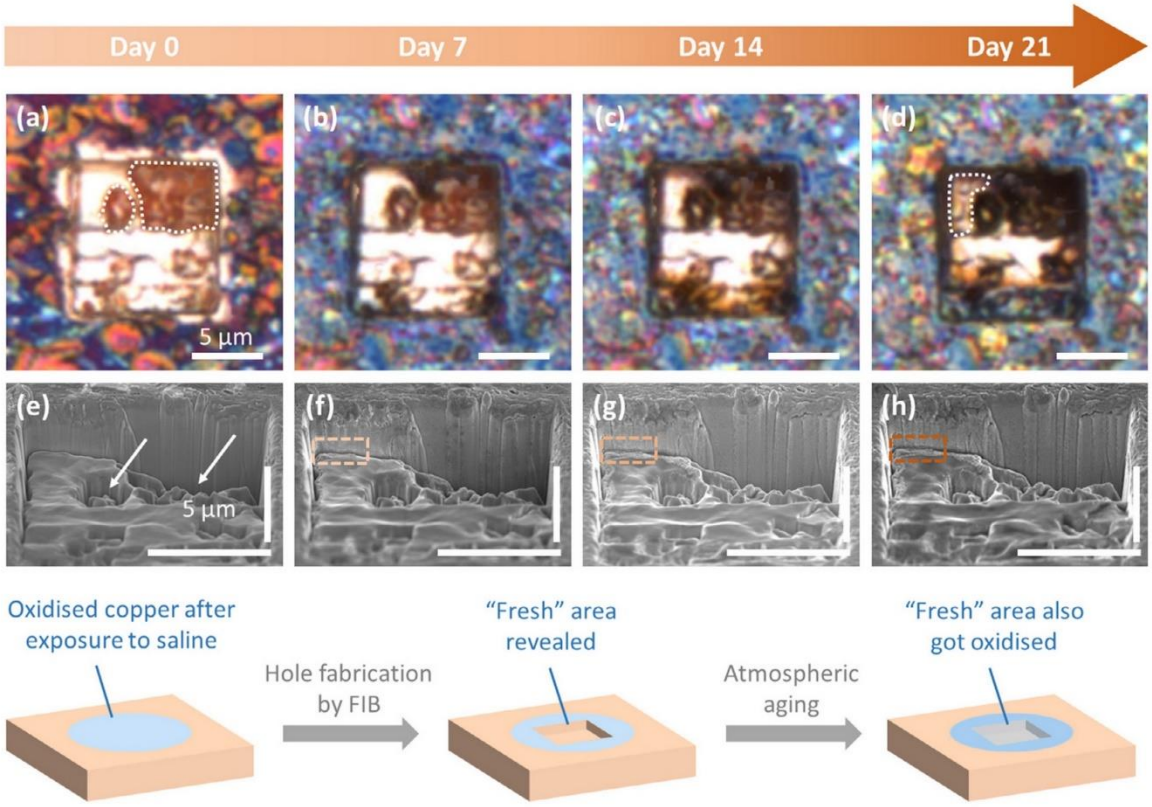

Fig. 7. OM images **(a-d)** and SEM images **(e-k)** (SE, 5 kV, coupon being 52° tilted) of fresh section of copper surface prepared by FIB after 3 h explosure to 0.9% NaCl. OM images and SEM images share the same scale bars presented in **(a)** and **(e)**, respectively. This position was repeatedly examined every 7 days. Dark areas surrounded by dotted lines in **(a)** are the regions pointed out by arrows in **(e)**. Area marked with dotted line in **(d)** serves as an example for positions that suffered colour change compared to the same positions in **(a)**. High magnification images of the square dash marked regions in **(f–h)** are further shown in the following Fig. 8. A schematic description of the treatment process is shown below the SEM images.

confirmed by SEM images.

However, as the aging experiment proceeds, the bright zones shown in OM turned darker from the boundaries inwardly. This is related to the morphological changes displayed in Fig. 8: submicron particles were forming on top of these surfaces. Being continuously exposed to atmosphere, part of this region extended, from the cross-section (edge of the hole) towards the bottom of it. Meanwhile, coarsening can be observed on some of these particles. At the cross-section (invisible in OM owing to observation angle) which is supposed to be relatively smooth at the original state, similar particle formation and coarsening phenomenon are also found. Although the exact chemical or phase composition has yet to be determined, these locations do contain an extra amount of oxygen content (Fig. 8 (d&e), obvious O K_α radiation at 0.525 keV), suggesting the formation oxygen-containing species. Served as the control groups, same type of FIB cross-sections was produced on copper coupon exposed to either pure water or *E. coli* water suspension for the same duration. Neither of these surfaces shows such changes after 3 weeks (data not included), excluding the potential additional effects brought by Ga ion implantation during FIB operation.

All these comparisons help to preliminarily pin down the cause of atmospheric aging: NaCl, as it is the only varied environmental parameter. In the end of corrosion test where the solution cannot been withdrawn completely, NaCl crystallised locally on the copper surface after the remained water evaporated. However, this is not yet the final fate of these crystals. Atmospheric corrosion continues to play a role. For example, these salts could go through a process so-called deliquescence [23], thereby absorbs the water from the atmosphere and induce aqueous corrosion. But this process requires a relatively high humidity (79% RH for pure NaCl), which is usually not fulfilled in the lab environment.

In spite of this, NaCl crystals could transform in another way, which is still related to water absorption, not by NaCl itself, but by the general surface: it is common to find monolayers of water forming on surfaces [24]. Therefore, the copper surface could still be regarded as being exposed to a quasi-aqueous environment. In fact, the properties of the water layer could already affect the nucleation and formation rate of Cu_2O in a certain range of relative humidity [39]. Besides, these monolayers dissolve NaCl and transform itself to electrolyte. Meanwhile, Cl^- are able to diffuse through these monolayers, reaching to the other parts of the surface [25]. Considering all these events, corrosion related phenomena are not a surprise. In addition, Cl^- may not be the only ions that would diffuse through the surface, as copper ions should also participate a similar process. Take the saline corroded surface as an example (Fig. 6 (b)), without copper ion diffusion to the top of the existing Cu_2O, it is hard to imagine how the secondary layer of Cu_2O actually formed on top.

3.6. Insight into antibacterial surface research

Firstly, the current results suggest the significance of buffer selection in antibacterial surface research. Buffers are more than a friendly environment designed for microbes. On the contrary, depending on their components as well as the corresponding properties (corrosivity in this case), they may react with the investigated surface in different

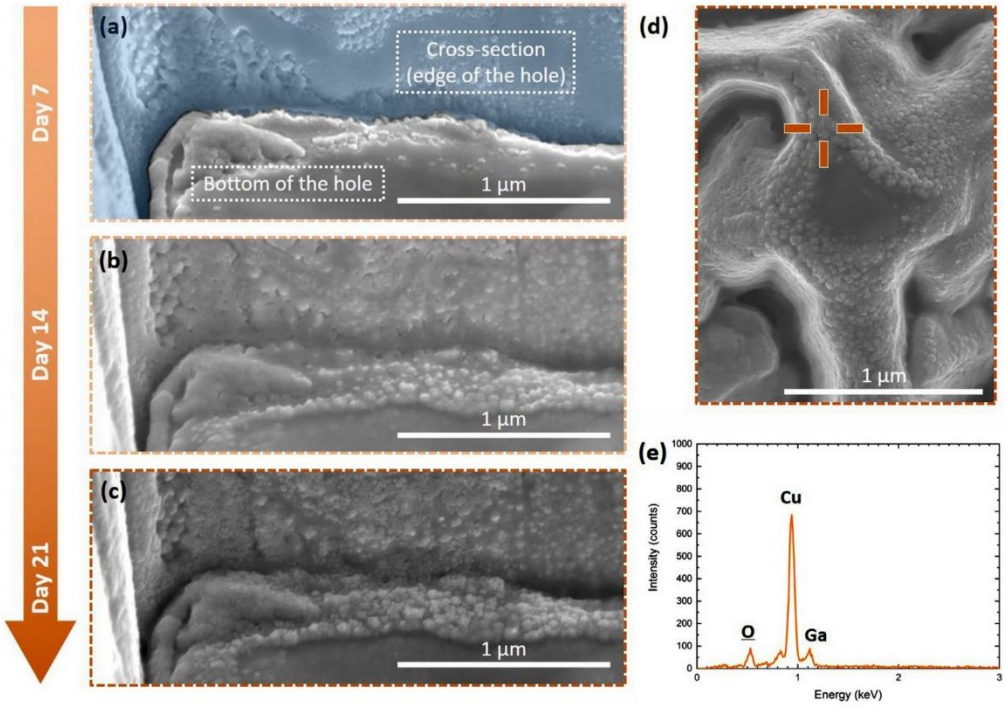

Fig. 8. High resolution SEM images **(a-c)** (SE, 5 kV, coupon being 52° tilted) of fresh section of copper surface prepared by FIB after 3 h exposure to 0.9% NaCl solution. This position was repeatedly examined every 7 days **(a-c)**, whose lower magnification images are already presented in Fig. 7. Zone covered by light blue colour in **(a)** highlights the cross-section (edge of the hole). Image **(d)** (SE, 5 kV) was taken from the Day 21 coupon. The cross shape indicator points out the position where the EDS spectrum **(e)** was collected.

ways, resulting in an enhanced antibacterial efficiency or vice versa. Evidences for this can also be obtained from other comparisons such as PBS vs Na-HEPES [27], or nutrient broth (NB) vs minimal media (MM) [40]. For the same reason, design of materials with weaker corrosion resistance could enhance release of antibacterial substances [41], meanwhile considering that the cytotoxicity might need to be and definitely can be avoided in specific scenarios [42].

Secondly, growth and coverage of passive layer as a result of the subsequent atmospheric corrosion, may not be beneficial for the long-term antibacterial property of copper surfaces [26]. Therefore, it should particularly inspire the applied research closely related to touched surfaces, as NaCl is also one of the major residues of perspiration. To evaluate its effect on antibacterial efficiency, cyclic test [43] should be one of the effective ways to be included in the future work.

4. Conclusion

NaCl as a common component in many popular buffers, was examined in this work in view of its roles in copper corrosion. Some concluding remarks are summarised as below:

- Ground copper coupon undergoes severe localised corrosion attacks in the environment of 0.9% saline, regardless of whether *E. coli* is added or not.
- A layer of Cu_2O grows on copper surface when being exposed to pure 0.9% saline. In the case of its *E. coli* suspension, formation of Cu_2O has been inhibited at least in 3 h.
- A faster killing rate of ground copper surface against *E. coli* (98% in 1 h) is recorded in 0.9% saline, compared to pure water (22%), which is attributed to the accelerated corrosion process in the presence of Cl^-.
- Increase of Cl^- concentration may accelerate copper release, forming Cu_2O even in *E. coli* suspension. However, it can be counteracted by increasing the concentration of *E. coli*, as this enhances the copper ion accumulation effect.
- Residual NaCl crystals on copper surface promote the formation of additional Cu_2O as corrosion products. A Cl^--assisted atmospheric corrosion process is revealed by a FIB-assisted 3-week aging experiment.

Data availability

The data that support the findings of this study are available from the corresponding author on request.

CRediT authorship contribution statement

Jiaqi Luo: Conceptualization, Validation, Investigation, Writing - original draft, Visualization, Project administration. **Christina Hein:** Validation, Investigation, Resources. **Jean-François Pierson:** Writing - review & editing, Supervision, Funding acquisition. **Frank Mücklich:** Resources, Supervision, Funding acquisition.

Declaration of Competing Interest

The authors declare that they have no known competing financial interests or personal relationships that could have appeared to influence the work reported in this paper.

Acknowledgements

This study was supported by Erasmus Mundus Joint European Doctoral Programme in Advanced Materials Science and Engineering

(DocMASE, 512225-1-2010-1-DE-EMJD, European Commission) and the PhD-Track-Programme (PhD02-14, Franco-German University). The ICP-MS experiments were supported by Dr. Ralf Kautenburger from the chair of Inorganic Solid State Chemistry. J. L. particularly thank Prof. Tomáš Prošek from University of Chemistry and Technology, Prague, for his inspiring perspective during EUROCORR 2018 and 2019, making this work possible.

References

[1] M. Vincent, R.E. Duval, P. Hartemann, M. Engels-Deutsch, Contact killing and antimicrobial properties of copper, J. Appl. Microbiol. 124 (2018) 1032–1046.
[2] S. Rigo, C. Cai, G. Gunkel-Grabole, L. Maurizi, X. Zhang, J. Xu, C.G. Palivan, Nanoscience-based strategies to engineer antimicrobial surfaces, Adv. Sci. 5 (2018) 1700892.
[3] M.P. Muller, C. MacDougall, M. Lim, I. Armstrong, A. Bialachowski, S. Callery, W. Ciccotelli, M. Cividino, J. Dennis, S. Hota, G. Garber, J. Johnstone, K. Katz, A. McGeer, V. Nankoosingh, C. Richard, M. Vearncombe, Antimicrobial surfaces to prevent healthcare-associated infections: a systematic review, J. Hosp. Infect. 92 (2018) 7–13.
[4] S.S. Dunne, M. Ahonen, M. Modic, F.R.L. Crijns, M.M. Keinänen-Toivola, R. Meinke, C.W. Keevil, J. Gray, N.H. O'Connell, C.P. Dunne, Specialised cleaning associated with antimicrobial coatings for reduction of hospital acquired infection. Opinion of the COST Action Network AMiCI (CA15114), J. Hosp. Infect. (2018).
[5] M. Colin, F. Klingelschmitt, E. Charpentier, J. Josse, L. Kanagaratnam, C. De Champs, S.C. Gangloff, Copper alloy touch surfaces in healthcare facilities: an effective solution to prevent bacterial spreading, Materials 11 (2018) 2479.
[6] S. Chyderiotis, C. Legeay, D. Verjat-Trannoy, F. Le Gallou, P. Astagneau, D. Lepelletier, New insights on antimicrobial efficacy of copper surfaces in the healthcare environment: a systematic review, Clin. Microbiol. Infect. (2018).
[7] J.H. Michel, W.R. Moran, A.A. Estelle, K.E. Sexton, H.T. Michels, Antimicrobial benefits of copper alloy touch surfaces, Int. J. Powder Metall. 49 (2013) 33–36.
[8] G. Grass, C. Rensing, M. Solioz, Metallic copper as an antimicrobial surface, Appl. Environ. Microbiol. 77 (2011) 1541–1547.
[9] S.L. Warnes, C.W. Keevil, Mechanism of copper surface toxicity in Vancomycin-resistant enterococci following wet or dry surface contact, Appl. Environ. Microbiol. 77 (2011) 6049–6059.
[10] C. Molteni, H.K. Abicht, M. Solioz, Killing of bacteria by copper surfaces involves dissolved copper, Appl. Environ. Microbiol. 76 (2010) 4099–4101.
[11] S. Sonia, R. Jayasudha, N.D. Jayram, P.S. Kumar, D. Mangalaraj, S.R. Prabagaran, Synthesis of hierarchical CuO nanostructures: biocompatible antibacterial agents for gram-positive and gram-negative bacteria, Curr. Appl. Phys. 16 (2016) 914–921.
[12] Phosphate-Buffered Saline (PBS) 2006 Cold Spring Harbor Protocols, 2006 pdb.rec8247.
[13] Y. Sun, V. Tran, D. Zhang, W.B. Wang, S. Yang, Technology and antimicrobial properties of Cu/TiB2 composite coating on 304 steel surface prepared by laser cladding, Mater. Sci. Forum 944 (2019) 473–479.
[14] K. Steinhauer, S. Meyer, J. Pfannebecker, K. Teckemeyer, K. Ockenfeld, K. Weber, B. Becker, Antimicrobial efficacy and compatibility of solid copper alloys with chemical disinfectants, PLoS ONE 13 (2018) e0200748.
[15] C. Hahn, M. Hans, C. Hein, A. Dennstedt, F. Mücklich, P. Rettberg, C.E. Hellweg, L.I. Leichert, C. Rensing, R. Moeller, Antimicrobial properties of ternary eutectic aluminum alloys, BioMetals 31 (2018) 759–770.
[16] M. Solioz, Copper and Bacteria: Evolution, Homeostasis and Toxicity, Springer, 2018.
[17] C. Toparli, S.W. Hieke, A. Altin, O. Kasian, C. Scheu, A. Erbe, State of the surface of antibacterial copper in phosphate buffered saline, J. Electrochem. Soc. 164 (2017) H734–H742.
[18] B.J. Webster, S.E. Werner, D.B. Wells, P.J. Bremer, Microbiologically influenced corrosion of copper in potable water systems—pH effects, Corrosion 56 (2000) 942–950.
[19] S.M. Mayanna, T.H.V. Setty, Role of chloride ions in relation to copper corrosion and inhibition, Proc. Indian Acad. Sci.Sect. A 80 (1974) 184–193.
[20] A. El Warraky, H.A. El Shayeb, E.M. Sherif, Pitting corrosion of copper in chloride solutions, Anti-Corros. Methods Mater. 51 (2004) 52–61.
[21] N. Ciacotich, M. Kilstrup, P. Møller, L. Gram, Influence of chlorides and phosphates on the antiadhesive, antibacterial, and electrochemical properties of an electroplated copper-silver alloy, Biointerphases 14 (2019) 021005.
[22] L. Wang, Y. Miao, M. Lu, Z. Shan, S. Lu, J. Hou, Q. Yang, X. Liang, T. Zhou, D. Curry, K. Oakes, X. Zhang, Chloride-accelerated Cu-Fenton chemistry for biofilm removal, Chem. Commun. 53 (2017) 5862–5865.
[23] S.X. Li, L.H. Hihara, Atmospheric corrosion initiation on steel from predeposited NaCl salt particles in high humidity atmospheres, Corros. Eng. Sci. Technol. 45 (2010) 49–56.
[24] E. Schindelholz, R.G. Kelly, Wetting phenomena and time of wetness in atmospheric corrosion: a review, Corros. Rev. 30 (2012).
[25] Z.Y. Chen, S. Zakipour, D. Persson, C. Leygraf, Effect of sodium chloride particles on the atmospheric corrosion of pure copper, Corrosion 60 (2004) 479–491.
[26] M.J. Hutchison, J.R. Scully, Solute capture and doping of Al in Cu2O: corrosion, tarnish resistance, and cation release of high-purity Cu-Al alloys in artificial perspiration, J. Electrochem. Soc. 165 (2018) C689–C702.
[27] J. Luo, C. Hein, J.-F. Pierson, F. Mücklich, Early-stage corrosion, ion release, and the antibacterial effect of copper and cuprous oxide in physiological buffers: Phosphate-buffered saline vs Na-4-(2-hydroxyethyl)-1-piperazineethanesulfonic acid, Biointerphases 14 (2019) 061004.
[28] J. Luo, C. Hein, J. Ghanbaja, J.-F. Pierson, F. Mücklich, Bacteria accumulate copper ions and inhibit oxide formation on copper surface during antibacterial efficiency test, Micron 127 (2019) 102759.
[29] J. Luo, C. Hein, J.-F. Pierson, F. Mücklich, Localised corrosion attacks and oxide growth on copper in phosphate-buffered saline, Mater. Charact. 158 (2019) 109985.
[30] A. Vinogradov, T. Mimaki, S. Hashimoto, R. Valiev, On the corrosion behaviour of ultra-fine grain copper, Scr. Mater. 41 (1999) 319–326.
[31] C.A.C. Sequeira, physicochemical Inorganic, and microbial aspects of copper corrosion: literature survey, Br. Corros. J. 30 (1995) 137–153.
[32] H. Kakinuma, I. Muto, Y. Oya, Y. Kyo, Y. Sugawara, N. Hara, Mechanism for the morphological change from trenching to pitting around intermetallic particles in AA1050 aluminum, J. Electrochem. Soc. 166 (2019) C19–C32.
[33] A.K. Lee, D.K Newman, Microbial iron respiration: impacts on corrosion processes, Appl. Microbiol. Biotechnol. 62 (2003) 134–139.
[34] A. Hedin, A.J. Johansson, C. Lilja, M. Boman, P. Berastegui, R. Berger, M. Ottosson, Corrosion of copper in pure O2-free water? Corros. Sci. 137 (2018) 1–12.
[35] W.D. Bjorndahl, K. Nobe, Copper corrosion in chloride media. Effect of oxygen, Corrosion 40 (1984) 82–87.
[36] T. Prosek, A.L. Gac, D. Thierry, S.L. Manchet, C. Lojewski, A. Fanica, E. Johansson, C. Canderyd, F. Dupoiron, T. Snauwaert, F. Maas, B. Droesbeke, Low-temperature stress corrosion cracking of austenitic and duplex stainless steels under chloride deposits, Corrosion 70 (2014) 1052–1063.
[37] J.M. Cassells, M.T. Yahya, C.P. Gerba, J.B. Rose, Efficacy of a combined system of copper and silver and free chlorine for inactivation of Naegleria fowleri amoebas in water, Water Sci. Technol. 31 (1995) 119–122.
[38] I.R. Booth, P. Louis, Managing hypoosmotic stress: Aquaporins and mediumosensitive channels in Escherichia coli, Curr. Opin. Microbiol. 2 (1999) 166–169.
[39] T. Aastrup, M. Wadsak, M. Schreiner, C. Leygraf, Experimental in situ studies of copper exposed to humidified air, Corros. Sci. 42 (2000) 957–967.
[40] M.A. Javed, P.R. Stoddart, E.A. Palombo, S.L. McArthur, S.A. Wade, Inhibition or acceleration: bacterial test media can determine the course of microbiologically influenced corrosion, Corros. Sci. 86 (2014) 149–158.
[41] S.C. Tao, J.L. Xu, L. Yuan, J.M. Luo, Y.F. Zheng, Microstructure, mechanical properties and antibacterial properties of the microwave sintered porous Ti–3Cu alloys, J.Alloys Compd. 812 (2020) 152142.
[42] L. Fowler, H. Engqvist, C. Öhman-Mägi, Effect of copper ion concentration on bacteria and cells, Materials 12 (2019) 3798.
[43] S. Rtimi, R. Sanjines, M. Bensimon, C. Pulgarin, J. Kiwi, Accelerated Escherichia coli inactivation in the dark on uniform copper flexible surfaces, Biointerphases 9 (2014) 029012.

7. Conclusions and Outlook

Since the detailed conclusions have been listed in the end of each chapter, here is a short outline, not only to briefly summarise the main results, but also to outline the central research path.

What are the main observations? Corrosion attacks on copper surface. Ground copper surface and electropolished copper surface have been investigated, in terms of the corrosion attacks introduced by physiological buffer solutions. Several types have been detected, namely the intergranular corrosion, preferred corrosion on specific grain orientation, selective/crystallographic corrosion and so on.

What are the reasons these attacks? Chloride in the buffers (*e.g.* in PBS). This has been confirmed by studying pure saline treated copper surface. At the same time, the effect of bacterial addition (*E. coli* in this work) has also been excluded.

What are the impacts? Antibacterial copper ion release and oxide formation. Corrosion attacks transform the solid-state copper into antibacterial copper ions, which are crucial in deactivating bacteria in antibacterial efficiency test. However, if the bacteria are missing from the aqueous environment, then oxide formation can be observed. Furthermore, this formation process could already occur even in a "dry" condition, through an atmospheric corrosion process.

What's next? As a thesis, it is compulsory to be completed at a certain point. But some findings acquired still suggest how the following research should be extended. The following suggestions, nevertheless, could already exceed the scope of antibacterial copper surface:

Keep considering the potential interactions between buffers and the antibacterial surfaces examined. It has already been shown on metallic copper surface (Chapter 3 and 6), the composition of buffer evidently affects the way how copper is corroded. Difference in antibacterial efficiency can thus be obtained as the copper ion release differentiates. Therefore, for the similar metal/alloy based antibacterial surfaces, it could be "unfair" to compare their antibacterial behaviour without considering the buffer, namely the corrosion environment.

Technically, to properly isolate the additional effects introduced by various buffers could be a better approach. This could probably mean, to totally exclude the buffers from the design of antibacterial efficiency test. For example, dry plating could be a promising attempt, especially if the deposits from the buffers could also be removed from the tested surfaces.

Modify the parameter/procedure of currently existing antibacterial efficiency test, in order to better reflect a surface antibacterial ability in actual scenarios. Antibacterial surfaces always have their own potential applied fields. It is, unfortunately, true that most of them could only be examined in lab tests in view of the huge expense of time and budget for clinical or *in vivo* tests. But this does not change the fact that environmental parameters are still the key to correlate surface

antibacterial efficiency. Therefore, it is crucial to find out a better way to mimic each corresponding scenario so as to obtain representative results. So far, adjusting the composition of the buffer is still a usual way, for instance, artificial perspiration is already commercially available and has been applied in a few studies. Further identification of the relevant environments helps to achieve this aim.

Aging of antibacterial surfaces deserves much more attention. In Chapter 6, aging (*i.e.* atmospheric oxidation) of copper surface has been observed in the presence of NaCl deposits. This phenomenon indicates the potential aging effect of antibacterial copper surface, which could present in the long-term atmospheric practise. The situation on copper could still be optimistic, since its main 3-week aging product Cu_2O is also an antibacterial substance, although less efficient. While similar scenarios may not be true on other surfaces, where antibacterial activity could completely lose after passivation or other aging mechanisms in the specific environment. Therefore it is essential to evaluate the effectiveness of antibacterial touched surfaces in a long-term.

Design (or at least consideration) of antibacterial surfaces based on the material microstructure. As we have seen in Chapter 5, grain boundaries as well as grains with specific orientations on copper surface are subject to localised corrosion attacks. This suggests the possibility to tailor the antibacterial copper ion release by delicate microstructure engineering, where research/outcomes of material science can play a big role. Besides, it reminds us that it is always necessary to have a full comprehension of the actual surface state of coupons, which can be easily altered through common preparation processes.

References

[1] S.B. Griffith, Sun Tzu: The art of war, Oxford University Press, London, 1963.

[2] C.R. Mahon, D.C. Lehman, G. Manuselis, Textbook of diagnostic microbiology, Elsevier Saunders, St. Louis, 2019.

[3] P. Ziegler, The black death, Faber & Faber, London, 2013.

[4] D.A. Rasko, D.R. Webster, J.W. Sahl, A. Bashir, N. Boisen, F. Scheutz, E.E. Paxinos, R. Sebra, C.-S. Chin, D. Iliopoulos, Origins of the E. coli strain causing an outbreak of hemolytic–uremic syndrome in Germany, New England Journal of Medicine, 365 (2011) 709-717.

[5] G. Gault, F.-X. Weill, P. Mariani-Kurkdjian, N. Jourdan-da Silva, L. King, B. Aldabe, M. Charron, N. Ong, C. Castor, M. Mace, Outbreak of haemolytic uraemic syndrome and bloody diarrhoea due to Escherichia coli O104: H4, south-west France, June 2011, Europe's journal on infectious disease surveillance, epidemiology, prevention and control, 16 (2011) 19905.

[6] Y. Xiong, P. Wang, R. Lan, C. Ye, H. Wang, J. Ren, H. Jing, Y. Wang, Z. Zhou, X. Bai, A novel Escherichia coli O157: H7 clone causing a major hemolytic uremic syndrome outbreak in China, PLoS ONE, 7 (2012) e36144.

[7] G. Pankey, L. Sabath, Clinical relevance of bacteriostatic versus bactericidal mechanisms of action in the treatment of Gram-positive bacterial infections, Clinical infectious diseases, 38 (2004) 864-870.

[8] R. Hare, New light on the history of penicillin, Medical history, 26 (1982) 1-24.

[9] R.I. Aminov, A brief history of the antibiotic era: lessons learned and challenges for the future, Frontiers in Microbiology, 1 (2010) 134.

[10] L.A. Reynolds, E. Tansey, Superbugs and Superdrugs: A history of MRSA, Wellcome Trust Centre for the History of Medicine at UCL, London, 2008.

[11] J. Wang, P. Wang, X. Wang, Y. Zheng, Y. Xiao, Use and prescription of antibiotics in primary health care settings in China, JAMA internal medicine, 174 (2014) 1914-1920.

[12] L. Zhao, P.K. Chu, Y. Zhang, Z. Wu, Antibacterial coatings on titanium implants, Journal of Biomedical Materials Research Part B: Applied Biomaterials, 91 (2009) 470-480.

[13] M.M. Querido, L. Aguiar, P. Neves, C.C. Pereira, J.P. Teixeira, Self-disinfecting surfaces and infection control, Colloids and Surfaces B: Biointerfaces, 178 (2019) 8-21.

[14] T.R. Garrett, M. Bhakoo, Z. Zhang, Bacterial adhesion and biofilms on surfaces, Progress in Natural Science, 18 (2008) 1049-1056.

[15] A. Pearson, Historical and changing epidemiology of healthcare-associated infections, Journal of Hospital Infection, 73 (2009) 296-304.

[16] D.J. Weber, D. Anderson, W.A. Rutala, The role of the surface environment in healthcare-

associated infections, Curr Opin Infect Dis, 26 (2013) 338-344.
[17] C. Rock, B.A. Small, K.A. Thom, Innovative Methods of Hospital Disinfection in Prevention of Healthcare-Associated Infections, Current Treatment Options in Infectious Diseases, 10 (2018) 65-77.
[18] A. Różańska, A. Chmielarczyk, D. Romaniszyn, G. Majka, M. Bulanda, Antimicrobial effect of copper alloys on Acinetobacter species isolated from infections and hospital environment, Antimicrobial Resistance & Infection Control, 7 (2018) 10.
[19] M. Souli, I. Galani, D. Plachouras, T. Panagea, A. Armaganidis, G. Petrikkos, H. Giamarellou, Antimicrobial activity of copper surfaces against carbapenemase-producing contemporary Gram-negative clinical isolates, Journal of Antimicrobial Chemotherapy, 68 (2013) 852-857.
[20] S. Mehtar, I. Wiid, S.D. Todorov, The antimicrobial activity of copper and copper alloys against nosocomial pathogens and Mycobacterium tuberculosis isolated from healthcare facilities in the Western Cape: an in-vitro study, Journal of Hospital Infection, 68 (2008) 45-51.
[21] S.L. Warnes, S.M. Green, H.T. Michels, C.W. Keevil, Biocidal Efficacy of Copper Alloys against Pathogenic Enterococci Involves Degradation of Genomic and Plasmid DNAs, Applied and Environmental Microbiology, 76 (2010) 5390-5401.
[22] M. Colin, F. Klingelschmitt, E. Charpentier, J. Josse, L. Kanagaratnam, C. De Champs, S.C. Gangloff, Copper Alloy Touch Surfaces in Healthcare Facilities: An Effective Solution to Prevent Bacterial Spreading, Materials, 11 (2018) 2479.
[23] M.G. Schmidt, H.H. Attaway Iii, S.E. Fairey, L.L. Steed, H.T. Michels, C.D. Salgado, Copper Continuously Limits the Concentration of Bacteria Resident on Bed Rails within the Intensive Care Unit, Infection Control and Hospital Epidemiology, 34 (2013) 530-533.
[24] C.D. Salgado, K.A. Sepkowitz, J.F. John, J.R. Cantey, H.H. Attaway, K.D. Freeman, P.A. Sharpe, H.T. Michels, M.G. Schmidt, Copper Surfaces Reduce the Rate of Healthcare-Acquired Infections in the Intensive Care Unit, Infection Control and Hospital Epidemiology, 34 (2013) 479-486.
[25] S. Rai, B.E. Hirsch, H.H. Attaway, R. Nadan, S. Fairey, J. Hardy, G. Miller, D. Armellino, W.R. Moran, P. Sharpe, A. Estelle, J.H. Michel, H.T. Michels, M.G. Schmidt, Evaluation of the Antimicrobial Properties of Copper Surfaces in an Outpatient Infectious Disease Practice, Infection Control and Hospital Epidemiology, 33 (2012) 200-201.
[26] F. Marais, S. Mehtar, L. Chalkley, Antimicrobial efficacy of copper touch surfaces in reducing environmental bioburden in a South African community healthcare facility, Journal of Hospital Infection, 74 (2010) 80-82.
[27] A.L. Casey, T.J. Karpanen, D. Adams, P.A. Lambert, P. Nightingale, L. Miruszenko, T.S.J.

Elliott, A comparative study to evaluate surface microbial contamination associated with copper-containing and stainless steel pens used by nurses in the critical care unit, American Journal of Infection Control, 39 (2011) e52-e54.

[28] A.L. Casey, D. Adams, T.J. Karpanen, P.A. Lambert, B.D. Cookson, P. Nightingale, L. Miruszenko, R. Shillam, P. Christian, T.S.J. Elliott, Role of copper in reducing hospital environment contamination, Journal of Hospital Infection, 74 (2010) 72-77.

[29] K. Steinhauer, S. Meyer, J. Pfannebecker, K. Teckemeyer, K. Ockenfeld, K. Weber, B. Becker, Antimicrobial efficacy and compatibility of solid copper alloys with chemical disinfectants, PLoS ONE, 13 (2018) e0200748.

[30] N. Sykaras, A.M. Iacopino, V.A. Marker, R.G. Triplett, R.D. Woody, Implant materials, designs, and surface topographies: their effect on osseointegration. A literature review, International Journal of Oral & Maxillofacial Implants, 15 (2000) 675-690.

[31] C.R. Arciola, F. Alvi, Y. An, D. Campoccia, L. Montanaro, Implant infection and infection resistant materials: a mini review, The International journal of artificial organs, 28 (2005) 1119-1125.

[32] S.-J. Cheng, I.-Y. Tseng, J.-J. Lee, S.-H. Kok, A prospective study of the risk factors associated with failure of mini-implants used for orthodontic anchorage, International Journal of Oral & Maxillofacial Implants, 19 (2004) 100-106.

[33] J. Costerton, L. Montanaro, C.R. Arciola, Biofilm in implant infections: its production and regulation, The International journal of artificial organs, 28 (2005) 1062-1068.

[34] D. Campoccia, L. Montanaro, C.R. Arciola, A review of the biomaterials technologies for infection-resistant surfaces, Biomaterials, 34 (2013) 8533-8554.

[35] J. Gallo, M. Holinka, C. Moucha, Antibacterial Surface Treatment for Orthopaedic Implants, International Journal of Molecular Sciences, 15 (2014) 13849-13880.

[36] G.A. Norambuena, R. Patel, M. Karau, C.C. Wyles, P.J. Jannetto, K.E. Bennet, A.D. Hanssen, R.J. Sierra, Antibacterial and Biocompatible Titanium-Copper Oxide Coating May Be a Potential Strategy to Reduce Periprosthetic Infection: An In Vitro Study, Clinical Orthopaedics and Related Research®, 475 (2017) 722-732.

[37] T. Shirai, H. Tsuchiya, T. Shimizu, K. Ohtani, Y. Zen, K. Tomita, Prevention of pin tract infection with titanium-copper alloys, Journal of Biomedical Materials Research Part B: Applied Biomaterials, 91B (2009) 373-380.

[38] J. Valle, S. Burgui, D. Langheinrich, C. Gil, C. Solano, A. Toledo-Arana, R. Helbig, A. Lasagni, I. Lasa, Evaluation of Surface Microtopography Engineered by Direct Laser Interference for Bacterial Anti-Biofouling, Macromolecular Bioscience, 15 (2015) 1060-1069.

[39] K. Bazaka, M.V. Jacob, R.J. Crawford, E.P. Ivanova, Efficient surface modification of biomaterial to prevent biofilm formation and the attachment of microorganisms, Applied Microbiology and Biotechnology, 95 (2012) 299-311.

[40] K. Bruellhoff, J. Fiedler, M. Möller, J. Groll, R.E. Brenner, Surface coating strategies to prevent biofilm formation on implant surfaces, Int J Artif Organs, 33 (2010) 646-653.

[41] C. Bower, J. McGuire, M. Daeschel, The adhesion and detachment of bacteria and spores on food-contact surfaces, Trends in Food Science & Technology, 7 (1996) 152-157.

[42] G. Faúndez, M. Troncoso, P. Navarrete, G. Figueroa, Antimicrobial activity of copper surfaces against suspensions of Salmonella enterica and Campylobacter jejuni, Bmc Microbiology, 4 (2004) 1-7.

[43] D. Berry, C. Xi, L. Raskin, Microbial ecology of drinking water distribution systems, Current opinion in biotechnology, 17 (2006) 297-302.

[44] M.W. LeChevallier, C.D. Lowry, R.G. Lee, D.L. Gibbon, Examining the relationship between iron corrosion and the disinfection of biofilm bacteria, Journal - American Water Works Association, 85 (1993) 111-123.

[45] M. Li, L. Nan, D. Xu, G. Ren, K. Yang, Antibacterial Performance of a Cu-bearing Stainless Steel against Microorganisms in Tap Water, Journal of Materials Science & Technology, 31 (2015) 243-251.

[46] S. Triantafyllidou, D. Lytle, C. Muhlen, J. Swertfeger, Copper-silver ionization at a US hospital: Interaction of treated drinking water with plumbing materials, aesthetics and other considerations, Water Research, 102 (2016) 1-10.

[47] Y. Lou, L. Lin, D. Xu, S. Zhao, C. Yang, J. Liu, Y. Zhao, T. Gu, K. Yang, Antibacterial ability of a novel Cu-bearing 2205 duplex stainless steel against Pseudomonas aeruginosa biofilm in artificial seawater, International Biodeterioration & Biodegradation, 110 (2016) 199-205.

[48] L. Nan, D. Xu, T. Gu, X. Song, K. Yang, Microbiological influenced corrosion resistance characteristics of a 304L-Cu stainless steel against Escherichia coli, Materials Science and Engineering: C, 48 (2015) 228-234.

[49] K. Ellinas, D. Kefallinou, K. Stamatakis, E. Gogolides, A. Tserepi, Is There a Threshold in the Antibacterial Action of Superhydrophobic Surfaces?, ACS Applied Materials & Interfaces, 9 (2017) 39781-39789.

[50] D. Wojcieszak, M. Mazur, D. Kaczmarek, B. Szponar, M. Grobelny, M. Kalisz, A. Pelczarska, I. Szczygiel, A. Poniedzialek, M. Osekowska, Structural and surface properties of semitransparent and antibacterial (Cu,Ti,Nb)Ox coating, Applied Surface Science, 380 (2016) 159-164.

[51] N. Thewes, P. Loskill, P. Jung, H. Peisker, M. Bischoff, M. Herrmann, K. Jacobs, Hydrophobic

interaction governs unspecific adhesion of staphylococci: a single cell force spectroscopy study, Beilstein Journal of Nanotechnology, 5 (2014) 1501-1512.

[52] S. Wu, S. Altenried, A. Zogg, F. Zuber, K. Maniura-Weber, Q. Ren, Role of the Surface Nanoscale Roughness of Stainless Steel on Bacterial Adhesion and Microcolony Formation, ACS Omega, 3 (2018) 6456-6464.

[53] R. Helbig, D. Gunther, J. Friedrichs, Ro, A. Lasagni, C. Werner, The impact of structure dimensions on initial bacterial adhesion, Biomaterials Science, 4 (2016) 1074-1078.

[54] V. Gadenne, L. Lebrun, T. Jouenne, P. Thebault, Role of molecular properties of ulvans on their ability to elaborate antiadhesive surfaces, Journal of Biomedical Materials Research Part A, 103 (2015) 1021-1028.

[55] G. Cheng, Z. Zhang, S. Chen, J.D. Bryers, S. Jiang, Inhibition of bacterial adhesion and biofilm formation on zwitterionic surfaces, Biomaterials, 28 (2007) 4192-4199.

[56] R.J. Turner, Metal‐based antimicrobial strategies, Microbial Biotechnology, 10 (2017) 1062-1065.

[57] M. Walkowicz, P. Osuch, B. Smyrak, T. Knych, E. Rudnik, Ł. Cieniek, A. Różańska, A. Chmielarczyk, D. Romaniszyn, M. Bulanda, Impact of oxidation of copper and its alloys in laboratory-simulated conditions on their antimicrobial efficiency, Corrosion Science, 140 (2018) 321-332.

[58] H. Liu, D. Xu, K. Yang, H. Liu, Y.F. Cheng, Corrosion of antibacterial Cu-bearing 316L stainless steels in the presence of sulfate reducing bacteria, Corrosion Science, 132 (2018) 46-55.

[59] Y. Yin, X. Zhang, D. Wang, L. Nan, Study of antibacterial performance of a type 304 Cu bearing stainless steel against airborne bacteria in real life environments, Materials Technology, 30 (2015) B104-B108.

[60] V. Champagne, K. Sundberg, D. Helfritch, Kinetically Deposited Copper Antimicrobial Surfaces, Coatings, 9 (2019) 257.

[61] N. LIN, J. GUO, R. HANG, J. ZOU, B. TANG, Double glow plasma surface alloying antibacterial silver coating on pure titanium, Surface Review and Letters, 21 (2014) 1450032.

[62] V.M. Villapún, C.C. Lukose, M. Birkett, L.G. Dover, S. González, Tuning the antimicrobial behaviour of Cu85Zr15 thin films in “wet” and “dry” conditions through structural modifications, Surface and Coatings Technology, 350 (2018) 334-345.

[63] M. Souli, A. Antoniadou, I. Katsarolis, I. Mavrou, E. Paramythiotou, E. Papadomichelakis, M. Drogari-Apiranthitou, T. Panagea, H. Giamarellou, G. Petrikkos, A. Armaganidis, Reduction of Environmental Contamination With Multidrug-Resistant Bacteria by Copper-Alloy Coating of Surfaces in a Highly Endemic Setting, Infection Control and Hospital Epidemiology, 38 (2017)

765-771.

[64] Y. Sun, V. Tran, D. Zhang, W.B. Wang, S. Yang, Technology and Antimicrobial Properties of Cu/TiB2 Composite Coating on 304 Steel Surface Prepared by Laser Cladding, Materials Science Forum, 944 (2019) 473-479.

[65] A.M. Kumar, A. Khan, R. Suleiman, M. Qamar, S. Saravanan, H. Dafalla, Bifunctional CuO/TiO2 nanocomposite as nanofiller for improved corrosion resistance and antibacterial protection, Progress in Organic Coatings, 114 (2018) 9-18.

[66] N.K. Eswar, R. Gupta, P.C. Ramamurthy, G. Madras, Influence of copper oxide grown on various conducting substrates towards improved performance for photoelectrocatalytic bacterial inactivation, Molecular Catalysis, 451 (2018) 161-169.

[67] A. Mahmoodi, S. Solaymani, M. Amini, N.B. Nezafat, M. Ghoranneviss, Structural, Morphological and Antibacterial Characterization of CuO Nanowires, Silicon, 10 (2018) 1427-1431.

[68] M.M. Momeni, M. Mirhosseini, Z. Nazari, A. Kazempour, M. Hakimiyan, Antibacterial and photocatalytic activity of CuO nanostructure films with different morphology, Journal of Materials Science: Materials in Electronics, 27 (2016) 8131-8137.

[69] E.I. Zamulaeva, A.N. Sheveyko, A.Y. Potanin, I.Y. Zhitnyak, N.A. Gloushankova, I.V. Sukhorukova, N.V. Shvindina, S.G. Ignatov, E.A. Levashov, D.V. Shtansky, Comparative investigation of antibacterial yet biocompatible Ag-doped multicomponent coatings obtained by pulsed electrospark deposition and its combination with ion implantation, Ceramics International, 44 (2018) 3765-3774.

[70] G.I. Nkou Bouala, A. Etiemble, C. Der Loughian, C. Langlois, J.F. Pierson, P. Steyer, Silver influence on the antibacterial activity of multi-functional Zr-Cu based thin film metallic glasses, Surface and Coatings Technology, 343 (2017) 108-114.

[71] F. Costa, I.F. Carvalho, R.C. Montelaro, P. Gomes, M.C.L. Martins, Covalent immobilization of antimicrobial peptides (AMPs) onto biomaterial surfaces, Acta Biomaterialia, 7 (2011) 1431-1440.

[72] N.R. Sudarshan, D.G. Hoover, D. Knorr, Antibacterial action of chitosan, Food Biotechnology, 6 (1992) 257-272.

[73] E.P. Ivanova, J. Hasan, H.K. Webb, G. Gervinskas, S. Juodkazis, V.K. Truong, A.H.F. Wu, R.N. Lamb, V.A. Baulin, G.S. Watson, J.A. Watson, D.E. Mainwaring, R.J. Crawford, Bactericidal activity of black silicon, Nature Communications, 4 (2013) 2838.

[74] E.P. Ivanova, J. Hasan, H.K. Webb, V.K. Truong, G.S. Watson, J.A. Watson, V.A. Baulin, S. Pogodin, J.Y. Wang, M.J. Tobin, C. Löbbe, R.J. Crawford, Natural Bactericidal Surfaces:

Mechanical Rupture of Pseudomonas aeruginosa Cells by Cicada Wings, Small, 8 (2012) 2489-2494.

[75] V.T.H. Pham, V.K. Truong, M.D.J. Quinn, S.M. Notley, Y. Guo, V.A. Baulin, M. Al Kobaisi, R.J. Crawford, E.P. Ivanova, Graphene Induces Formation of Pores That Kill Spherical and Rod-Shaped Bacteria, ACS Nano, 9 (2015) 8458-8467.

[76] T. Wei, Z. Tang, Q. Yu, H. Chen, Smart Antibacterial Surfaces with Switchable Bacteria-Killing and Bacteria-Releasing Capabilities, ACS Applied Materials & Interfaces, 9 (2017) 37511-37523.

[77] J. Luo, C. Hein, F. Mücklich, M. Solioz, Killing of bacteria by copper, cadmium, and silver surfaces reveals relevant physicochemical parameters, Biointerphases, 12 (2017) 020301.

[78] M. Hans, J.C. Támara, S. Mathews, B. Bax, A. Hegetschweiler, R. Kautenburger, M. Solioz, F. Mücklich, Laser cladding of stainless steel with a copper–silver alloy to generate surfaces of high antimicrobial activity, Applied Surface Science, 320 (2014) 195-199.

[79] C. Molteni, H.K. Abicht, M. Solioz, Killing of Bacteria by Copper Surfaces Involves Dissolved Copper, Applied and Environmental Microbiology, 76 (2010) 4099-4101.

[80] L. Zhu, J. Elguindi, C. Rensing, S. Ravishankar, Antimicrobial activity of different copper alloy surfaces against copper resistant and sensitive Salmonella enterica, Food Microbiology, 30 (2012) 303-310.

[81] A. Różańska, A. Chmielarczyk, D. Romaniszyn, A. Sroka-Oleksiak, M. Bulanda, M. Walkowicz, P. Osuch, T. Knych, Antimicrobial Properties of Selected Copper Alloys on Staphylococcus aureus and Escherichia coli in Different Simulations of Environmental Conditions: With vs. without Organic Contamination, International Journal of Environmental Research and Public Health, 14 (2017) 813.

[82] N. Tripathy, R. Ahmad, S.H. Bang, G. Khang, J. Min, Y.-B. Hahn, Outstanding Antibiofilm Features of Quanta-CuO Film on Glass Surface, ACS Applied Materials & Interfaces, 8 (2016) 15128-15137.

[83] H. Kawakami, K. Yoshida, Y. Nishida, Y. Kikuchi, Y. Sato, Antibacterial Properties of Metallic Elements for Alloying Evaluated with Application of JIS Z 2801:2000, ISIJ International, 48 (2008) 1299-1304.

[84] E. Robine, L. Boulangé-Petermann, D. Derangère, Assessing bactericidal properties of materials: the case of metallic surfaces in contact with air, Journal of Microbiological Methods, 49 (2002) 225-234.

[85] N. Ciacotich, R.U. Din, J.J. Sloth, P. Møller, L. Gram, An electroplated copper–silver alloy as antibacterial coating on stainless steel, Surface and Coatings Technology, 345 (2018) 96-104.

[86] C. Espírito Santo, P.V. Morais, G. Grass, Isolation and Characterization of Bacteria Resistant

to Metallic Copper Surfaces, Applied and Environmental Microbiology, 76 (2010) 1341-1348.
[87] J. Elguindi, S. Moffitt, H. Hasman, C. Andrade, S. Raghavan, C. Rensing, Metallic copper corrosion rates, moisture content, and growth medium influence survival of copper ion-resistant bacteria, Applied Microbiology and Biotechnology, 89 (2011) 1963-1970.
[88] H.T. Michels, J.O. Noyce, C.W. Keevil, Effects of temperature and humidity on the efficacy of methicillin-resistant Staphylococcus aureus challenged antimicrobial materials containing silver and copper, Letters in Applied Microbiology, 49 (2009) 191-195.
[89] C.E. Santo, E.W. Lam, C.G. Elowsky, D. Quaranta, D.W. Domaille, C.J. Chang, G. Grass, Bacterial Killing by Dry Metallic Copper Surfaces, Applied and Environmental Microbiology, 77 (2011) 794-802.
[90] R. Hong, T.Y. Kang, C.A. Michels, N. Gadura, Membrane Lipid Peroxidation in Copper Alloy-Mediated Contact Killing of Escherichia coli, Applied and Environmental Microbiology, 78 (2012) 1776-1784.
[91] J.O. Noyce, H. Michels, C.W. Keevil, Potential use of copper surfaces to reduce survival of epidemic meticillin-resistant Staphylococcus aureus in the healthcare environment, Journal of Hospital Infection, 63 (2006) 289-297.
[92] L. Weaver, J.O. Noyce, H.T. Michels, C.W. Keevil, Potential action of copper surfaces on meticillin-resistant Staphylococcus aureus, Journal of Applied Microbiology, 109 (2010) 2200-2205.
[93] C.E. Santo, D. Quaranta, G. Grass, Antimicrobial metallic copper surfaces kill Staphylococcus haemolyticus via membrane damage, MicrobiologyOpen, 1 (2012) 46-52.
[94] N. Ciacotich, K.N. Kragh, M. Lichtenberg, J.E. Tesdorpf, T. Bjarnsholt, L. Gram, In Situ Monitoring of the Antibacterial Activity of a Copper–Silver Alloy Using Confocal Laser Scanning Microscopy and pH Microsensors, Global Challenges, 3 (2019) 1900044.
[95] A. Mikolay, S. Huggett, L. Tikana, G. Grass, J. Braun, D.H. Nies, Survival of bacteria on metallic copper surfaces in a hospital trial, Applied Microbiology and Biotechnology, 87 (2010) 1875-1879.
[96] B. von Dessauer, M.S. Navarrete, D. Benadof, C. Benavente, M.G. Schmidt, Potential effectiveness of copper surfaces in reducing health care–associated infection rates in a pediatric intensive and intermediate care unit: A nonrandomized controlled trial, American Journal of Infection Control, 44 (2016) e133-e139.
[97] T. Pandiyarajan, R. Udayabhaskar, S. Vignesh, R.A. James, B. Karthikeyan, Synthesis and concentration dependent antibacterial activities of CuO nanoflakes, Materials Science and Engineering: C, 33 (2013) 2020-2024.

[98] N. Ekthammathat, T. Thongtem, S. Thongtem, Antimicrobial activities of CuO films deposited on Cu foils by solution chemistry, Applied Surface Science, 277 (2013) 211-217.
[99] S. Sonia, R. Jayasudha, N.D. Jayram, P.S. Kumar, D. Mangalaraj, S.R. Prabagaran, Synthesis of hierarchical CuO nanostructures: Biocompatible antibacterial agents for Gram-positive and Gram-negative bacteria, Current Applied Physics, 16 (2016) 914-921.
[100] E. Zhang, F. Li, H. Wang, J. Liu, C. Wang, M. Li, K. Yang, A new antibacterial titanium–copper sintered alloy: Preparation and antibacterial property, Materials Science and Engineering: C, 33 (2013) 4280-4287.
[101] M. Radetzki, Seven thousand years in the service of humanity—the history of copper, the red metal, Resources Policy, 34 (2009) 176-184.
[102] J.R. Davis, Copper and copper alloys, ASM international, Ohio, 2001.
[103] I. Platzman, R. Brener, H. Haick, R. Tannenbaum, Oxidation of Polycrystalline Copper Thin Films at Ambient Conditions, The Journal of Physical Chemistry C, 112 (2008) 1101-1108.
[104] G. Borkow, J. Gabbay, Copper as a Biocidal Tool, Current Medicinal Chemistry, 12 (2005) 2163-2175.
[105] D.L. de Romaña, M. Olivares, R. Uauy, M. Araya, Risks and benefits of copper in light of new insights of copper homeostasis, Journal of Trace Elements in Medicine and Biology, 25 (2011) 3-13.
[106] G. Borkow, Using Copper to Fight Microorganisms, Current Chemical Biology, 6 (2012) 93-103.
[107] M. Solioz, Copper and Bacteria: Evolution, Homeostasis and Toxicity, Springer, Cham, 2018.
[108] C.E. Santo, N. Taudte, D.H. Nies, G. Grass, Contribution of Copper Ion Resistance to Survival of Escherichia coli on Metallic Copper Surfaces, Applied and Environmental Microbiology, 74 (2008) 977-986.
[109] M. Saphier, E. Silberstein, Y. Shotland, S. Popov, O. Saphier, Prevalence of Monovalent Copper Over Divalent in Killing Escherichia coli and Staphylococcus aureus, Current Microbiology, 75 (2018) 426-430.
[110] W.-X. Tian, S. Yu, M. Ibrahim, A.W. Almonaofy, L. He, Q. Hui, Z. Bo, B. Li, G.-l. Xie, Copper as an antimicrobial agent against opportunistic pathogenic and multidrug resistant Enterobacter bacteria, Journal of Microbiology, 50 (2012) 586-593.
[111] X. Zhang, X. Huang, Y. Ma, N. Lin, A. Fan, B. Tang, Bactericidal behavior of Cu-containing stainless steel surfaces, Applied Surface Science, 258 (2012) 10058-10063.
[112] L. Wang, Y. Miao, M. Lu, Z. Shan, S. Lu, J. Hou, Q. Yang, X. Liang, T. Zhou, D. Curry, K. Oakes, X. Zhang, Chloride-accelerated Cu-Fenton chemistry for biofilm removal, Chemical

Communications, 53 (2017) 5862-5865.
[113] S.L. Warnes, C.W. Keevil, Lack of Involvement of Fenton Chemistry in Death of Methicillin-Resistant and Methicillin-Sensitive Strains of Staphylococcus aureus and Destruction of Their Genomes on Wet or Dry Copper Alloy Surfaces, Applied and Environmental Microbiology, 82 (2016) 2132-2136.
[114] D.A. Palmer, P. Bénézeth, J. Simonson, Solubility of copper oxides in water and steam, 14th International Conference on the Properties of Water and Steam in Kyoto, 2004, pp. 491-496.
[115] I.A. Hassan, I.P. Parkin, S.P. Nair, C.J. Carmalt, Antimicrobial activity of copper and copper(i) oxide thin films deposited via aerosol-assisted CVD, Journal of Materials Chemistry B, 2 (2014) 2855-2860.
[116] M. Hans, A. Erbe, S. Mathews, Y. Chen, M. Solioz, F. Mücklich, Role of Copper Oxides in Contact Killing of Bacteria, Langmuir, 29 (2013) 16160-16166.
[117] R. Katwal, H. Kaur, G. Sharma, M. Naushad, D. Pathania, Electrochemical synthesized copper oxide nanoparticles for enhanced photocatalytic and antimicrobial activity, Journal of Industrial and Engineering Chemistry, 31 (2015) 173-184.
[118] O. Akhavan, E. Ghaderi, Cu and CuO nanoparticles immobilized by silica thin films as antibacterial materials and photocatalysts, Surface and Coatings Technology, 205 (2010) 219-223.
[119] J.D. Moore, A. Avellan, C.W. Noack, Y. Guo, G.V. Lowry, K.B. Gregory, Time-dependent bacterial transcriptional response to CuO nanoparticles differs from that of Cu2+ and provides insights into CuO nanoparticle toxicity mechanisms, Environmental Science: Nano, 4 (2017) 2321-2335.
[120] A. Rotini, A. Tornambè, R. Cossi, F. Iamunno, G. Benvenuto, M.T. Berducci, C. Maggi, M.C. Thaller, A.M. Cicero, L. Manfra, L. Migliore, Salinity-Based Toxicity of CuO Nanoparticles, CuO-Bulk and Cu Ion to Vibrio anguillarum, Frontiers in Microbiology, 8 (2017) 2076.
[121] L. Wang, C. Hu, L. Shao, The antimicrobial activity of nanoparticles: present situation and prospects for the future, International Journal of Nanomedicine, 12 (2017) 1227-1249.
[122] L. Ren, J. Chong, A. Loya, Q. Kang, J.L. Stair, L. Nan, G. Ren, Determination of Cu2+ ions release rate from antimicrobial copper bearing stainless steel by joint analysis using ICP-OES and XPS, Materials Technology, 30 (2015) B86-B89.
[123] J.O. Noyce, H. Michels, C.W. Keevil, Use of Copper Cast Alloys To Control Escherichia coli O157 Cross-Contamination during Food Processing, Applied and Environmental Microbiology, 72 (2006) 4239-4244.
[124] D.J. Horton, H. Ha, L.L. Foster, H.J. Bindig, J.R. Scully, Tarnishing and Cu Ion release in Selected Copper-Base Alloys: Implications towards Antimicrobial Functionality, Electrochimica

Acta, 169 (2015) 351-366.
[125] G. Grass, C. Rensing, M. Solioz, Metallic Copper as an Antimicrobial Surface, Applied and Environmental Microbiology, 77 (2011) 1541-1547.
[126] A. Tripathy, S. Sreedharan, C. Bhaskarla, S. Majumdar, S.K. Peneti, D. Nandi, P. Sen, Enhancing the Bactericidal Efficacy of Nanostructured Multifunctional Surface Using an Ultrathin Metal Coating, Langmuir, 33 (2017) 12569-12579.
[127] M. Zeiger, M. Solioz, H. Edongué, E. Arzt, A.S. Schneider, Surface structure influences contact killing of bacteria by copper, MicrobiologyOpen, 3 (2014) 327-332.
[128] V.K. Champagne, D.J. Helfritch, A demonstration of the antimicrobial effectiveness of various copper surfaces, Journal of Biological Engineering, 7 (2013) 1-7.
[129] I. Codiþã, D.M. Caplan, E.-C. Drãgulescu, B.a.-E. Lixandru, I.L. Coldea, C.C. Dragomirescu, C. Surdu-Bob, M. Bãdulescu, Antimicrobial activity of copper and silver nanofilms on nosocomial bacterial species, ROMANIAN ARCHIVES, 18 (2010) 204-212.
[130] S. Rtimi, R. Sanjines, M. Bensimon, C. Pulgarin, J. Kiwi, Accelerated Escherichia coli inactivation in the dark on uniform copper flexible surfaces, Biointerphases, 9 (2014) 029012.
[131] H.M. Yates, P. Sheel, J.L. Hodgkinson, M.E.A. Warwick, S.O. Elfakhri, H.A. Foster, Dual functionality anti-reflection and biocidal coatings, Surface and Coatings Technology, 324 (2017) 201-207.
[132] Y. Kang, J. Park, D.-W. Kim, H. Kim, Y.-C. Kang, Controlling the antibacterial activity of CuSn thin films by varying the contents of Sn, Applied Surface Science, 389 (2016) 1012-1016.
[133] A. Javid, M. Kumar, S. Yoon, J.H. Lee, J.G. Han, Size-controlled growth and antibacterial mechanism for Cu:C nanocomposite thin films, Physical Chemistry Chemical Physics, 19 (2017) 237-244.
[134] M. Turalija, P. Merschak, B. Redl, U. Griesser, H. Duelli, T. Bechtold, Copper(i)oxide microparticles - synthesis and antimicrobial finishing of textiles, Journal of Materials Chemistry B, 3 (2015) 5886-5892.
[135] Y.-J. Lee, S. Kim, S.-H. Park, H. Park, Y.-D. Huh, Morphology-dependent antibacterial activities of Cu2O, Materials Letters, 65 (2011) 818-820.
[136] L.M. Gilbertson, E.M. Albalghiti, Z.S. Fishman, F. Perreault, C. Corredor, J.D. Posner, M. Elimelech, L.D. Pfefferle, J.B. Zimmerman, Shape-Dependent Surface Reactivity and Antimicrobial Activity of Nano-Cupric Oxide, Environmental Science & Technology, 50 (2016) 3975-3984.
[137] R.K. Swarnkar, J.K. Pandey, K.K. Soumya, P. Dwivedi, S. Sundaram, S. Prasad, R. Gopal, Enhanced antibacterial activity of copper/copper oxide nanowires prepared by pulsed laser ablation

in water medium, Applied Physics A, 122 (2016) 1-7.
[138] S.V.P. Ramaswamy, S. Narendhran, R. Sivaraj, Potentiating effect of ecofriendly synthesis of copper oxide nanoparticles using brown alga: antimicrobial and anticancer activities, Bulletin of Materials Science, 39 (2016) 361-364.
[139] Udayabhanu, P.C. Nethravathi, M.A. Pavan Kumar, D. Suresh, K. Lingaraju, H. Rajanaika, H. Nagabhushana, S.C. Sharma, Tinospora cordifolia mediated facile green synthesis of cupric oxide nanoparticles and their photocatalytic, antioxidant and antibacterial properties, Materials Science in Semiconductor Processing, 33 (2015) 81-88.
[140] K. Lingaraju, H.R. Naika, K. Manjunath, G. Nagaraju, D. Suresh, H. Nagabhushana, Rauvolfia serpentina-Mediated Green Synthesis of CuO Nanoparticles and Its Multidisciplinary Studies, Acta Metallurgica Sinica (English Letters), 28 (2015) 1134-1140.
[141] O.V. Zakharova, A.Y. Godymchuk, A.A. Gusev, S.I. Gulchenko, I.A. Vasyukova, D.V. Kuznetsov, Considerable Variation of Antibacterial Activity of Cu Nanoparticles Suspensions Depending on the Storage Time, Dispersive Medium, and Particle Sizes, BioMed Research International, 2015 (2015) 11.
[142] H.-Y. Jung, Y. Seo, H. Park, Y.-D. Huh, Morphology-controlled Synthesis of Octahedral-to-Rhombic Dodecahedral Cu2O Microcrystals and Shape-dependent Antibacterial Activities, Bulletin of the Korean Chemical Society, 36 (2015) 1828-1833.
[143] H. Pang, F. Gao, Q. Lu, Morphology effect on antibacterial activity of cuprous oxide, Chemical Communications, (2009) 1076-1078.
[144] A. Sedighi, M. Montazer, Tunable shaped N-doped CuO nanoparticles on cotton fabric through processing conditions: synthesis, antibacterial behavior and mechanical properties, Cellulose, 23 (2016) 2229-2243.
[145] A. Errokh, A.M. Ferraria, D.S. Conceição, L.F. Vieira Ferreira, A.M. Botelho do Rego, M. Rei Vilar, S. Boufi, Controlled growth of Cu2O nanoparticles bound to cotton fibres, Carbohydrate Polymers, 141 (2016) 229-237.
[146] H.E. Emam, A.P. Manian, B. Široká, H. Duelli, P. Merschak, B. Redl, T. Bechtold, Copper(I)oxide surface modified cellulose fibers—Synthesis, characterization and antimicrobial properties, Surface and Coatings Technology, 254 (2014) 344-351.
[147] S. Shankar, J.-W. Rhim, Facile approach for large-scale production of metal and metal oxide nanoparticles and preparation of antibacterial cotton pads, Carbohydrate Polymers, 163 (2017) 137-145.
[148] A. M.El Saeed, M. Abd El-Fattah, A.M. Azzam, M.M. Dardir, M.M. Bader, Synthesis of cuprous oxide epoxy nanocomposite as an environmentally antimicrobial coating, International

Journal of Biological Macromolecules, 89 (2016) 190-197.
[149] R.F. Tylecote, A history of metallurgy, Institute of Materials, London, 1992.
[150] S.D. Cramer, B.S. Covino Jr, C. Moosbrugger, B.R. Sanders, G.J. Anton, N. Hrivnak, J. Kinson, C. Polakowski, K. Muldoon, S.D. Henry, ASM handbook, ASM international, Ohio, 2003.
[151] F. Ijsseling, General guidelines for corrosion testing of materials for marine applications: Literature review on sea water as test environment, British Corrosion Journal, 24 (1989) 53-78.
[152] J. Nawrocki, U. Raczyk-Stanisławiak, J. Świetlik, A. Olejnik, M.J. Sroka, Corrosion in a distribution system: Steady water and its composition, Water Research, 44 (2010) 1863-1872.
[153] R. Heidersbach, Metallurgy and corrosion control in oil and gas production, John Wiley & Sons, Hoboken, 2018.
[154] P. Dillmann, D. Watkinson, E. Angelini, A. Adriaens, Corrosion and conservation of cultural heritage metallic artefacts, Woodhead Publishing Limited, Cambridge, 2013.
[155] N. LeBozec, N. Blandin, D. Thierry, Accelerated corrosion tests in the automotive industry: a comparison of the performance towards cosmetic corrosion, Materials and Corrosion, 59 (2008) 889-894.
[156] S. Benavides, Corrosion control in the aerospace industry, Woodhead Publishing Limited, Cambridge, 2009.
[157] D.C. Hansen, Metal corrosion in the human body: the ultimate bio-corrosion scenario, The Electrochemical Society Interface, 17 (2008) 31-34.
[158] G. Petzow, Metallographic etching: techniques for metallography, ceramography, plastography, ASM international, Ohio, 1999.
[159] D.M. Bastidas, M. Criado, S. Fajardo, V.M. La Iglesia, E. Cano, J.M. Bastidas, Copper deterioration: causes, diagnosis and risk minimisation, International Materials Reviews, 55 (2010) 99-127.
[160] A. Hedin, A.J. Johansson, C. Lilja, M. Boman, P. Berastegui, R. Berger, M. Ottosson, Corrosion of copper in pure O2-free water?, Corrosion Science, 137 (2018) 1-12.
[161] A. Vinogradov, T. Mimaki, S. Hashimoto, R. Valiev, On the corrosion behaviour of ultra-fine grain copper, Scripta Materialia, 41 (1999) 319-326.
[162] T. Weisser, The de-alloying of copper alloys, Studies in Conservation, 20 (1975) 207-214.
[163] M.B. Valcarce, S.R. de Sánchez, M. Vázquez, Brass dezincification in a tap water bacterial suspension, Electrochimica Acta, 51 (2006) 3736-3742.
[164] K. Hashimoto, S. Ogawa, S. Shimodaira, Dezincification of Alpha Brass, Transactions of the Japan Institute of Metals, 4 (1963) 42-45.
[165] E. Martinez-Lombardia, L. Lapeire, I. De Graeve, K. Verbeken, L.A.I. Kestens, H. Terryn,

Study of the influence of the microstructure on the corrosion properties of pure copper, Materials and Corrosion, 67 (2016) 847-856.

[166] L. Lapeire, E. Martinez Lombardia, I. De Graeve, H. Terryn, K. Verbeken, Influence of grain size on the electrochemical behavior of pure copper, Journal of Materials Science, 52 (2017) 1501-1510.

[167] Y. Zhao, I.C. Cheng, M.E. Kassner, A.M. Hodge, The effect of nanotwins on the corrosion behavior of copper, Acta Materialia, 67 (2014) 181-188.

[168] E. Martinez-Lombardia, L. Lapeire, V. Maurice, I. De Graeve, K. Verbeken, L.H. Klein, L.A.I. Kestens, P. Marcus, H. Terryn, In situ scanning tunneling microscopy study of the intergranular corrosion of copper, Electrochemistry Communications, 41 (2014) 1-4.

[169] J.W. Sowards, E. Mansfield, Corrosion of copper and steel alloys in a simulated underground storage-tank sump environment containing acid-producing bacteria, Corrosion Science, 87 (2014) 460-471.

[170] E. Martinez-Lombardia, V. Maurice, L. Lapeire, I. De Graeve, K. Verbeken, L. Kestens, P. Marcus, H. Terryn, In Situ Scanning Tunneling Microscopy Study of Grain-Dependent Corrosion on Microcrystalline Copper, The Journal of Physical Chemistry C, 118 (2014) 25421-25428.

[171] E. Martinez-Lombardia, Y. Gonzalez-Garcia, L. Lapeire, I. De Graeve, K. Verbeken, L. Kestens, J.M.C. Mol, H. Terryn, Scanning electrochemical microscopy to study the effect of crystallographic orientation on the electrochemical activity of pure copper, Electrochimica Acta, 116 (2014) 89-96.

[172] L. Lapeire, E. Martinez Lombardia, K. Verbeken, I. De Graeve, L.A.I. Kestens, H. Terryn, Effect of neighboring grains on the microscopic corrosion behavior of a grain in polycrystalline copper, Corrosion Science, 67 (2013) 179-183.

[173] N. Ebejer, A.G. Güell, S.C.S. Lai, K. McKelvey, M.E. Snowden, P.R. Unwin, Scanning Electrochemical Cell Microscopy: A Versatile Technique for Nanoscale Electrochemistry and Functional Imaging, Annual Review of Analytical Chemistry, 6 (2013) 329-351.

[174] J.H. Seo, J.-H. Ryu, D.N. Lee, Formation of Crystallographic Etch Pits during AC Etching of Aluminum, Journal of The Electrochemical Society, 150 (2003) B433-B438.

[175] B.J. Cruickshank, A.A. Gewirth, R.M. Rynders, R.C. Alkire, In Situ Observations of Shape Evolution during Copper Dissolution Using Atomic Force Microscopy, Journal of The Electrochemical Society, 139 (1992) 2829-2832.

[176] J.D. Livingston, The density and distribution of dislocations in deformed copper crystals, Acta Metallurgica, 10 (1962) 229-239.

[177] J.D. Livingston, Etch Pits at Dislocations in Copper, Journal of Applied Physics, 31 (1960)

1071-1076.
[178] A.W. Ruff, Dislocations and Chemical Etch Pits in Copper, Journal of Applied Physics, 33 (1962) 3392-3400.
[179] H. Kakinuma, I. Muto, Y. Oya, Y. Kyo, Y. Sugawara, N. Hara, Mechanism for the Morphological Change from Trenching to Pitting around Intermetallic Particles in AA1050 Aluminum, Journal of The Electrochemical Society, 166 (2019) C19-C32.
[180] F.W. Young, Etch Pits at Dislocations in Copper, Journal of Applied Physics, 32 (1961) 192-201.
[181] A. El Warraky, H.A. El Shayeb, E.M. Sherif, Pitting corrosion of copper in chloride solutions, Anti-Corrosion Methods and Materials, 51 (2004) 52-61.
[182] C.A.C. Sequeira, Inorganic, physicochemical, and microbial aspects of copper corrosion: literature survey, British Corrosion Journal, 30 (1995) 137-153.
[183] W. Fischer, H.H. Paradies, D. Wagner, I. Hänßel, Copper deterioration in a water distribution system of a county hospital in Germany caused by microbially induced corrosion – I. Description of the problem, Materials and Corrosion, 43 (1992) 56-62.
[184] D. Wagner, W. Fischer, H.H. Paradies, Copper deterioration in a water distribution system of a county hospital in Germany caused by microbially influenced corrosion – II. Simulation of the corrosion process in two test rigs installed in this hospital, Materials and Corrosion, 43 (1992) 496-502.
[185] B.J. Webster, S.E. Werner, D.B. Wells, P.J. Bremer, Microbiologically Influenced Corrosion of Copper in Potable Water Systems—pH Effects, Corrosion, 56 (2000) 942-950.
[186] A.K. Lee, D.K. Newman, Microbial iron respiration: impacts on corrosion processes, Applied Microbiology and Biotechnology, 62 (2003) 134-139.
[187] W.P. Iverson, Microbial Corrosion of Metals, Advances in Applied Microbiology, Academic Press, New York, 1987, pp. 1-36.
[188] M.A. Javed, P.R. Stoddart, E.A. Palombo, S.L. McArthur, S.A. Wade, Inhibition or acceleration: Bacterial test media can determine the course of microbiologically influenced corrosion, Corrosion Science, 86 (2014) 149-158.
[189] K.R. Lawless, The oxidation of metals, Reports on Progress in Physics, 37 (1974) 231-316.
[190] K.R. Lawless, G.T. Miller, Jnr, The epitaxial relationships of cuprous oxide formed on copper single crystals immersed in an aqueous solution of copper sulfate, Acta Crystallographica, 12 (1959) 594-600.
[191] N. Ikemiya, T. Kubo, S. Hara, In situ AFM observations of oxide film formation on Cu(111) and Cu (100) surfaces under aqueous alkaline solutions, Surface Science, 323 (1995) 81-90.

[192] J. Kunze, V. Maurice, L.H. Klein, H.-H. Strehblow, P. Marcus, In Situ Scanning Tunneling Microscopy Study of the Anodic Oxidation of Cu(111) in 0.1 M NaOH, The Journal of Physical Chemistry B, 105 (2001) 4263-4269.

[193] J. Kunze, V. Maurice, L.H. Klein, H.-H. Strehblow, P. Marcus, In situ STM study of the duplex passive films formed on Cu(111) and Cu(001) in 0.1 M NaOH, Corrosion Science, 46 (2004) 245-264.

[194] M.J. Hutchison, J.R. Scully, Solute Capture and Doping of Al in Cu2O: Corrosion, Tarnish Resistance, and Cation Release of High-Purity Cu-Al Alloys in Artificial Perspiration, Journal of The Electrochemical Society, 165 (2018) C689-C702.

[195] N. Ciacotich, M. Kilstrup, P. Møller, L. Gram, Influence of chlorides and phosphates on the antiadhesive, antibacterial, and electrochemical properties of an electroplated copper-silver alloy, Biointerphases, 14 (2019) 021005.

[196] S.M. Mayanna, T.H.V. Setty, Role of chloride ions in relation to copper corrosion and inhibition, Proceedings of the Indian Academy of Sciences - Section A, 80 (1974) 184-193.

[197] X. Li, D. Gupta, H.-J. Eom, H. Kim, C.-U. Ro, Deliquescence and efflorescence behavior of individual NaCl and KCl mixture aerosol particles, Atmospheric Environment, 82 (2014) 36-43.

[198] E. Schindelholz, R.G. Kelly, Wetting phenomena and time of wetness in atmospheric corrosion: a review, Corrosion Reviews, 30 (2012) 135-170.

[199] Z.Y. Chen, S. Zakipour, D. Persson, C. Leygraf, Effect of Sodium Chloride Particles on the Atmospheric Corrosion of Pure Copper, Corrosion, 60 (2004) 479-491.

[200] S.X. Li, L.H. Hihara, Atmospheric corrosion initiation on steel from predeposited NaCl salt particles in high humidity atmospheres, Corrosion Engineering, Science and Technology, 45 (2010) 49-56.

List of units, abbreviations and symbols

AFM	Atomic Force Microscope
BF	Bright Field
BSE	Backscatter Electron(s)
CD	Crystal Direction
cfu	Colony-forming Unit
CI	Confidence Index
CVD	Chemical Vapour Deposition
DF	Dark Field
DNA	Deoxyribonucleic Acid
E. coli	*Escherichia coli*
EBSD	Electron Backscatter Diffraction
EDS	Energy Dispersive X-ray Spectroscopy
EPA	Environmental Protection Agency
EPS	Extracellular Polymeric Substances
FIB	Focused Ion Beam
GIXRD	Grazing Incidence X-ray Diffraction
HAADF	High-angle Annular Dark-field
HAIs	Healthcare-associated Infections
IAIs	Implant-Associated Infections
ICP	Inductively Coupled Plasma
IPF	Inverse Pole Figure
IQ	Image Quality
LB	Lysogeny Broth
LSM	Laser Scanning Microscope
MIC	Microbiologically Influenced Corrosion
MRSA	Multiple-resistant *Staphylococcus aureus*
MS	Mass Spectrometry
Na-HEPES	Na-4-(2-hydroxyethyl)-1-piperazineethanesulfonic Acid
OM	Optical Microscope
PBS	Phosphate-buffered Saline
PVD	Physical Vapour Deposition
Raman	Raman Spectroscopy

RCS	Reactive Chlorine Species
redox	Oxidation-reduction
RH	Relative Humidity
ROS	Reactive Oxygen Species
S. aureus	*Staphylococcus aureus*
S. cohnii	*Staphylococcus cohnii*
SE	Secondary Electron(s)
SECCM	Scanning Electrochemical Cell Microscope
SECM	Scanning Electrochemical Microscope
SEM	Scanning Electron Microscope
STEM	Scanning Transmission Electron Microscope
STM	Scanning Tunnelling Microscope
TEM	Transmission Electron Microscope
TSB	Tryptic Soy Broth

Acknowledgements

(I put this chapter in the end just like how we usually do in China. In this way, whenever one searches if his/her name is mentioned here, he/she looks like reading carefully the chapter of Conclusion…Well, these two sections might not be essentially different, in some ways.)

At the same time when I am starting this part, the public transport in Saarbruecken is undergoing an unprecedented strike, already for nearly a week. For this reason, like many others, I have to walk from Dudweiler (the "village" where I stay at nights), through a tiny hill and forest, to our institute (the "home" where I stay during the days, some of you like to put it in this way). This kind of travelling is, unexpectedly, pretty fine for me. Simply because exactly four years ago, in September 2015, I was making the same way to the institute for almost the whole month, starting from my first day as a PhD student.

Of course, I did not meet Prof. Frank Mücklich, our "Chef", so awkward on my first day. Not even the second day, since he was participating in a wonderful DocMASE summer school in Barcelona. If it were me, I would not want to come back as well, but he did. And he did more than that. He did enjoy looking at me whenever I tried to carefully start our conversations in German, and friendly offering me a chance to switch to English. He therefore got an upper hand in the beginning of our negotiations. Thanks to his trust, I was provided with some tasks in which I get myself trained, although it is obvious that there are always some other colleagues who are more capable in accomplishing them. As a result, I was able to learn the best things from others.

So, who actually introduced me to the institute on my first day? It was Dr. Michael Hans, who also drafted my original project as an outlook of his doctoral thesis. We shared an office in the first half year, where so many lab procedures as well as German culture were covered. I hope I did not fail his expectation of how the work is continued in my hands.

Because of Michael, I also got a chance to work with (for, to be honest) Prof. Marc Solioz. We spent one whole week together in the lab and tried get some results from the no-one-dare-touch Cadmium plate. So guys, if something happens to me in the rest of my life, it should not be hard to deduce why. Most importantly, it is also why this thesis has been developed in such a way: everything sprouts from a small observation from that week. Despite of this, I am always grateful to have been appointed as the first author of the publication as a result of these experiments. One thing I haven't told him yet is how much I have learned from the way he delivers his thoughts, especially from

those replies to the reviewers, although I got warned when I tried to copy his style in my own submissions.

For the same reason, I got to know Dr. Christina Hein and Dr. Ralf Kautenburger, who support our ICP-MS measurements, all the way from their old site in Dudweiler to new building in Campus. Without those experiments, I cannot imagine if any conclusions can be drawn within this thesis. On the other hand, I have to say sorry to my "Wissenschaftliche Begleiter" (Scientific Companion) Prof. Rolf Müller, for having forgotten how to properly arrange an appointment, more than once. However, he never refuses to examine the summaries and offer comments from a totally different viewpoint. Some of them have been transformed to some enlightening moments from which this study benefited a lot.

As one may expect, I should start listing some people, claiming how significant their support and care are in these years. But I am not anymore a big fan of this norm: it is such a challenge for people who have a bad memory like me (and probably also a disaster for those who have a good one), considering the unexpected longitude of one's doctoral study. Besides, this kind of list also seems to emphasise the existence of some mystery groups. So, why don't we simply express thanks to the group?

First, my gratitude goes to my numerous former/current/short-term/long-term officemates as well as the colleagues I visited frequently, who always endure me and never let me feel unwelcome (not like bacteria on copper). Thereby I also got to know how imperfect I am and has been putting efforts in understanding others, not to mention the academic or technical support, cultural exchanges and language courses that have been running almost every day and always free of charge.

On the other hand, unlike Saarbruecken, which literally means "bridges on the Saar river", Nancy is a French city that simply sounds much gentle and attractive. Since I was asked more than once who the girl Nancy I was staying with, I had to spend days in picking up its pronunciation in its original French way. But as you may know, both the difficulty and beauty of the French language, is that you can never tell if you are pronouncing it correctly. The good news is, I do not have to face this problem when I talk with another supervisor of this thesis, Prof. Jean-François Pierson. Among those things inspired by him, an important one is definitely about setting goals. Without this creed, this thesis would not have a chance to be finalised. During my first week in Nancy, it was another person, Dr. Yong Wang who displayed me the deposition techniques. He offered almost everything

I need to survive in the lab, as well as the mental instructions to survive my PhD. For those friends met in this city, I don't think I have brought enough German chocolate to them, compared to the happy hours they have given me, transforming my stays in Nancy to kind of holidays.

I will not forget those who work in the secretary rooms and administration offices, who have assisted me in many paper works. It is their patience and instructions that ensure everything goes smoothly before every deadline.

Obviously, without the strong and continuous financial support, I would not be able to know all of you or to feel all of these. It is Dr. Flavio Soldera, Michael Engstler and Daniel Müller who applied/shared their project from European Commission or Deutsche Forschungsgemeinschaft for/with me, whom I am always grateful for. Additionally, Claudia Heß should not be forgotten since she managed to obtain the support from Franco-German University.

Being in these two campuses also rewards me with relationships found in language courses, sport courses or other activities. These fellows occasionally remind me of those who I already got to know when I was in China before this doctoral study. The moments we shared have been appearing from time to time, having me supported in this wonderful journey. Sometimes I even believe that it is easier to see things clearer, if there is a chance to step back and be far away.

No one would deny that to offer suggestions requires both wisdom and bravery. Without the kind and critical feedback from the mystery reviewers of the publications, our internal reviewers Daniel Müller and Lucía Campo, or other warm-hearted colleagues who challenged in seminars, conferences, rehearsal and other casual occasions, this thesis could have been presented in a much more confused way. (Very constructive comments and corrections from the defence committee also play an important role in the final version.)

After being far away from home for more than ten years, I hope it is not too late to recognise how fortunate I am to have my family members who always care about me, at home, at the airport, or even here in Saarbruecken. Especially my parents, you offered me a couple of months to show you how Europe looks like, in the very same way you showed me how this wonderful world looked like when I was a child.

Finalised on May 3, 2020, the last Sunday of COVID-19 lockdown, at Dudweiler.